

การประเมินวิธีการยิงท่อกูในหลุมผลิตก๊าซธรรมชาติในอ่าวไทย



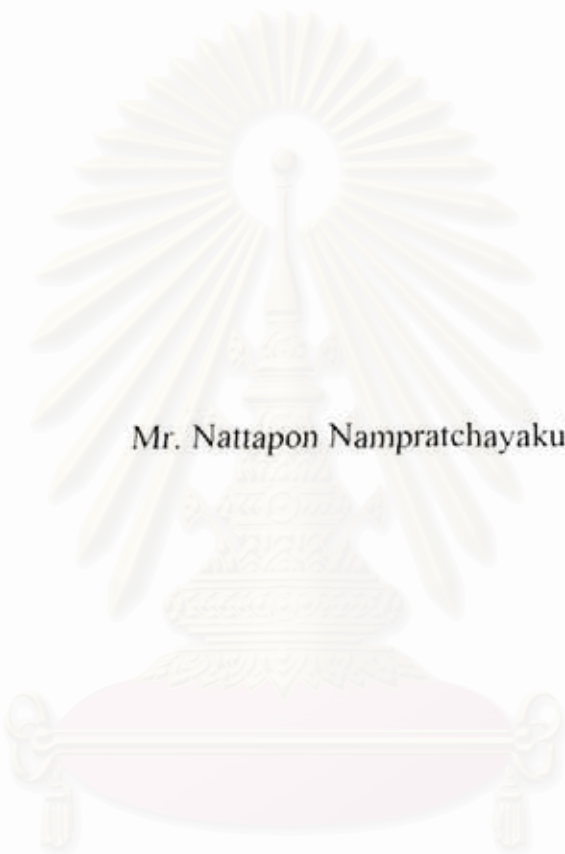
นายรัฐพล นำปรัชญากุล

สถาบันวิทยบริการ จุฬาลงกรณ์มหาวิทยาลัย

วิทยานิพนธ์นี้เป็นส่วนหนึ่งของการศึกษาดตามหลักสูตรปริญญาวิศวกรรมศาสตรมหาบัณฑิต
สาขาวิชาวิศวกรรมปิโตรเลียม ภาควิชาวิศวกรรมเหมืองแร่และปิโตรเลียม
คณะวิศวกรรมศาสตร์ จุฬาลงกรณ์มหาวิทยาลัย
ปีการศึกษา 2549
ลิขสิทธิ์ของจุฬาลงกรณ์มหาวิทยาลัย

491202

EVALUATION OF PERFORATION STRATEGIES OF
GAS WELLS IN THE GULF OF THAILAND



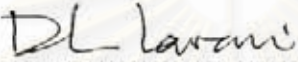
Mr. Nattapon Nampratchayakul

สถาบันวิทยบริการ
จุฬาลงกรณ์มหาวิทยาลัย

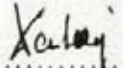
A Thesis Submitted in Partial Fulfillment of the Requirements
for the Degree of Master of Engineering Program in Petroleum Engineering
Department of Mining and Petroleum Engineering
Faculty of Engineering Chulalongkorn University
Academic Year 2006
Copyright of Chulalongkorn University


Thesis Title EVALUATION OF PERFORATION STRATEGIES OF
 GAS WELLS IN THE GULF OF THAILAND
By Mr. Nattapon Nampratchayakul
Field of Study Petroleum Engineering
Thesis Advisor Assistant Professor Suwat Athichanagorn, Ph.D.


Accepted by the Faculty of Engineering, Chulalongkorn University in
Partial Fulfillment of the Requirements for the Master's Degree


..... Dean of the Faculty of Engineering
(Professor Direk Lavansiri, Ph.D.)

THESIS COMMITTEE


..... Chairman
(Associate Professor Sarithdej Pathanasetpong)


..... Thesis Advisor
(Assistant Professor Suwat Athichanagorn, Ph.D.)


..... Member
(Jirawat Chewaroungroj, Ph.D.)

นัฐพล นำปรัชญากุล : การประเมินวิธีการยิงท่อกรูในหลุมผลิตก๊าซธรรมชาติในอ่าวไทย (EVALUATION OF PERFORATION STRATEGIES OF GAS WELLS IN THE GULF OF THAILAND) อ.ที่ปรึกษา : ศศ.ดร. สุวัฒน์ อธิชนากร, 189 หน้า.

การยิงท่อกรูในหลุมผลิตในสภาวะที่ความดันในหลุมผลิตน้อยกว่าความดันของแหล่งกักเก็บ เป็นวิธีที่ยอมรับกันมานานแล้วว่าเป็นวิธีที่ดีที่สุดวิธีหนึ่งในการลดความเสียหายของแหล่งกักเก็บที่เกิดจากการยิงท่อกรู อย่างไรก็ตามประสิทธิภาพในการไหลของหลุมผลิตที่ได้จากการยิงท่อกรูขึ้นอยู่กับปัจจัย เช่น ระดับความแตกต่างของความดันในหลุมผลิตและความดันของแหล่งกักเก็บ ขนาดของปืนยิงท่อกรู จำนวนลูกปืนต่อหนึ่งฟุตของปืนยิงท่อกรู องศาที่ต่างกันของลูกปืนแต่ละลูกในหนึ่งฟุต และชนิดของดินปืน การศึกษาในวิทยานิพนธ์ฉบับนี้ได้ทำการวิเคราะห์ผลการทดสอบหลุมหรือการวิเคราะห์การเปลี่ยนแปลงของความดันเมื่ออัตราการผลิตเปลี่ยนไปของแหล่งกักเก็บก๊าซธรรมชาติจำนวน 70 แหล่ง จาก 70 หลุมผลิตก๊าซธรรมชาติในอ่าวไทย แหล่งกักเก็บก๊าซธรรมชาติ 70 แหล่งนี้มีค่าความพรุนที่แตกต่างกัน ถูกยิงท่อกรูด้วยปืนยิงท่อกรูที่ต่างกัน ในสภาวะความดันที่ต่างกัน

จากการวิเคราะห์ข้อมูลของแหล่งกักเก็บก๊าซธรรมชาติจำนวนเจ็ดสิบแหล่ง สามารถสรุปได้ว่าระดับความแตกต่างของความดันในหลุมผลิตและความดันของแหล่งกักเก็บ ขณะทำการยิงท่อกรู มีผลกระทบโดยตรงต่อขนาดของความเสียหายและประสิทธิภาพในการไหลของแหล่งกักเก็บ ระดับความแตกต่างของความดันสูงๆ จะทำให้ขนาดของความเสียหายค่าและประสิทธิภาพในการไหลของแหล่งกักเก็บสูง อย่างไรก็ตาม ระดับความแตกต่างของความดันมีผลกระทบมากกับประสิทธิภาพในการไหลของแหล่งกักเก็บที่มีค่าความพรุนน้อยกว่า 18%

นอกจากนี้ จากการศึกษา สามารถหาสมการความสัมพันธ์ระหว่างระดับความแตกต่างของความดันที่จำเป็นเพื่อให้ความเสียหายของแหล่งกักเก็บที่เกิดจากการยิงท่อกรูเป็นศูนย์ สำหรับแหล่งกักเก็บที่มีค่าความพรุนหรือค่าความสามารถในการไหลผ่านใดๆ สมการความสัมพันธ์นี้ยังได้ถูกนำไปเปรียบเทียบกับความสัมพันธ์จากการศึกษาอื่นๆ ก่อนหน้านี้ จากการเปรียบเทียบ แหล่งกักเก็บที่อยู่ต่างแหล่งต่างพื้นที่กันต้องการระดับความแตกต่างของความดันไม่เหมือนกันเพื่อให้ความเสียหายของแหล่งกักเก็บที่เกิดจากการยิงท่อกรูเป็นศูนย์

การยิงท่อกรูโดยการใช้ดินปืนที่ต่างกัน จำเป็นต้องใช้ระดับความแตกต่างของความดัน 1500 ถึง 1777 ปอนด์ต่อตารางนิ้ว ขณะทำการยิงท่อกรู เพื่อให้ความเสียหายของแหล่งกักเก็บที่เกิดจากการยิงท่อกรูเป็นศูนย์ และจากการศึกษาพบว่าที่ระดับความแตกต่างของความดันที่น้อยกว่า 1300 ปอนด์ต่อตารางนิ้ว มีดินปืนอยู่สองชนิดที่ให้ความเสียหายของแหล่งกักเก็บต่ำกว่า

ภาควิชาวิศวกรรมเหมืองแร่และปิโตรเลียม.....ลายมือชื่อนิสิต *Nattaporn Namprachayakul*
สาขาวิชาวิศวกรรมปิโตรเลียม.....ลายมือชื่ออาจารย์ที่ปรึกษา *Suwanat Attichanagorn*
ปีการศึกษา 2549.....

4671637121 : MAJOR PETROLEUM ENGINEERING

KEY WORD : PERFORATION/GAS WELL/SKIN/FLOW EFFICIENCY

NATTAPON NAMPRATCHAYAKUL : EVALUATION OF
PERFORATION STRATEGIES OF GAS WELLS IN THE GULF OF
THAILAND. THESIS ADVISOR : ASSIST. PROF. SUWAT
ATHICHANAGORN, Ph.D. 189 pp.

Underbalance perforation has long been recognized as one of the best techniques for mitigating perforating damage. However, the flow efficiency of the perforated wells is controlled by several parameters such as underbalance condition, perforation gun size, shot density, phase angle, and charge type. In this study, seventy pressure transients of seventy gas reservoirs from different wells in the Gulf of Thailand have been analyzed. These reservoirs have different porosities and were perforated with various perforation gun assemblies under different pressure conditions.

After analyzing results obtained from seventy gas reservoirs, it can be concluded that the underbalance pressure condition directly affects the perforation damage or skin of perforated gas reservoir, as well as corrected flow efficiency. The higher the underbalance pressure the lower the perforation skin is. As a result, the higher flow efficiency and recovery of gas reservoir can be achieved. However, the underbalance pressure has more impact on the corrected flow efficiency of tight gas reservoirs which have porosity equal to or lower than 18%.

The correlations of underbalance pressure required to achieve zero perforation skin for any reservoir porosity or permeability were obtained and compared to published correlations. From comparison, reservoirs located in different fields require different underbalance pressure condition to achieve zero perforation skin.

Regardless of reservoirs properties, depending on perforation charge type, 1500 to 1777 psi underbalance pressure is required to achieve zero perforation skin. There are two recommended charge types for better perforation performance when available or achievable underbalance pressure is lower than 1300 psi.

Department of Mining and Petroleum Engineering... Student's signature *Nattapon Nampratchayakul*
Field of Study: Petroleum Engineering..... Advisor's signature *Suwat Athichanagorn*
Academic Year: 2006.....

Acknowledgements

My utmost appreciation and gratitude are expressed to my thesis advisor, Assist. Prof. Dr. Suwat Athichanagorn, Department of Mining and Petroleum Engineering, Chulalongkorn University, for his guidance and advice during this study. His understanding, encouragement and personal guidance have provided a good basis, not only for this thesis, but also during the course works both Bachelor and Master degrees.

Special thanks are also extended to all professors in Department of Mining and Petroleum Engineering, Chulalongkorn University, for infinite valuable knowledge that I have been using for my career for last 6 years and also in the future.

A deep appreciation is also expressed to Chevron Thailand Exploration and Production, Ltd for providing all information for this thesis, as well as a financial support.

Finally, I would like to take this opportunity to thank my parents for their infinite support and endless love.

สถาบันวิทยบริการ
จุฬาลงกรณ์มหาวิทยาลัย

Contents

	Page
Abstract (in Thai)	iv
Abstract (in English)	v
Acknowledgements	vi
Table of Contents	vii
List of Tables	ix
List of Figures	x
Nomenclature	xix
 Chapter	
I Introduction	1
II Theoretical Considerations	3
2.1 Underbalance Perforation.....	3
2.2 Pressure Transient (Well Test) Analysis.....	7
2.3 Skin.....	8
2.3.1 Rate Dependent (Non-Darcy) Skin.....	9
2.3.2 Partial Penetration Skin.....	10
2.3.3 Perforation Skin and Flow Efficiency.....	14
 III Evaluation of Perforation Strategies of Gas Wells in the Gulf of Thailand	 16
3.1 Perforation of Gas Wells.....	20
3.2 Pressure Transient (Well Test) Analysis.....	23
3.2.1 Skin and Corrected Flow Efficiency for Perforated Gas Wells.....	26
3.3 Relationship between Skin and Underbalance Pressure.....	28
3.4 Relationship between Corrected Flow Efficiency and Underbalance Pressure.....	32

	Page
3.5 Relationship between Underbalance and Permeability.....	36
3.6 Relationship between Underbalance and Porosity.....	39
3.7 Relationship between Corrected Flow Efficiency and Perforation Charge Type.....	41
IV Conclusions.....	44
Reference.....	46
Appendix.....	48
Vitae.....	189

สถาบันวิทยบริการ
จุฬาลงกรณ์มหาวิทยาลัย

List of Tables

Table	Page
2.1 Typical ranges of underbalance pressure for perforated system cleanup.	4
3.1 Gas reservoir properties.....	19
3.2 Swabbing depths and perforation information.....	22
3.3 Results of pressure transient analyses.....	24
3.4 Calculated partial penetration skin and corrected data.....	27
3.5 Information for relationship study.....	29
3.6 Coefficient of determination, R^2 , of each porosity cutoff on perforation skin versus underbalance pressure.....	30
3.7 Coefficient of determination, R^2 , of each porosity cutoff on corrected flow efficiency versus underbalance pressure	33
3.8 Minimal underbalance pressure to obtain zero perforation skin for each perforation charge type.....	43

สถาบันวิทยบริการ
จุฬาลงกรณ์มหาวิทยาลัย

List of Figures

Figure	Page
2.1 Underbalance used in perforating oil reservoir in sandstone formation...	5
2.2 Underbalance used in perforating gas reservoir in sandstone formation..	5
2.3 Drawdown test.....	8
2.4 Buildup test.....	8
2.5 Flow after flow well test.....	9
2.6 Total skin versus flow rate.....	10
2.7 Yeh and Reynolds' correlation for C' – multilayer reservoir.....	13
3.1 Histogram of porosity.....	16
3.2 Histogram of water saturation.....	17
3.3 Gulf of Thailand pressure profile.....	18
3.4 Histogram of permeability.....	25
3.5 Average permeability versus porosity of 70 gas reservoirs.....	26
3.6 Total skin and perforation skin versus underbalance pressure	28
3.7 Perforation skin versus underbalance pressure – cutoff porosity of 18%.	31
3.8 Corrected flow efficiency versus underbalance pressure – all 70 gas reservoirs of interest.....	32
3.9 Corrected flow efficiency versus underbalance pressure – cutoff porosity of 18%.....	34
3.10 Underbalance pressure versus gas reservoir permeability at corrected flow efficiency higher than 60, 80, and 100%.....	36
3.11 Underbalance pressure versus gas reservoir permeability at corrected flow efficiency higher than 100% (zero-perforation skin) compared with King's field correlation and Hsia & Behrmann's correlation.....	38
3.12 Underbalance pressure versus gas reservoir porosity at corrected flow efficiency higher than 60, 80, and 100%.....	39
3.13 Corrected flow efficiency versus underbalance pressure for each perforation charge type.....	41

Figure	Page
3.14 Corrected flow efficiency versus underbalance pressure for each perforation charge type, 2-1/8" gun size, 60 degree phasing, 5-6 shot per foot, and HMX explosive.....	42
A.1 Well-01 testing overview.....	49
A.2 Well-01 main build-up, log-log plot.....	50
A.3 Well-01 main build-up, semi-log plot.....	50
A.4 Well-02 testing overview.....	51
A.5 Well-02 main build-up, log-log plot.....	51
A.6 Well-02 main build-up, semi-log plot.....	52
A.7 Well-03 testing overview.....	53
A.8 Well-03 main build-up, log-log plot.....	53
A.9 Well-03 main build-up, semi-log plot.....	54
A.10 Well-04 testing overview.....	55
A.11 Well-04 main build-up, log-log plot.....	55
A.12 Well-04 main build-up, semi-log plot.....	56
A.13 Well-05 testing overview.....	57
A.14 Well-05 main build-up, log-log plot.....	57
A.15 Well-05 main build-up, semi-log Plot.....	58
A.16 Well-06 testing overview.....	59
A.17 Well-06 main build-up, log-log plot.....	59
A.18 Well-06 main build-up, semi-log plot.....	60
A.19 Well-07 testing overview.....	61
A.20 Well-07 main build-up, log-log plot.....	61
A.21 Well-07 main build-up, semi-log plot.....	62
A.22 Well-08 testing overview.....	63
A.23 Well-08 main build-up, log-log plot.....	63
A.24 Well-08 main build-up, semi-log plot.....	64
A.25 Well-09 testing overview.....	65
A.26 Well-09 main build-up, log-log plot.....	65
A.27 Well-09 main build-up, semi-log plot.....	66
A.28 Well-10 testing overview.....	67

Figure	Page
A.29 Well-10 main build-up, log-log plot.....	67
A.30 Well-10 main build-up, semi-log plot.....	68
A.31 Well-10 rate dependent skin plot.....	68
A.32 Well-11 testing overview.....	69
A.33 Well-11 main build-up, log-log plot.....	69
A.34 Well-11 main build-up, semi-log plot.....	70
A.35 Well-11 rate dependent skin plot.....	70
A.36 Well-12 testing overview.....	71
A.37 Well-12 main build-up, log-log plot.....	71
A.38 Well-12 main build-up, semi-log plot.....	72
A.39 Well-12 rate dependent skin plot.....	72
A.40 Well-13 testing overview.....	73
A.41 Well-13 main build-up, log-log plot.....	73
A.42 Well-13 main build-up, semi-log plot.....	74
A.43 Well-14 testing overview.....	75
A.44 Well-14 main build-up, log-log plot.....	75
A.45 Well-14 main build-up, semi-log plot.....	76
A.46 Well-14 rate dependent skin plot.....	76
A.47 Well-15 testing overview.....	77
A.48 Well-15 main build-up, log-log plot.....	77
A.49 Well-15 main build-up, semi-log plot.....	78
A.50 Well-15 rate dependent skin plot.....	78
A.51 Well-16 testing overview.....	79
A.52 Well-16 main build-up, log-log plot.....	79
A.53 Well-16 main build-up, semi-log plot.....	80
A.54 Well-16 rate dependent skin plot.....	80
A.55 Well-17 testing overview.....	81
A.56 Well-17 main build-up, log-log plot.....	81
A.57 Well-17 main build-up, semi-log plot.....	82
A.58 Well-18 testing overview.....	83
A.59 Well-18 main build-up, log-log plot.....	83

Figure	Page
A.60 Well-18 main build-up, semi-log plot.....	84
A.61 Well-18 rate dependent skin plot.....	84
A.62 Well-19 testing overview.....	85
A.63 Well-19 main build-up, log-log plot.....	85
A.64 Well-19 main build-up, semi-log plot.....	86
A.65 Well-20 testing overview.....	87
A.66 Well-20 main build-up, log-log plot.....	87
A.67 Well-20 main build-up, semi-log plot.....	88
A.68 Well-21 testing overview.....	89
A.69 Well-21 main build-up, log-log plot.....	89
A.70 Well-21 main build-up, semi-log plot.....	90
A.71 Well-22 testing overview.....	91
A.72 Well-22 main build-up, log-log plot.....	91
A.73 Well-22 main build-up, semi-log plot.....	92
A.74 Well-23 testing overview.....	93
A.75 Well-23 main build-up, log-log plot.....	93
A.76 Well-23 main build-up, semi-log plot.....	94
A.77 Well-24 testing overview.....	95
A.78 Well-24 main build-up, log-log plot.....	95
A.79 Well-24 main build-up, semi-log plot.....	96
A.80 Well-25 testing overview.....	97
A.81 Well-25 main build-up, log-log plot.....	97
A.82 Well-25 main build-up, semi-log plot.....	98
A.83 Well-26 testing overview.....	99
A.84 Well-26 main build-up, log-log plot.....	99
A.85 Well-26 main build-up, semi-log plot.....	100
A.86 Well-27 testing overview.....	101
A.87 Well-27 main build-up, log-log plot.....	101
A.88 Well-27 main build-up, semi-log plot.....	102
A.89 Well-28 testing overview.....	103
A.90 Well-28 main build-up, log-log plot.....	103

Figure	Page
A.91 Well-28 main build-up, semi-log plot.....	104
A.92 Well-29 testing overview.....	105
A.93 Well-29 main build-up, log-log plot.....	105
A.94 Well-29 main build-up, semi-log plot.....	106
A.95 Well-30 testing overview.....	107
A.96 Well-30 main build-up, log-log plot.....	107
A.97 Well-30 main build-up, semi-log plot.....	108
A.98 Well-31 testing overview.....	109
A.99 Well-31 main build-up, log-log plot.....	109
A.100 Well-31 main build-up, semi-log plot.....	110
A.101 Well-32 testing overview.....	111
A.102 Well-32 main build-up, log-log plot.....	111
A.103 Well-32 main build-up, semi-log plot.....	112
A.104 Well-33 testing overview.....	113
A.105 Well-33 main build-up, log-log plot.....	113
A.106 Well-33 main build-up, semi-log plot.....	114
A.107 Well-34 testing overview.....	115
A.108 Well-34 main build-up, log-log plot.....	115
A.109 Well-34 main build-up, semi-log plot.....	116
A.110 Well-35 testing overview.....	117
A.111 Well-35 main build-up, log-log plot.....	117
A.112 Well-35 main build-up, semi-log plot.....	118
A.113 Well-36 testing overview.....	119
A.114 Well-36 main build-up, log-log plot.....	119
A.115 Well-36 main build-up, semi-log plot.....	120
A.116 Well-37 testing overview.....	121
A.117 Well-37 main build-up, log-log plot.....	121
A.118 Well-37 main build-up, semi-log plot.....	122
A.119 Well-38 testing overview.....	123
A.120 Well-38 main build-up, log-log plot.....	123
A.121 Well-38 main build-up, semi-log plot.....	124

Figure	Page
A.122 Well-39 testing overview.....	125
A.123 Well-39 main build-up, log-log plot.....	125
A.124 Well-39 main build-up, semi-log plot.....	126
A.125 Well-40 testing overview.....	127
A.126 Well-40 main build-up, log-log plot.....	127
A.127 Well-40 main build-up, semi-log plot.....	128
A.128 Well-41 testing overview.....	129
A.129 Well-41 main build-up, log-log plot.....	129
A.130 Well-41 main build-up, semi-log plot.....	130
A.131 Well-42 testing overview.....	131
A.132 Well-42 main build-up, log-log plot.....	131
A.133 Well-42 main build-up, semi-log plot.....	132
A.134 Well-43 testing overview.....	133
A.135 Well-43 main build-up, log-log plot.....	133
A.136 Well-43 main build-up, semi-log plot.....	134
A.137 Well-44 testing overview.....	135
A.138 Well-44 main build-up, log-log plot.....	135
A.139 Well-44 main build-up, semi-log plot.....	136
A.140 Well-45 testing overview.....	137
A.141 Well-45 main build-up, log-log plot.....	137
A.142 Well-45 main build-up, semi-log plot.....	138
A.143 Well-46 testing overview.....	139
A.144 Well-46 main build-up, log-log plot.....	139
A.145 Well-46 main build-up, semi-log plot.....	140
A.146 Well-47 testing overview.....	141
A.147 Well-47 main build-up, log-log plot.....	141
A.148 Well-47 main build-up, semi-log plot.....	142
A.149 Well-48 testing overview.....	143
A.150 Well-48 main build-up, log-log plot.....	143
A.151 Well-48 main build-up, semi-log plot.....	144
A.152 Well-49 testing overview.....	145

Figure	Page
A.153 Well-49 main build-up, log-log plot.....	145
A.154 Well-49 main build-up, semi-log plot.....	146
A.155 Well-50 testing overview.....	147
A.156 Well-50 main build-up, log-log plot.....	147
A.157 Well-50 main build-up, semi-log plot.....	148
A.158 Well-51 testing overview.....	149
A.159 Well-51 main build-up, log-log plot.....	149
A.160 Well-51 main build-up, semi-log plot.....	150
A.161 Well-52 testing overview.....	151
A.162 Well-52 main build-up, log-log plot.....	151
A.163 Well-52 main build-up, semi-log plot.....	152
A.164 Well-53 testing overview.....	153
A.165 Well-53 main build-up, log-log plot.....	153
A.166 Well-53 main build-up, semi-log plot.....	154
A.167 Well-54 testing overview.....	155
A.168 Well-54 main build-up, log-log plot.....	155
A.169 Well-54 main build-up, semi-log plot.....	156
A.170 Well-55 testing overview.....	157
A.171 Well-55 main build-up, log-log plot.....	157
A.172 Well-55 main build-up, semi-log plot.....	158
A.173 Well-56 testing overview.....	159
A.174 Well-56 main build-up, log-log plot.....	159
A.175 Well-56 main build-up, semi-log plot.....	160
A.176 Well-57 testing overview.....	161
A.177 Well-57 main build-up, log-log plot.....	161
A.178 Well-57 main build-up, semi-log plot.....	162
A.179 Well-58 testing overview.....	163
A.180 Well-58 main build-up, log-log plot.....	163
A.181 Well-58 main build-up, semi-log plot.....	164
A.182 Well-59 testing overview.....	165
A.183 Well-59 main build-up, log-log plot.....	165

Figure	Page
A.184 Well-59 main build-up, semi-log plot.....	166
A.185 Well-60 testing overview.....	167
A.186 Well-60 main build-up, log-log plot.....	167
A.187 Well-60 main build-up, semi-log plot.....	168
A.188 Well-61 testing overview.....	169
A.189 Well-61 main build-up, log-log plot.....	169
A.190 Well-61 main build-up, semi-log plot.....	170
A.191 Well-62 testing overview.....	171
A.192 Well-62 main build-up, log-log plot.....	171
A.193 Well-62 main build-up, semi-log plot.....	172
A.194 Well-63 testing overview.....	173
A.195 Well-63 main build-up, log-log plot.....	173
A.196 Well-63 main build-up, semi-log plot.....	174
A.197 Well-64 testing overview.....	175
A.198 Well-64 main build-up, log-log plot.....	175
A.199 Well-64 main build-up, semi-log plot.....	176
A.200 Well-65 testing overview.....	177
A.201 Well-65 main build-up, log-log plot.....	177
A.202 Well-65 main build-up, semi-log plot.....	178
A.203 Well-66 testing overview.....	179
A.204 Well-66 main build-up, log-log plot.....	179
A.205 Well-66 main build-up, semi-log plot.....	180
A.206 Well-67 testing overview.....	181
A.207 Well-67 main build-up, log-log plot.....	181
A.208 Well-67 main build-up, semi-log plot.....	182
A.209 Well-68 testing overview.....	183
A.210 Well-68 main build-up, log-log plot.....	183
A.211 Well-68 main build-up, semi-log plot.....	184
A.212 Well-69 testing overview.....	185
A.213 Well-69 main build-up, log-log plot.....	185
A.214 Well-69 main build-up, semi-log plot.....	186

Figure	Page
A.215 Well-70 testing overview.....	187
A.216 Well-70 main build-up, log-log plot.....	187
A.217 Well-70 main build-up, semi-log plot.....	188



สถาบันวิทยบริการ
จุฬาลงกรณ์มหาวิทยาลัย

Nomenclature

b	penetration ratio
C'	correlating coefficient
D	rate dependent skin coefficient
f_i	dimensionless flow capacity
FE	flow efficiency
h	reservoir pay thickness
h_D	dimensionless pay thickness
h_p	limited interval open to flow
k	average reservoir permeability
\bar{k}	thickness-average horizontal permeability
k_h	horizontal permeability
k_j	horizontal permeability of layer j
k_v	vertical permeability
h_{wD}	dimensionless wellbore length
p_i	initial reservoir pressure
p_w	wellbore pressure
q_{sc}	tested flow rate
R^2	coefficient of determination
r_w	wellbore radius
S'	total skin factor
S	skin due to wellbore damage effect
$S_{non-Darcy}$	non-Darcy skin
S_p	perforation skin
S_{pp}	partial penetration skin
y	distance from the top of formation to the top of perforated interval
Δp	underbalance pressure
Δp_{upper}	upper bound underbalance pressure
Δp_{lower}	lower bound underbalance pressure

Greek Letter

ϕ	porosity
π	pi value, approximately of 3.1415926

Subscripts

D	dimensionless
h	horizontal
i	initial
j	layer index
p	perforated interval
pp	partial penetration
sc	standard condition
v	vertical
w	wellbore



สถาบันวิทยบริการ
จุฬาลงกรณ์มหาวิทยาลัย

CHAPTER I

INTRODUCTION

"The fate of a well hinges on years of exploration, months of well planning and weeks of drilling. But it ultimately depends on performing the optimal completion, which begins with the millisecond of perforation. Profitability is strongly influenced by this critical link between the reservoir and wellbore."

Quoted from Oilfield Review, Oct 1992

As per quotation in Oilfield Review, the perforation is not only a common operation to complete oil and gas wells, but also the critical link between the reservoir and wellbore. The flow efficiency of a perforated well might be higher than that of an openhole when the perforating parameters are optimized. At the moment, underbalance perforation has been widely accepted and applied in oil and gas well completion, especially in development wells. However, the flow efficiency of the perforated wells is controlled by several parameters, such as, perforation length, perforation diameter, shot density, phase angle, and degree of the damage around the perforation tunnels.

Numerous laboratory tests have been performed under simulated downhole conditions to obtain zero-perforation damage skin or the best flow efficiency. In addition, many field studies attempt to identify the minimum required underbalance pressure to obtain clean perforation and zero-perforation skin for different gas reservoir permeabilities and porosities.

The damage or skin around the perforations can be quantified indirectly by means of flow efficiency (*FE*). A poor flow efficiency requires a much higher pressure drop to obtain a certain rate. Thus, the flow efficiency is directly related to oil and gas reserves and recovery efficiency.

The pressure transient analysis (well test) can be used to evaluate the overall damage or total skin. However, the reservoir damage or skin could be caused by several factors, such as drilling operation, perforation, partial penetration, and high velocity flow. In order to determine the perforation skin, it is necessary to subtract skins caused by other factors from the total skin.

The perforation skin depends on various factors, such as wellbore condition (under balance) and perforation gun assembly in term of gun size, charge type, shot density, and phase angle.

The objective of this study is to define the guidelines for underbalance condition that leads to the best flow efficiency and an increase in recovery efficiency for various reservoir permeability (k) and porosities (ϕ) of gas wells in the Gulf of Thailand environment.



สถาบันวิทยบริการ
จุฬาลงกรณ์มหาวิทยาลัย

CHAPTER II

THEORITICAL CONSIDERATIONS

2.1 Underbalance Perforation

Underbalance perforation has gained a wide acceptance and become a more common practice than overbalance perforation which provides a lower flow efficiency, less well productivity, and higher degree of reservoir damage.

Perforation damage cleanup during underbalance perforation is the result of the transient decompression of the reservoir fluid around the perforation once the reservoir/wellbore pressure differential is established during the perforation process. It is assumed that cleanup of the perforation damage is from the dynamic force, from the pressure differential, on the fractured sand grain particles that progressively move these particles from the perforation tunnel walls, thus moving the permeability damaged region.

The first reservoir in multi-layered reservoirs that is perforated and used to unload the completion fluid is called unloading reservoir. Prior to perforation on the unloading reservoir, the conditions of both reservoir and within the wellbore are usually known.

Before the first perforation, the well is usually filled with the completion fluid. Thus, the hydrostatic pressure within the wellbore at any depth could be determined by Equation 2.1.

$$\text{Hydrostatic pressure} = 0.052 \times \text{completion fluid density (ppg)} \times \text{vertical depth (ft)} \quad [2.1]$$

With the initial reservoir pressure obtained from the wireline formation testing (or from general pressure profile in the particular area) and calculated Hydrostatic

pressure, the under balance perforation condition could be estimated and obtained from the Equation 2.2.

$$\text{Under Balance Pressure} = \text{Initial Reservoir Pressure} - \text{Hydrostatic Pressure} \quad [2.2]$$

The underbalance condition may be naturally existed in the case where initial reservoir pressure is higher than hydrostatic pressure. However, the required underbalance condition can be achieved by the certain operation such gas lift, liquid swabbing, etc.

Bell¹ first estimated the ranges of necessary underbalance pressure on the basis of both permeability and well performance. Bell conducted a perforation experimental test based on API RP 43, "Standard Procedure for Evaluation of Well Perforators". However, his estimation is useful in only two permeability ranges listed in Table 2.1.

Table 2.1: Typical ranges of underbalance pressure for perforated system cleanup¹.

	Liquid	Gas
High Permeability (> 100 MD)	200 to 500 psi	1,000 to 2,000 psi
Lower Permeability (< 100 MD)	1,000 to 2,000 psi	2,000 to 5,000 psi

After Bell's study, King² *et al.* conducted a field study of 90 wells with sandstone pays in five different regions which are the Rocky Mountain overthrust, Alberta, Canada, New Mexico Morrow sandstone, Lafayette Tuscaloosa trend, and U.S. gulf coast. Those 90 wells of King's study were perforated with tubing-conveyed systems at various levels of underbalance pressure.

The underbalance pressure was considered sufficient, and the perforation was assumed clean wherever the subsequent acidizing did not improve the well's performance. King's data show a clear correlation between a minimum required underbalance pressure and the formation permeability, determined from either core tests or pressure transient analysis, as shown in Figures 2.1 and 2.2, for oil and gas

reservoirs, respectively. In Figures 2.1 and 2.2, black and white points represent the reservoirs that well performance did improved and did not improved after acidizing, respectively.,

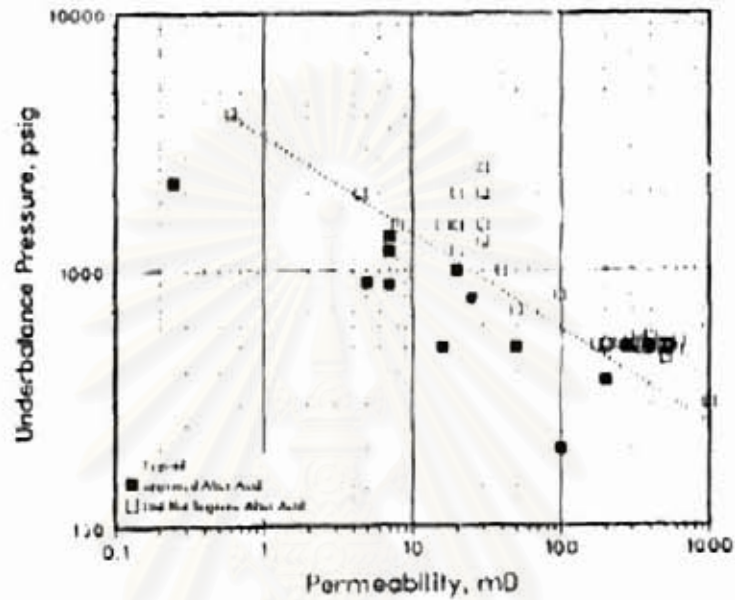


Figure 2.1: Underbalance pressure used in perforating oil reservoirs in sandstone formation.

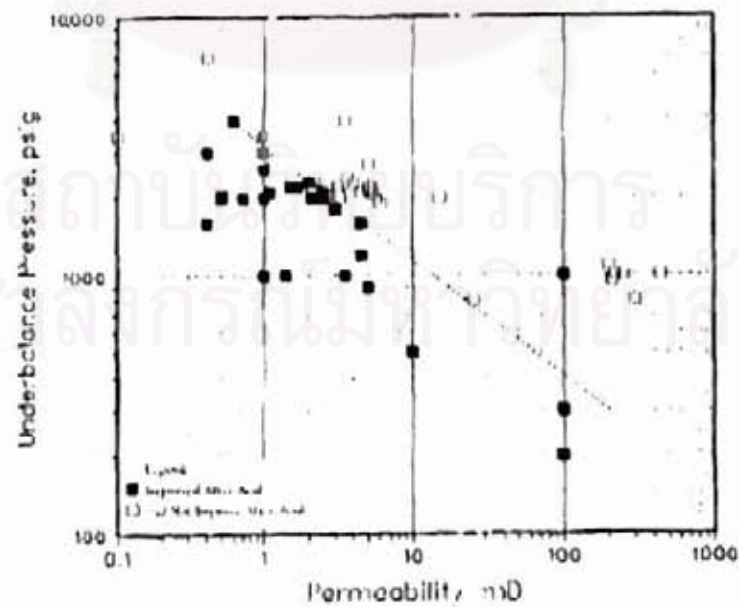


Figure 2.2: Underbalance pressure used in perforating gas reservoirs in sandstone formation.

Statistical analysis of King's field data was undertaken to find the best straight lines for correlations by Tariq⁴, as shown in Equations 2.3, 2.4, and 2.5. These equations provide a general guideline to estimate the minimum underbalance pressure requirement to obtain minimum perforation skin damage skin, based on the formation permeability.

$$\text{Overall,} \quad \Delta p = \frac{2900}{k^{0.36}} \quad [2.3]$$

$$\text{Oil,} \quad \Delta p = \frac{3100}{k^{0.37}} \quad [2.4]$$

$$\text{Gas,} \quad \Delta p = \frac{3000}{k^{0.4}} \quad [2.5]$$

where Δp = underbalance pressure, psi
 k = average reservoir permeability, md

Tariq concluded that there is no significant difference between underbalance requirements for oil and gas reservoirs. Therefore, King's field data for oil and gas wells have been combined as a single graph. Thus, the best straight line to determine sufficient underbalance pressure points for King's field data is given by Equation 2.3.

However, King's field data and Tariq's Equation 2.3 represents the minimum underbalance pressure for which acidization is not effective in any further reduction of perforation damage skin, but not for zero-perforation skin.

Hsia and Behrmann⁶ performed experimental tests to determine the minimum underbalance necessary to obtain zero-perforation damage skin. Single-shot perforation flow tests were conducted in nominally 100 md and 200 md sandstone cores under various underbalance pressure conditions. Prior to the perforation, the virgin whole core diametral and axial permeabilities were measured. Perforation damage skin was determined using analytical and finite elements models.

From the perforation experimental tests, Hsia and Behrmann presented the upper and lower bound underbalance pressure requirement, as shown in Equations 2.6 and 2.7, for zero-perforation skin for fluid properties similar to King's field data.

$$\Delta p_{\text{Upper bound}}, \quad \Delta p_{\text{upper}} = \frac{5.06 \times 10^4}{k^{0.913}} \quad [2.6]$$

$$\Delta p_{\text{Lower bound}}, \quad \Delta p_{\text{lower}} = \frac{1.7 \times 10^4}{k^{0.7}} \quad [2.7]$$

King's filed study and Hsia and Behrmann experimental tests were based on sandstone formation only. Since all gas reservoirs of interest in this study are sandstone formation, their equations can be used to compare with Gulf of Thailand data.

Not only the underbalance pressure, the combination of perforation gun assembly also affect the reservoir productivity and degree of reservoir damage. The Following perforation gun assemblies are generally used in the Gulf of Thailand petroleum industry.

- a. Gun size - 1.56", 2", 2.5"
- b. Charge Type - PowerJet Plus, Predator, Predator XP, Owen HERO
- c. Shot Density - 2, 4, 5, or 6 shot per foot
- d. Phasing - 0, 60, 180 phasing degree
- e. Explosive - HMX, HTX, HNS

2.2 Pressure Transient (Well Test) Analysis

A pressure transient (well test), in its simplest form, consists of disturbing the reservoir by producing from or injecting into a well at a controlled flow rate for a period of time and measuring the pressure response at the production or injection well, or at some nearby observation well. The pressure response, which depends on the reservoir rock and fluid properties, is then analyzed for reservoir parameters.

One of the main objective of pressure transient analysis is to determine the skin around wellbore which may be caused by wellbore damage, partial penetration, perforation, turbulence flow, etc. However, skin obtained from pressure transient analysis is the total skin of the area near the wellbore. To identify whether the reservoir is damaged and needs well cleaning or well-stimulation treatments, the total skin have to be subtracted by skin due to other factors, such as partial penetration skin, non-Darcy skin, etc.

For reservoir evaluation, there are several types of well test, such as drawdown, buildup, injection, falloff. In a drawdown test (Figure 2.3), a well that shut-in is opened to flow. For the purposes of traditional analysis, the flow rate is controlled to be as constant as possible. In a buildup test (Figure 2.4), a well which is already flowing (ideally at constant rate) is shut-in, and the downhole pressure is measured as the pressure builds up. In this study, most of pressure transient tests are buildup tests.

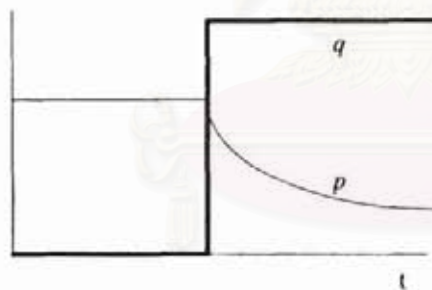


Figure 2.3: Drawdown test.

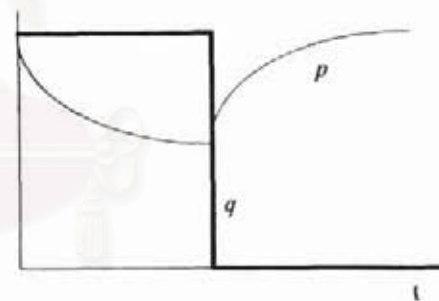


Figure 2.4: Buildup test.

2.3 Skin

It is well known that the properties of the reservoir near the wellbore are usually altered during drilling, completion, and stimulation procedures. The invasion of drilling fluids, the presence of mudcakes and cement, partial penetration of the formation, and insufficient perforation density are some of the factors that cause "damage" to the formation and, more importantly, cause an additional localized pressure drop during flow.

Skin is the term used to refer to the alteration of permeability that exists near the wellbore. The skin factor, S , is used to quantify the skin. If the well has been damaged, there is an additional pressure drop at the wellbore for a given flow rate and the skin factor is positive. If the well has been stimulated and the pressure drop at the wellbore has been decreased, the skin factor is negative. As stated in the previous section, the total skin can be determined by pressure transient analysis. However, other technique or correlation is required to determine other skin factors caused by turbulent flow and partial penetration.

2.3.1 Rate Dependent (Non-Darcy) Skin

For gas which has low viscosity, turbulent or non-Darcy flow may occur in the vicinity of the wellbore and cause the rate dependent skin effect. To determine the rate dependent or Non-Darcy skin ($S_{non-Darcy}$), a multi rate or flow after flow well test (Figure 2.5) must be performed and analyzed.

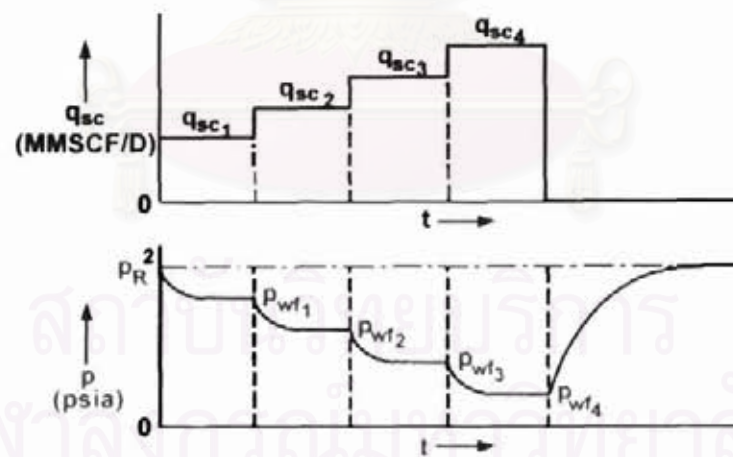


Figure 2.5: Flow after flow well test.

The total skin at a particular flow rate can be determined from pressure transient analysis of that flow period. The plot between the total skin and flow rate yields a straight line as shown in Figure 2.4. The linear equation of total skin and flow rate is as follows:

$$S = S' + Dq_{sc} \quad [2.8]$$

where

S = total skin (interpreted result from well test analysis)

S' = skin due to other factors

D = Rate dependent skin coefficient

q_{sc} = flow rate

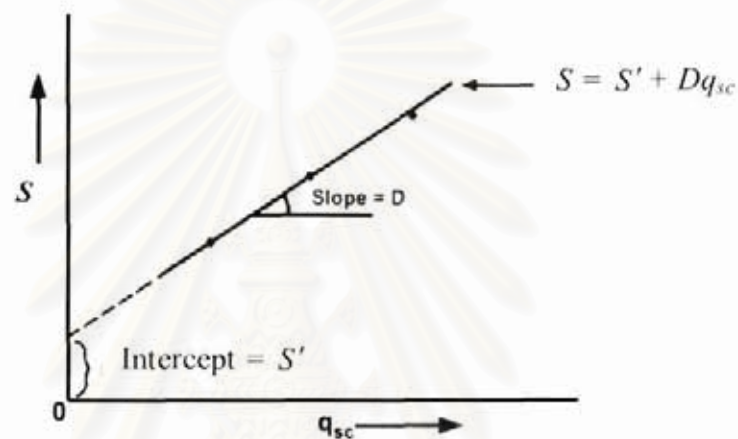


Figure 2.6: Total skin versus flow rate.

2.3.2 Partial Penetration Skin (S_{pp})

Partial completion or perforation of gas wells to inhibit the water coning has been a common practice in the petroleum industry for many years. However, partial perforation of a well will force the flow near the wellbore to converge with high velocity towards the perforations, resulting in flow turbulence and spherical flow which incurs the higher pressure loss in the formation and hence the deviation from the ideal Darcy' flow occur.

Numerous studies, based on a variety of assumptions, have investigated the theoretical pressure response, productivity, and additional skin called partial penetration skin (S_{pp}) of such well. Common correlations used to compute the partial penetration skin (S_{pp}) are summarized as follows:

1. Brons and Marting¹¹

Brons and Marting expressed the additional kind of productivity impairment or partial penetration skin (S_{pp}). They presented the following equation for estimation, regardless the location of the perforated interval on the formation.

$$S_{pp} = \left(\frac{1}{b} - 1\right) [\ln h_D - G(b)] \quad [2.9]$$

where

$$G(b) = 2.948 - 7.363b + 11.45b^2 - 4.675b^3$$

$$h_D = \frac{h}{r_w} \sqrt{\frac{k_h}{k_v}}, \text{ dimensionless pay thickness}$$

$$b = \frac{h_p}{h}, \text{ penetration ratio}$$

$$h = \text{reservoir pay thickness (ft)}$$

$$r_w = \text{wellbore radius (ft)}$$

$$h_p = \text{limited interval open to flow (ft)}$$

$$k_h = \text{horizontal permeability (md)}$$

$$k_v = \text{vertical permeability (md)}$$

2. Odeh¹²

Odeh stated that the location of the perforated interval is usually dictated by formation characteristics and reservoir behavior. Therefore, by considering the location of perforated interval of formation, Odeh suggested the Equation 2.10 to determine the partial penetration skin (S_{pp}):

$$S_{pp} = 1.35 \left(\frac{1}{b} - 1\right)^{0.825} \left[\ln(r_w h_D + 7) - 1.95 - [0.49 + 0.1 \ln(r_w h_D)] \ln r_{wc} \right] \quad [2.10]$$

where

$$r_{wc} = r_w e^{0.2126 \left(2.753 + \frac{z_m}{h}\right)}, \quad 0 < \frac{z_m}{h} < 0.5$$

$$r_{wc} = r_w \quad \text{if } y = 0$$

$$z_m = y + \frac{h_p}{2}$$

y = distance from the top of formation to the top of perforated interval

If $\frac{z_m}{h}$ is greater than 0.5, then use $1 - \frac{z_m}{h}$ instead.

In this study, all reservoirs of interest were perforated at the topmost part; as a result, all y values are zero. So, Equation 2.5 can be rewritten as the Equation 2.11:

$$S_{pp} = 1.35 \left(\frac{1}{b} - 1 \right)^{0.825} \left[\ln(r_w h_D + 7) - 1.95 - [0.49 + 0.1 \ln(r_w h_D)] \ln r_w \right] \quad [2.11]$$

3. Papatzacos¹³

Papatzacos presented Equation 2.12 to determine the partial penetration skin. The equation was derived based on an infinite-conductivity well in an infinite reservoir.

$$S_{pp} = \left(\frac{1}{b} - 1 \right) \ln \left(\frac{\pi h_D}{2} \right) + \frac{1}{b} \ln \left[\frac{b}{2+b} \left(\frac{A-1}{B-1} \right)^{1.2} \right] \quad [2.12]$$

where

$$A = \frac{1}{\left(\frac{y}{h} \right) + \frac{b}{4}}$$

$$B = \frac{1}{\left(\frac{y}{h} \right) + \frac{3b}{4}}$$

As previously mentioned, all y values in this study are zero because all reservoirs were perforated at the topmost part. So, the equations to calculate A and B can be rewritten as follows:

$$A = \frac{1}{0.25b} = \frac{h}{0.25h_p}$$

$$B = \frac{1}{0.75b} = \frac{h}{0.75h_p}$$

4. Yeh and Reynolds¹⁴

Yeh and Reynolds showed the general equation to determine the partial penetration skin (S_{pp}) for either single or multilayer reservoirs:

$$S_{pp} = \left(\frac{1-f_1}{f_1} \right) \ln(h_{wD}) \quad [2.13]$$

where

$$f_1 = \frac{\bar{k}_p h_p}{kh}, \text{ dimensionless flow capacity}$$

$$\bar{k}_p = \frac{1}{h_p} \sum_{j=n_o}^{m_o} k_j h_{pj}, \text{ thickness-average horizontal permeability}$$

of open interval

$$\bar{k} = \frac{1}{h} \sum_{j=1}^m k_j h_j, \text{ thickness-average horizontal permeability}$$

$$k_j = \text{horizontal permeability of layer } j$$

$$h_{wD} = \frac{C' f_1 (1-f_1) h_D}{\exp(C_1)}, \text{ dimensionless wellbore length}$$

$$C_1 = 0.481 + 1.01(f_1) - 0.838(f_1)^2$$

$$C' = \text{correlating coefficient that can be obtain from Figure 2.7}$$

$$\Delta z_D = \text{dimensionless distance from top of open interval to top of reservoir}$$

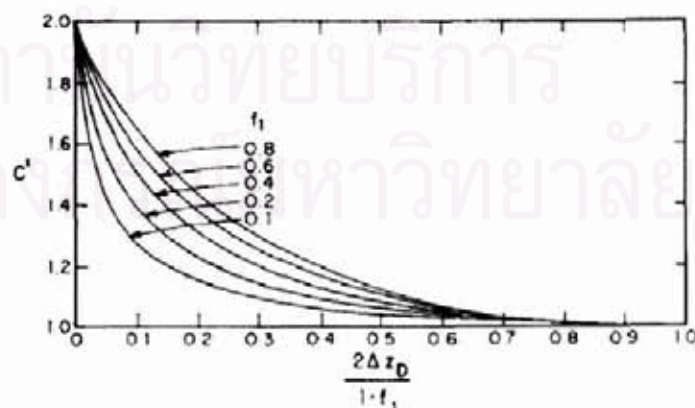


Figure 2.7: Yeh and Reynolds' correlation for C' – multilayer reservoir.

However, for single-layer reservoirs, many parameters can be simplified: $f_1 = b = \frac{h_p}{h}$, $\Delta z_D = 0$, $C' = 2$

Thus, Yeh and Reynolds partial penetration skin correlation can be rewritten as follows:

$$S_{pp} = \left(\frac{1-b}{b} \right) \ln h_{wD} \quad [2.14]$$

where

$$h_{wD} = \frac{2b(1-b)h_D}{\exp(C_1)}$$

$$C_1 = 0.481 + 1.01(b) - 0.838(b)^2$$

Since this study is considering only single reservoir, Equation 2.14 was used to estimate the partial penetration skin.

2.3.3 Perforation Skin and Flow Efficiency

The damage or skin around the perforations could be quantified indirectly by means of flow efficiency (FE).

$$FE = \frac{\Delta p_{zero\ skin}}{\Delta p_{total}} = \frac{q_{actual\ skin}}{q_{zero\ skin}} \quad [2.15]$$

In order to evaluate different perforation strategies, the pressure drop due to skin will be corrected by subtracting pressure drop due to skin caused by non-Darcy flow and partial penetration.

$$corrected\ FE = \frac{\Delta p_{zero\ skin}}{\Delta p_{corrected\ skin}} = \frac{q_{corrected\ skin}}{q_{zero\ skin}} \quad [2.16]$$

where

$$Corrected\ Skin = Skin_{total} - Skin_{non-Darcy} - Skin_{partial\ penetration} \quad [2.17]$$

However, rather than non-Darcy and partial penetration skins, other skins caused by other factors are unknown and assumed to be the same for all wells. Thus, the corrected flow efficiency could be relatively compared and used to evaluate the perforation strategies. In this study, the corrected skin is called perforation skin.



สถาบันวิทยบริการ
จุฬาลงกรณ์มหาวิทยาลัย

CHAPTER III

EVALUATION OF PERFORATION STRATEGIES OF GAS WELLS IN THE GULF OF THAILAND

In this study, data from 70 gas reservoirs penetrated by 70 gas wells were used for perforation evaluation. The reservoir properties of these sands vary in a wide range as detailed in Table 3.1. The subsea vertical depths of these sands vary from 5216 feet to 9563 feet with sand thickness in a range between 5 and 92 feet vertical depth. Porosity and water saturation are in the range of 13 to 28% and 10 to 62%, respectively. Figures 3.1 and 3.2 show the histogram of reservoir porosity and water saturation, respectively. The mean and the standard deviation of porosity are 18.67 and 3.16, respectively, while the mean and the standard deviation of water saturation are 39.9 and 12.2, respectively.

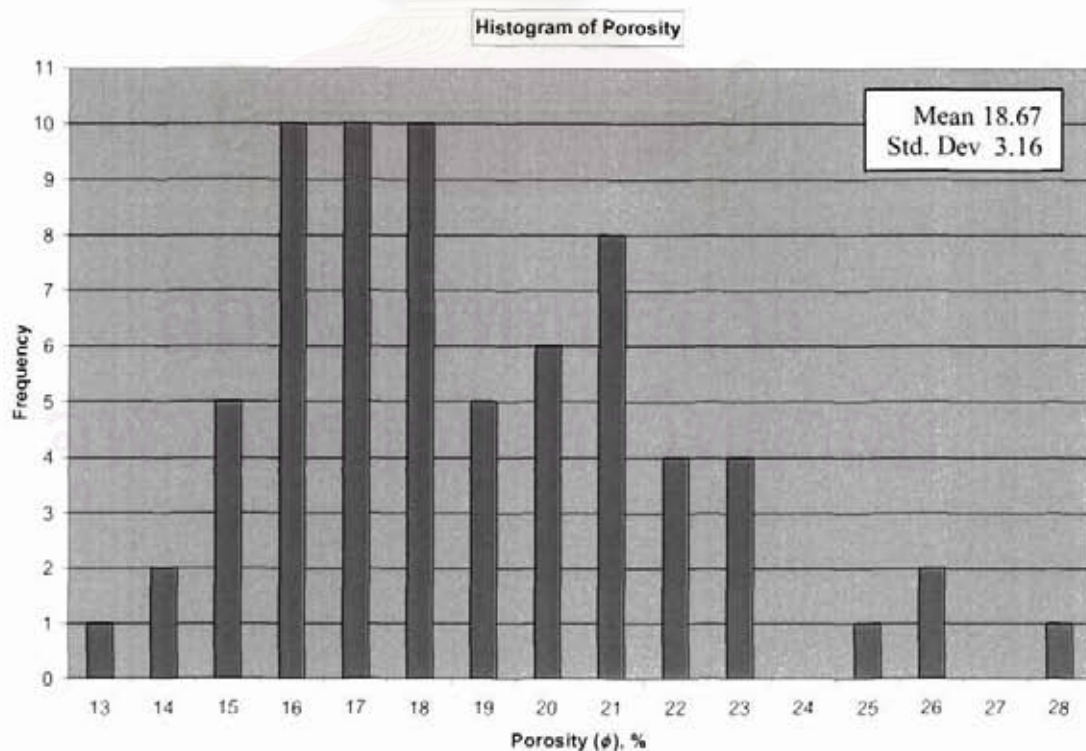


Figure 3.1 Histogram of porosity.

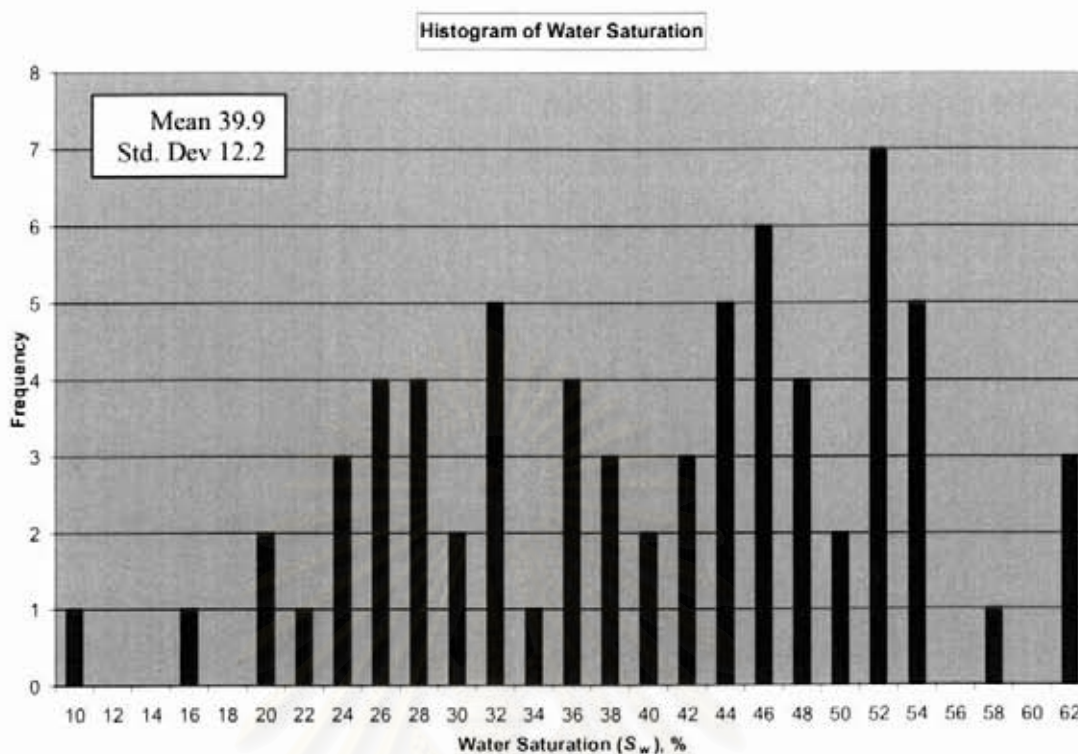


Figure 3.2 Histogram of water saturation.

The reservoir initial pressure can be obtained from either Repeated Formation Tester (*RFT*) or interpretation results from pressure transient analysis, which are presented in Table 3.1. For the condition inside wellbore, the pressure can be estimated from completion fluid gradient and completion fluid level.

For gas wells in the Gulf of Thailand, the completion fluid is typically brine with 3% Potassium Chloride (KCL), with a density of 8.6 pound per gallon. However, saline oil based completion fluid is used in some cases to lower the hydrostatic pressure, especially in oil wells. Thus, prior to perforation, the wellbore pressure (p_w) can be estimated by hydrostatic pressure caused by completion fluid.

Figure 3.3 illustrates the Gulf of Thailand's pressure profile, 3% Potassium Chloride (KCL) completion fluid gradient at 8.6 ppg, and initial pressure of 70 gas reservoirs chosen for this study. All red points in Figure 3.3 are the initial reservoir pressures obtained from Repeated Formation Tester (*RFT*). Some reservoirs were depleted by existing wells prior to pressure measurement. The black dash line shows the upper limit of the initial reservoir pressure of gas reservoirs in the Gulf of

Thailand. For the gas reservoirs that have initial pressure on the right hand side of the completion fluid gradient at 8.6 ppg ($P_i > P_w$), the perforation can be performed with the natural existing of underbalance pressure. However, for the gas reservoirs that have initial pressure on the left hand side of the completion fluid gradient at 8.6 ppg ($P_i < P_w$), additional work prior to perforation is required to achieve the underbalance pressure condition.

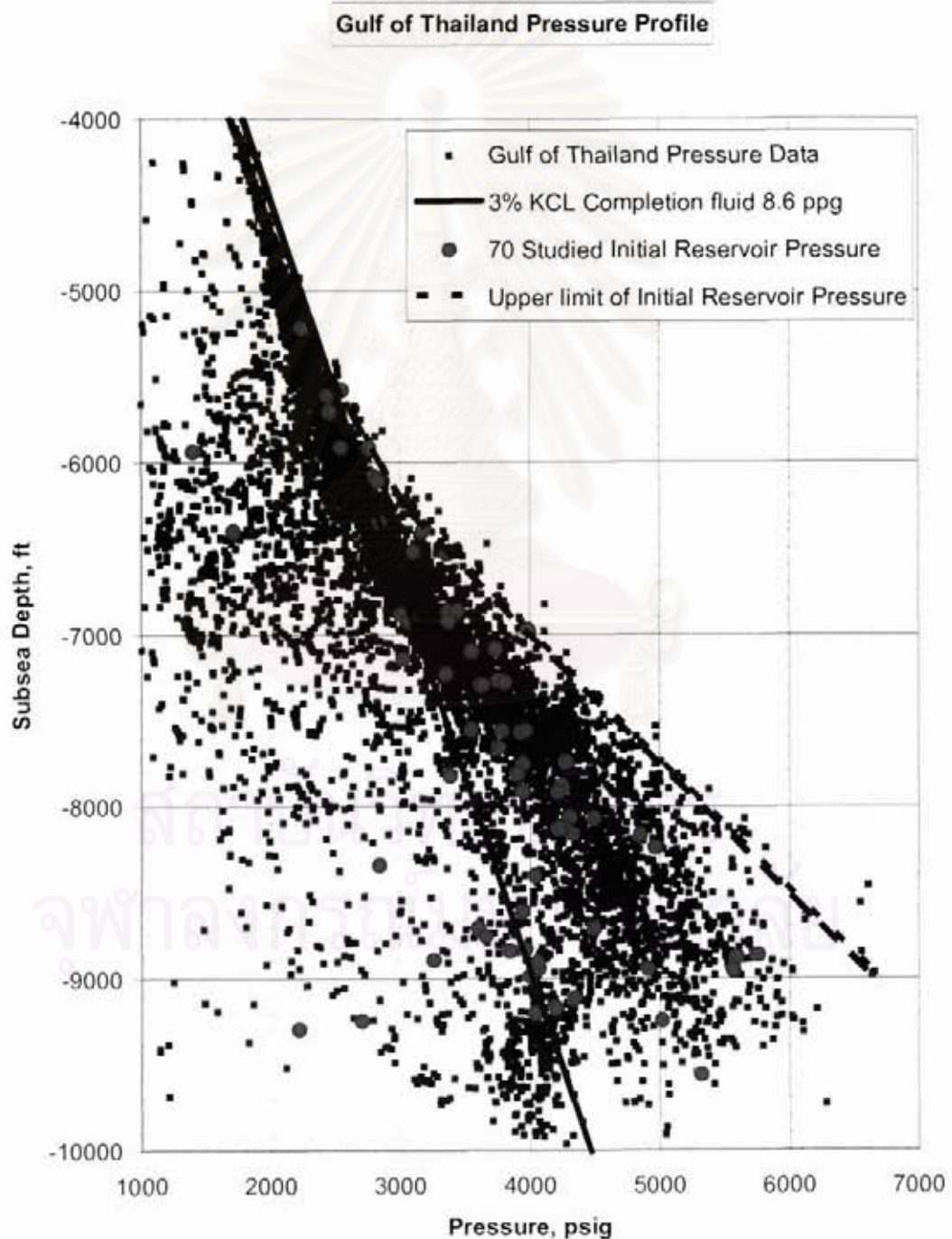


Figure 3.3: Gulf of Thailand pressure profile.

Table 3.1: Gas reservoir properties.

Well	Res. Name	Gas Reservoir Properties						
		Res. depth, TVD ft	RFT Initial Res. Pressure, psi	PBU, Initial Res. Pressure, psi	Thickness		Porosity, %	Sw, %
					ft MD	ft TVD		
Well-01	68-8	6884	3,010	2,901	8	5	13	58
Well-02	82-4	8240	4,966	4,780	27	22	16	62
Well-03	92-4	9243	none	5,017	20	18	13	30
Well-04	95-6	9563	none	5,320	13	10	16	39
Well-05	75-6	7560	none	3,790	37	27	18	45
Well-06	69-2	6920	3,070	2,721	25	20	20	26
Well-07	81-7	8170	4,852	4,254	18	10	17	38
Well-08	63-4	6343	2,840	2,835	51	41	22	28
Well-09	89-5	8952	5,568	5,504	16	11	17	46
Well-10	52-2	5216	none	2,238	63	45	28	23
Well-11	55-8	5581	2,553	2,514	68	54	21	10
Well-12	56-1	5612	none	2,440	64	53	26	32
Well-13	59-1	5911	none	2,545	25	23	26	16
Well-14	72-7	7266	none	3,757	41	28	18	44
Well-15	75-5	7553	none	3,555	57	49	20	52
Well-16	60-8	6082	none	2,799	61	47	25	23
Well-17	59-2	5916	none	2,764	70	52	21	41
Well-18	61-0	6104	none	2,826	37	28	23	31
Well-19	81-6	8159	4,334	4,334	27	20	15	52
Well-20	72-9	7292	none	3,629	31	22	21	25
Well-21	73-0	7296	none	3,640	26	19	17	50
Well-22	78-2	7822	none	3,389	52	38	23	37
Well-23	59-4	5938	none	1,404	23	19	21	36
Well-24	88-3	8832	none	3,964	52	37	22	47
Well-25	71-0	7098	none	3,555	42	32	18	52
Well-26	65-3	6528	3,360	3,261	82	60	19	30
Well-27	57-0	5704	2,453	2,209	47	28	17	47
Well-28	80-6	8063	none	4,315	45	28	15	45
Well-29	92-5	9246	none	2,705	27	22	21	19
Well-30	88-4	8842	none	3,842	33	25	19	32
Well-31	86-1	8611	none	3,946	38	23	20	52
Well-32	84-0	8404	none	4,014	46	34	15	53
Well-33	78-8	7880	4,257	4,047	61	42	17	54
Well-34	92-9	9293	none	2,220	63	50	17	36
Well-35	87-1	8708	none	4,500	35	24	16	54
Well-36	91-7	9170	4,202	3,997	32	11	14	31
Well-37	64-0	6399	none	1,712	38	34	22	25
Well-38	89-9	8988	3,998	3,619	42	34	23	27
Well-39	87-1	8710	none	3,604	78	45	19	35
Well-40	83-4	8344	none	2,843	29	25	20	49
Well-41	69-8	6978	none	3,989	48	40	23	43
Well-42	77-5	7754	3,952	3,853	15	13	16	48
Well-43	75-7	7568	none	3,938	25	20	18	62
Well-44	79-2	7916	none	3,949	46	20	22	52
Well-45	80-7	8068	none	4,499	32	26	17	28
Well-46	88-6	8864	none	5,756	78	59	16	46
Well-47	77-4	7742	4,288	4,266	28	24	21	40
Well-48	76-6	7660	none	3,765	24	20	19	36
Well-49	79-2	7917	none	4,223	42	36	18	54
Well-50	68-7	6865	none	3,372	62	49	18	24
Well-51	72-8	7276	none	3,811	44	27	17	42
Well-52	68-6	6860	none	3,447	78	58	16	32
Well-53	91-1	9114	4,346	4,293	35	27	16	33
Well-54	89-4	8943	none	4,070	74	31	15	20
Well-55	89-1	8906	4,062	4,000	30	22	21	26
Well-56	75-6	7560	none	3,972	49	32	16	52
Well-57	87-6	8757	3,663	3,555	120	92	19	22
Well-58	88-9	8894	none	3,258	49	32	16	57
Well-59	88-8	8877	none	5,596	68	45	18	45
Well-60	69-2	6921	none	3,376	56	41	17	51
Well-61	78-2	7815	none	3,908	49	30	20	42
Well-62	70-8	7084	none	3,738	75	56	20	54
Well-63	81-2	8121	none	4,259	29	16	15	62
Well-64	92-0	9199	none	4,053	55	43	18	43
Well-65	89-5	8946	none	4,913	48	42	14	38
Well-66	64-0	6397	3,178	3,142	78	61	21	28
Well-67	81-3	8130	none	4,230	23	19	18	46
Well-68	71-4	7141	none	3,024	41	32	17	43
Well-69	72-3	7228	3,357	3,073	52	42	18	48

3.1 Perforation of Gas Wells

In the Gulf of Thailand, the underbalance pressure perforation technique is commonly applied, in order to achieve the lower completion or perforation skin. The lower skin helps maximize the production rate and also reduce the abandonment pressure, resulting in a higher recovery efficiency. The underbalance condition can be achieved by:

1. **Swabbing** fluid out of the well by the wireline swabbing cup, lowering the fluid column, as a result, lowering the hydrostatic pressure on the reservoir face.
2. **Displacing with low density** of completion fluid (sarlaline, base oil), to lower the hydrostatic pressure on the reservoir face.
3. **Flowing the well** by opening the choke and drawing the pressure down in the wellbore.
4. **Leaving the naturally existing underbalance** when $P_{Reservoir} > P_{Wellbore}$
5. **Injecting gas (N₂ or produced gas) to lift** into annulus and unloading completion fluid via gas lift valve. This method is typically applied in oil wells.

To obtain the desired underbalance condition, the swabbing technique seems to be the most popular choice comparing to others since it is the cheapest and fastest execution. However, the wireline unit is capable of swabbing liquid down to a certain level, depending on well deviation, due to tension limitation. If the desired depth is deeper than the limit, a coiled tubing unit might be required for gas lifting which is more expensive.

Table 3.2 contains the data related to swabbing operation and perforation for all 70 wells chosen in this study. All wells were filled with 3% KCL completion fluid which exerts a hydrostatic weight of 8.6 ppg.

All wells were perforated with underbalance pressure varying from 185 to 1792 psi, with an average of 865 psi. Fifty wells out of seventy wells achieved the

underbalance condition by swabbing at depth between 500 to 6100 feet (measured depth). The completion fluids of other twenty wells were not swabbed out; however, the underbalance conditions were still achieved due to naturally existing underbalance condition.

Speaking of gun assembly, charge type is the only parameter that has sufficient variation of data for evaluation. Other parameters such as gun size, slot density, phasing, and explosive cannot be evaluated because the ranges of the data values are too narrow.

Fifteen gas reservoirs out of seventy were perforated full-to-base without any gap. These fifteen wells were completed using an old fashion strategy based on the idea of lowering the pressure drop across the sand face as much as possible in order to maximize the recovery. However, many operators in the Gulf of Thailand experienced many problems, especially water shut-off related issues, in full-to-base perforated gas reservoirs. The longer the perforated interval, the more difficulty the water shut-off can be performed.

To shut the water off, the long perforated interval may require expensive chemical treatment, such as cement squeeze or polymer treatment, instead of cheaper mechanical shut-off, such as permanent or retrievable tubing patch.

The other fifty five gas reservoirs out of seventy were partially perforated. At this moment, partial perforation now becomes the best practice for all gas wells in the Gulf of Thailand. The short interval of partial perforation eliminates or reduces the difficulty for future remedial well work, especially water shut-off. However, this partial perforation causes an additional skin, called partial penetration skin, as mentioned in the previous chapter.

Table 3.2: Swabbing depths and perforation information.

Well	Res. Name	Swabbing Depth, ft		Under balance pressure, psi	Gun Assembly					Perforated Interval	
		measured depth, ft	true vertical depth, ft		Gun size, inch	Charge Type	Shot Density	Phasing	Explosive	ft MD	ft TVD
Well-01	68-8	5,600	3,558	1523	2-1/8"	Predator XP	6	60	HMX	8	5.0
Well-02	82-4	0	0	1281	2-1/8"	Power Jet	6	60	HMX	15	12.2
Well-03	92-4	0	0	884	2-1/8"	Power Jet	4	60	HMX	10	9.0
Well-04	95-6	0	0	1043	2-1/8"	Power Jet	4	60	HMX	6	4.6
Well-05	75-6	2050	1516	1087	2-1/8"	Owen Hero	6	60	HMX	24	17.5
Well-06	69-2	4030	2673	1171	2-1/8"	Owen Hero	6	60	HMX	20	16.0
Well-07	81-7	0	0	1198	2-1/8"	Owen Hero	6	60	HMX	14	7.8
Well-08	63-4	1,250	1,164	524	2-1/8"	Predator	6	60	HMX	9	7.2
Well-09	89-5	0	0	1565	2-1/8"	Power Jet	6	60	HMX	9	6.2
Well-10	52-2	1,000	982	344	2-1/8"	Predator	5	60	HMX	9	6.4
Well-11	55-8	1,200	1,200	594	2-1/8"	Predator	5	60	HMX	40	31.8
Well-12	56-1	1,160	1,157	447	2-1/8"	Predator	6	60	HMX	9	7.5
Well-13	59-1	1,200	1,168	424	2-1/8"	Power Jet	6	60	HMX	18	16.6
Well-14	72-7	1,044	993	951	2-1/8"	Power Jet	6	60	HMX	29	19.8
Well-15	75-5	5,000	3,104	1565	2-1/8"	Power Jet	6	60	HMX	40	34.4
Well-16	60-8	1,250	1,215	622	2-1/8"	Power Jet	6	60	HMX	61	47.0
Well-17	59-2	1,200	1,195	653	2-1/8"	Power Jet	6	60	HMX	44	32.7
Well-18	61-0	1,160	1,160	615	2-1/8"	Power Jet	6	60	HMX	27	20.4
Well-19	81-6	0	0	685	2-1/8"	Power Jet	6	60	HMX	20	14.8
Well-20	72-9	2057	1707	1131	2-1/8"	Power Jet	6	60	HMX	31	22.0
Well-21	73-0	0	0	377	2-1/8"	Power Jet	6	60	HMX	15	11.0
Well-22	78-2	974	959	320	2-1/8"	Predator	5	60	HMX	36	26.3
Well-23	59-4	5,500	3,658	385	2-1/8"	Power Jet	6	60	HMX	18	14.9
Well-24	88-3	1,021	1,021	471	2-1/8"	Power Jet	6	60	HMX	20	14.4
Well-25	71-0	1,200	1,092	869	2-1/8"	Predator	5	60	HMX	9	6.9
Well-26	65-3	3,060	2,213	1430	2-1/8"	Owen Hero	6	60	HMX	20	14.6
Well-27	57-0	1,200	1,000	349	2-1/8"	Owen Hero	6	60	HMX	5	3.0
Well-28	80-6	0	0	709	2-1/8"	Power Jet	6	60	HMX	30	18.7
Well-29	92-5	5,500	3,835	285	2-1/8"	Predator	5	60	HMX	18	14.7
Well-30	88-4	1,010	1,004	337	2"	Predator	5	60	HNS	18	13.6
Well-31	86-1	1,000	982	535	2-1/8"	Power Jet	6	60	HMX	38	23.0
Well-32	84-0	1,300	1,246	843	2-1/8"	Predator	5	60	HMX	46	34.0
Well-33	78-8	720	718	1054	2-1/8"	Owen Hero	6	60	HMX	30	20.7
Well-34	92-9	5,500	4,743	185	2"	Predator	5	60	HNS	14	11.1
Well-35	87-1	0	0	606	2-1/8"	Power Jet	6	60	HMX	20	13.7
Well-36	91-7	3,320	3,183	1525	2-1/8"	Power Jet	6	60	HMX	32	11.0
Well-37	64-0	5,500	4,765	982	2-1/8"	Power Jet	6	60	HMX	30	26.8
Well-38	89-9	4,150	3,453	1523	2-1/8"	Predator XP	6	60	HMX	10	8.1
Well-39	87-1	6,100	3,561	1301	2-1/8"	Predator XP	6	60	HMX	45	26.0
Well-40	83-4	5,000	3,229	555	2-1/8"	Predator	5	60	HMX	20	17.2
Well-41	69-8	1,065	1,024	1327	2-1/8"	Predator	5	60	HMX	9	7.5
Well-42	77-5	2,800	2,307	1516	2-1/8"	Owen Hero	6	60	HMX	7	6.1
Well-43	75-7	0	0	554	2-1/8"	Predator	6	60	HMX	25	20.0
Well-44	79-2	1,000	996	855	2-1/8"	Predator	6	60	HMX	46	20.0
Well-45	80-7	550	548	1137	2-1/8"	Predator	5	60	HMX	20	16.3
Well-46	88-6	0	0	1792	2-1/8"	Power Jet	6	60	HMX	30	22.7
Well-47	77-4	2000	1702	1587	2-1/8"	Power Jet	6	60	HMX	21	18.0
Well-48	76-6	2010	1711	1105	2-1/8"	Predator	5	60	HMX	18	15.0
Well-49	79-2	2020	1726	1454	2-1/8"	Predator	5	60	HMX	27	23.1
Well-50	68-7	0	0	302	2-1/8"	Owen Hero	6	60	HMX	18	14.2
Well-51	72-8	2000	1724	1328	2-1/8"	Predator XP	6	60	HMX	8	4.9
Well-52	68-6	1000	944	801	2-1/8"	Predator XP	6	60	HMX	9	6.7
Well-53	91-1	3500	2397	1342	1-9/16"	Predator XP	6	60	HMX	8	6.2
Well-54	89-4	3500	3170	1488	1-9/16"	Predator XP	6	60	HMX	40	16.8
Well-55	89-1	2100	2000	974	1-9/16"	Predator XP	6	60	HMX	10	7.3
Well-56	75-6	0	0	591	2-1/8"	Power Jet	6	60	HMX	10	6.5
Well-57	87-6	2000	1998	640	2-1/8"	Power Jet	6	60	HMX	80	61.3
Well-58	88-9	2500	2231	279	2-1/8"	Power Jet	6	60	HMX	49	32.0
Well-59	88-8	0	0	1626	2-1/8"	Power Jet	6	60	HMX	30	19.9
Well-60	69-2	0	0	280	2-1/8"	Power Jet	6	60	HMX	56	41.0
Well-61	78-2	500	500	637	2-1/8"	Power Jet	6	60	HSD	49	30.0
Well-62	70-8	0	0	570	2-1/8"	Power Jet	4	60	HMX	75	56.0
Well-63	81-2	0	0	627	2-1/8"	Power Jet	6	60	HSD	29	16.0
Well-64	92-0	2500	2076	867	2-1/8"	Power Jet	6	60	HSD	55	43.0
Well-65	89-5	0	0	912	2-1/8"	Predator	5	60	HMX	40	35.0
Well-66	64-0	0	0	317	2-1/8"	Power Jet	6	60	HMX	40	31.3
Well-67	81-3	1000	980	1033	2-1/8"	Power Jet	6	60	HMX	8	6.6
Well-68	71-4	1500	1381	449	2-1/8"	Predator	6	60	HMX	27	21.1
Well-69	72-3	3000	2054	1043	2-1/8"	Predator	6	60	HMX	41	33.1
Well-70	65-2	0	0	191	2-1/8"	Predator	6	60	HMX	24	11.0

3.2 Pressure Transient (Well Test) Analysis

To evaluate the perforation strategies of gas wells in the Gulf of Thailand, seventy pressure transient tests were interpreted for permeability, total skin, non-Darcy skin coefficient, and pressure drop due to skin. The results from these pressure transient analyses were then used along with other parameters, such as gas reservoir properties and underbalance condition, for perforation evaluation.

In this study, PanSystem version 3.1.1 software was used for all seventy pressure transient analyses. Suitable models were chosen based on the characteristic of the pressure responses. Rate dependent skin coefficient (D) can also be incorporated, by trial and error, into each model for better matching between actual and model pressure responses. The trial and error was performed by changing the Rate Dependent Skin Coefficient in order to match pressure transient data acquired in different flow periods. However, the rate dependent skin factor sometimes cannot be simply obtained from the trial and error approach. In this case, the rate dependent skin plot is required for Rate Dependent Skin Coefficient determination.

The details of pressure transient analysis, including test overview, log-log and semi-log plots, and rate dependent skin plot (if available), of each perforated gas reservoir is presented in Appendix A. The summary of interpreted results of all pressure transient analyses is presented in Table 3.3.

In addition, by using the total pressure drop and pressure drop due to total skin from the pressure transient analysis, the flow efficiency then can be calculated. These results are shown in Table 3.3. These flow efficiencies were calculated based on total skin. So, these flow efficiencies do not represent perforation performance of gas wells.

Table 3.3: Results of pressure transient analyses.

Well	Res. Name	Pressure Transient Analyses								Flow Efficiency, %
		Main Gas Flow Rate, MMsct/d	Permeability (k), md	Total Skin	Non-Darcy		Initial Pressure, psi	Total Pressure Drop, psi	Pressure Drop from Total Skin, psi	
					Coefficient, 1/(Mscf/day)	Skin				
Well-01	68-8	0.40	1.65	0.52	0.00000	0.0	2,901	1,598	117	93%
Well-02	82-4	4.86	2.98	4.97	0.00000	0.0	4,780	3,277	1,552	53%
Well-03	92-4	1.05	1.77	21.43	0.00000	0.0	5,017	3,727	2,923	22%
Well-04	95-6	0.85	2.29	19.50	0.00000	0.0	5,320	3,911	2,905	26%
Well-05	75-6	6.66	9.07	8.67	0.00030	2.0	3,790	2,714	922	66%
Well-06	69-2	6.02	16.60	3.05	0.00025	1.5	2,721	801	253	68%
Well-07	81-7	3.03	4.30	3.60	0.00003	0.1	4,254	3,090	1,268	59%
Well-08	63-4	13.10	520.00	101.13	0.00310	40.6	2,835	239	224	6%
Well-09	89-5	7.03	9.06	6.89	0.00015	1.0	5,504	3,277	1,697	48%
Well-10	52-2	12.00	850.00	104.00	0.00621	74.5	2,238	132	122	7%
Well-11	55-8	15.70	250.00	6.60	0.00005	0.8	2,514	67	27	59%
Well-12	56-1	14.80	850.00	45.30	0.00026	3.8	2,440	91	59	35%
Well-13	59-1	14.40	700.00	23.00	0.00000	0.0	2,545	222	79	65%
Well-14	72-7	11.70	28.00	17.50	0.00060	7.0	3,757	1,187	787	34%
Well-15	75-5	13.25	100.00	16.20	0.00142	18.8	3,555	220	145	34%
Well-16	60-8	15.00	160.00	2.20	0.00020	3.0	2,799	77	23	70%
Well-17	59-2	14.80	152.80	5.50	0.00000	0.0	2,764	105	29	72%
Well-18	61-0	13.30	123.00	5.80	0.00024	3.2	2,826	198	84	58%
Well-19	81-6	3.00	100.00	10.00	0.00000	0.0	4,334	90	48	46%
Well-20	72-9	9.10	8.90	-0.95	0.00000	0.0	3,629	1,252	232	119%
Well-21	73-0	6.64	18.34	15.00	0.00000	0.0	3,640	1,781	1,356	74%
Well-22	78-2	9.12	70.00	2.00	0.00000	0.0	3,389	168	20	88%
Well-23	59-4	4.75	80.00	6.60	0.00000	0.0	1,404	297	115	61%
Well-24	88-3	9.10	14.00	14.30	0.00000	0.0	3,964	1,458	904	38%
Well-25	71-0	8.80	13.00	14.25	0.00000	0.0	3,555	1,698	1,167	31%
Well-26	65-3	13.60	40.00	23.80	0.00000	0.0	3,261	630	463	27%
Well-27	57-0	3.51	65.00	135.00	0.00000	0.0	2,209	1,409	1,344	5%
Well-28	80-6	1.40	1.66	16.86	0.00000	0.0	4,315	3,624	2,658	27%
Well-29	92-5	7.66	130.73	5.43	0.00004	0.3	2,705	190	57	70%
Well-30	88-4	8.71	15.10	8.90	0.00000	0.0	3,842	1,676	784	53%
Well-31	86-1	8.55	83.00	1.00	0.00000	0.0	3,946	360	14	96%
Well-32	84-0	0.82	0.17	2.40	0.00000	0.0	4,044	2,975	1,378	54%
Well-33	78-8	3.50	1.86	7.07	0.00000	0.0	4,047	2,920	1,578	46%
Well-34	92-9	5.45	80.00	127.71	0.00050	2.7	2,220	1,035	967	7%
Well-35	87-1	5.00	70.00	10.00	0.00000	0.0	4,500	169	94	44%
Well-36	91-7	4.20	7.69	-2.20	0.00000	0.0	3,997	2,088	569	127%
Well-37	64-0	4.05	81.68	3.10	0.00000	0.0	1,712	78	22	72%
Well-38	89-9	14.48	200.00	13.60	0.00000	0.0	3,619	342	114	67%
Well-39	87-1	13.93	50.00	1.40	0.00000	0.0	3,604	234	27	88%
Well-40	83-4	7.87	31.36	7.15	0.00000	0.0	2,843	792	355	55%
Well-41	69-8	10.30	104.27	26.02	0.00001	0.1	3,989	227	170	25%
Well-42	77-5	4.50	6.00	2.40	0.00000	0.0	3,853	2,656	695	74%
Well-43	75-7	1.66	3.00	15.50	0.00000	0.0	3,938	3,166	2,368	25%
Well-44	79-2	6.10	7.10	3.30	0.00000	0.0	3,949	1,761	590	67%
Well-45	80-7	6.83	3.80	3.40	0.00000	0.0	4,499	2,538	945	63%
Well-46	88-6	6.00	30.00	41.58	0.00500	30.0	5,756	530	446	16%
Well-47	77-4	11.11	183.71	4.11	0.00001	0.1	4,266	116	31	73%
Well-48	76-6	11.27	24.18	2.76	0.00026	3.0	3,765	991	234	76%
Well-49	79-2	4.00	1.81	1.92	0.00001	0.0	4,223	2,459	611	75%
Well-50	68-7	9.10	60.00	84.0	0.00000	0.0	3,372	1,336	1,066	20%
Well-51	72-8	1.80	2.77	23.00	0.00000	0.0	3,811	2,972	2,419	19%
Well-52	68-6	11.10	60.00	81.50	0.00000	0.0	3,447	959	875	9%
Well-53	91-1	9.80	16.00	16.00	0.00000	0.0	4,293	1,883	1,326	30%
Well-54	89-4	15.87	39.00	4.97	0.00000	0.0	4,070	576	235	59%
Well-55	89-1	16.70	633.00	36.50	0.00200	33.4	4,000	188	139	26%
Well-56	75-6	3.93	20.00	94.67	0.00000	0.0	3,972	2,615	2,442	7%
Well-57	87-6	15.30	300.00	30.00	0.00010	1.5	3,555	122	62	49%
Well-58	88-9	7.23	43.00	23.50	0.00000	0.0	3,258	806	554	31%
Well-59	88-8	5.00	60.00	10.00	0.00000	0.0	5,596	274	139	49%
Well-60	69-2	2.53	1.20	4.90	0.00000	0.0	3,376	2,678	1,491	44%
Well-61	78-2	7.41	410.55	20.22	0.00000	0.0	3,908	163	51	69%
Well-62	70-8	8.22	19.00	18.00	0.00000	0.0	3,738	1,460	701	52%
Well-63	81-2	2.79	4.40	9.30	0.00000	0.0	4,259	3,078	1,982	36%
Well-64	92-0	11.70	27.68	7.17	0.00000	0.0	4,053	559	266	52%
Well-65	89-5	2.10	0.95	12.87	0.00000	0.0	4,913	3,810	2,677	30%
Well-66	64-0	15.20	65.00	12.51	0.00001	0.2	3,142	268	156	42%
Well-67	81-3	7.78	13.65	8.96	0.00000	0.0	4,230	2,078	1,129	46%
Well-68	71-4	10.50	58.00	19.98	0.00001	0.1	3,024	612	430	30%
Well-69	72-3	8.00	18.87	18.95	0.00150	12.0	3,073	1,280	913	29%

Figure 3.4 shows the histogram reservoir permeabilities which obtained from pressure transient analyses. The mean and the standard deviation of permeability are 102.45 and 188.51, respectively.

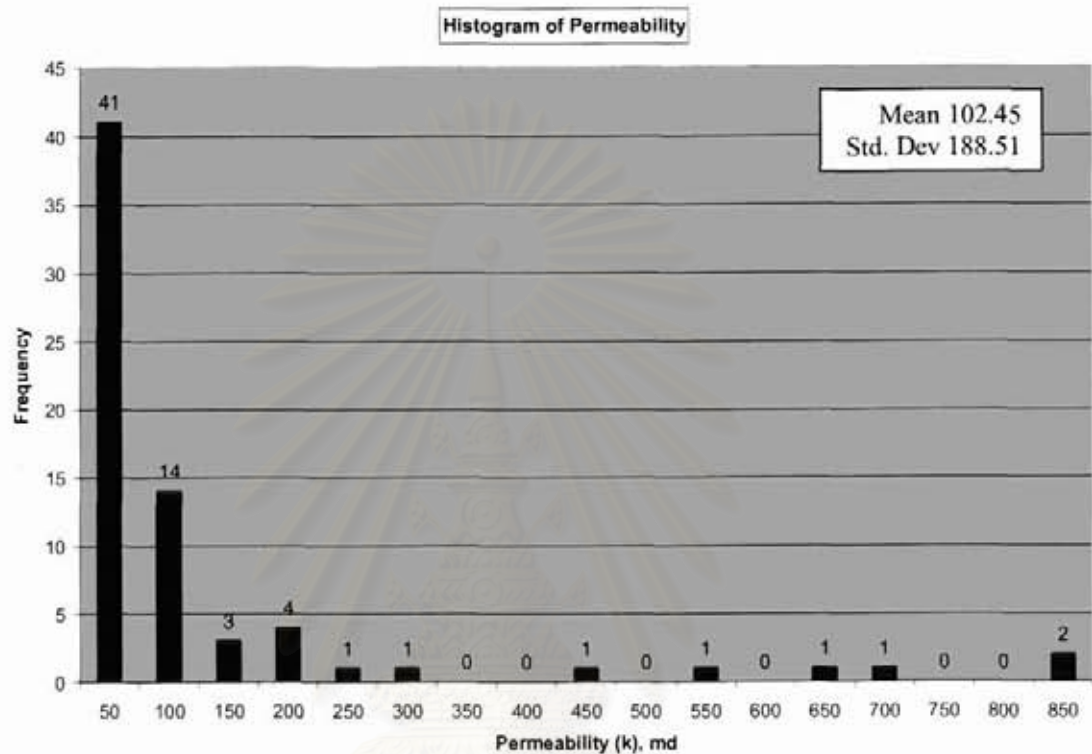


Figure 3.4 Histogram of permeability.

In addition, the relationship of reservoir permeability and porosity was also obtained as shown in Figure 3.5. From the trend line, which has coefficient of determination (R^2) at 0.4754, the permeability can be estimated for any reservoir porosity by the following equation:

$$k = 0.0141e^{40.329\phi} \quad [3.1]$$

where

k = average reservoir permeability, md

ϕ = gas reservoir porosity, %

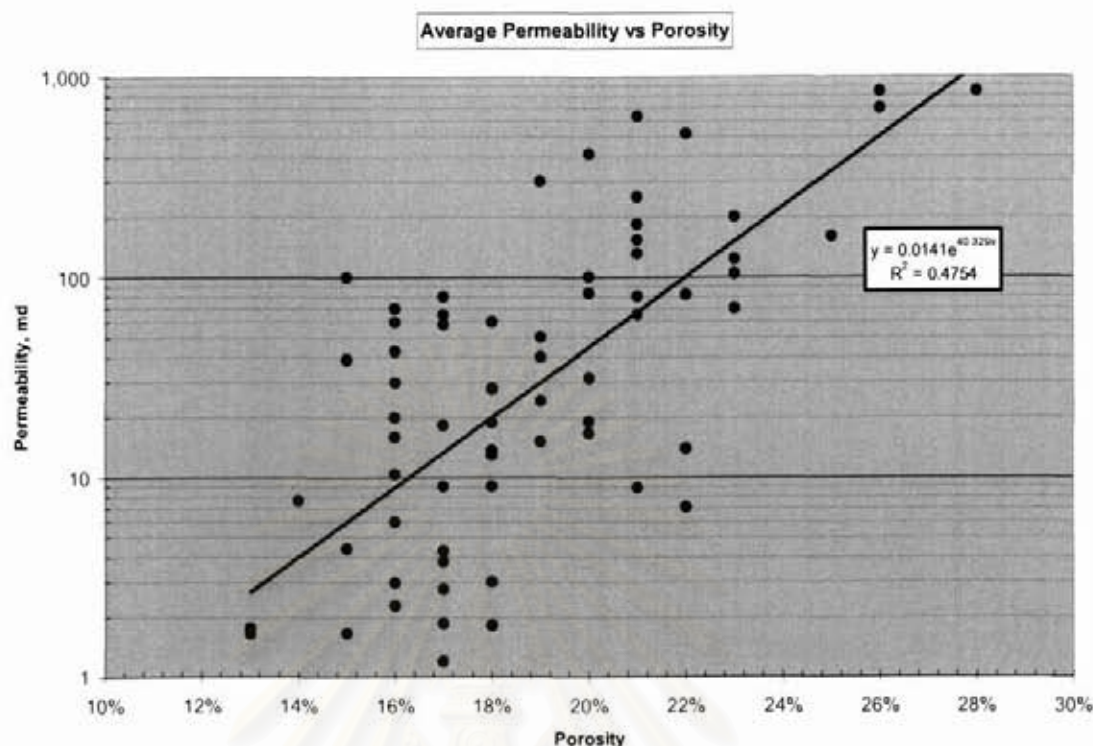


Figure 3.5: Average permeability versus porosity of 70 gas reservoirs.

3.2.1 Skin and Corrected Flow Efficiency for Perforated Gas Wells

In addition to non-Darcy skin, partial penetration skin was calculated from wellbore configuration, perforation interval, and an assumption of reservoir permeability ratio (k_v/k_h) of 0.2, using four correlations as described in Chapter 2. The calculated value from each correlation and the average value are presented in Table 3.4

To obtain the skin that represents the performance of perforation, the average partial penetration skin and non-Darcy skin were then subtracted from the total skin estimated from pressure transient analysis. Finally, the corrected flow efficiency can be determined from the pressure drop due to perforation skin using Equation 2.16.

To evaluate the perforation strategy, the impact of underbalance pressure on flow efficiency and skin was analyzed. The effect of reservoir porosity and charge type would also be discussed.

Table 3.4: Calculated partial penetration skin and corrected data.

Well	Res. Name	Calculated Partial Penetration Skin					Corrected Data		
		Brons & Marting	Odeh	Yeh & Reynolds	Papatzacos	Avg	Perforation Skin	Pressure Drop due to Perforation Skin, psi	Flow Efficiency, %
Well-01	68-8	0.00	0.00	0.00	0.00	0.00	0.52	117	93%
Well-02	82-4	2.94	3.68	3.02	3.16	3.20	1.77	553	83%
Well-03	92-4	3.52	4.16	3.59	3.73	3.75	17.68	2,412	35%
Well-04	95-6	3.44	3.87	3.51	3.64	3.61	15.89	2,367	39%
Well-05	75-6	2.03	2.84	2.11	2.26	2.31	4.36	464	83%
Well-06	69-2	0.79	1.37	0.82	0.96	0.99	0.54	45	94%
Well-07	81-7	0.72	1.21	0.76	0.90	0.90	2.61	920	70%
Well-08	63-4	18.22	18.90	18.74	18.72	18.65	41.87	93	61%
Well-09	89-5	2.31	2.86	2.39	2.54	2.53	3.33	821	75%
Well-10	52-2	23.17	23.85	23.78	23.73	23.63	5.85	7	95%
Well-11	55-8	3.17	4.25	3.26	3.40	3.52	2.29	10	86%
Well-12	56-1	24.54	25.27	25.15	25.10	25.02	16.44	21	76%
Well-13	59-1	1.35	2.06	1.41	1.56	1.59	21.41	73	67%
Well-14	72-7	1.53	2.30	1.59	1.74	1.79	8.69	391	67%
Well-15	75-5	1.81	2.75	1.88	2.03	2.11	-4.73	-42	119%
Well-16	60-8	0.00	0.00	0.00	0.00	0.00	-0.80	-8	111%
Well-17	59-2	2.62	3.66	2.70	2.85	2.96	2.54	14	87%
Well-18	61-0	1.35	2.10	1.41	1.56	1.60	1.00	15	93%
Well-19	81-6	1.15	1.81	1.20	1.35	1.38	8.62	42	54%
Well-20	72-9	0.00	0.00	0.00	0.00	0.00	-0.95	-232	119%
Well-21	73-0	2.57	3.28	2.65	2.80	2.82	12.18	1,101	38%
Well-22	78-2	1.79	2.66	1.86	2.01	2.08	-0.08	-1	100%
Well-23	59-4	0.88	1.47	0.91	1.05	1.08	5.52	96	68%
Well-24	88-3	6.68	7.50	6.76	6.87	6.95	7.35	464	68%
Well-25	71-0	13.89	14.46	14.26	14.27	14.22	0.02	2	100%
Well-26	65-3	13.95	14.90	14.23	14.26	14.33	9.47	184	71%
Well-27	57-0	27.00	27.57	27.42	27.38	27.34	107.66	1,072	24%
Well-28	80-6	1.88	2.69	1.96	2.11	2.16	14.70	2,318	36%
Well-29	92-5	1.76	2.50	1.83	1.98	2.02	3.07	32	83%
Well-30	88-4	3.18	3.96	3.26	3.40	3.45	5.45	481	71%
Well-31	86-1	0.00	0.00	0.00	0.00	0.00	1.00	14	96%
Well-32	84-0	0.00	0.00	0.00	0.00	0.00	2.40	1,378	54%
Well-33	78-8	4.51	5.49	4.59	4.72	4.83	2.24	500	83%
Well-34	92-9	14.90	15.72	15.25	15.26	15.28	109.70	830	20%
Well-35	87-1	2.81	3.59	2.89	3.03	3.08	6.92	65	61%
Well-36	91-7	0.00	0.00	0.00	0.00	0.00	-2.20	-569	127%
Well-37	64-0	0.99	1.69	1.02	1.17	1.22	1.88	13	83%
Well-38	89-9	12.53	13.15	12.83	12.86	12.84	0.76	6	98%
Well-39	87-1	3.20	4.21	3.28	3.43	3.53	-2.13	-42	118%
Well-40	83-4	1.62	2.38	1.69	1.84	1.89	5.27	261	67%
Well-41	69-8	16.99	17.66	17.47	17.45	17.39	8.52	56	76%
Well-42	77-5	3.66	4.17	3.74	3.87	3.86	-1.46	-422	116%
Well-43	75-7	0.00	0.00	0.00	0.00	0.00	15.50	2,368	25%
Well-44	79-2	0.00	0.00	0.00	0.00	0.00	3.30	590	67%
Well-45	80-7	2.25	3.06	2.33	2.48	2.53	0.87	242	90%
Well-46	88-6	7.53	8.60	7.61	7.72	7.86	3.71	40	92%
Well-47	77-4	1.15	1.84	1.20	1.35	1.38	2.59	20	83%
Well-48	76-6	1.09	1.74	1.14	1.29	1.31	-1.52	-129	113%
Well-49	79-2	2.25	3.15	2.33	2.48	2.55	-0.68	-218	109%
Well-50	68-7	10.76	11.63	10.93	11.00	11.08	72.92	925	31%
Well-51	72-8	15.78	16.30	16.28	16.26	16.16	6.84	720	76%
Well-52	68-6	30.57	31.18	31.10	31.06	30.98	50.52	543	43%
Well-53	91-1	12.35	12.85	12.68	12.70	12.65	3.35	278	85%
Well-54	89-4	3.43	4.29	3.50	3.65	3.72	1.25	59	90%
Well-55	89-1	7.34	7.85	7.45	7.54	7.54	-4.44	-17	109%
Well-56	75-6	14.64	15.21	15.06	15.06	14.99	79.68	2,055	21%
Well-57	87-6	2.47	3.66	2.55	2.70	2.85	25.62	53	56%
Well-58	88-9	0.00	0.00	0.00	0.00	0.00	23.50	554	31%
Well-59	88-8	5.64	6.61	5.71	5.83	5.95	4.05	56	79%
Well-60	69-2	0.00	0.00	0.00	0.00	0.00	4.90	1,491	44%
Well-61	78-2	0.00	0.00	0.00	0.00	0.00	20.22	51	69%
Well-62	70-8	0.00	0.00	0.00	0.00	0.00	18.00	701	52%
Well-63	81-2	0.00	0.00	0.00	0.00	0.00	9.30	1,982	36%
Well-64	92-0	0.00	0.00	0.00	0.00	0.00	7.17	266	52%
Well-65	89-5	0.77	1.42	0.78	0.91	0.97	11.90	2,476	35%
Well-66	64-0	4.49	5.64	4.57	4.71	4.85	7.51	94	65%
Well-67	81-3	6.64	7.11	6.74	6.83	6.83	2.13	269	87%
Well-68	71-4	2.03	2.88	2.10	2.25	2.32	17.56	378	38%
Well-69	72-3	1.06	1.80	1.09	1.23	1.29	5.66	273	79%

3.3 Relationship between Skin and Underbalance Pressure

Only data for relationship study is re-presented in Table 3.5. The plot between skin versus underbalance pressure is shown in Figure 3.6. Both the total and perforation skins tend to decrease as underbalance pressure increases. However, the total skin values are more scattered. As a result, a relationship between the total skin and underbalance pressure cannot be established. From Figure 3.6, the linear trend line of perforation skin has coefficient of determination (R^2) of 0.2104 while the coefficient of determination for the total skin is only 0.0277.

As described in Chapter 2, the total skin is the combination of various skin factors: non-Darcy skin, partial penetration skin, perforation skin, and other pseudo skin factors. Non-Darcy skin is a rate dependent factor while partial penetration skin is a penetration ratio dependent factor. So, both non-Darcy and partial penetration skins are not function of underbalance pressure.

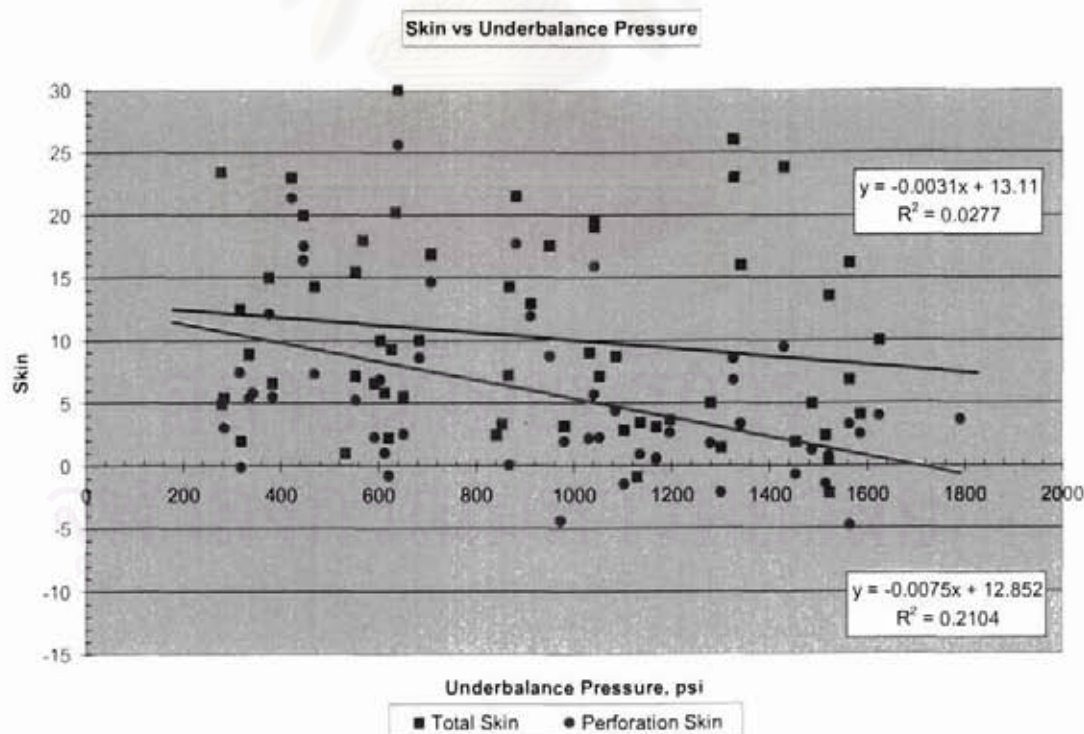


Figure 3.6: Total skin and perforation skin versus underbalance pressure.

Table 3.5: Information for relationship study.

Well	Res. Name	Gas Reservoir Properties		Under balance pressure, psi	Pressure Transient Analyses		Perforation Skin	Corrected Flow Efficiency, %
		Porosity, %	Sw, %		Permeability (k), md	Total Skin		
Well-01	68-8	13	58	1523	1.65	0.52	0.52	93%
Well-02	82-4	16	62	1281	2.98	4.97	1.77	83%
Well-03	92-4	13	30	884	1.77	21.43	17.68	35%
Well-04	95-6	16	39	1043	2.29	19.50	15.89	39%
Well-05	75-6	18	45	1087	9.07	8.67	4.36	83%
Well-06	69-2	20	26	1171	16.60	3.05	0.54	94%
Well-07	81-7	17	38	1198	4.30	3.60	2.61	70%
Well-08	63-4	22	28	524	520.00	101.13	41.87	61%
Well-09	89-5	17	46	1565	9.06	6.89	3.33	75%
Well-10	52-2	28	23	344	850.00	104.00	5.85	95%
Well-11	55-8	21	10	594	250.00	6.60	2.29	86%
Well-12	56-1	26	32	447	850.00	45.30	16.44	76%
Well-13	59-1	26	16	424	700.00	23.00	21.41	67%
Well-14	72-7	18	44	951	28.00	17.50	8.69	67%
Well-15	75-5	20	52	1565	100.00	16.20	-4.73	119%
Well-16	60-8	25	23	622	160.00	2.20	-0.80	111%
Well-17	59-2	21	41	653	152.80	5.50	2.54	87%
Well-18	61-0	23	31	615	123.00	5.80	1.00	93%
Well-19	81-6	15	52	685	100.00	10.00	8.62	54%
Well-20	72-9	21	25	1131	8.90	-0.95	-0.95	119%
Well-21	73-0	17	50	377	18.34	15.00	12.18	38%
Well-22	78-2	23	37	320	70.00	2.00	-0.08	100%
Well-23	59-4	21	36	385	80.00	6.60	5.52	68%
Well-24	88-3	22	47	471	14.00	14.30	7.35	68%
Well-25	71-0	18	52	869	13.00	14.25	0.02	100%
Well-26	65-3	19	30	1430	40.00	23.80	9.47	71%
Well-27	57-0	17	47	349	65.00	135.00	107.66	24%
Well-28	80-6	15	45	709	1.66	16.86	14.70	36%
Well-29	92-5	21	19	285	130.73	5.43	3.07	83%
Well-30	88-4	19	32	337	15.10	8.90	5.45	71%
Well-31	86-1	20	52	535	83.00	1.00	1.00	96%
Well-32	84-0	15	53	843	0.17	2.40	2.40	54%
Well-33	78-8	17	54	1054	1.86	7.07	2.24	83%
Well-34	92-9	17	36	185	80.00	127.71	109.70	20%
Well-35	87-1	16	54	606	70.00	10.00	6.92	61%
Well-36	91-7	14	31	1525	7.69	-2.20	-2.20	127%
Well-37	64-0	22	25	982	81.68	3.10	1.88	83%
Well-38	89-9	23	27	1523	200.00	13.60	0.76	98%
Well-39	87-1	19	35	1301	50.00	1.40	-2.13	118%
Well-40	83-4	20	49	555	31.36	7.15	5.27	67%
Well-41	69-8	23	43	1327	104.27	26.02	8.52	76%
Well-42	77-5	16	48	1516	6.00	2.40	-1.46	116%
Well-43	75-7	18	62	554	3.00	15.50	15.50	25%
Well-44	79-2	22	52	855	7.10	3.30	3.30	67%
Well-45	80-7	17	28	1137	3.80	3.40	0.87	90%
Well-46	88-6	16	46	1792	30.00	41.58	3.71	92%
Well-47	77-4	21	40	1587	183.71	4.11	2.59	83%
Well-48	76-6	19	36	1105	24.18	2.76	-1.52	113%
Well-49	79-2	18	54	1454	1.81	1.92	-0.68	109%
Well-50	68-7	18	24	302	60.00	84.0	72.92	31%
Well-51	72-8	17	42	1328	2.77	23.00	6.84	76%
Well-52	68-6	16	32	801	60.00	81.50	50.52	43%
Well-53	91-1	16	33	1342	16.00	16.00	3.35	85%
Well-54	89-4	15	20	1488	39.00	4.97	1.25	90%
Well-55	89-1	21	26	974	633.00	36.50	-4.44	109%
Well-56	75-6	16	52	591	20.00	94.67	79.68	21%
Well-57	87-6	19	22	640	300.00	30.00	25.62	56%
Well-58	88-9	16	57	279	43.00	23.50	23.50	31%
Well-59	88-8	18	45	1626	60.00	10.00	4.05	79%
Well-60	69-2	17	51	280	1.20	4.90	4.90	44%
Well-61	78-2	20	42	637	410.55	20.22	20.22	69%
Well-62	70-8	20	54	570	19.00	18.00	18.00	52%
Well-63	81-2	15	62	627	4.40	9.30	9.30	36%
Well-64	92-0	18	43	867	27.68	7.17	7.17	52%
Well-65	89-5	14	38	912	0.95	12.87	11.90	35%
Well-66	64-0	21	28	317	65.00	12.51	7.51	65%
Well-67	81-3	18	46	1033	13.65	8.96	2.13	87%
Well-68	71-4	17	43	449	58.00	19.98	17.56	38%
Well-69	72-3	18	48	1043	18.87	18.95	5.66	79%

From Figure 3.6, the relationship between perforation skin and underbalance pressure can be established as follows:

$$S_{\text{perforation}} = -0.0075\Delta p + 12.852 \quad [3.2]$$

where

$$\Delta p = \text{underbalance pressure, psi}$$

From Figure 3.6 and Equation 3.2, perforation skin less than 5 or even negative in some cases, can be achieved with underbalance pressure higher than 1,000 psi. In addition, the zero perforation skin can be obtained at an underbalance pressure of 1714 psi.

To better understand the effect of underbalance pressure on the perforation skin, the data were divided into two groups based on porosity. Based on all 70 gas reservoirs of interest data, trial and error was performed to identify the best porosity cutoff. Eighteen percent porosity yields the best average coefficient of determination for both groups of data as shown in Table 3.6.

Table 3.6: Coefficient of determination, R^2 , of each porosity cutoff on perforation skin versus underbalance pressure.

Porosity cutoff, %	Coefficient of determination, R^2	
	Lower or equal to cutoff	Higher than cutoff
17	0.4431	0.1112
18	0.4503	0.1276
19	0.3682	0.1247
20	0.3620	0.1054

Figure 3.7 was plotted using the same perforation skin data set as presented earlier in Figure 3.6, but the data were divided into two groups based on 18% porosity cutoff which has the best average coefficient of determination. The blue points represent data with porosity less than or equal to 18% (tight reservoirs) which have the coefficient of determination (R^2) of 0.4503, while others with porosity higher than 18% (porous reservoirs) are shown in red which have the coefficient of determination

(R^2) of 0.1276. Both categories indicate that the perforation skin decrease as underbalance pressure increases but with a different trend as shown in blue and red straight lines. The blue line is steeper than the red one indicating that underbalance pressure has more impact on the perforation skin in the case of lower reservoir porosity.

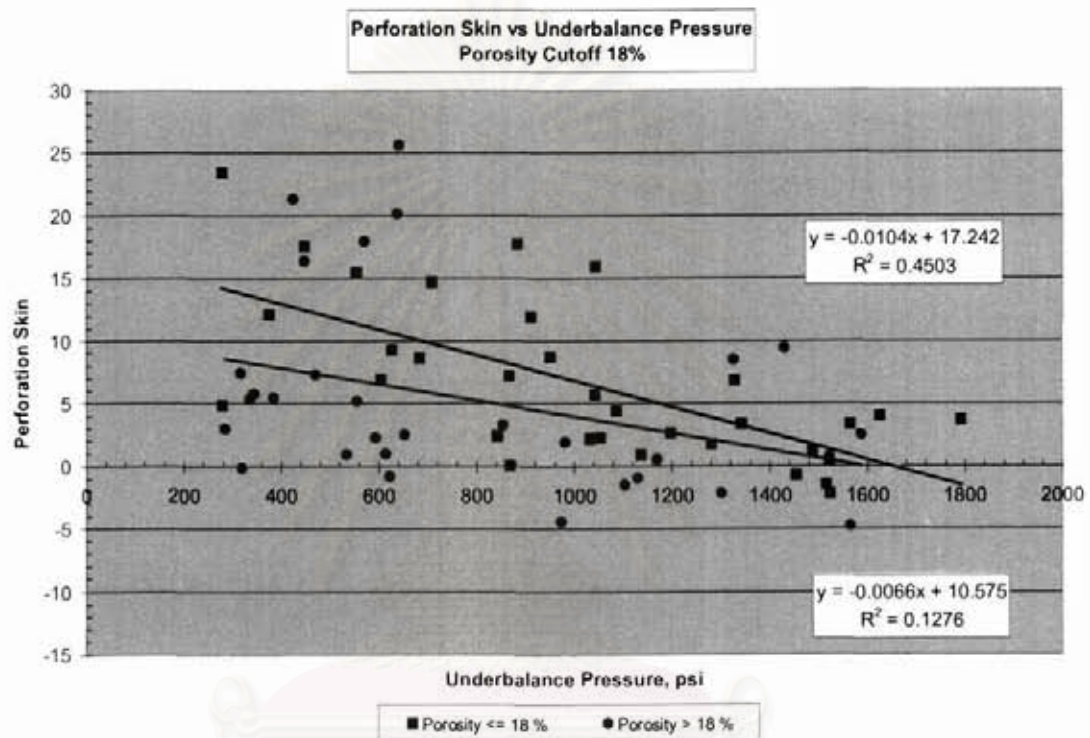


Figure 3.7: Perforation skin versus underbalance pressure – cutoff porosity of 18%.

From Figure 3.7, the linear relationship between perforation skin and underbalance pressure (Δp) for tight reservoir (porosity, $\phi \leq 18\%$) and porous reservoir (porosity, $\phi > 18\%$) can be established as follows:

$$\text{For } \phi \leq 18\%, \quad \text{Perforation Skin} = -0.0104\Delta p + 17.242 \quad [3.3]$$

$$\text{For } \phi > 18\%, \quad \text{Perforation Skin} = -0.0066\Delta p + 10.575 \quad [3.4]$$

From Equations 3.3 and 3.4, to achieve zero perforation skin, 1658 and 1602 psi underbalance pressure is required for tight and porous reservoirs.

3.4 Relationship between Corrected Flow Efficiency and Underbalance Pressure

According to the previous section, the higher the underbalance the higher corrected flow efficiency will be. This section describes more details on the relationship between underbalance pressure and corrected flow efficiency.

Figure 3.8 illustrates the relationship between corrected flow efficiency and underbalance pressure for 70 perforated gas reservoirs. The underbalance pressure of 185 to 1800 psi results in flow efficiency ranging from 12% to almost 130%. Although the data points are relatively scattered, an increasing trend can be observed. The trend indicates, as expected, that the higher the underbalance pressure, the higher the flow efficiency can be achieved. With a higher underbalance pressure, the degree of reservoir damage from perforation can be reduced and consequently resulting in a higher flow efficiency.

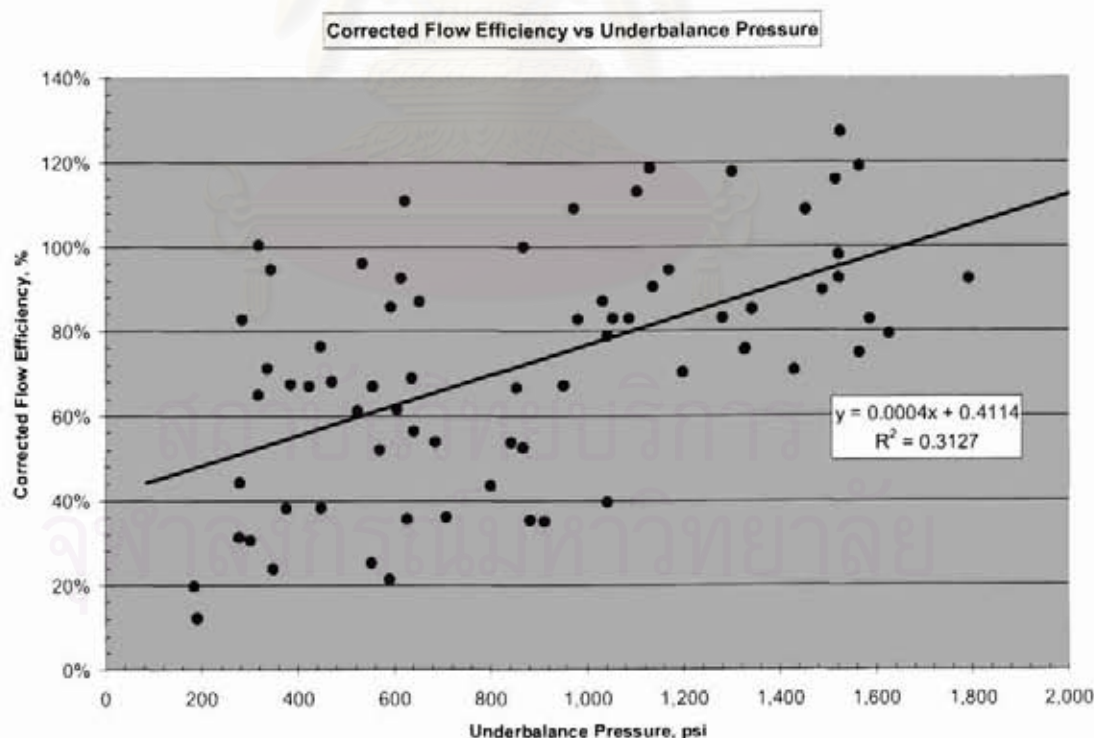


Figure 3.8: Corrected flow efficiency versus underbalance pressure – all 70 gas reservoirs of interest.

According to the trend line, a 50% corrected flow efficiency can be obtained by an underbalance pressure of 222 psi while a 100% efficiency or zero-perforation skin requires an underbalance pressure of 1472 psi. However, without underbalance pressure condition while perforation (perforate the gas reservoir at the equivalent pressure between reservoir and the wellbore), the corrected flow efficiency will be only 43%.

Based on all 70 gas reservoirs of interest data, as shown in Figure 3.8, the linear relationship between corrected flow efficiency (CFE) and underbalance pressure (Δp) can be established as follows:

$$CFE = 0.0004\Delta p + 0.4114 \quad [3.5]$$

However, the coefficient of determination (R^2) is only 0.3127 and the linear trend line in Figure 3.8 does not well represent all 70 gas reservoirs of interest. To better understand the effect of underbalance pressure on the corrected flow efficiency, the data were divided into two groups based on porosity. Similar to the previous section, trial and error was performed again to identify the best porosity cutoff. The same porosity of eighteen percent yields the best average coefficient of determination for both groups of data as shown in Table 3.7.

Table 3.7: Coefficient of determination, R^2 , of each porosity cutoff on corrected flow efficiency versus underbalance pressure.

Porosity cutoff, %	Coefficient of determination, R^2	
	Lower or equal to cutoff	Higher than cutoff
17	0.1870	0.6435
18	0.1900	0.6980
19	0.1719	0.6161
20	0.0844	0.5661

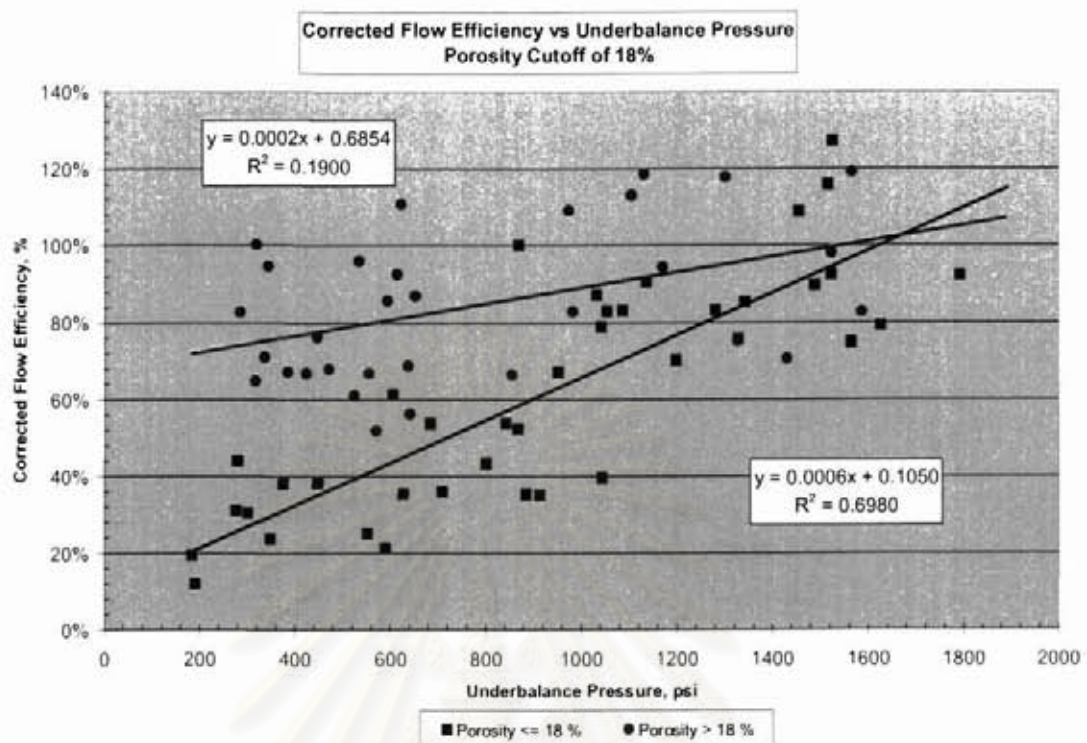


Figure 3.9: Corrected flow efficiency versus underbalance pressure – cutoff porosity of 18%.

Figure 3.9 was plotted using the same data set as presented earlier in Figure 3.8, but the data were divided into two groups based on 18% porosity cutoff which has the best average coefficient of determination. The blue points represent data with porosity less than or equal to 18% (39 tight reservoirs) which have the coefficient of determination (R^2) of 0.698, while others with porosity higher than 18% (31 porous reservoirs) are shown in red which have the coefficient of determination (R^2) of 0.19. Both categories indicate that the flow efficiency increase as underbalance pressure increases but with a different trend as shown in blue and red straight lines. The blue line is steeper than the red one indicating that underbalance pressure has more impact on the corrected flow efficiency in the case of lower reservoir porosity.

From Figure 3.9, the linear relationship between corrected flow efficiency (CFE) and underbalance pressure (Δp) for tight reservoir (porosity, $\phi \leq 18\%$) and porous reservoir (porosity, $\phi > 18\%$) can be established as follows:

$$\text{For } \phi \leq 18\%, \quad CFE = 0.0006\Delta p + 0.1050 \quad [3.6]$$

$$\text{For } \phi > 18\%, \quad CFE = 0.0002\Delta p + 0.6854 \quad [3.7]$$

By increasing the underbalance pressure from 500 to 1200 psi, the corrected flow efficiency doubles from 41% to 83% for the tight gas reservoirs but increases from 79% to only 93% for the porous gas reservoirs. This is because high porosity reservoirs naturally have high flow ability, thus the flow efficiency would only be slightly affected by underbalance pressure conditions, as seen from the less slope of the red line in Figure 3.9.

With equivalent pressure perforation (or zero underbalance pressure at the y-intercept shown in Figure 3.9), corrected flow efficiency will be 69% for gas reservoir with porosity higher than 18%, but only 11% for reservoir with porosity equal or lower than 18%.

In summary, porous gas reservoirs that have porosity higher than 18% require lower underbalance pressures compared to tight gas reservoirs to achieve the same corrected flow efficiency.

สถาบันวิทยบริการ
จุฬาลงกรณ์มหาวิทยาลัย

3.5 Relationship between Underbalance and Permeability

In order to prove whether the published correlations of required underbalance pressure for given reservoir permeability can be used for gas wells in the Gulf of Thailand, the relationship between underbalance pressure and reservoir permeability of all 70 gas reservoirs of interest has been studied and compared with the published correlations.

Figure 3.10 presents the relationship between underbalance pressure and reservoir permeability of all 70 gas reservoirs of interest, but arranged into 3 different groups based on corrected flow efficiency: higher than 60%, 80%, and 100%. Note that the first group is a subset of the second group and that the second is a subset of the third one.

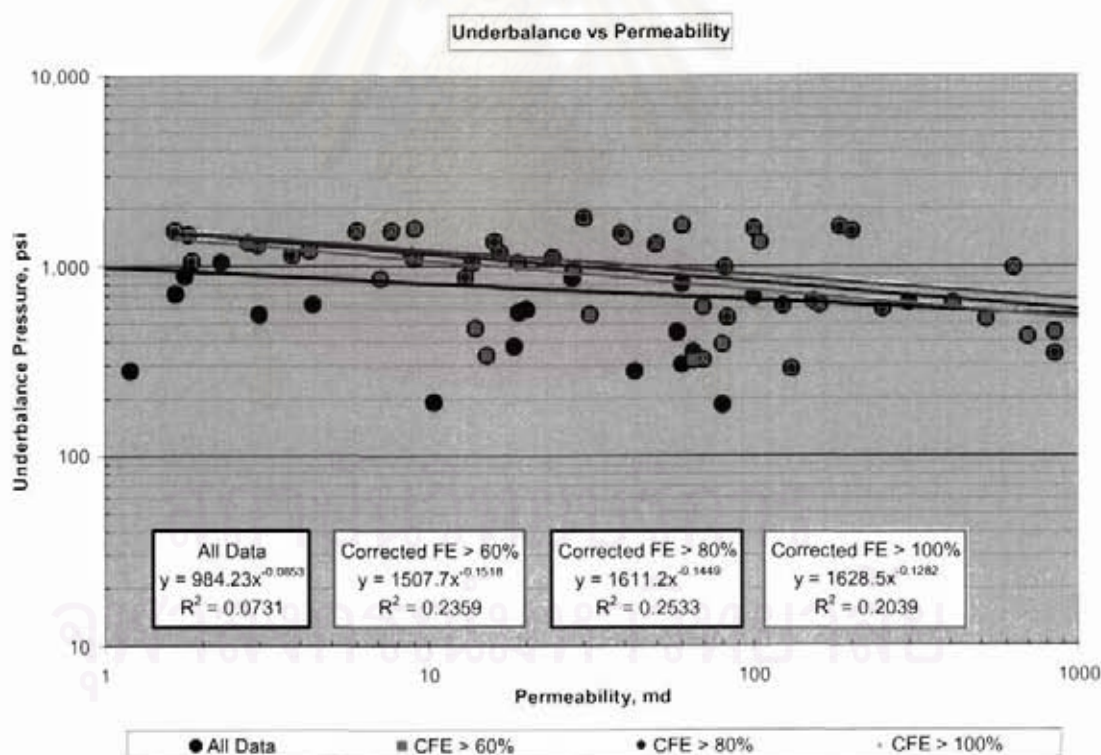


Figure 3.10: Underbalance pressure versus gas reservoir permeability at corrected flow efficiency higher than 60, 80, and 100%.

The coefficient of determination (R^2) of CFE higher than 80% is the highest, having a value of 0.2533, while CFE higher than 60% and 100% has R^2 of 0.2359 and 0.2039, respectively. From trend lines in Figure 3.10, the minimum required underbalance pressure (Δp) to obtain a certain level of corrected flow efficacy (CFE), can be determined as follows:

$$\text{To obtain } CFE > 60\%, \quad \Delta p = \frac{1507.7}{k^{0.1518}} \quad [3.8]$$

$$\text{To obtain } CFE > 80\%, \quad \Delta p = \frac{1611.2}{k^{0.1449}} \quad [3.9]$$

$$\text{To obtain } CFE > 100\%, \quad \Delta p = \frac{1628.5}{k^{0.1282}} \quad [3.10]$$

For any gas reservoir in the Gulf of Thailand, zero or negative perforation skin can be obtained by applying the underbalance pressure calculated from Equation 3.10 based on permeability.

To compare the result obtained from this study with published correlations, Equation 3.10 which represents zero-perforation skin was plotted together with King's and Hsia & Behrmann's correlations as shown in Figure 3.11. However, Equation 3.10 cannot directly be compared with King's correlation which is not entirely correct for zero-perforation skin as mentioned in Chapter 2.

It can be seen from Figure 3.11 that the published correlations cannot be used for Gulf of Thailand's gas reservoirs. It seems that different fields have different requirements for underbalance pressure condition to achieve zero-perforation skin.

In order to achieve zero-perforation skin, Behrmann's correlation requires much higher underbalance pressure for reservoirs that have permeability lower than 90 md, but requires lower underbalance pressure for reservoirs that have permeability higher than 90 md.

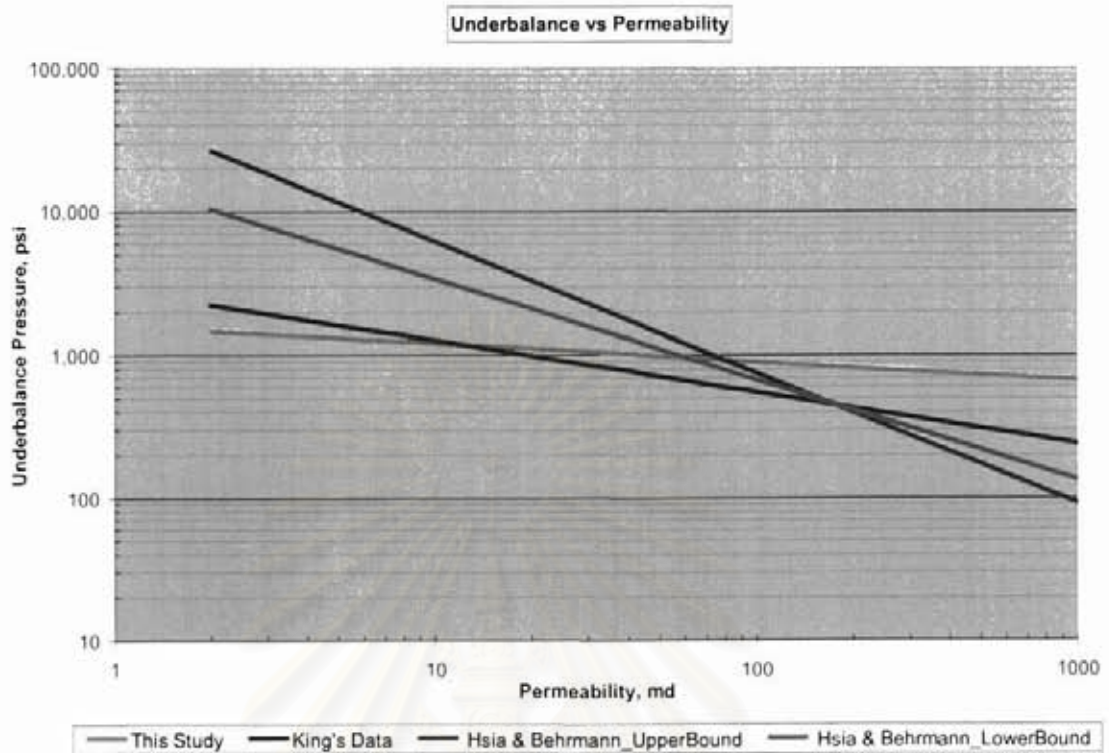


Figure 3.11: Underbalance pressure versus gas reservoir permeability at corrected flow efficiency higher than 100% (zero-perforation skin) compared with King's field correlation and Hsia & Behrmann's correlation.

สถาบันวิทยบริการ
จุฬาลงกรณ์มหาวิทยาลัย

3.6 Relationship between Underbalance and Porosity

The average permeability of each gas reservoir is unlikely available before perforation. Even though, for any gas reservoir in the Gulf of Thailand, the average permeability can be estimated by Equation 3.1 but with low accuracy. Typically, the gas reservoir porosity is known by either openhole wireline log or logging while drilling (LWD). So, the perforation plan is practically based on reservoir porosity, but not permeability.

To determine the minimum required underbalance pressure to obtain a certain level of corrected flow efficiency, the underbalance pressures and gas reservoir porosities are plotted in Figure 3.12. The data are arranged into three groups based on the corrected flow efficiency: higher than 60, 80, and 100%. As mentioned before, the first group is a subset of the second group and the second is a subset of the third one.

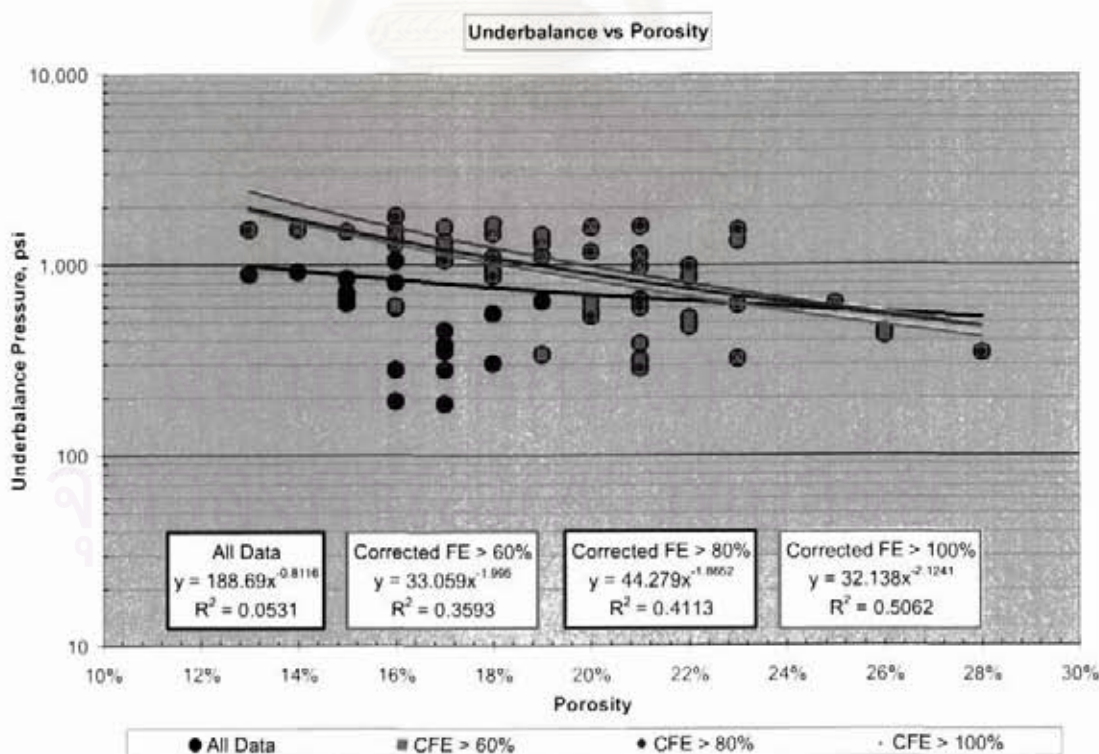


Figure 3.12: Underbalance pressure versus gas reservoir porosity at corrected flow efficiency higher than 60, 80, and 100%.

All trend lines in Figure 3.12 also support the results discussed in Section 3.4 that the higher the porosity the lower underbalance pressure is required to get the same corrected flow efficiency.

From Figure 3.12, the coefficient of determination (R^2) of CFE higher than 100% is the highest, having a value of 0.5062, while CFE higher than 60% and 80% has R^2 of 0.3593 and 0.4113, respectively. From trend lines in Figure 3.11, to obtain a certain level of corrected flow efficacy (CFE), the following minimum underbalance pressure (psi), Δp , is required:

$$\text{To obtain } CFE > 60\%, \quad \Delta p = \frac{33.059}{\phi^{1.995}} \quad [3.11]$$

$$\text{To obtain } CFE > 80\%, \quad \Delta p = \frac{44.279}{\phi^{1.8652}} \quad [3.12]$$

$$\text{To obtain } CFE > 100\%, \quad \Delta p = \frac{32.138}{\phi^{2.1241}} \quad [3.13]$$

For any gas reservoir in the Gulf of Thailand, zero or negative perforation skin can be obtained by applying the underbalance pressure calculated from Equation 3.13 based on porosity.

3.7 Relationship between Corrected Flow Efficiency and Perforation Charge Type

To evaluate the performance of different charge types, the same data set in Figure 3.8 was plotted again in Figure 3.13 but they are categorized into 4 groups according to 4 different charge types: Owen Hero, Power Jet, Predator, and Predator XP. The relationship between flow efficiency and underbalance pressure is similar among all 4 different charge types, increasing in underbalance pressure results in higher flow efficiency.

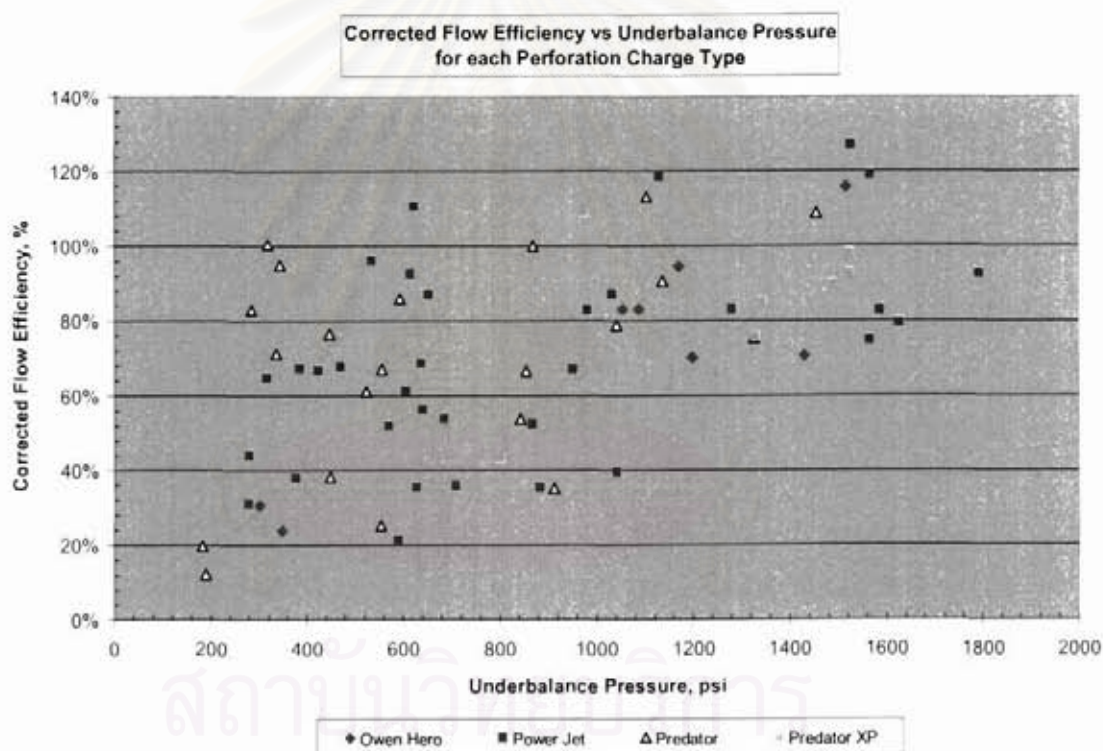


Figure 3.13: Corrected flow efficiency versus underbalance pressure for each perforation charge type.

To better understand the affect from only perforation charge type to the corrected flow efficiency, the data were narrowed down as shown in Figure 3.14, focusing only 2-1/8" gun size, 60 degree phasing, 5-6 shot per foot, and HMX explosive.

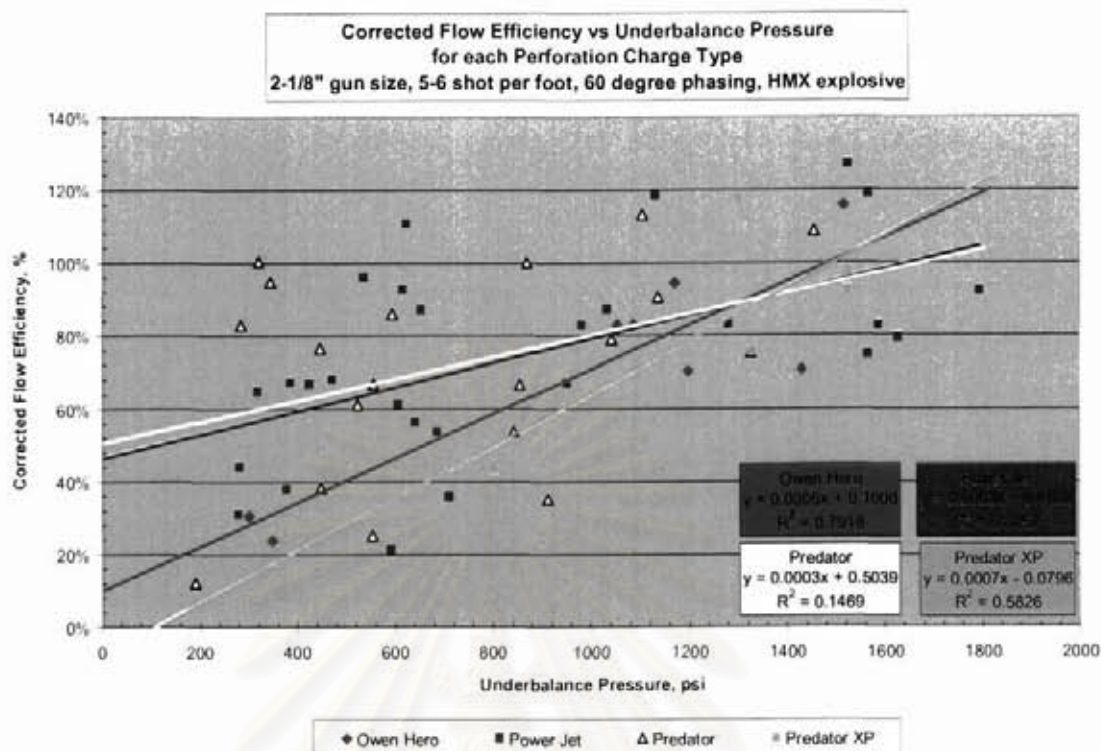


Figure 3.14: Corrected flow efficiency versus underbalance pressure for each perforation charge type, 2-1/8" gun size, 60 degree phasing, 5-6 shot per foot, and HMX explosive.

From Figure 3.14, the coefficient of determination (R^2) of Owen Hero is the highest, having a value of 0.7918, while Predator XP, Power Jet, and Predator has R^2 of 0.5826, 0.3257, and 0.1469, respectively. From trend lines in Figure 3.14, the linear relationship between corrected flow efficiency (CFE) and underbalance pressure (Δp) for each perforation charge type can be established as follows:

$$\text{For Owen Hero,} \quad CFE = 0.0006\Delta p + 0.1000 \quad [3.14]$$

$$\text{For Predator XP,} \quad CFE = 0.0007\Delta p - 0.0796 \quad [3.15]$$

$$\text{For Power Jet,} \quad CFE = 0.0003\Delta p + 0.4668 \quad [3.16]$$

$$\text{For Predator,} \quad CFE = 0.0003\Delta p + 0.5039 \quad [3.17]$$

From Figure 3.14, Power Jet and Predator perforation charges have similar trend lines which provide better corrected flow efficiency than Owen Hero and Predator XP when underbalance pressure lower than 1300 psi. However, from the trend lines, Owen Hero and Predator XP perforation charge types provide better corrected flow efficiency when underbalance pressure higher than 1300 psi.

To obtain zero perforation skin or 100% corrected flow efficiency, from Equations 3.14 to 3.17, following minimal underbalance pressure is required for each perforation charge type:

Table 3.8: Minimal underbalance pressure to obtain zero perforation skin for each perforation charge type.

Charge Type	Equation	Minimal underbalance pressure, psi
Owen Hero	$CFE = 0.0006 \Delta p + 0.1000$	1,500
Predator XP	$CFE = 0.0007 \Delta p - 0.0796$	1,542
Power Jet	$CFE = 0.0003 \Delta p + 0.4668$	1,777
Predator	$CFE = 0.0003 \Delta p + 0.5039$	1,654

From Table 3.8, the lowest required underbalance pressure is 1500 psi when using Owen Hero perforation charge while the highest is 1777 psi using Power Jet to obtain zero perforation skin or 100% corrected flow efficiency.

In summary, regardless of gas reservoir properties, the range of underbalance pressure of 1500 to 1777 psi, depending on perforation charge type, is required to achieve best perforation performance or zero perforation skin. However, if available or achievable underbalance pressure condition is lower than 1300 psi, Power Jet and Predator perforation charges are recommended for better perforation performance and lower perforation skin.

CHAPTER IV

CONCLUSIONS

This study was based on seventy perforations of gas wells in the Gulf of Thailand. Seventy interpreted results from pressure transient tests were used along with other skin factor correlations, and perforation information such as underbalance pressure, perforation charge type, etc. Perforation skin factors were obtained by subtracting the total skin by other skin factors such as partial penetration skin and non-Darcy skin.

After analyzing the skins of seventy tests, it can be concluded that the underbalance pressure condition directly affects the perforation damage or skin of perforated gas reservoirs, as well as corrected flow efficiency. The magnitude of the perforation skin depends on the degree of the underbalance pressure. The higher the underbalance pressure, the lower the perforation skin will be. As a result, a higher flow efficiency and recovery of gas reservoir can be achieved.

It was also found that the underbalance pressure has more impact on the corrected flow efficiency of tight gas reservoirs than that of porous sands. For the tight gas reservoirs (porosity less than 18%), every additional 100 psi underbalance pressure will provide an increase of 6% in corrected flow efficiency but only an increase of 2% can be obtained if the porosity is over 18%.

Without any underbalance pressure applied during the perforation, tight gas reservoirs will have only 11% corrected flow efficiency while porous gas reservoirs will have 69% corrected flow efficiency. In order to obtain 100% corrected flow efficiency, 1620 and 1550 psi underbalance pressures are required for tight and porous gas reservoirs, respectively.

To obtain the best corrected flow efficiency or zero-perforation skin for a given gas reservoir permeability or porosity, the minimum required underbalance pressure can be estimated by $\Delta p = \frac{1628.5}{k^{0.1282}}$, and $\Delta p = \frac{32.138}{\phi^{2.1741}}$, respectively.

However, these equations are applicable only for gas reservoirs in the Gulf of Thailand. Reservoirs with the same properties but located in different environments require different minimal underbalance pressures to achieve the same corrected flow efficiency or perforation skin.

Regardless of gas reservoir properties, at underbalance pressure lower than 1300 psi, Power Jet and Predator perforation charges provide better perforation performance and lower perforation skin. To achieve the zero perforation skin or 100% corrected flow efficiency, 1500, 1542, 1777, and 1654 psi underbalance pressure is required when using Owen Hero, Predator XP, Power Jet, and Predator charge, respectively.



สถาบันวิทยบริการ
จุฬาลงกรณ์มหาวิทยาลัย

References

1. Bell, W.T.: Perforating Underbalanced – Evolving Techniques. JPT (Oct 1984) :1653-62 SPE 13413
2. King, G. E., Anderson, A., and Bingham, M.: A Field Study of Underbalance Pressure Necessary To Obtain Clean Perforations Using Tubing Conveyed Perforating. JPT (June 1986): 662-664 SPE 14321
3. Halleck, P. M., and Deo, M.: Effects of Underbalance on Perforation Flow. paper SPE 16895
4. Tariq, S. M.: New, Generalized Criteria for Determining the Level of Underbalance for Obtaining Clean Perforations. paper SPE 20636
5. Behrmann, L.A. *et al.*: Measurement of Additional Skin Resulting From Perforation Damage. paper SPE 22809
6. Hsia, T.Y. and Behrmann, L.A.: Perforating Skin as a Function of Rock Permeability and Underbalance. paper SPE 22810
7. Kent Folsie *et al.*: Perforating System Selection for Optimum Well Inflow Performance. paper SPE 73762
8. Roostapour A. and Yildiz T.: Post-Perforation Flow Models For API Recommended Practices 19B. paper SPE 94245
9. Behrmann, L.A.: Underbalance Criteria for Minimum Perforating Damage. paper SPE 30081
10. Roland N. Horne: Modern Well Test Analysis. May 1995

11. Brons, F. and Marting, V. E.: The Effect of Restricted Fluid Entry on Well Productivity. JPT (Feb. 1961); 172-174
12. Odeh, A.S.: An Equation for Calculating Skin Factor Due to Restricted Entry. JPT 8879-PA
13. Paul Papatzacos: Approximate Partial-Penetration Pseudoskin for Infinite-Conductivity Wells. paper SPE 13956-PA
14. Yeh N. and Reynolds A. C.: Computation of the Pseudoskin Factor Caused by a Restricted-Entry Well Completed in a Multilayer Reservoir. paper SPE 15793-PA



สถาบันวิทยบริการ
จุฬาลงกรณ์มหาวิทยาลัย



APPENDICES

สถาบันวิทยบริการ
จุฬาลงกรณ์มหาวิทยาลัย

Appendix A

This appendix presents all pressure transient analyses of 70 gas reservoirs.

Well-01 Reservoir 68-8

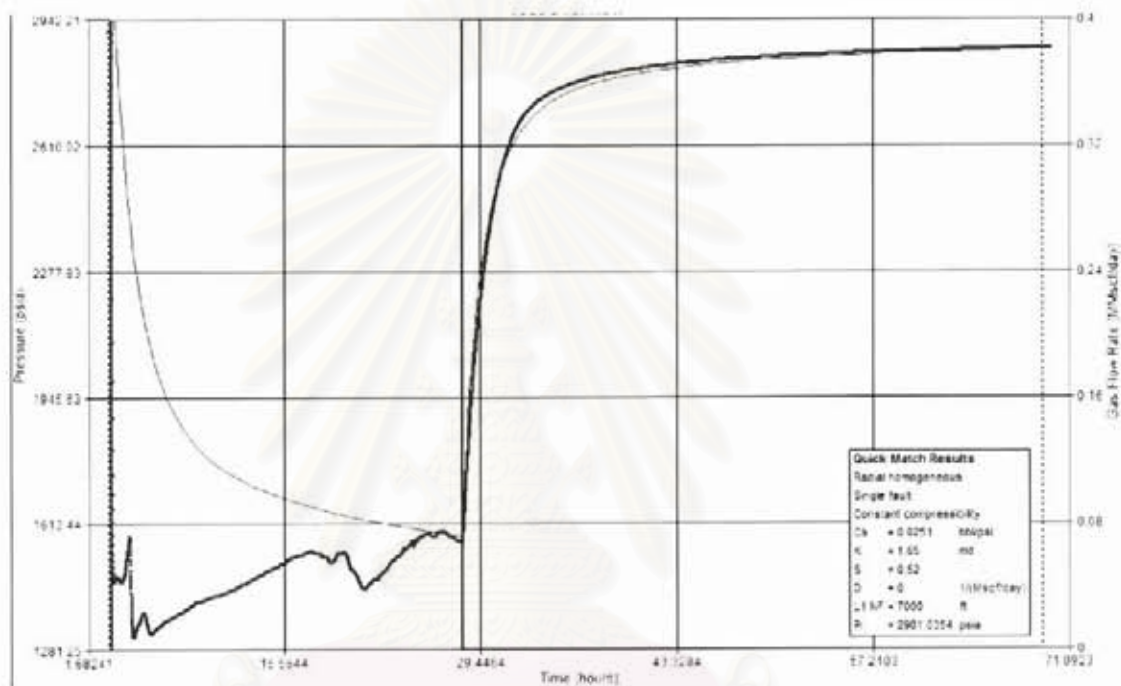


Figure A.1: Well-01 testing overview.

สถาบันวิทยบริการ
จุฬาลงกรณ์มหาวิทยาลัย

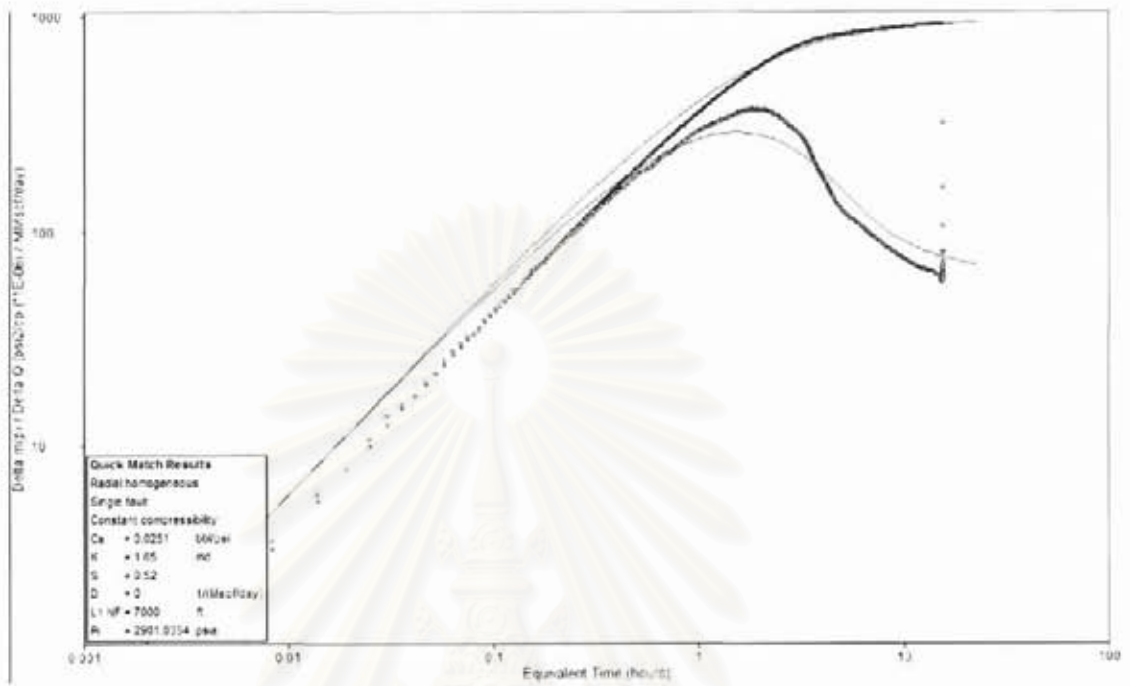


Figure A.2: Well-01 main build-up, log-log plot.

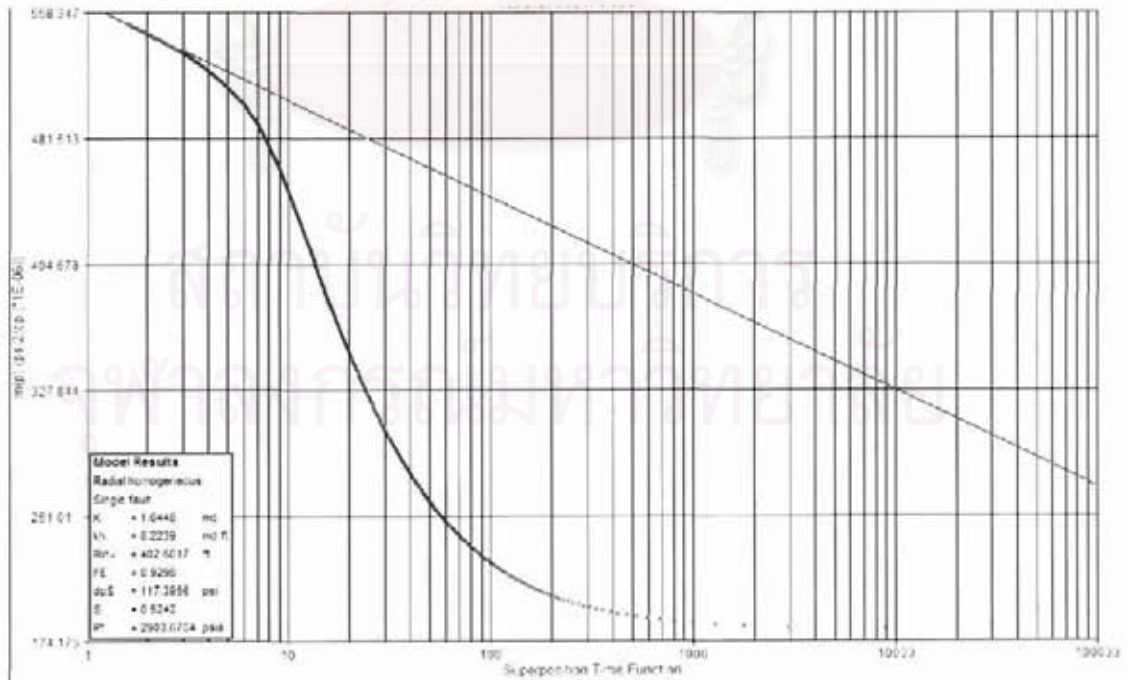


Figure A.3: Well-01 main build-up, semi-log plot.

Well-02 Reservoir 82-4

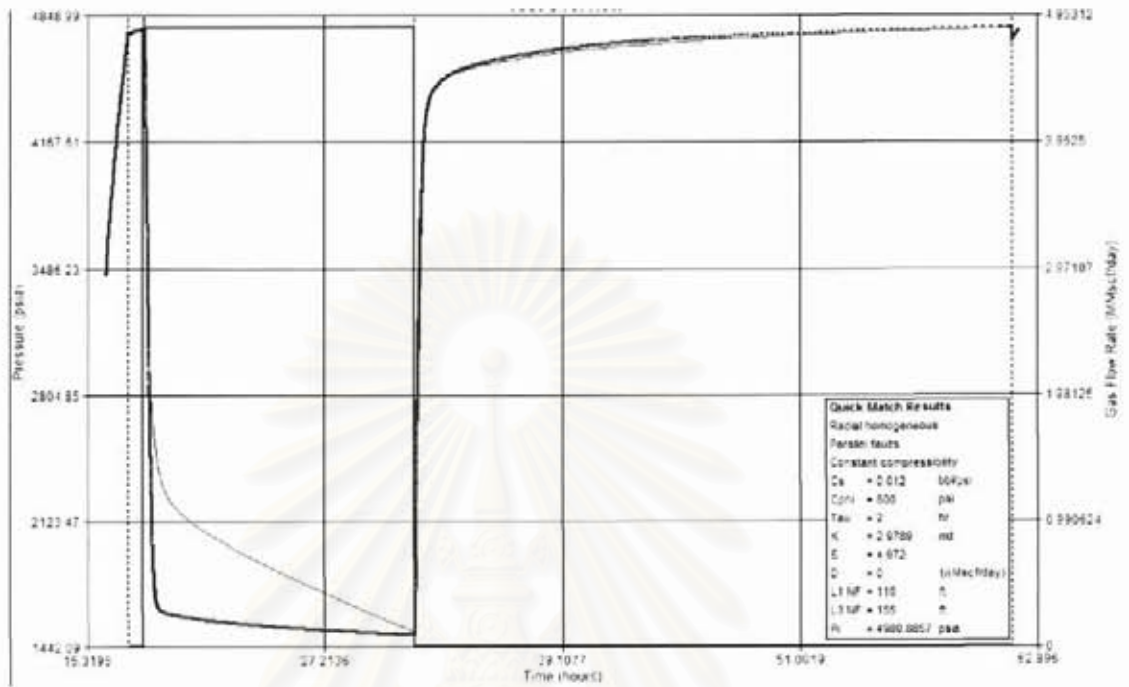


Figure A.4: Well-02 testing overview.

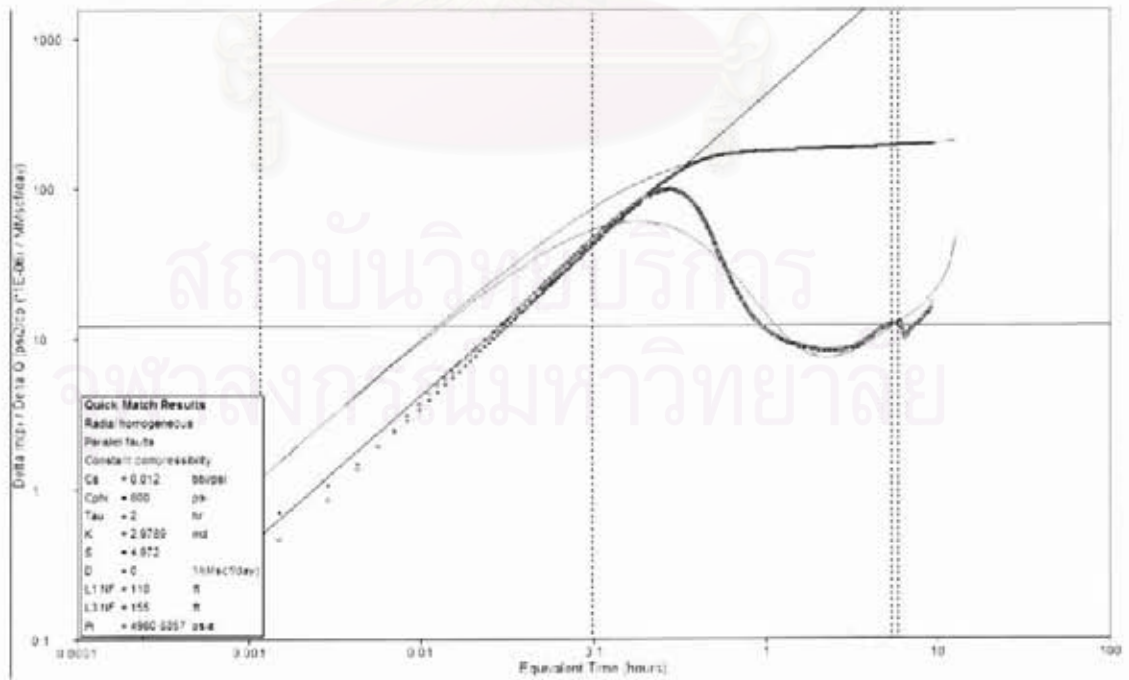


Figure A.5: Well-02 main build-up, log-log plot.

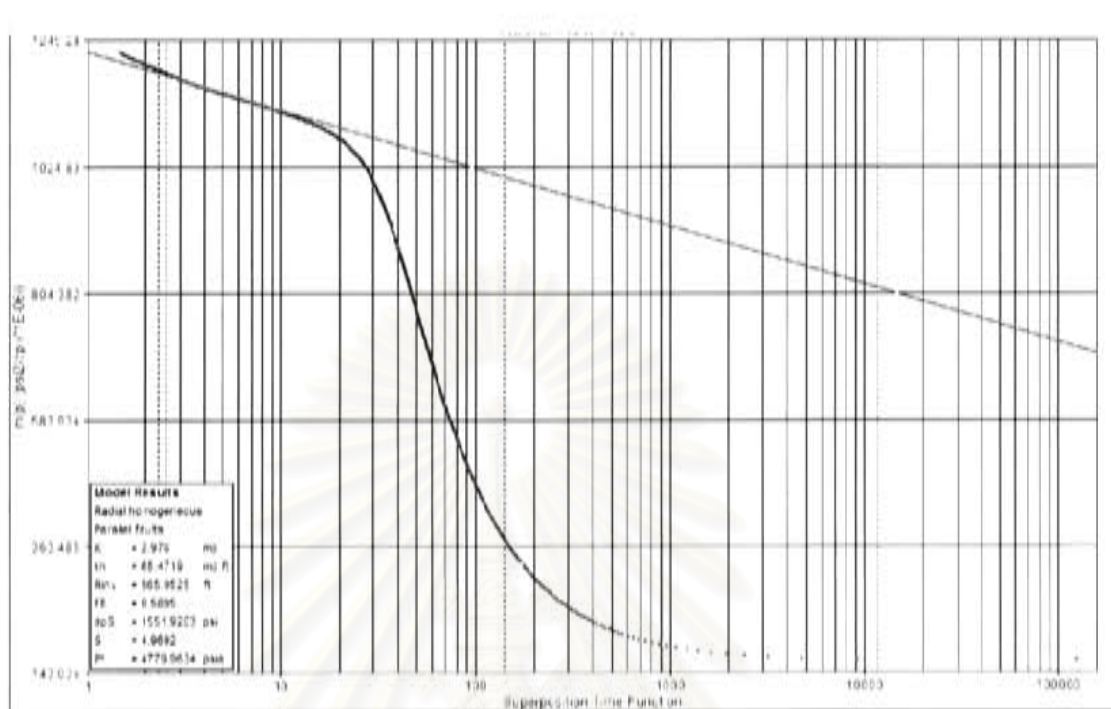


Figure A.6: Well-02 main build-up, semi-log plot.

สถาบันวิทยบริการ
 จุฬาลงกรณ์มหาวิทยาลัย

Well-03 Reservoir 92-4

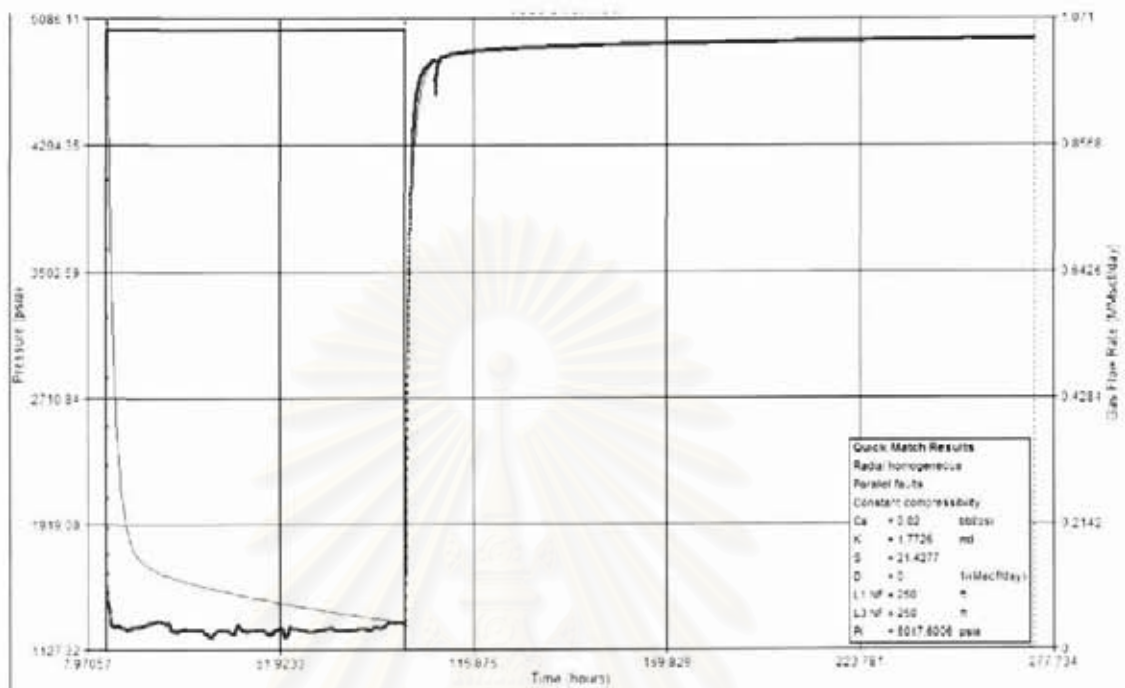


Figure A.7: Well-03 testing overview.

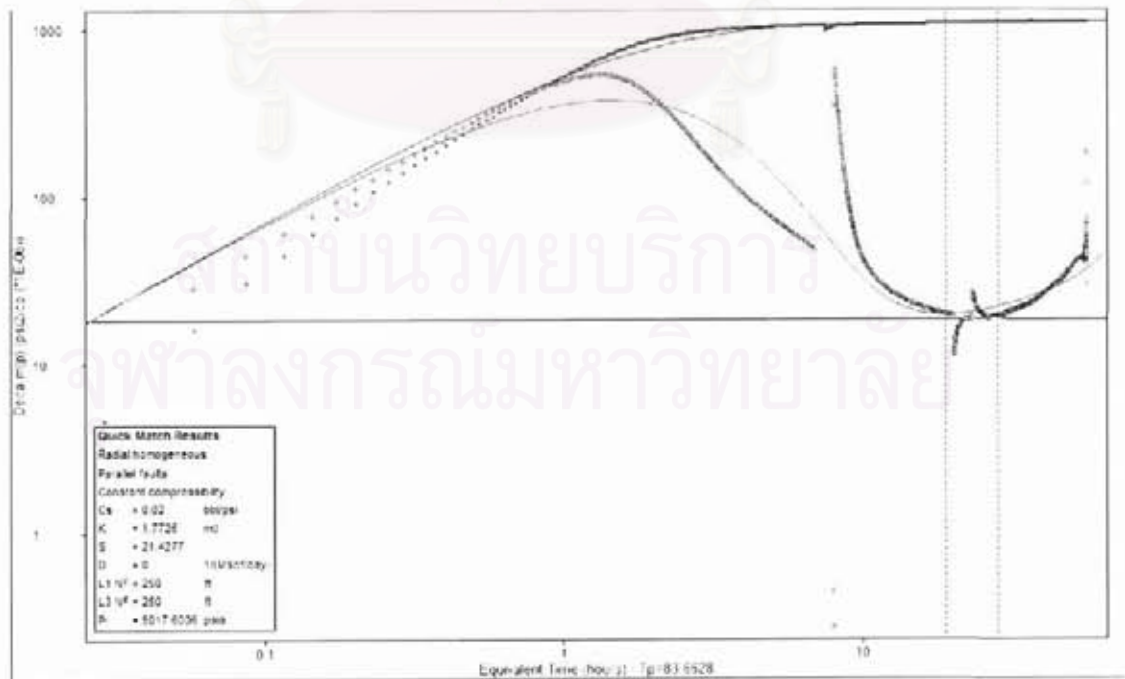


Figure A.8: Well-03 main build-up, log-log plot.

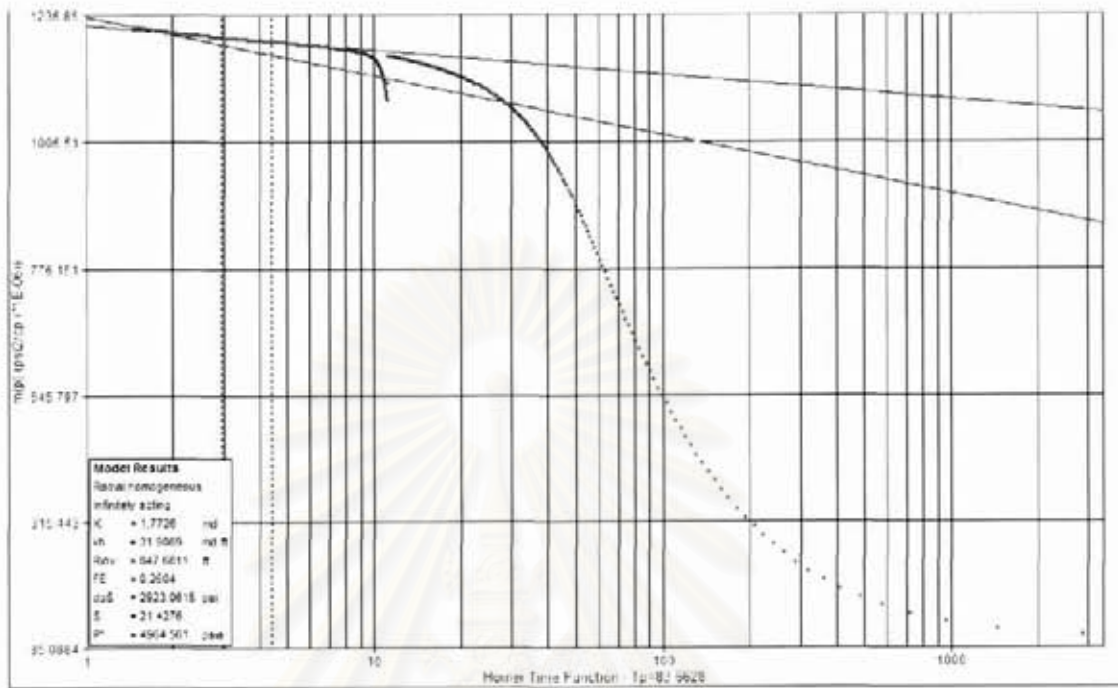


Figure A.9: Well-03 main build-up, semi-log plot.

สถาบันวิทยบริการ
จุฬาลงกรณ์มหาวิทยาลัย

Well-04 Reservoir 95-6

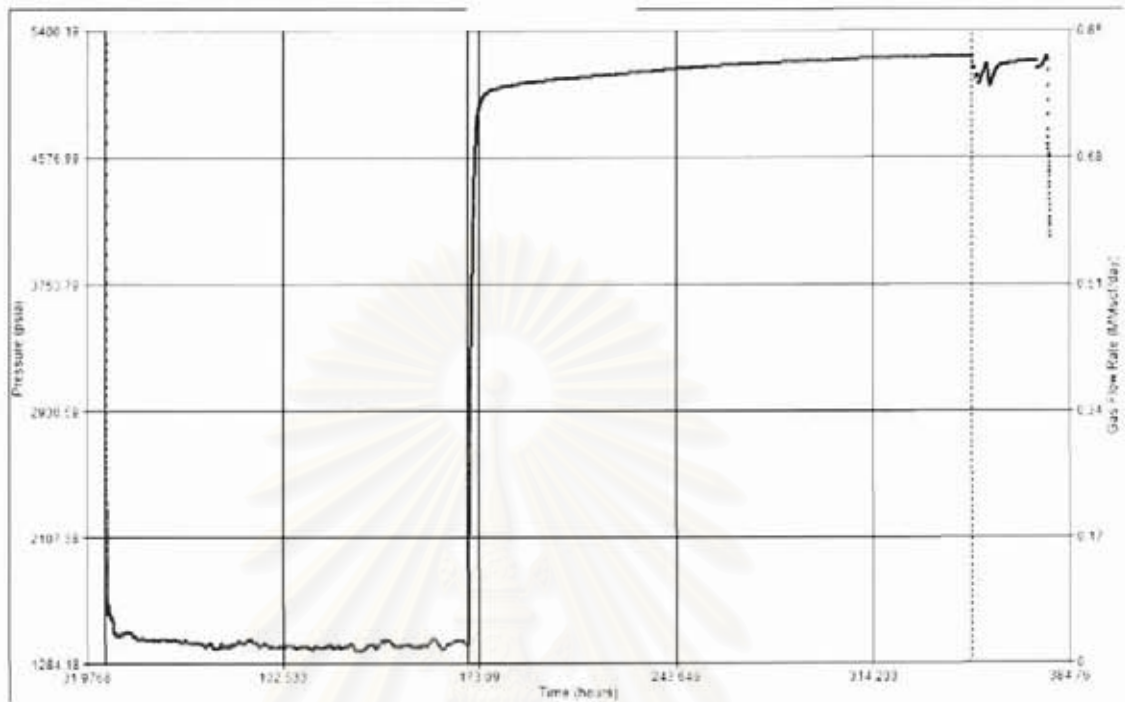


Figure A.10: Well-04 testing overview.

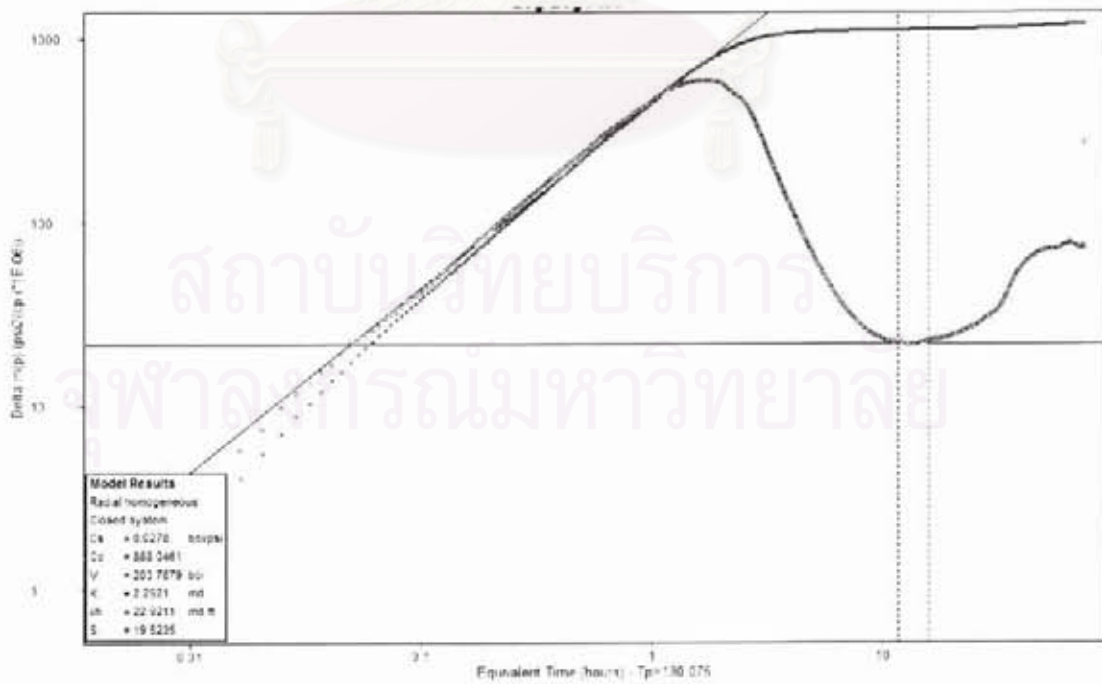


Figure A.11: Well-04 main build-up, log-log plot.

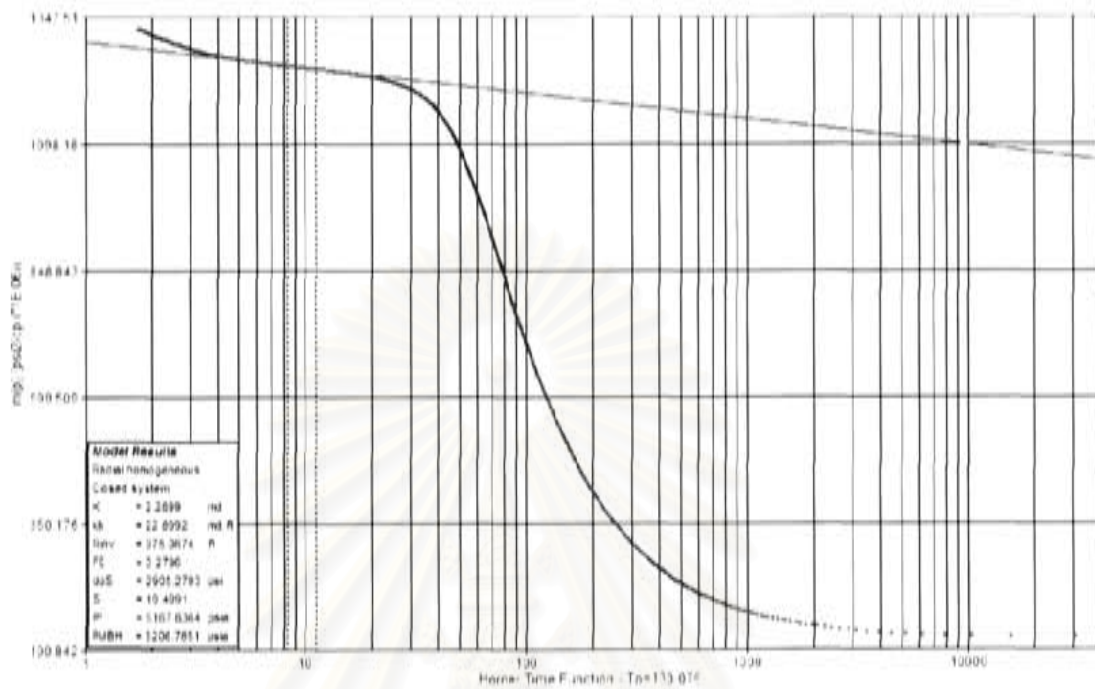


Figure A.12: Well-04 main build-up, semi-log plot.

สถาบันวิทยบริการ
จุฬาลงกรณ์มหาวิทยาลัย

Well-05 Reservoir 75-6

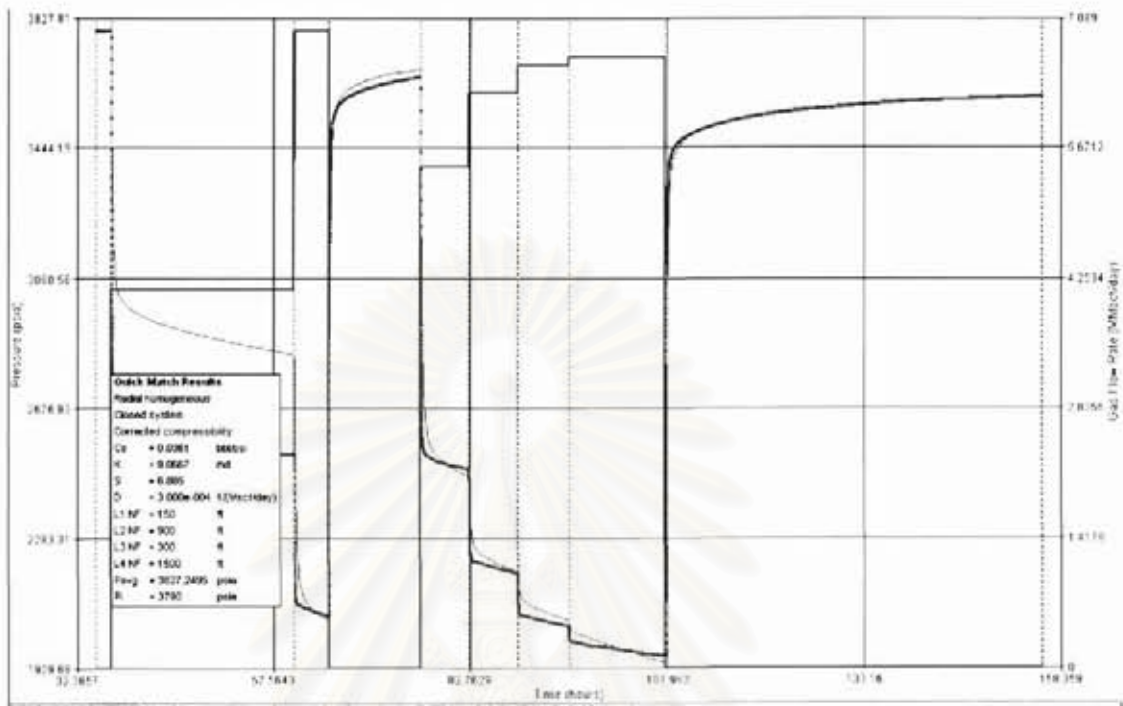


Figure A.13: Well-05 testing overview.

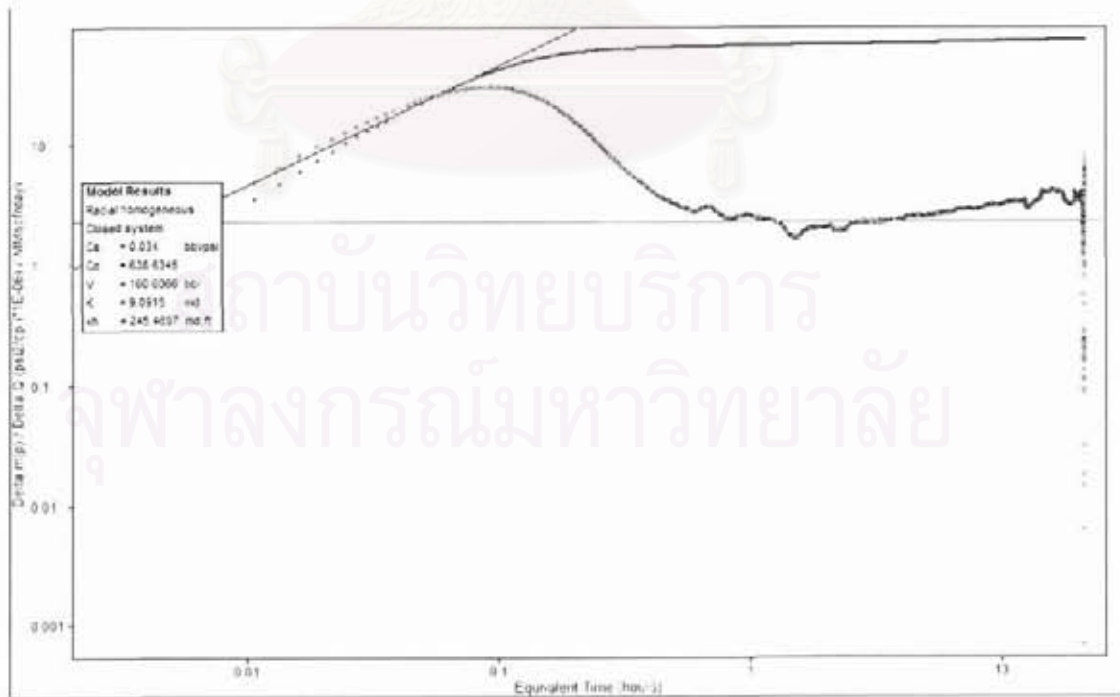


Figure A.14: Well-05 main build-up, log-log plot.

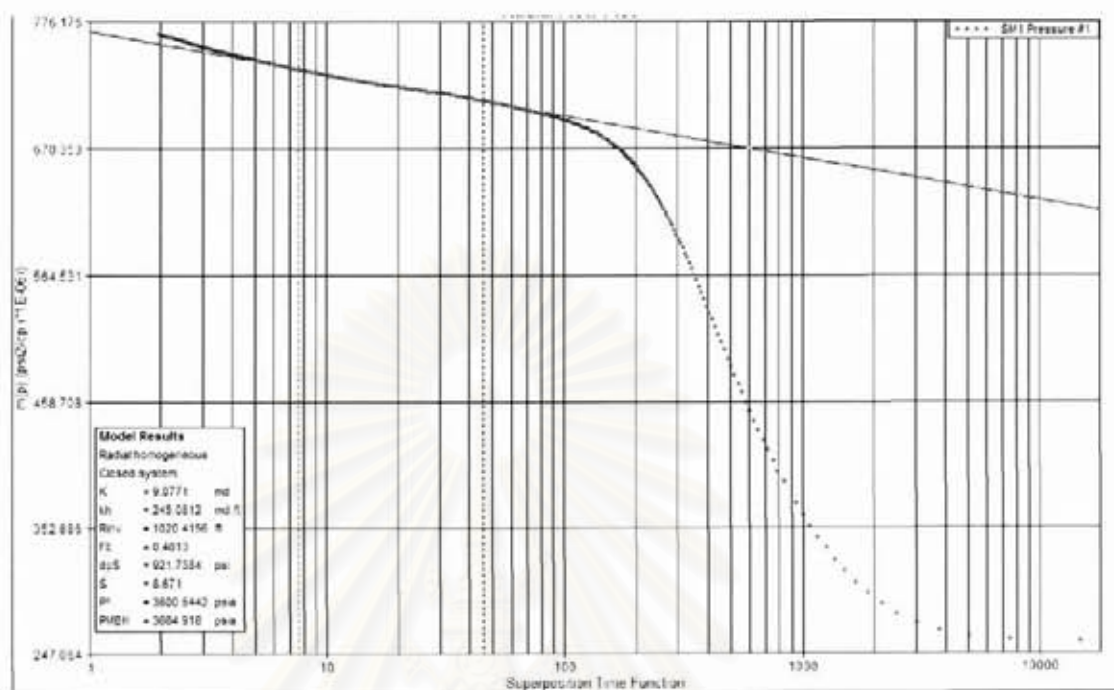


Figure A.15: Well-05 main build-up, semi-log plot.

สถาบันวิทยบริการ
จุฬาลงกรณ์มหาวิทยาลัย

Well-06 Reservoir 69-2

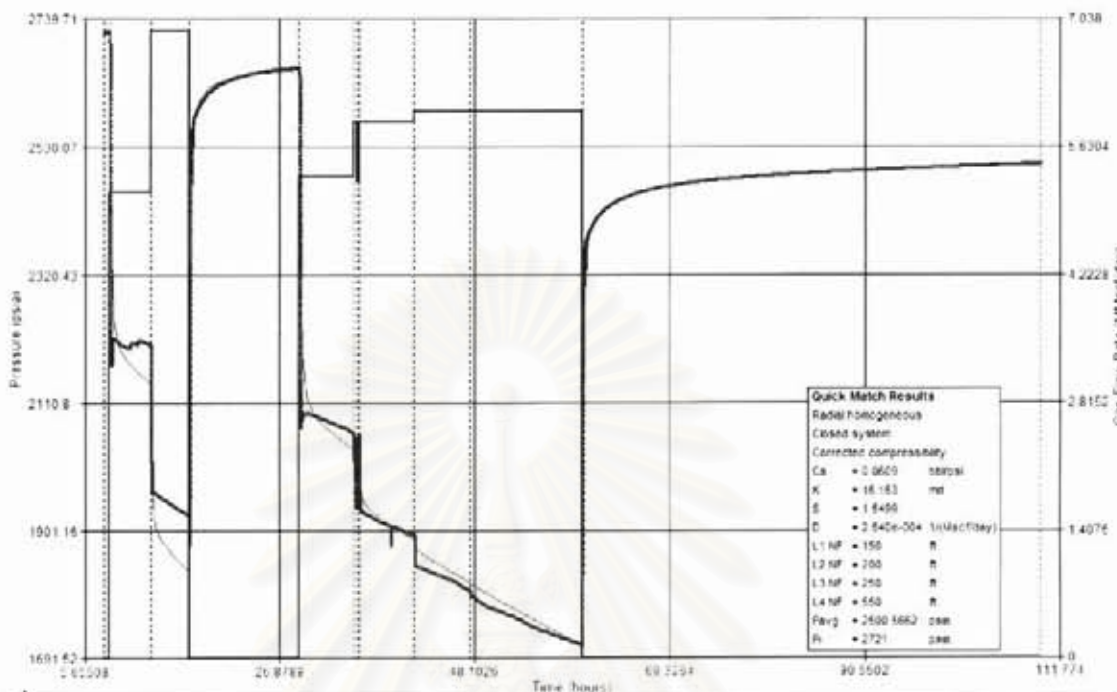


Figure A.16: Well-06 testing overview.

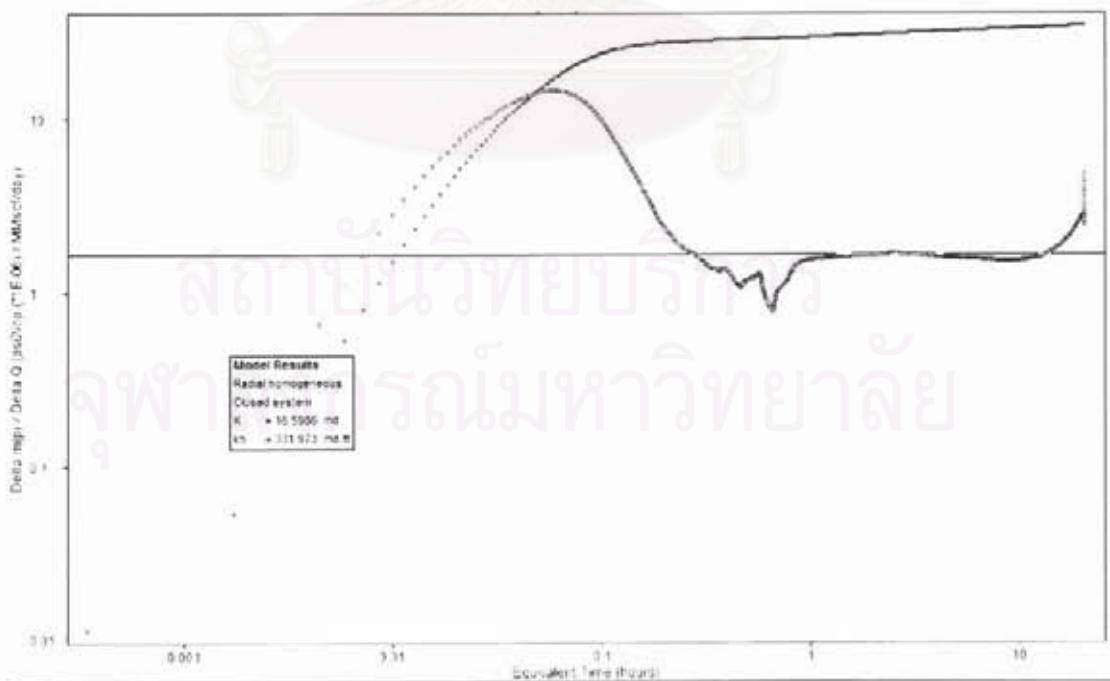


Figure A.17: Well-06 main build-up, log-log plot.

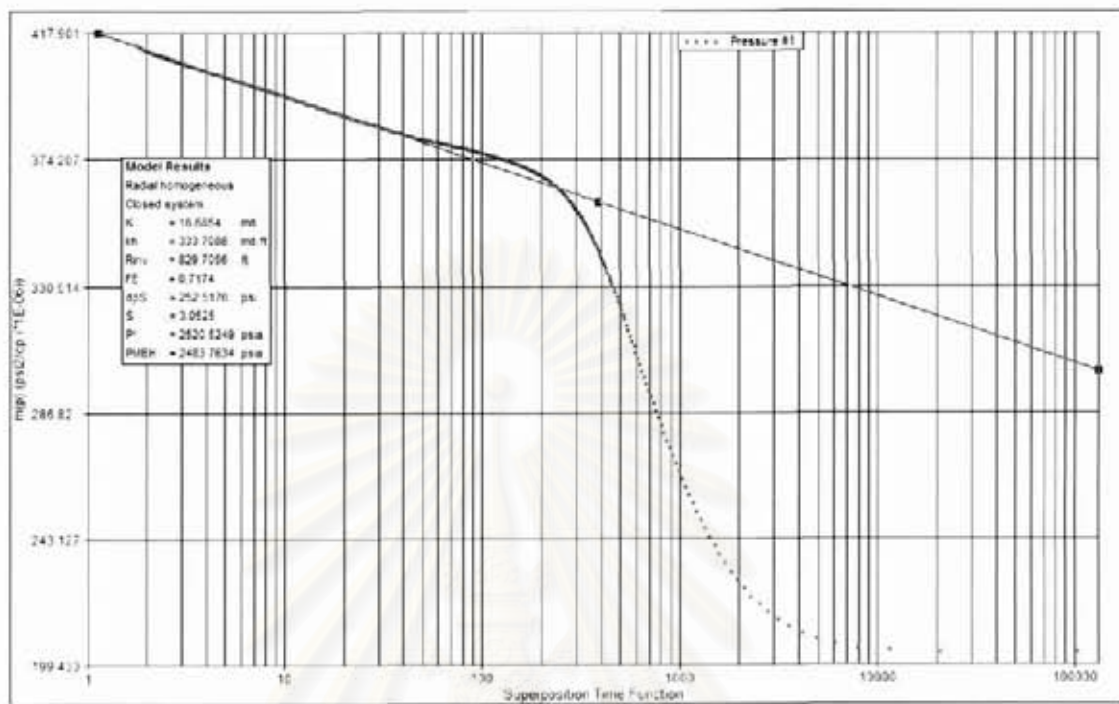


Figure A.18: Well-06 main build-up, semi-log plot.

สถาบันวิทยบริการ
 จุฬาลงกรณ์มหาวิทยาลัย

Well-07 Reservoir 81-7

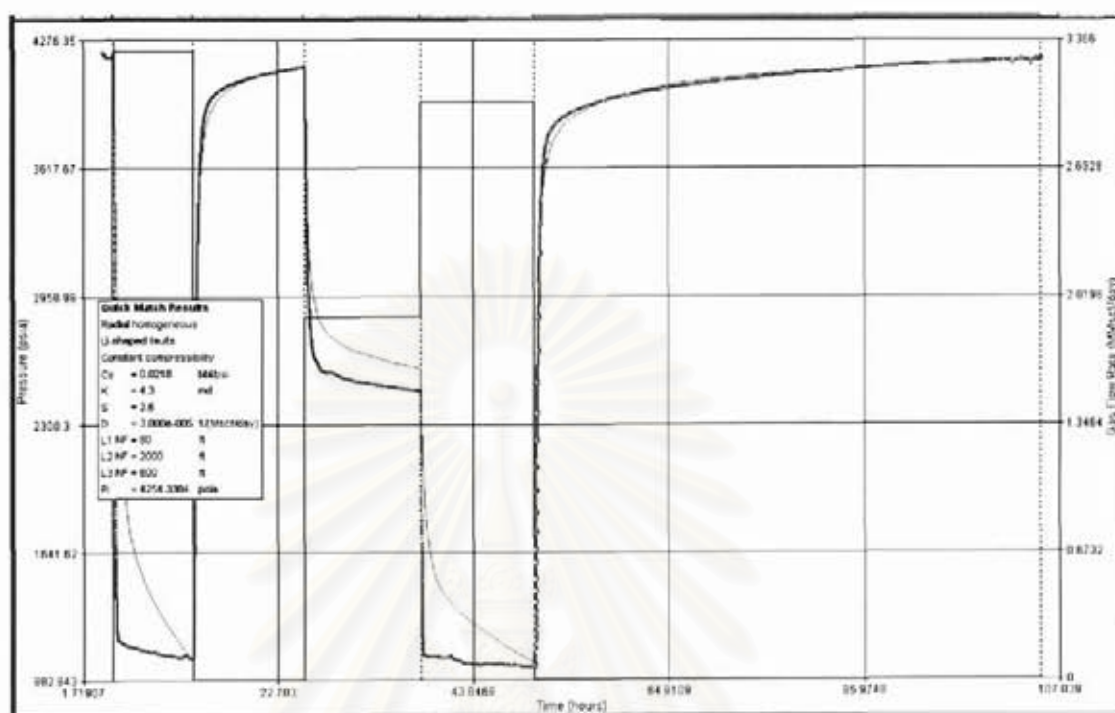


Figure A.19: Well-07 testing overview.

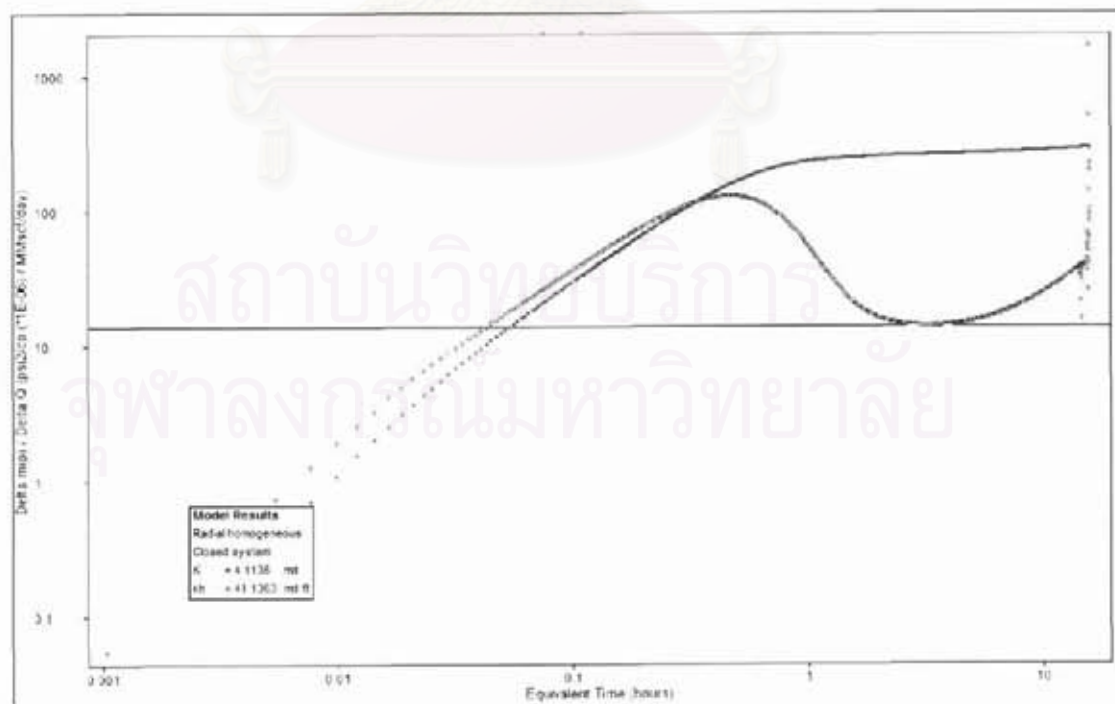


Figure A.20: Well-07 main build-up, log-log plot.

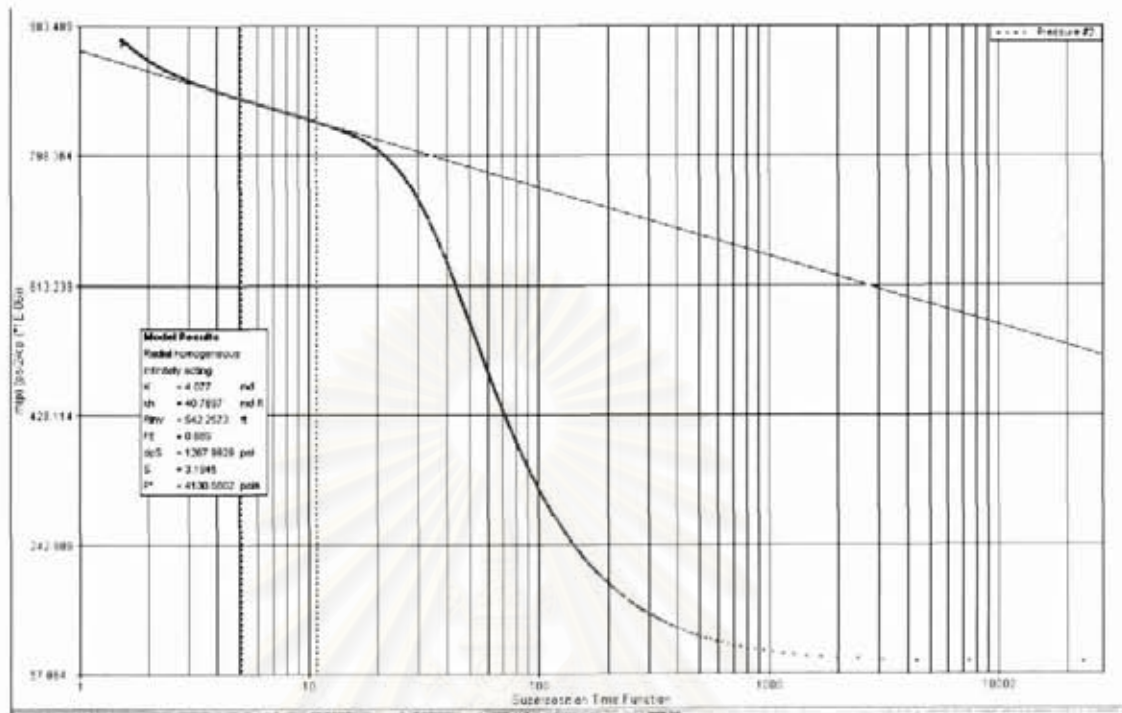


Figure A.21: Well-07 main build-up, semi-log plot.

สถาบันวิทยบริการ
จุฬาลงกรณ์มหาวิทยาลัย

Well-08 Reservoir 63-4

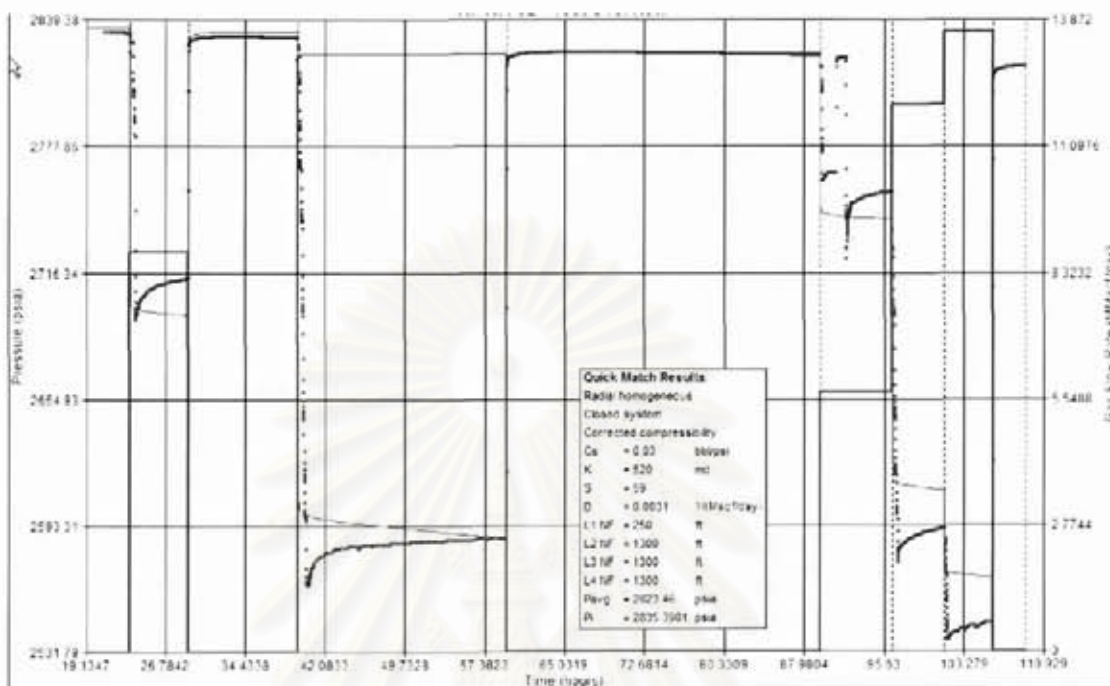


Figure A.22: Well-08 testing overview.

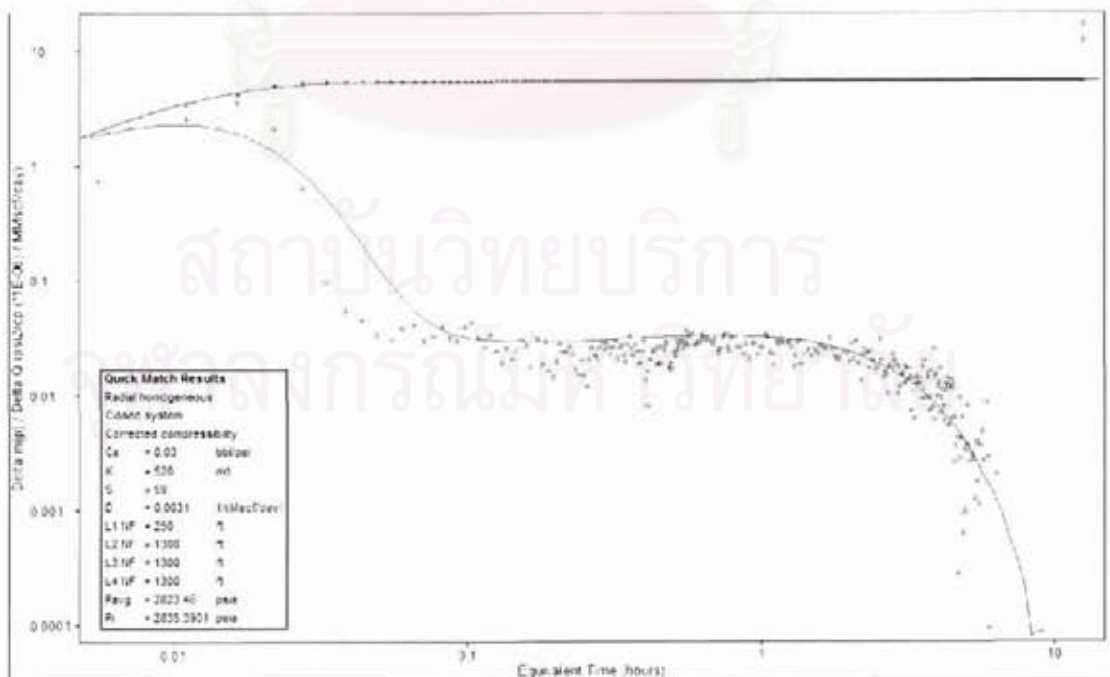


Figure A.23: Well-08 main build-up, log-log plot.

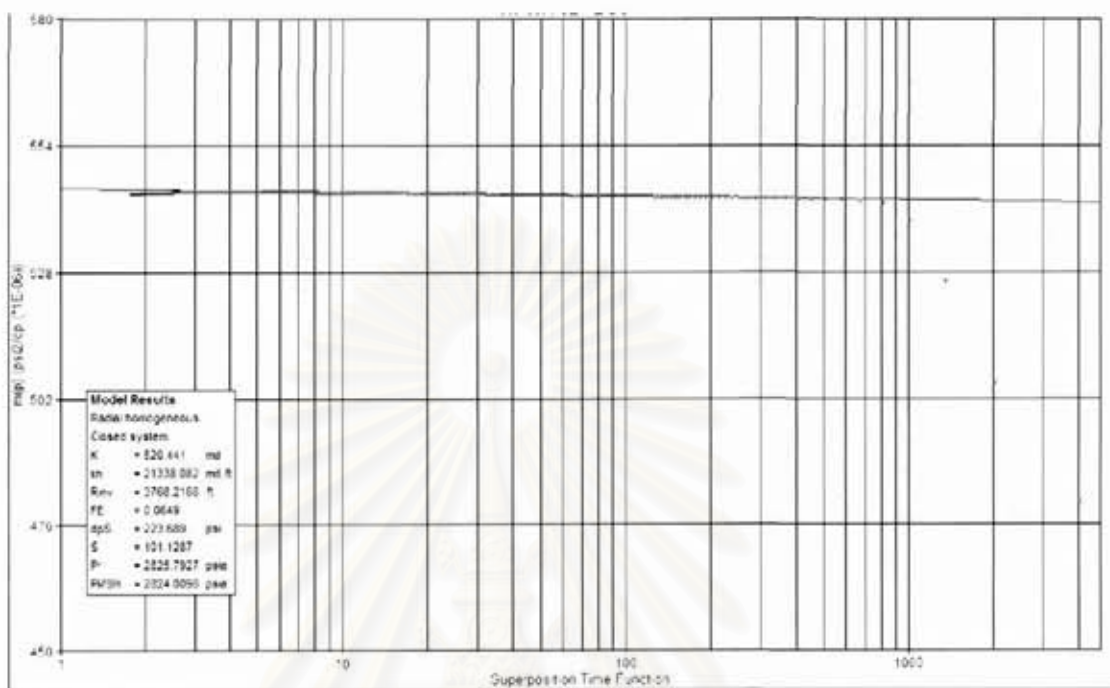


Figure A.24: Well-08 main build-up, semi-log plot.

สถาบันวิทยบริการ
จุฬาลงกรณ์มหาวิทยาลัย

Well-09 Reservoir 89-5

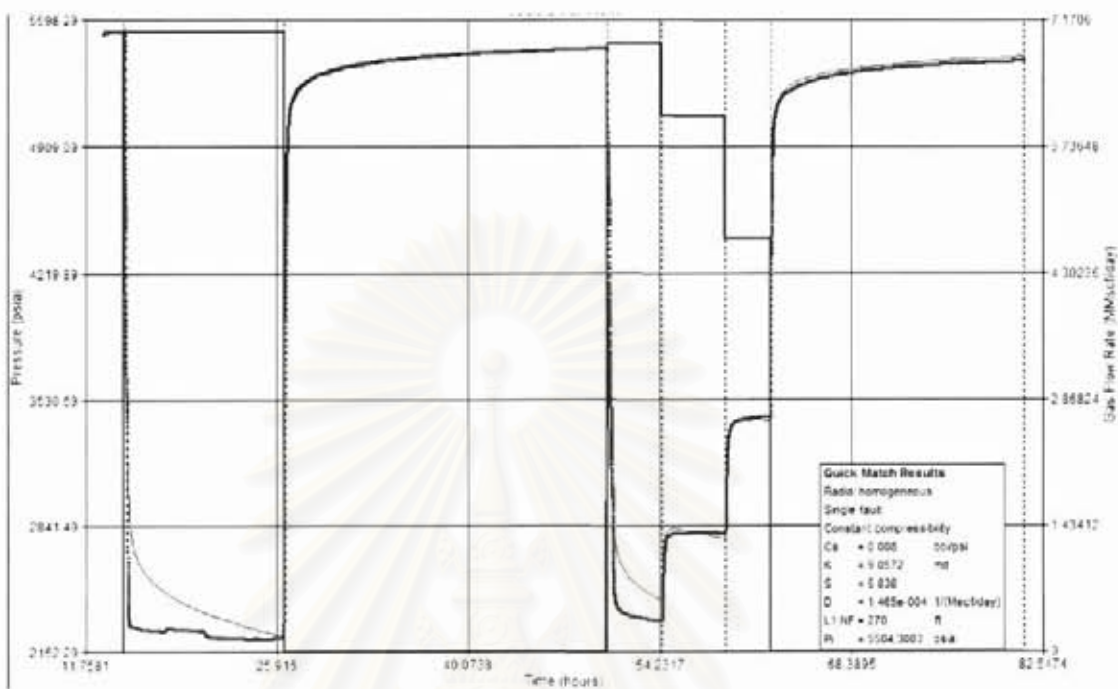


Figure A.25: Well-09 testing overview.

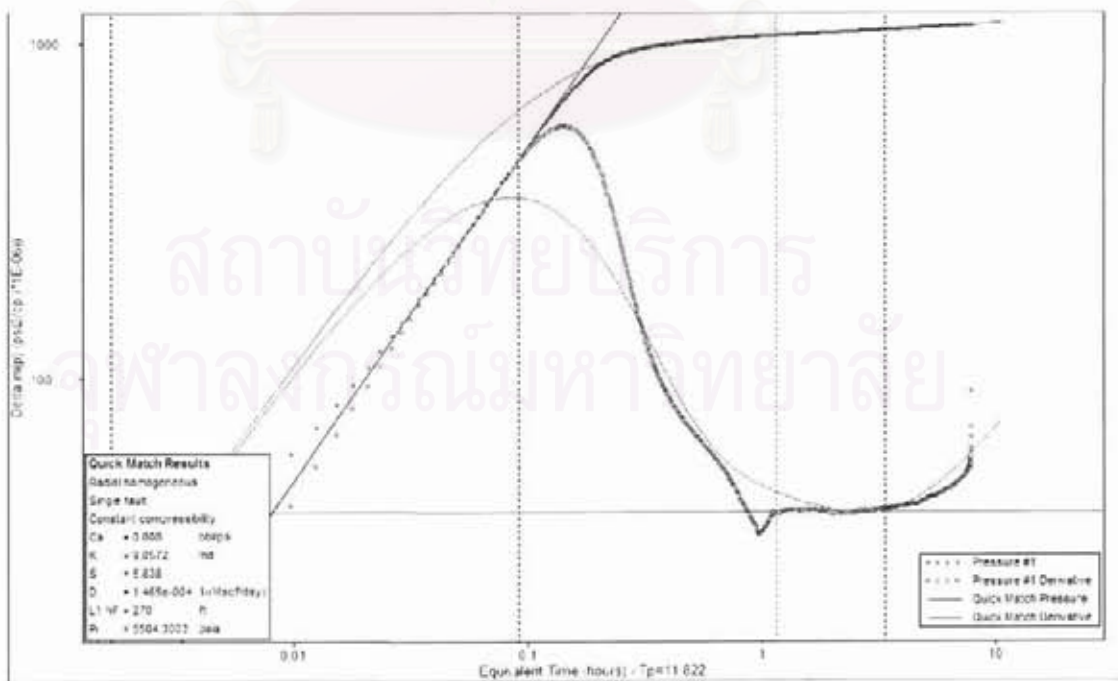


Figure A.26: Well-09 main build-up, log-log plot.

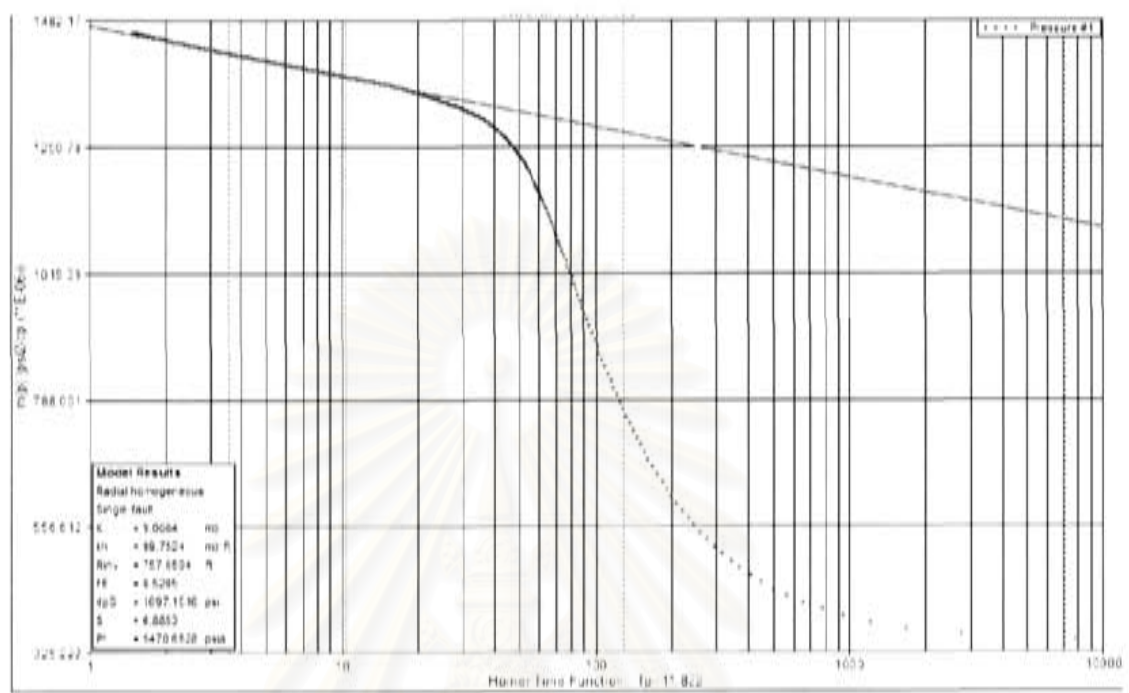


Figure A.27: Well-09 main build-up, semi-log plot.

สถาบันวิทยบริการ
 จุฬาลงกรณ์มหาวิทยาลัย

Well-10 Reservoir 52-2



Figure A.28: Well-10 testing overview.

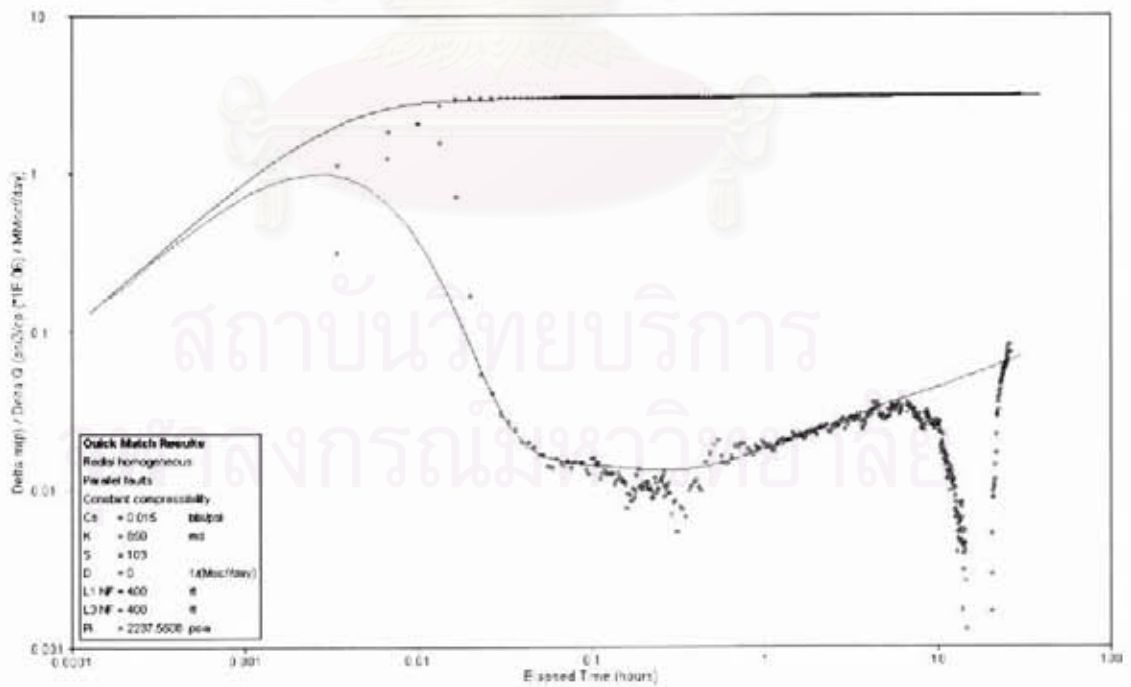


Figure A.29: Well-10 main build-up, log-log plot.

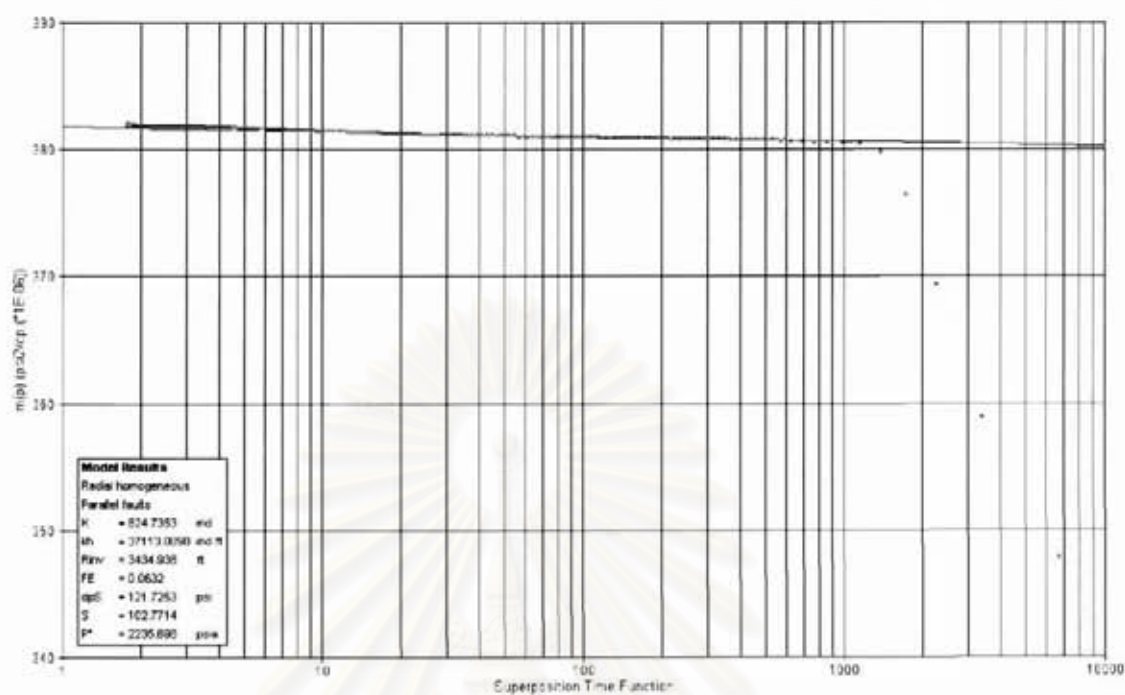


Figure A.30: Well-10 main build-up, semi-log plot.

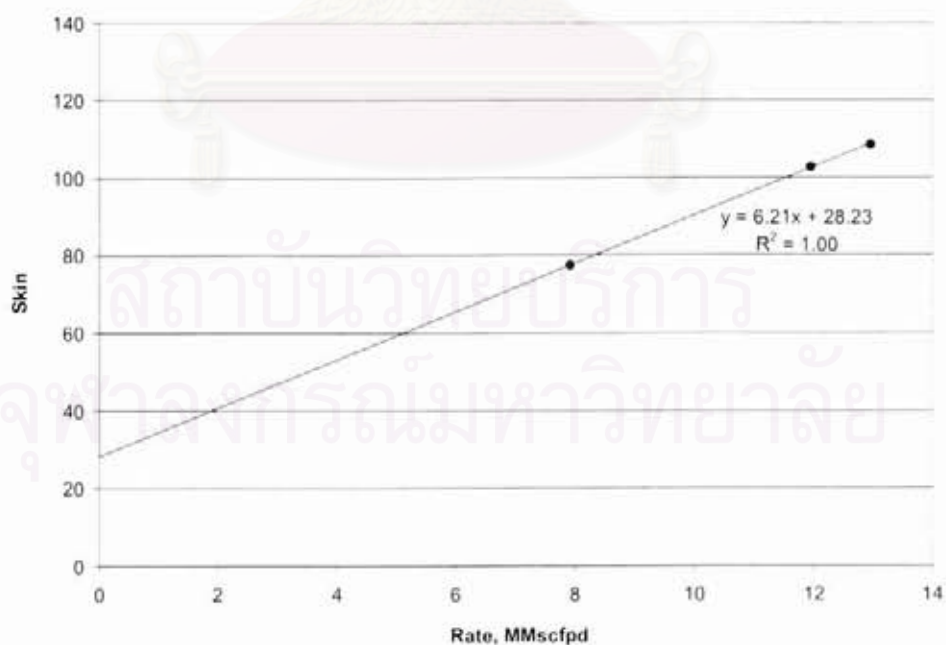


Figure A.31: Well-10 Rate Dependent Skin Plot

Well-11 Reservoir 55-8

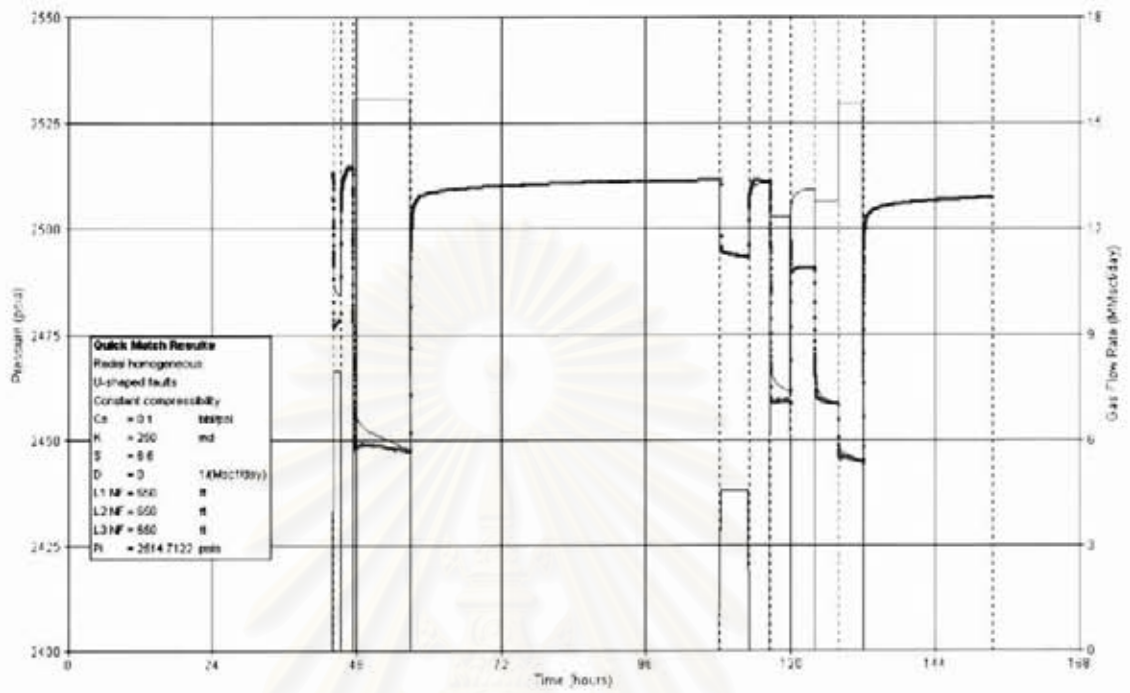


Figure A.32: Well-11 testing overview.

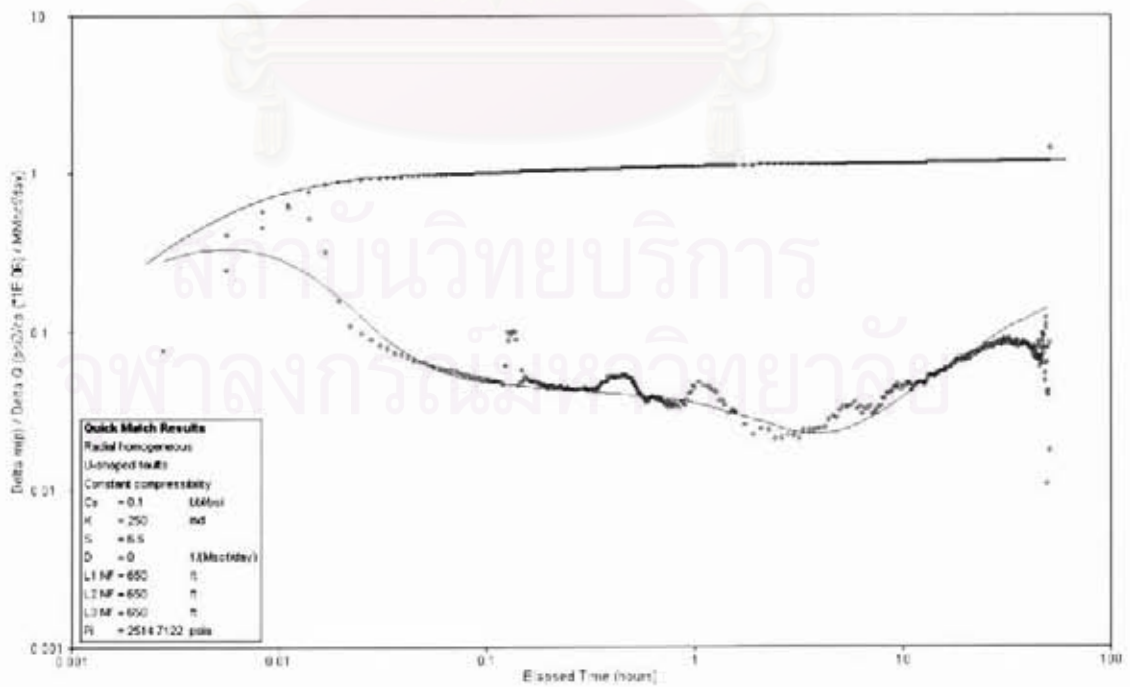


Figure A.33: Well-11 main build-up, log-log plot.

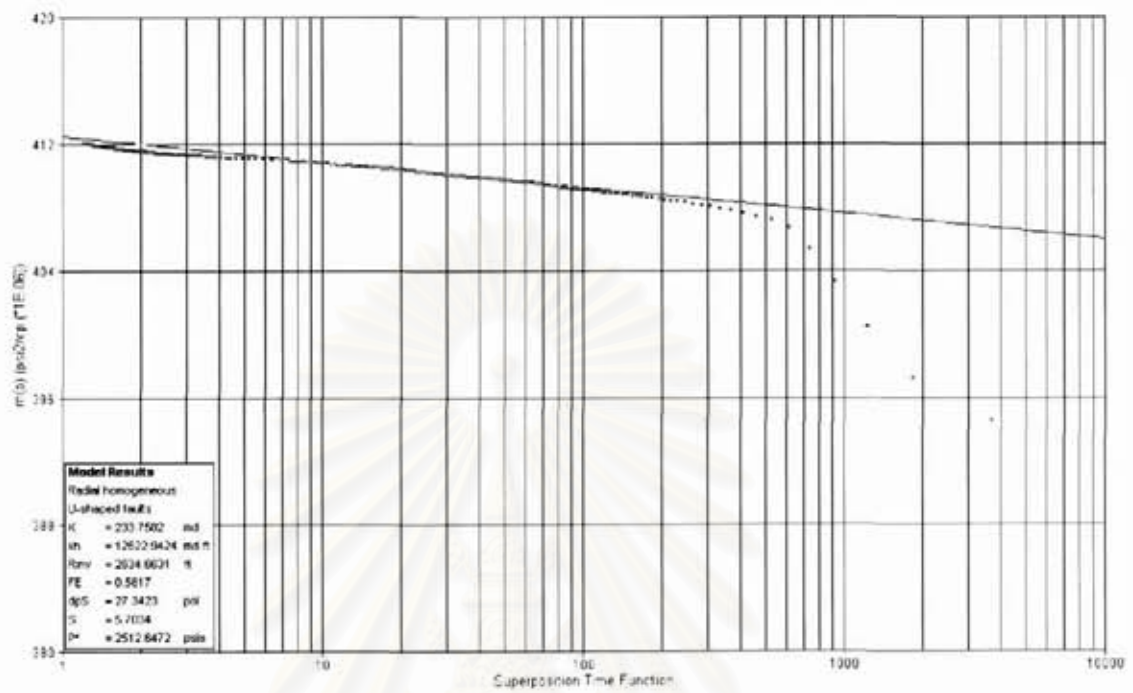


Figure A.34: Well-11 main build-up, semi-log plot.

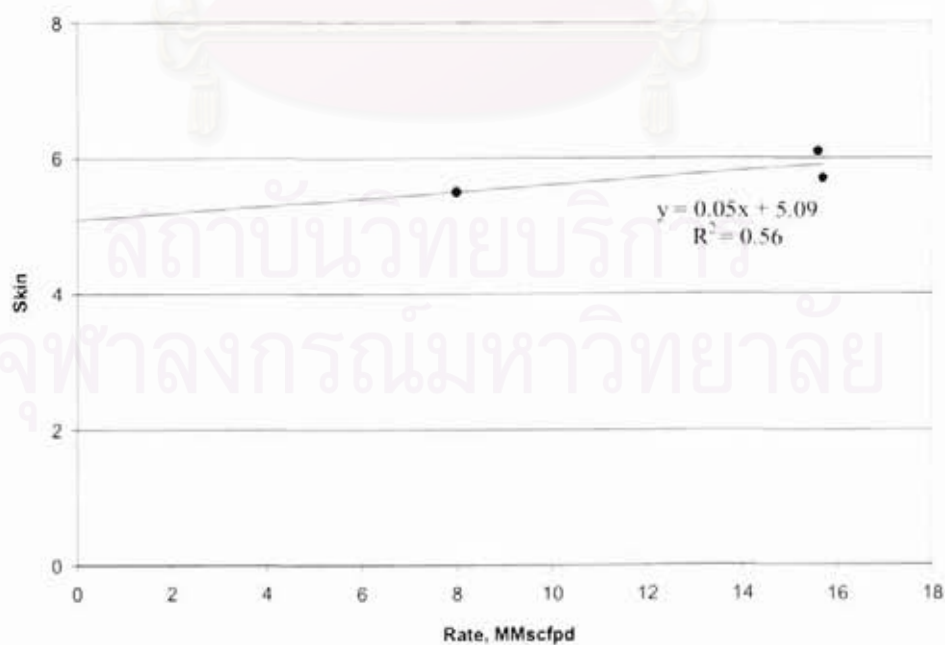


Figure A.35: Well-11 Rate Dependent Skin Plot

Well-12 Reservoir 56-1

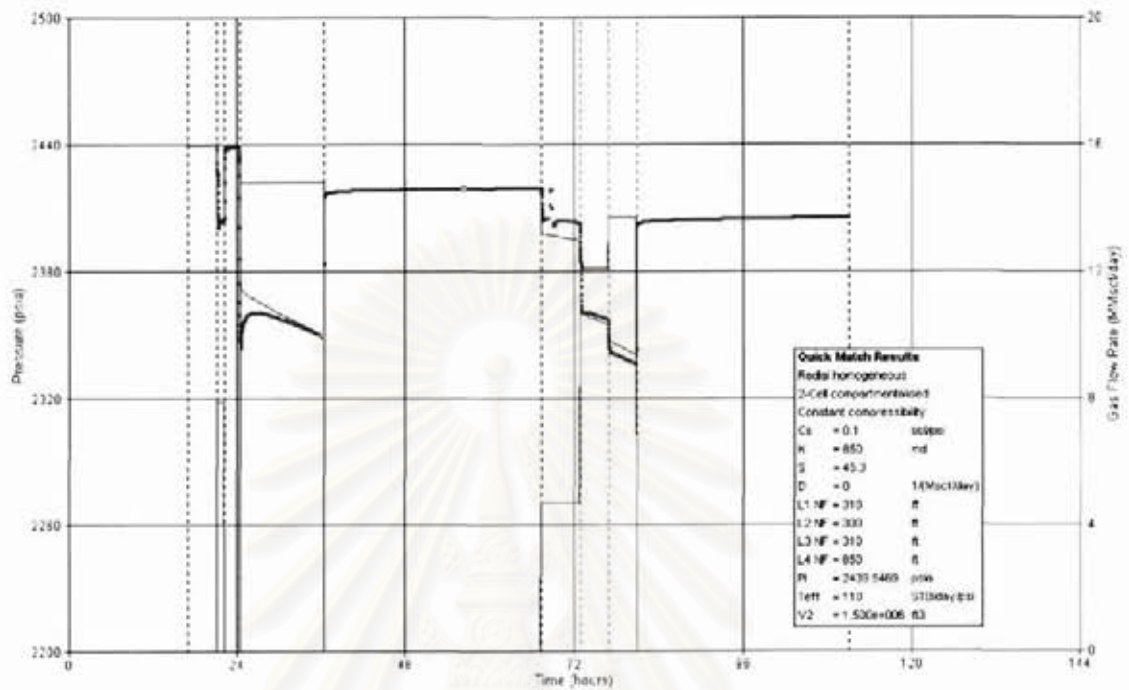


Figure A.36: Well-12 testing overview.

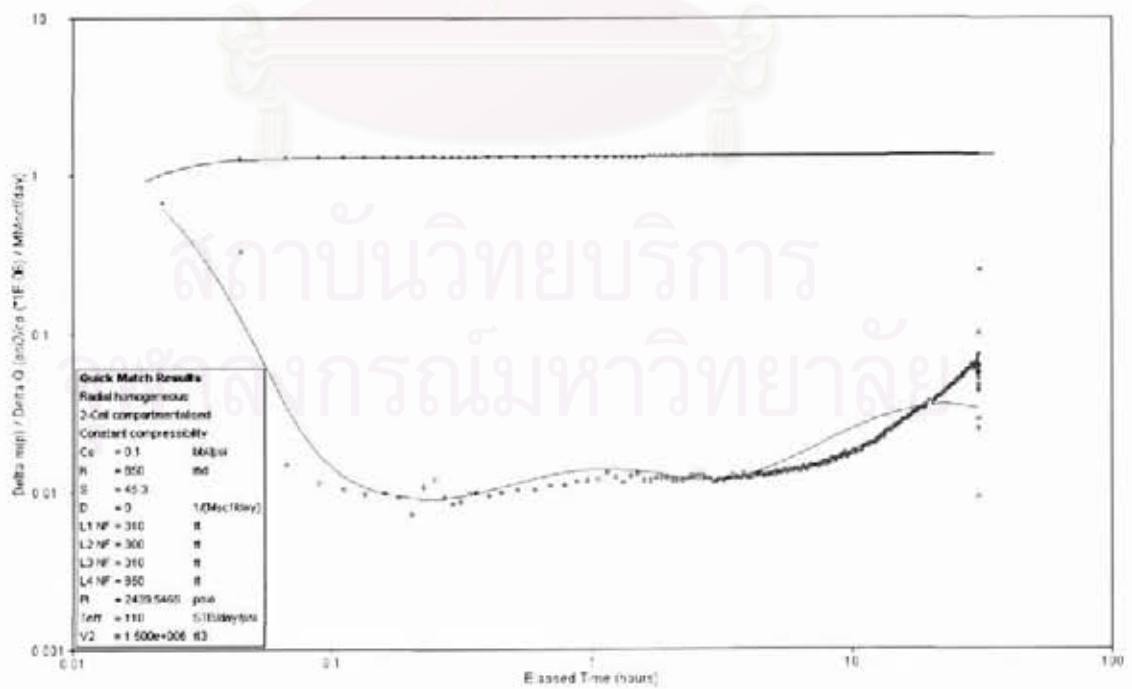


Figure A.37: Well-12 main build-up, log-log plot.

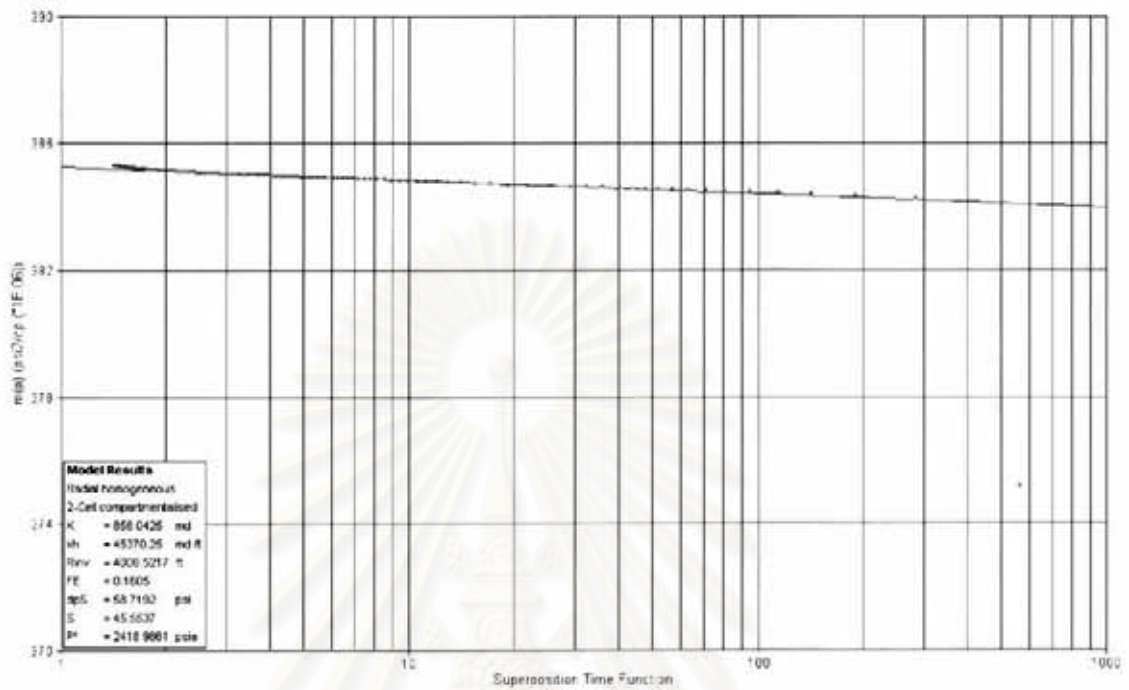


Figure A.38: Well-12 main build-up, semi-log plot.

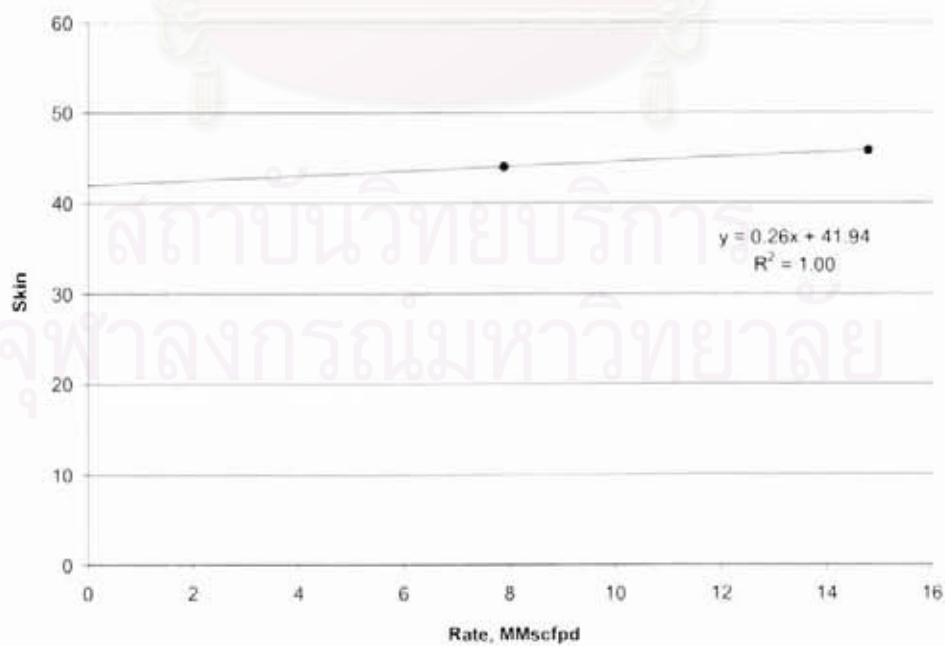


Figure A.39: Well-12 Rate Dependent Skin Plot

Well-13 Reservoir 59-1

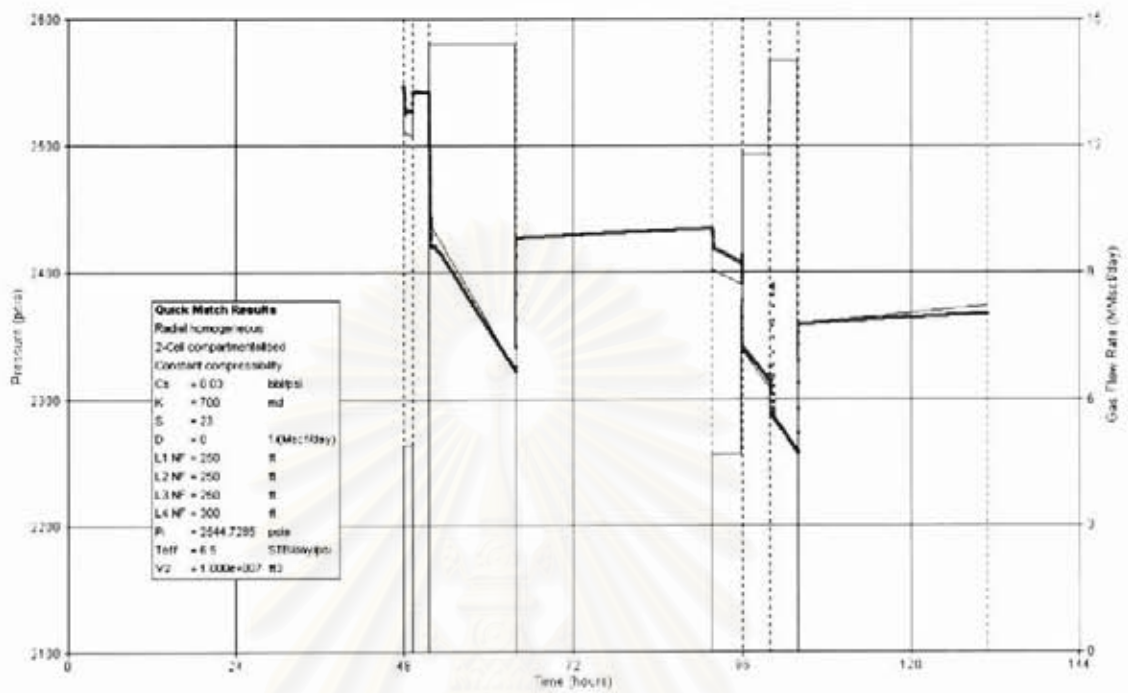


Figure A.40: Well-13 testing overview.

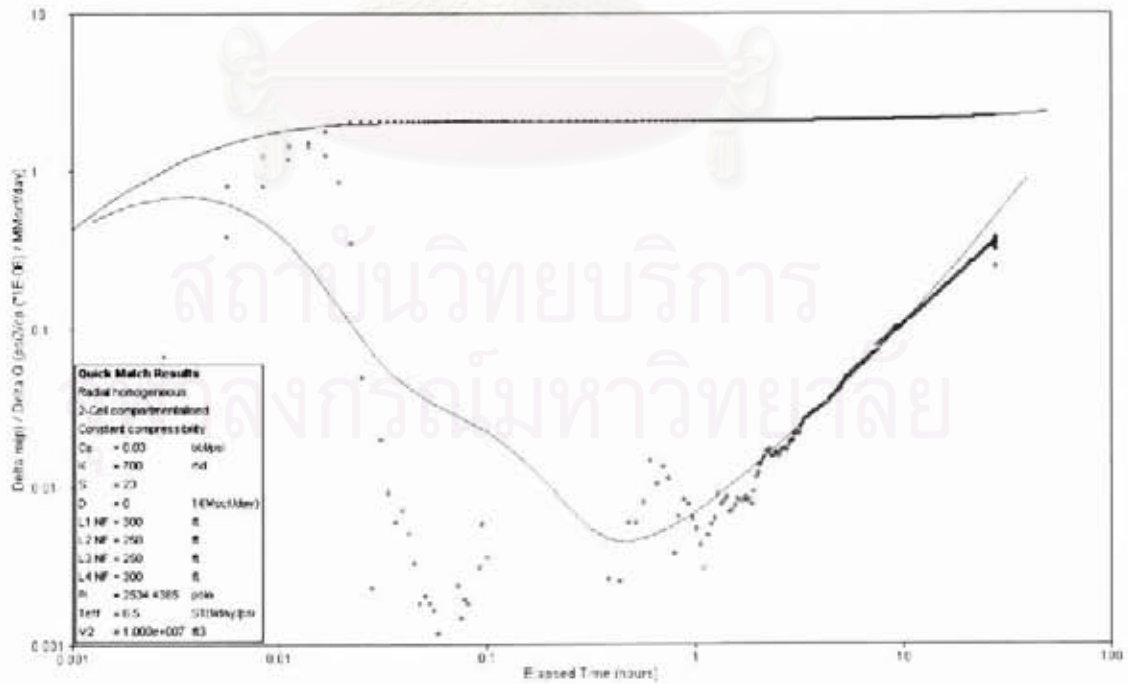


Figure A.41: Well-13 main build-up, log-log plot.

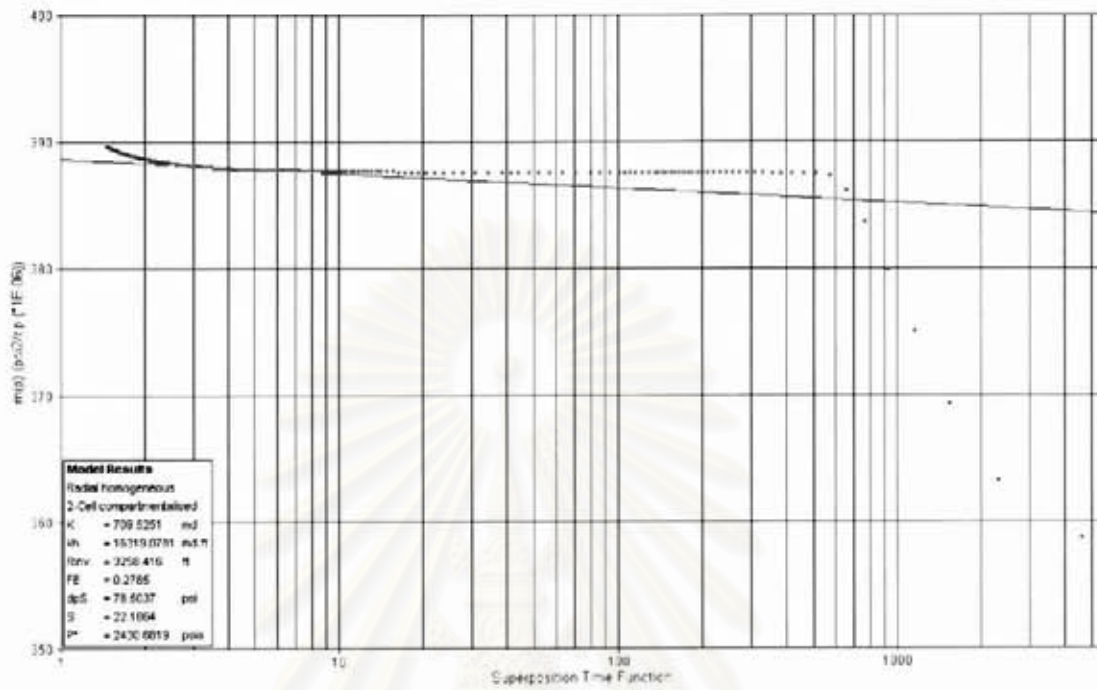


Figure A.42: Well-13 main build-up, semi-log plot.

สถาบันวิทยบริการ
จุฬาลงกรณ์มหาวิทยาลัย

Well-14 Reservoir 72-7

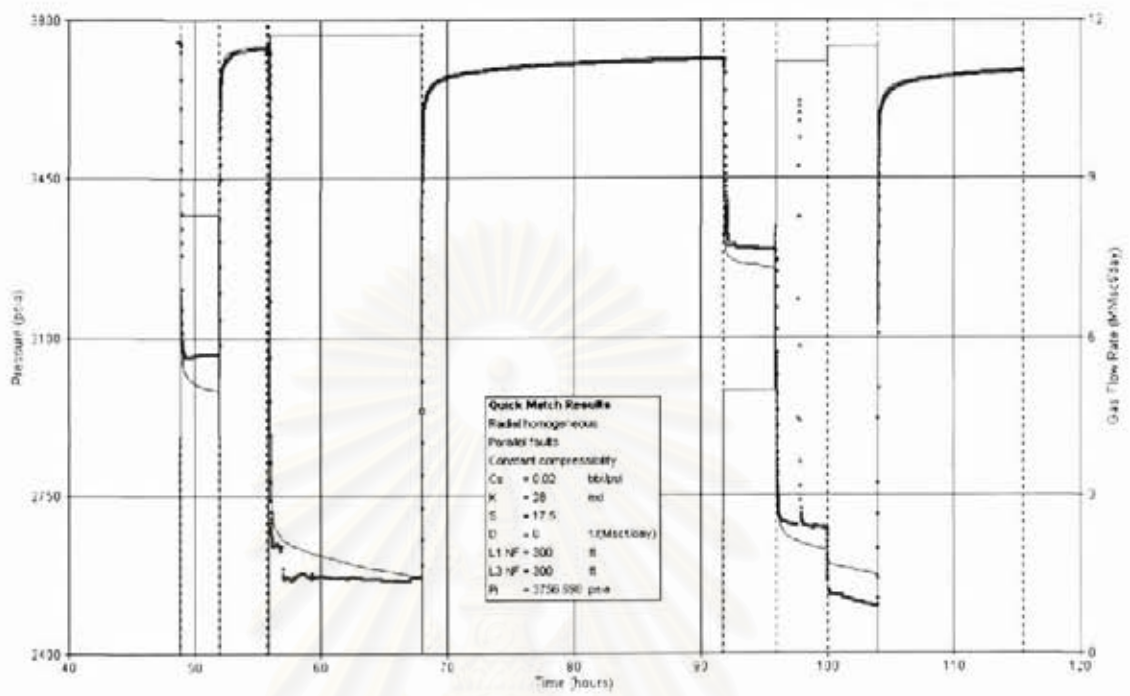


Figure A.43: Well-14 testing overview.

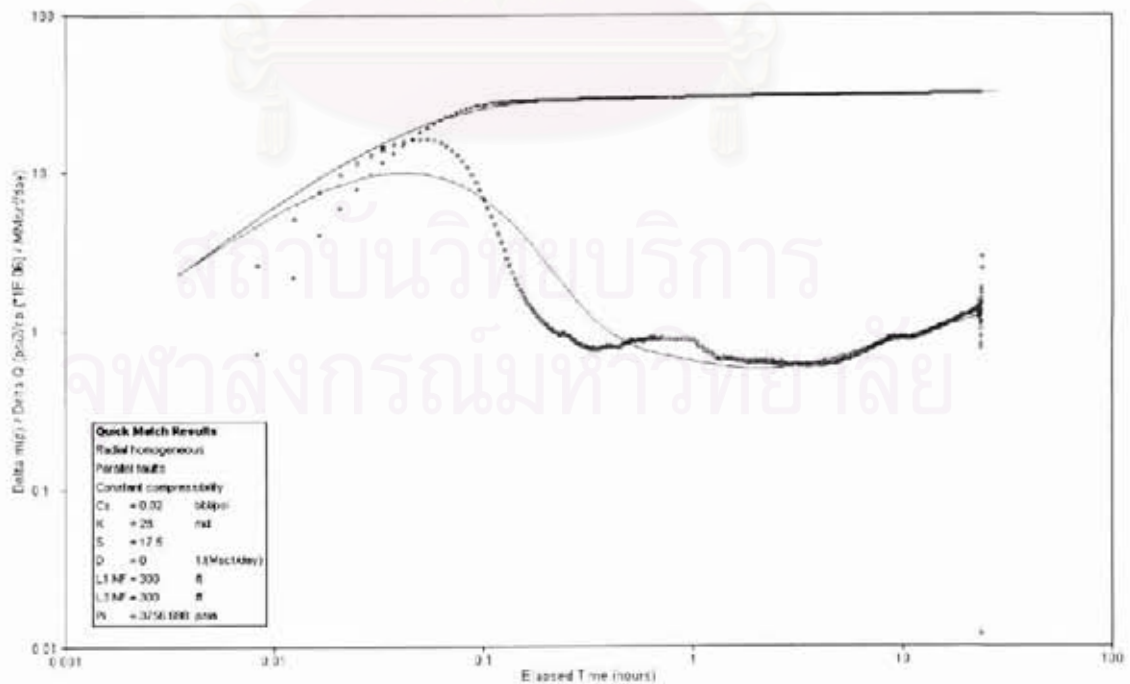


Figure A.44: Well-14 main build-up, log-log plot.

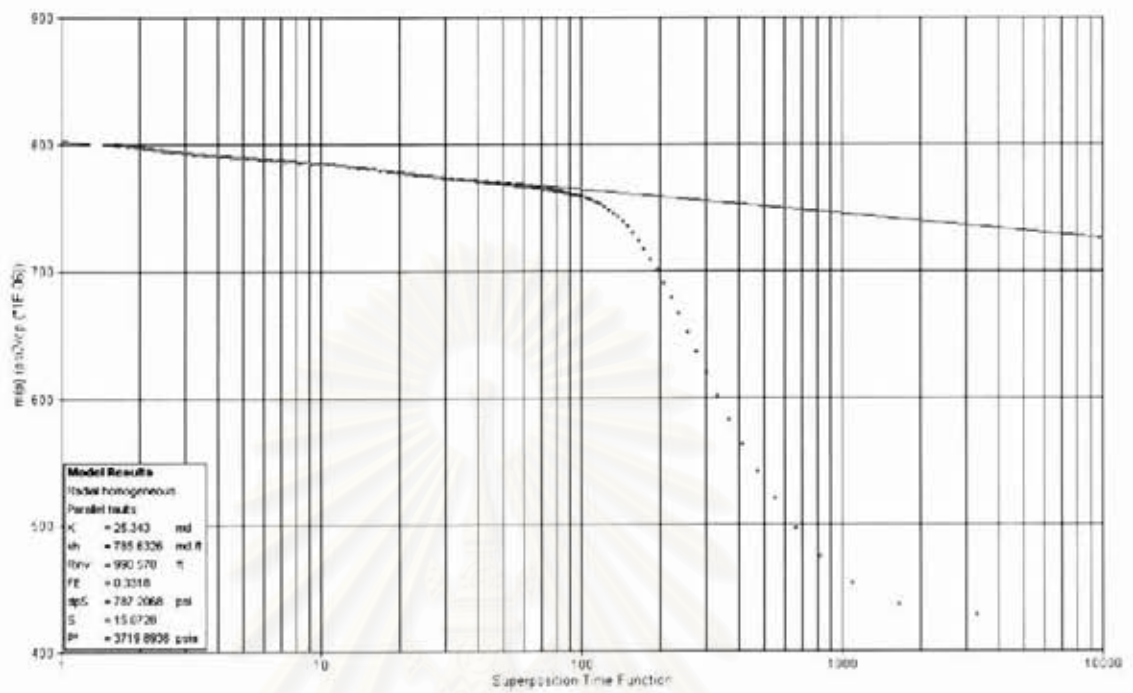


Figure A.45: Well-14 main build-up, semi-log plot.

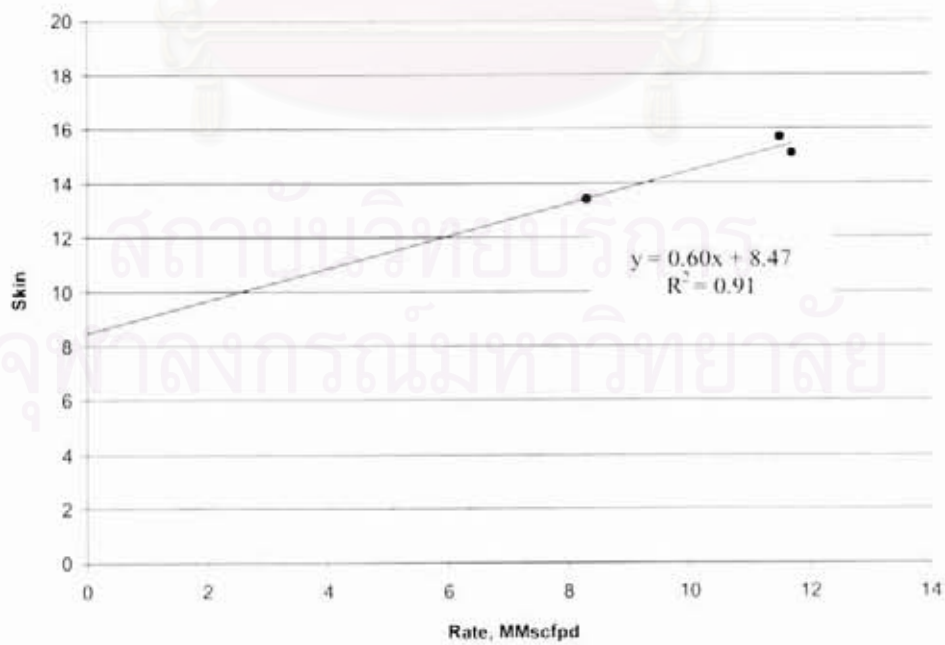


Figure A.46: Well-14 Rate Dependent Skin Plot

Well-15 Reservoir 75-5

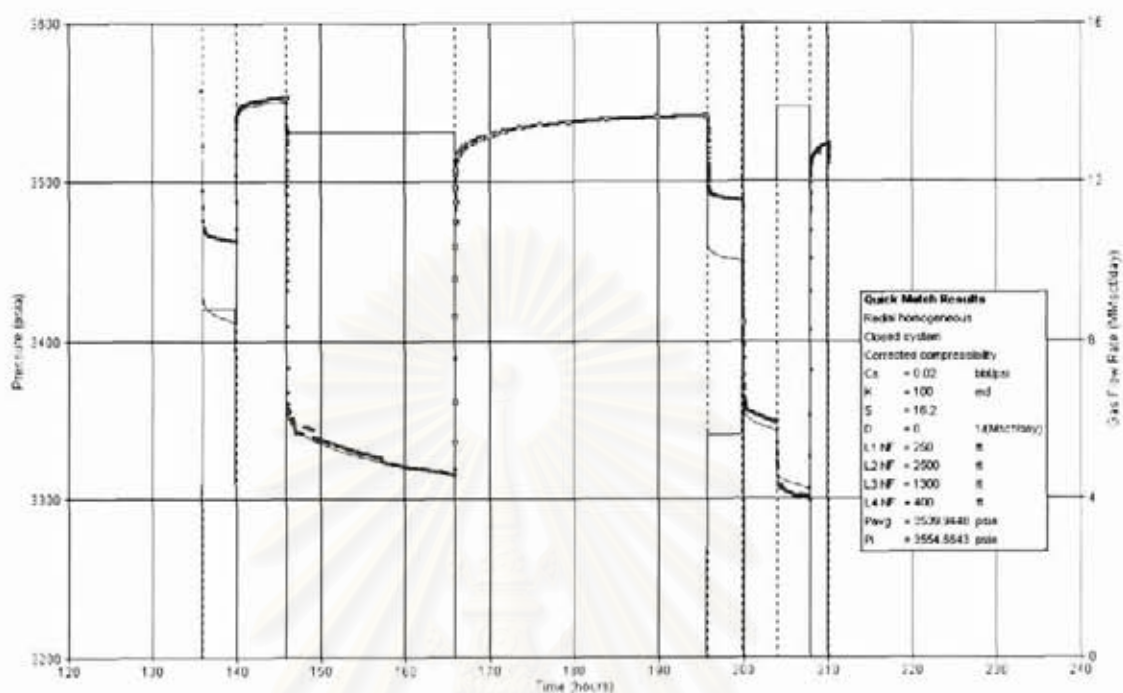


Figure A.47: Well-15 testing overview.

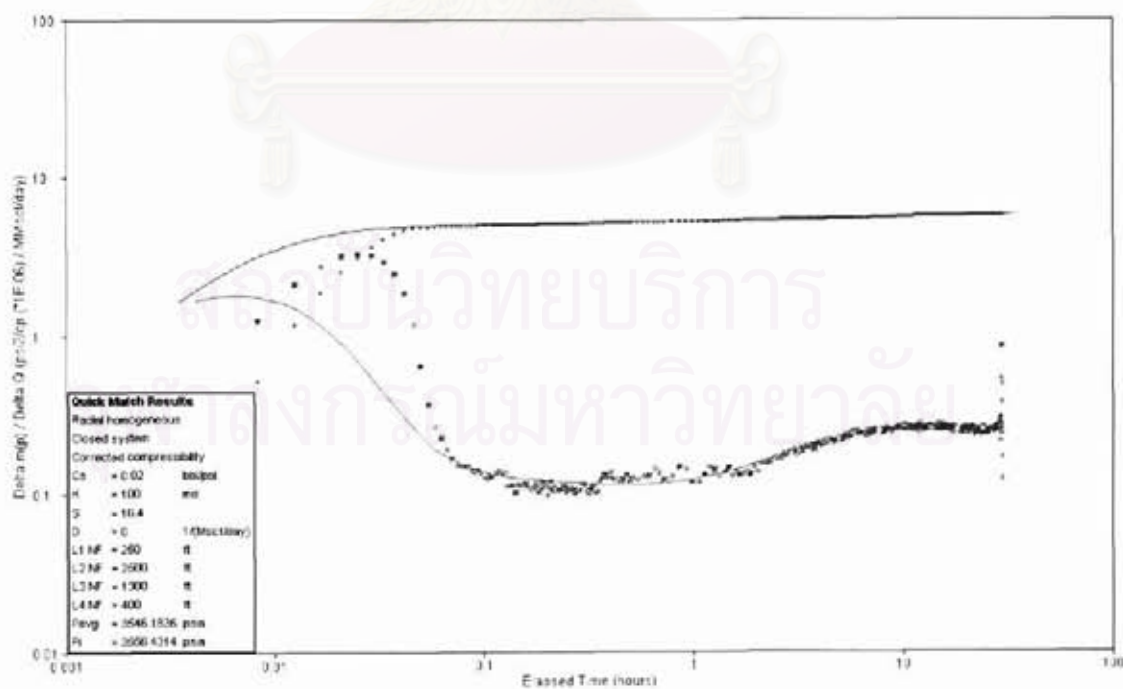


Figure A.48: Well-15 main build-up, log-log plot.

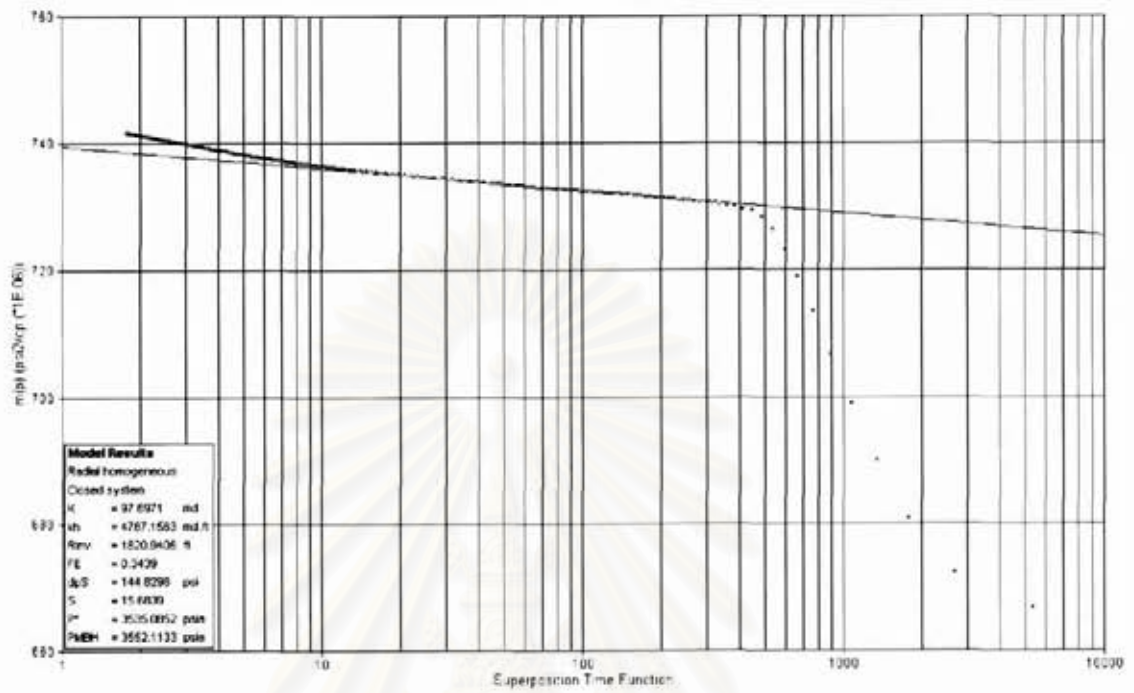


Figure A.49: Well-15 main build-up, semi-log plot.

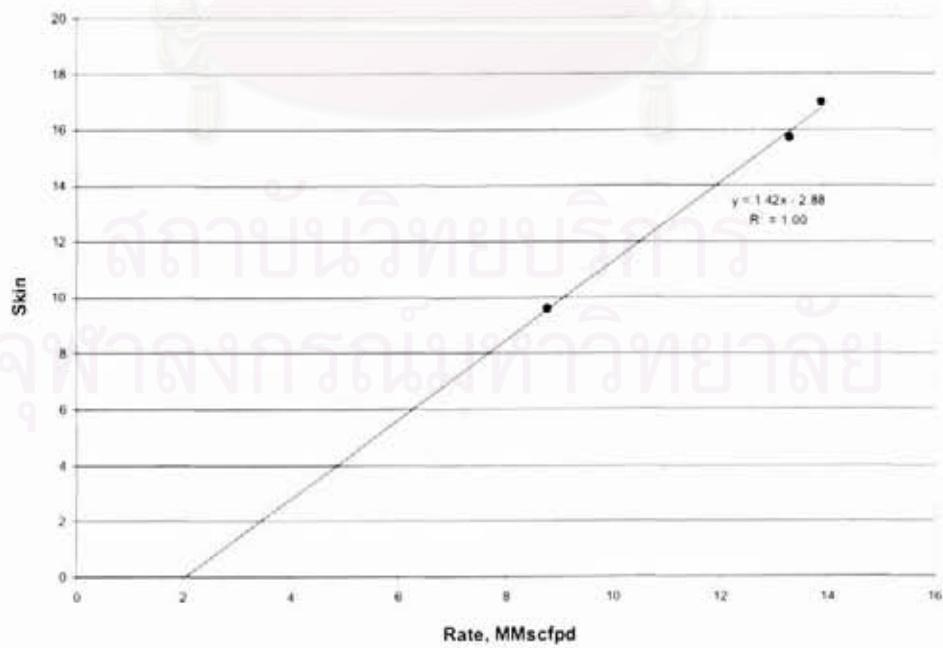


Figure A.50: Well-15 Rate Dependent Skin Plot

Well-16 Reservoir 60-8

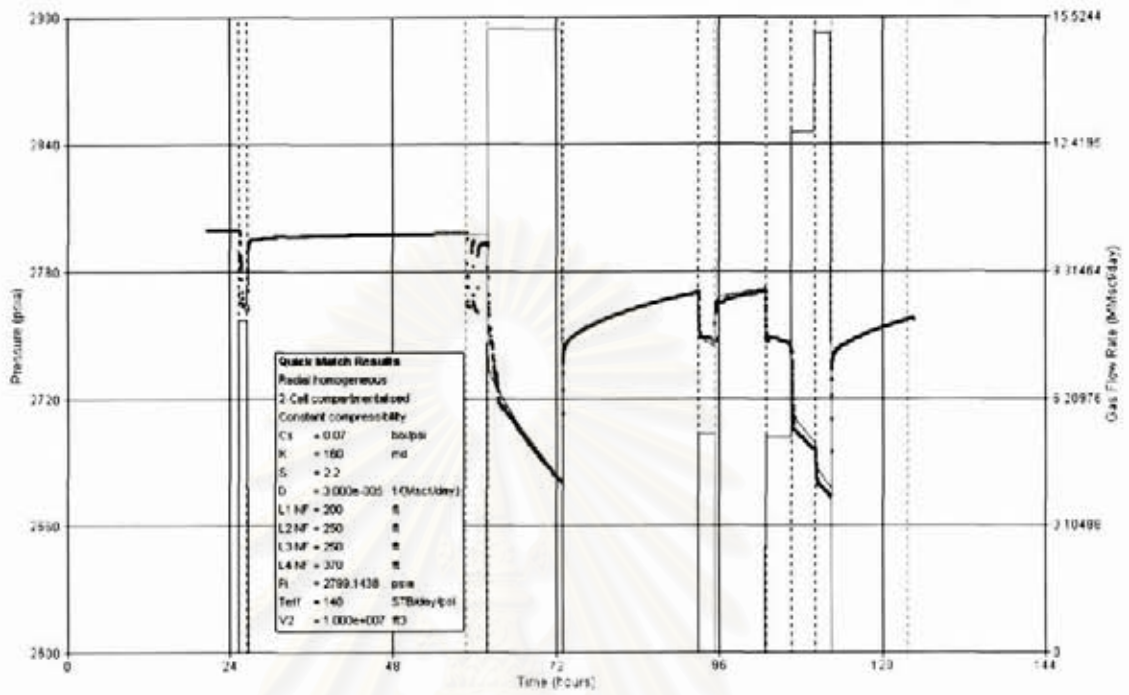


Figure A.51: Well-16 testing overview.

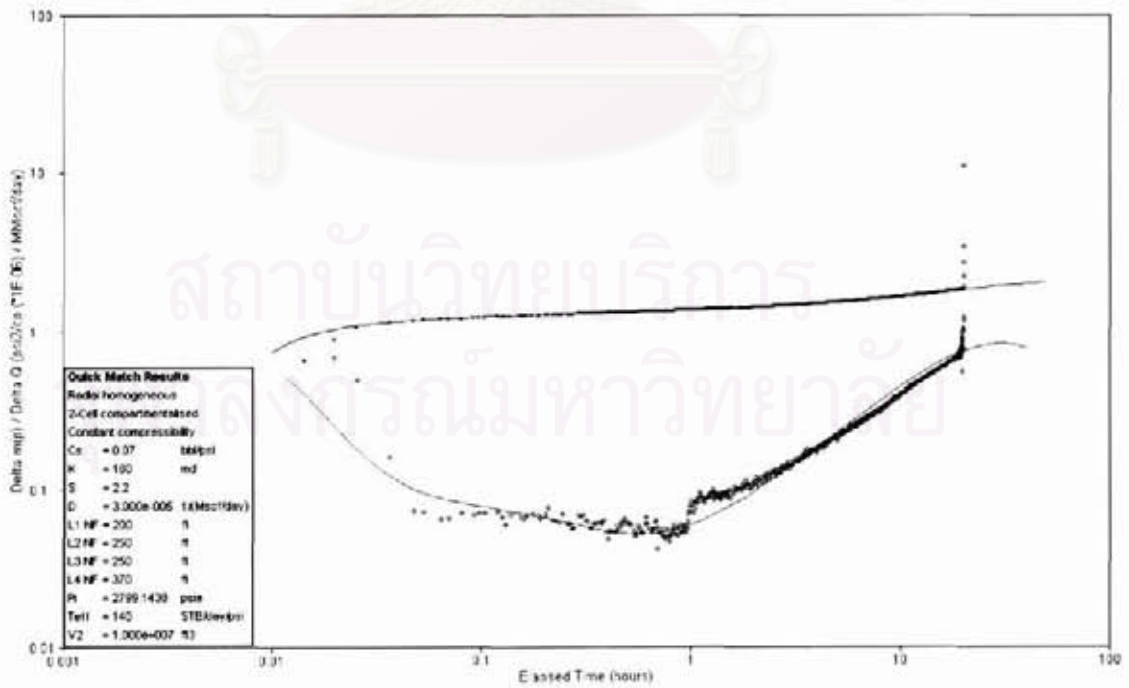


Figure A.52: Well-16 main build-up, log-log plot.

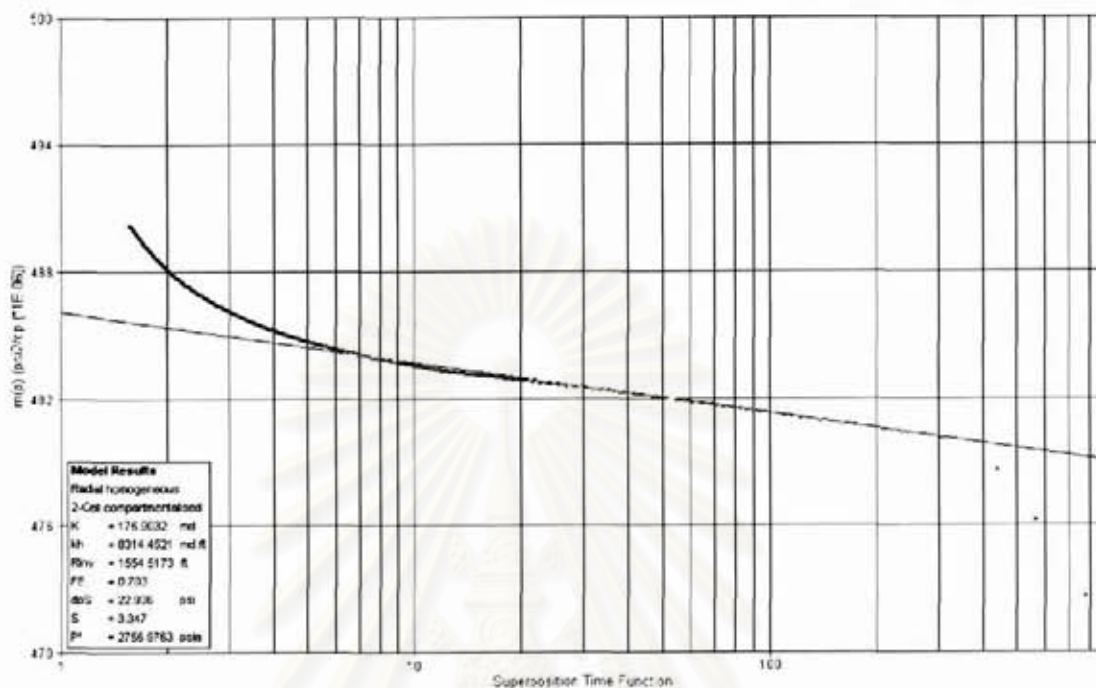


Figure A.53: Well-16 main build-up, semi-log plot.

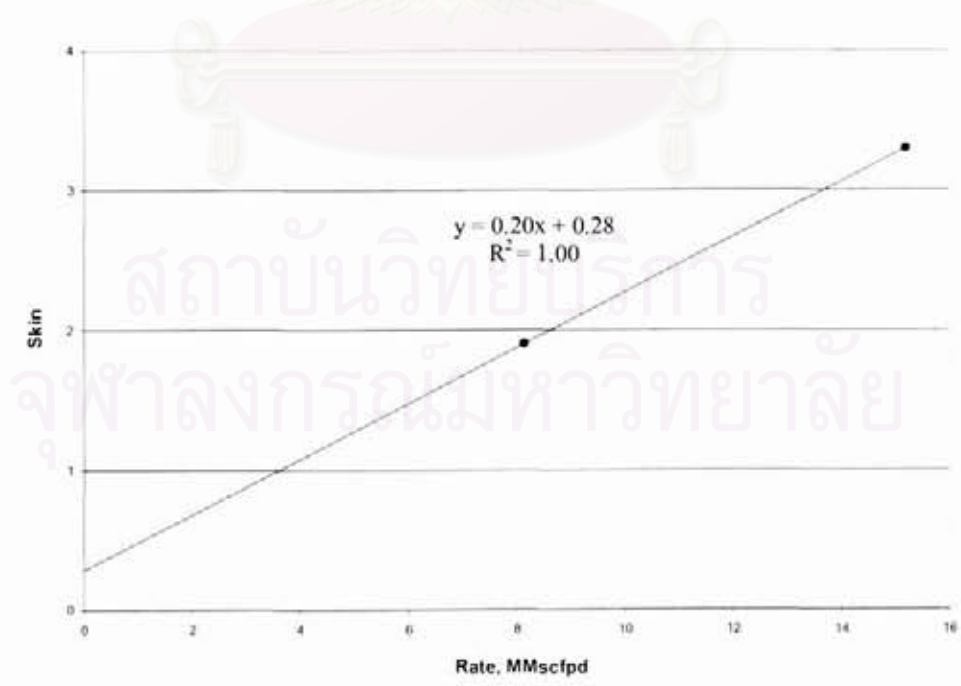


Figure A.54: Well-16 Rate Dependent Skin Plot

Well-17 Reservoir 59-2

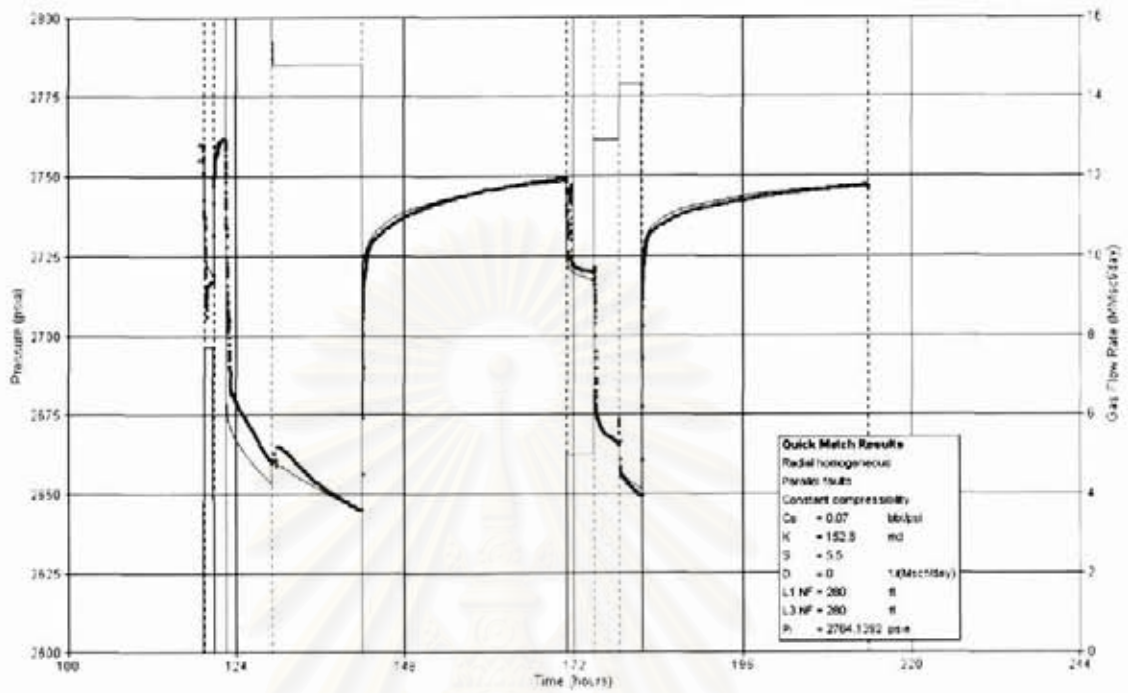


Figure A.55: Well-17 testing overview.

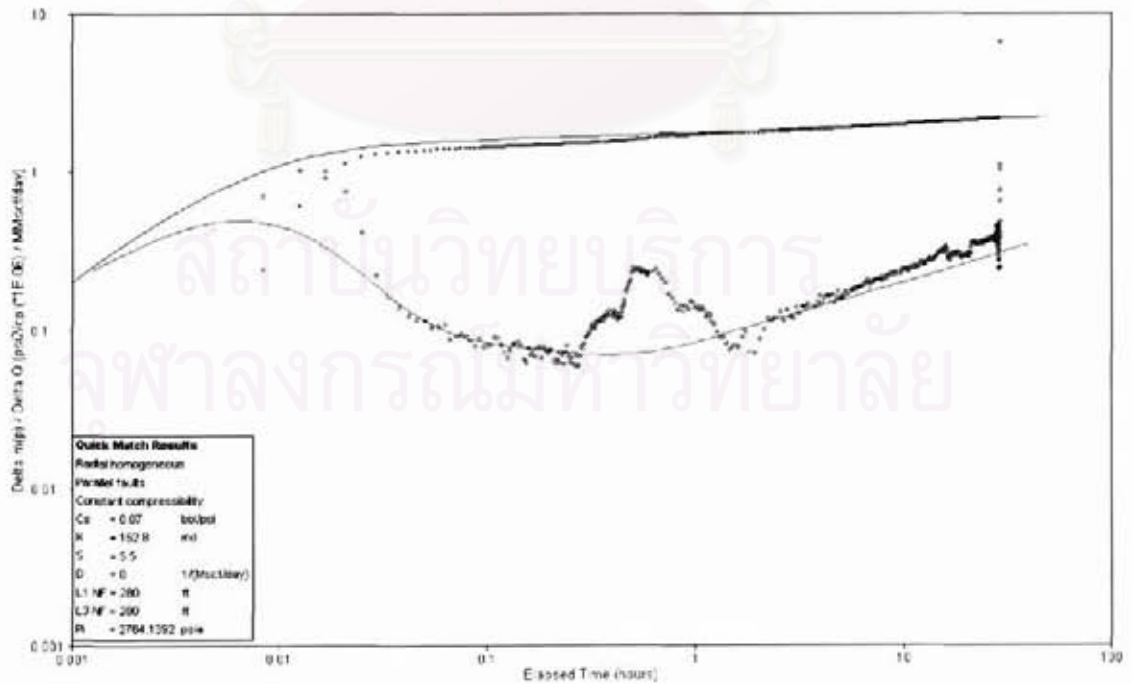


Figure A.56: Well-17 main build-up, log-log plot.

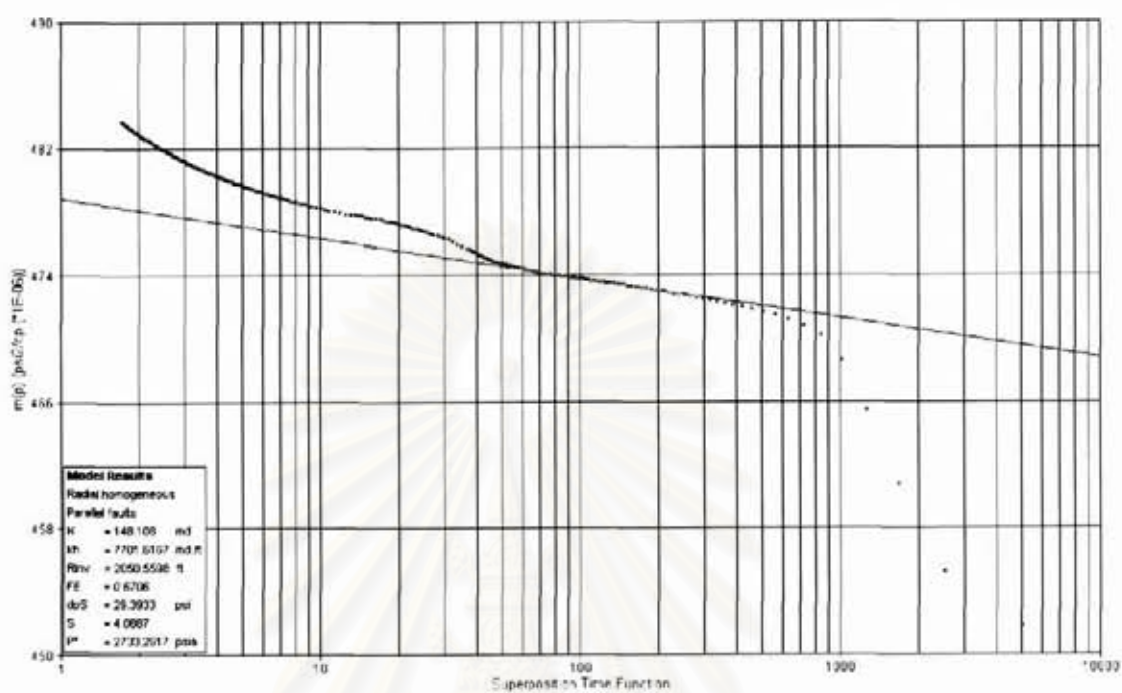


Figure A.57: Well-17 main build-up, semi-log plot.

สถาบันวิทยบริการ
จุฬาลงกรณ์มหาวิทยาลัย

Well-18 Reservoir 61-0

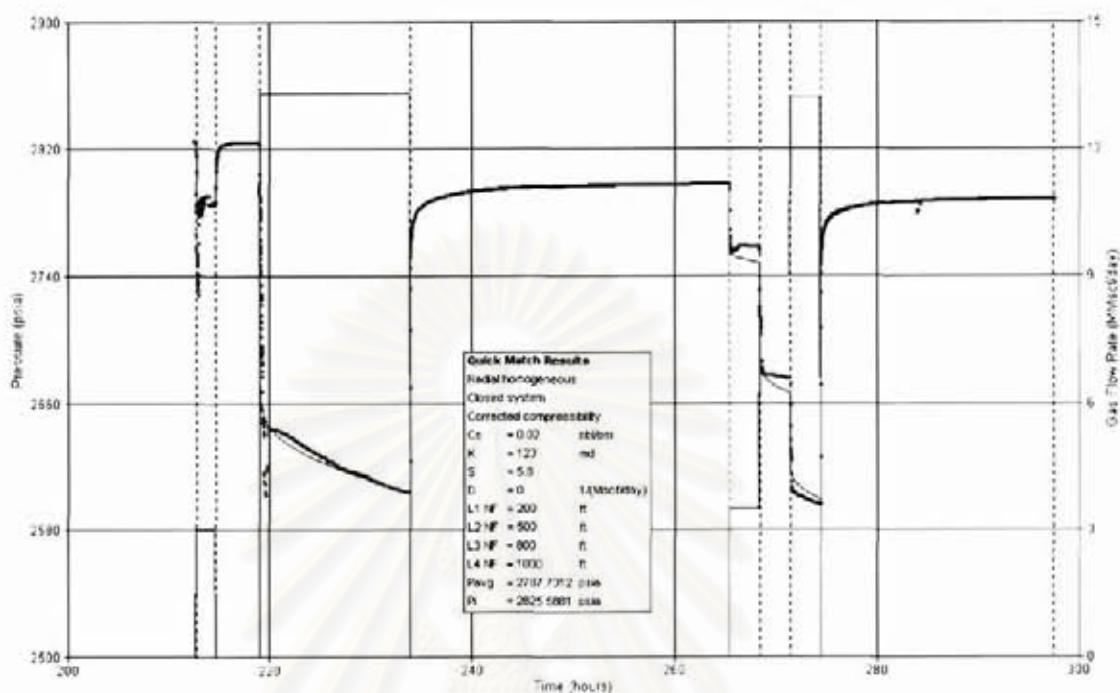


Figure A.58: Well-18 testing overview.

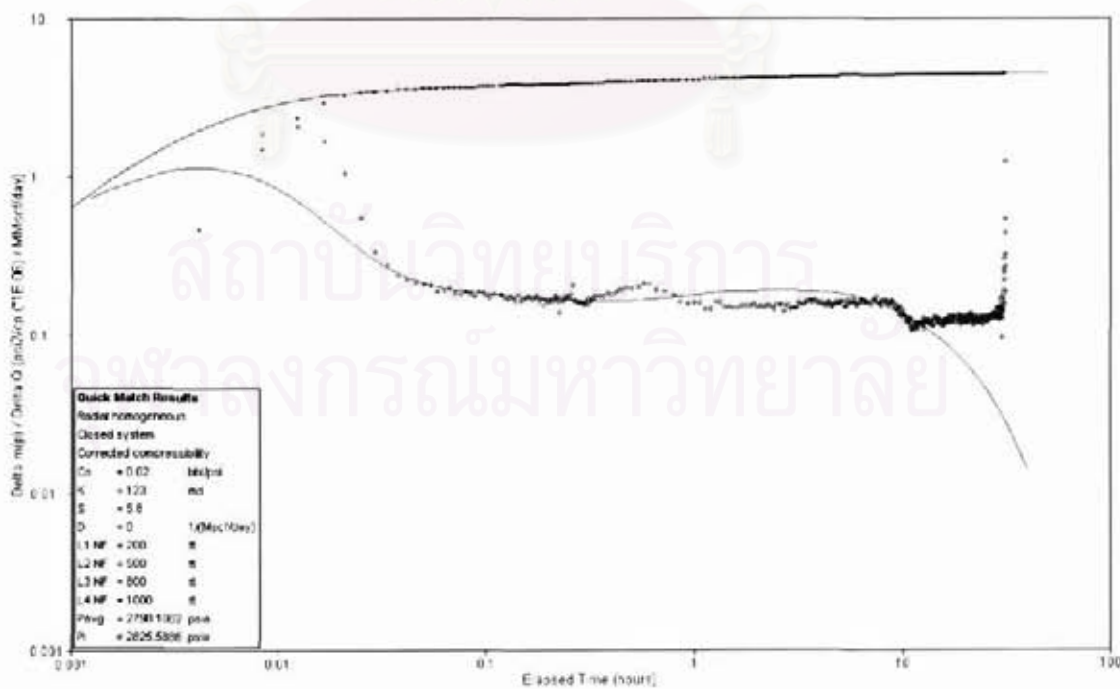


Figure A.59: Well-18 main build-up, log-log plot.

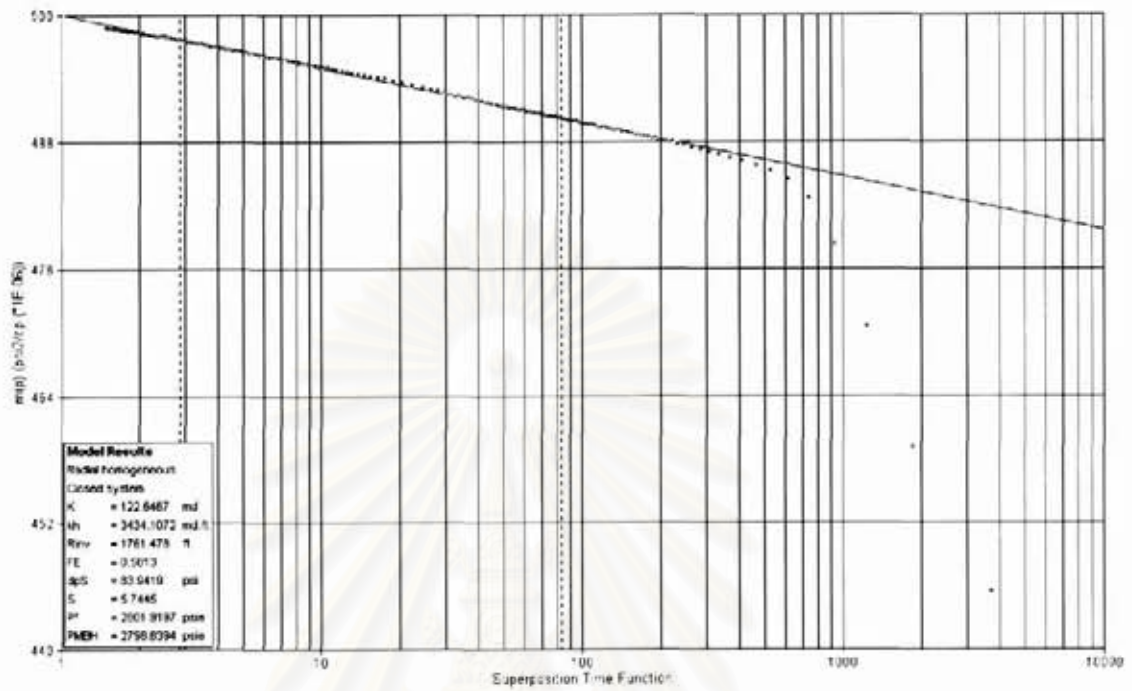


Figure A.60: Well-18 main build-up, semi-log plot.

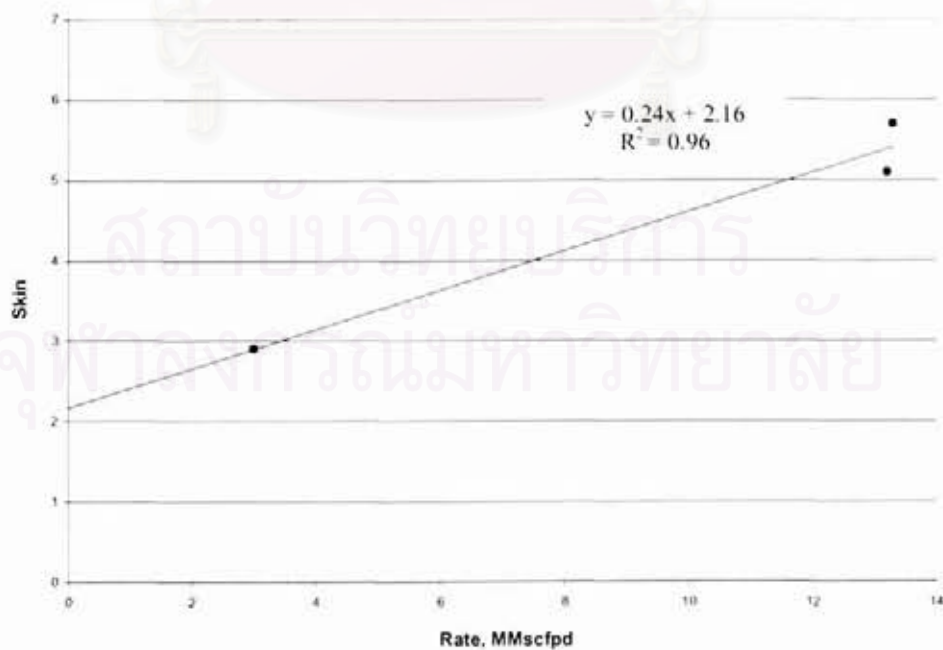


Figure A.61: Well-18 Rate Dependent Skin Plot

Well-19 Reservoir 81-6

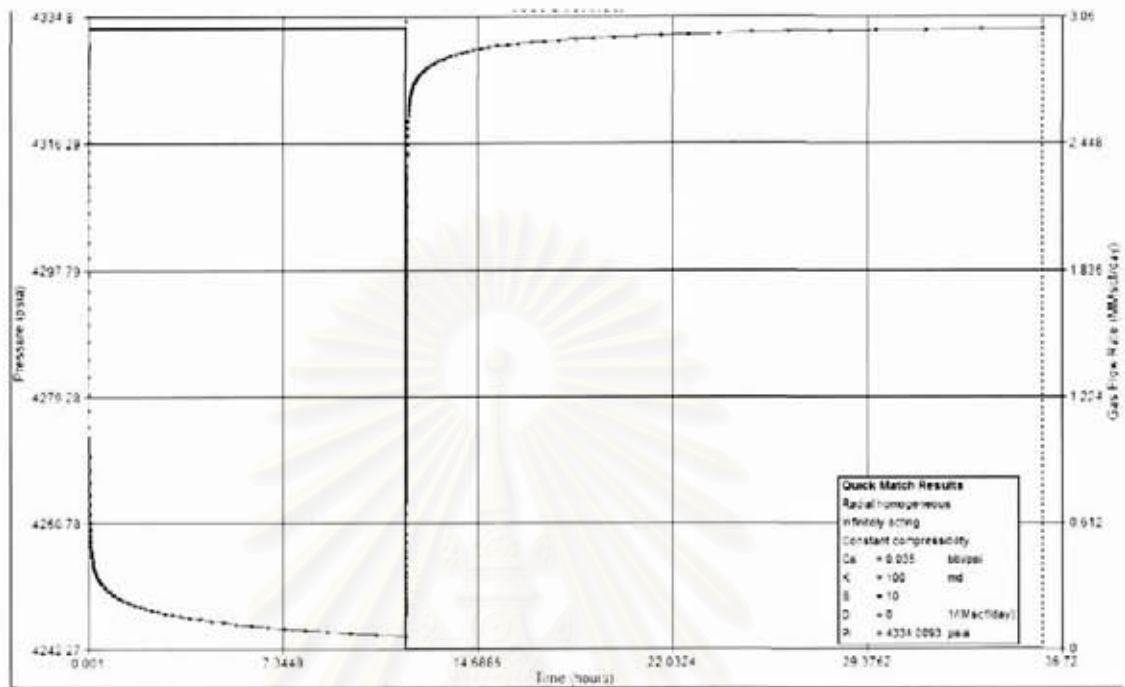


Figure A.62: Well-19 testing overview.

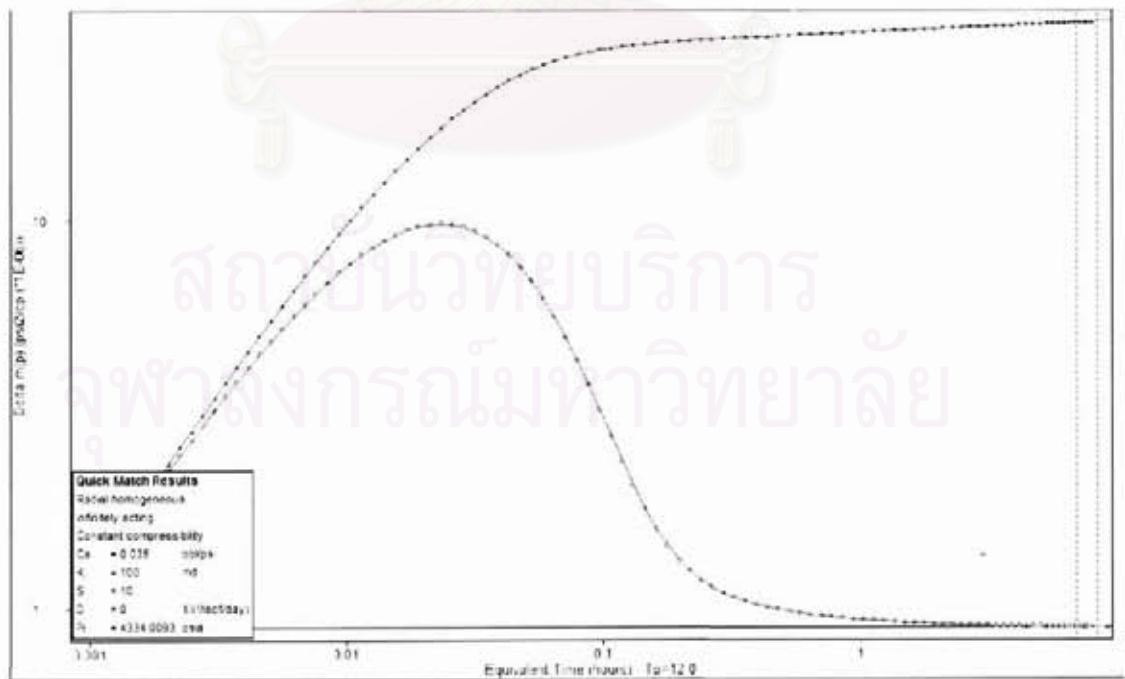


Figure A.63: Well-19 main build-up, log-log plot.

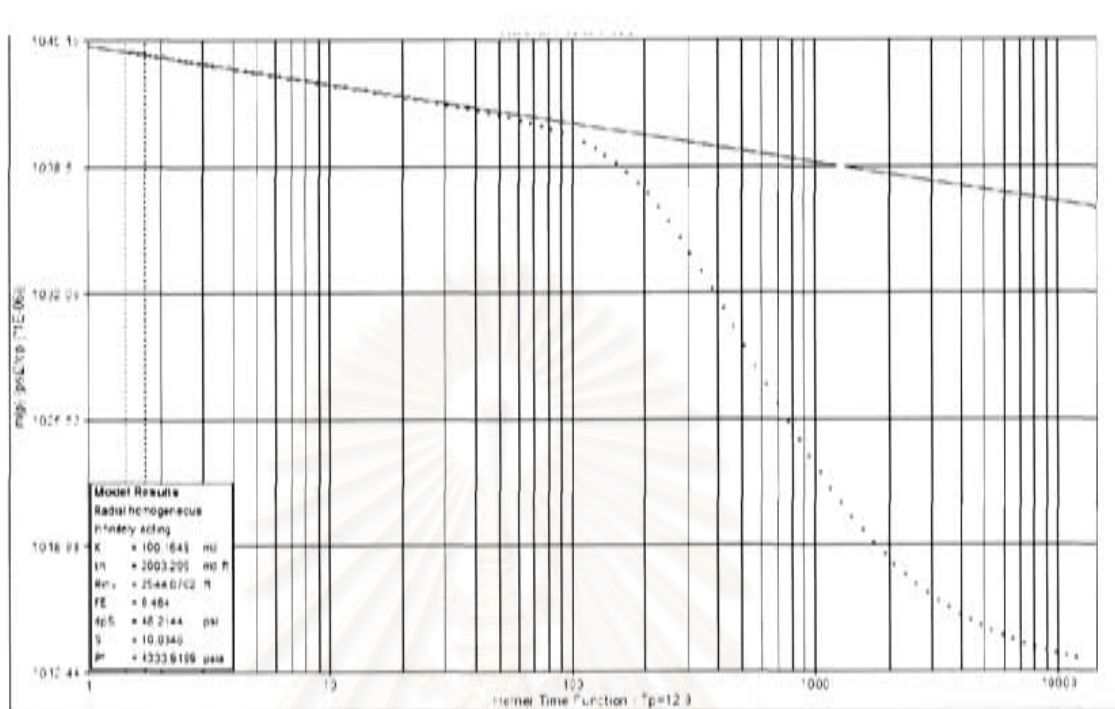


Figure A.64: Well-19 main build-up, semi-log plot.

สถาบันวิทยบริการ
 จุฬาลงกรณ์มหาวิทยาลัย

Well-20 Reservoir 72-9

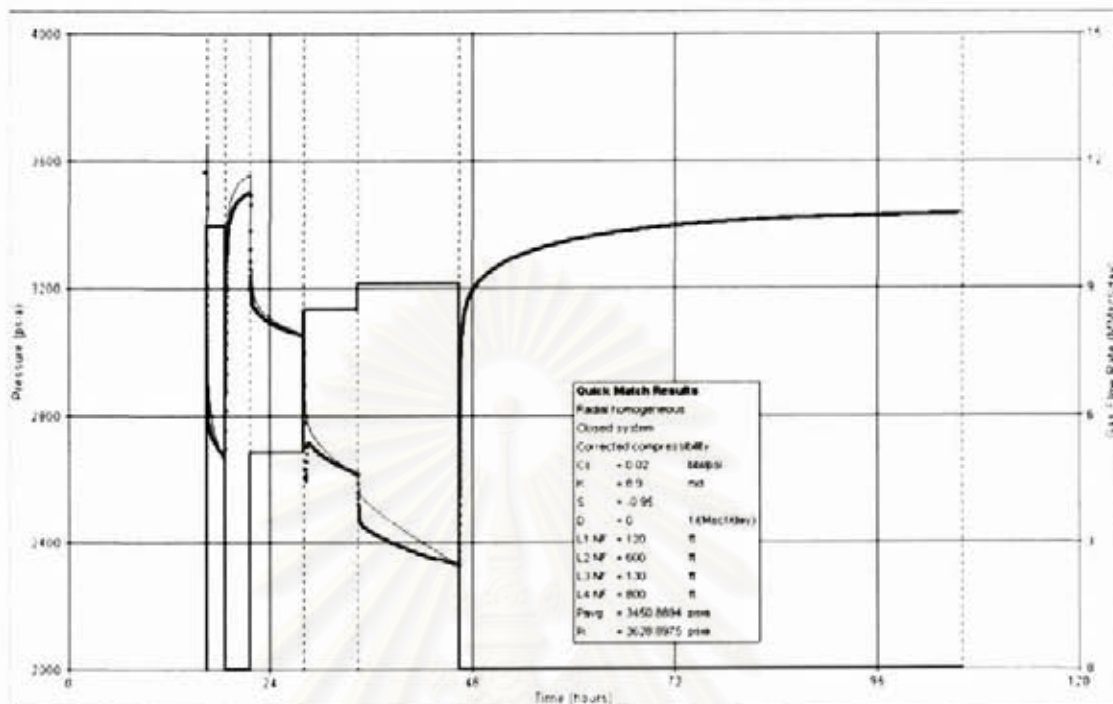


Figure A.65: Well-20 testing overview.

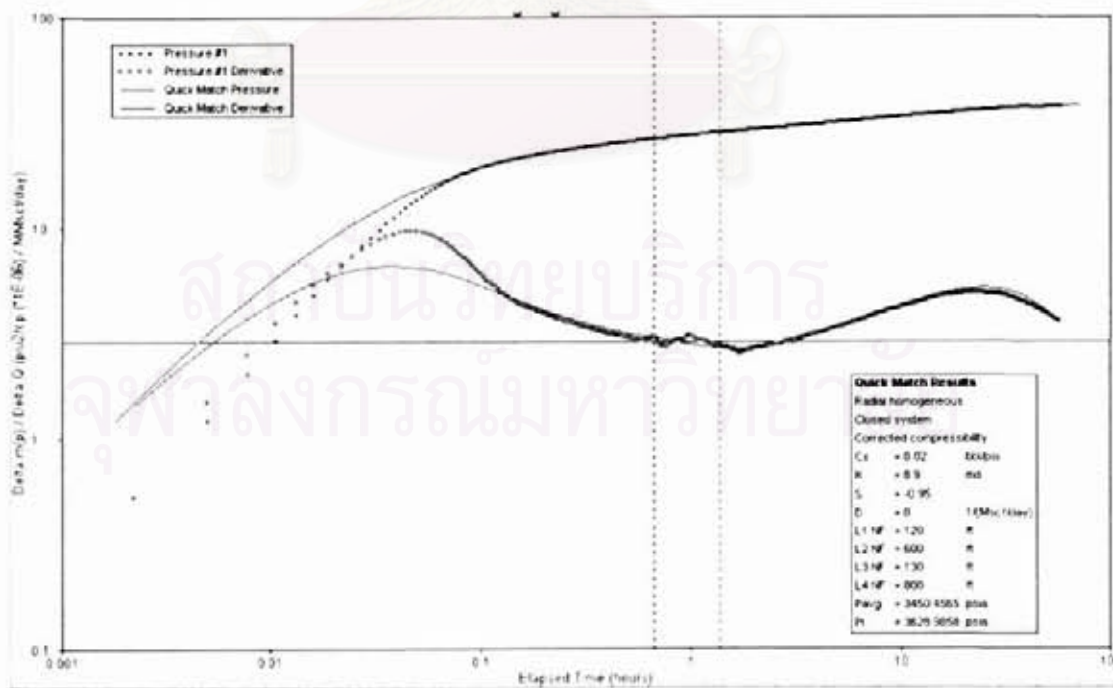


Figure A.66: Well-20 main build-up, log-log plot.

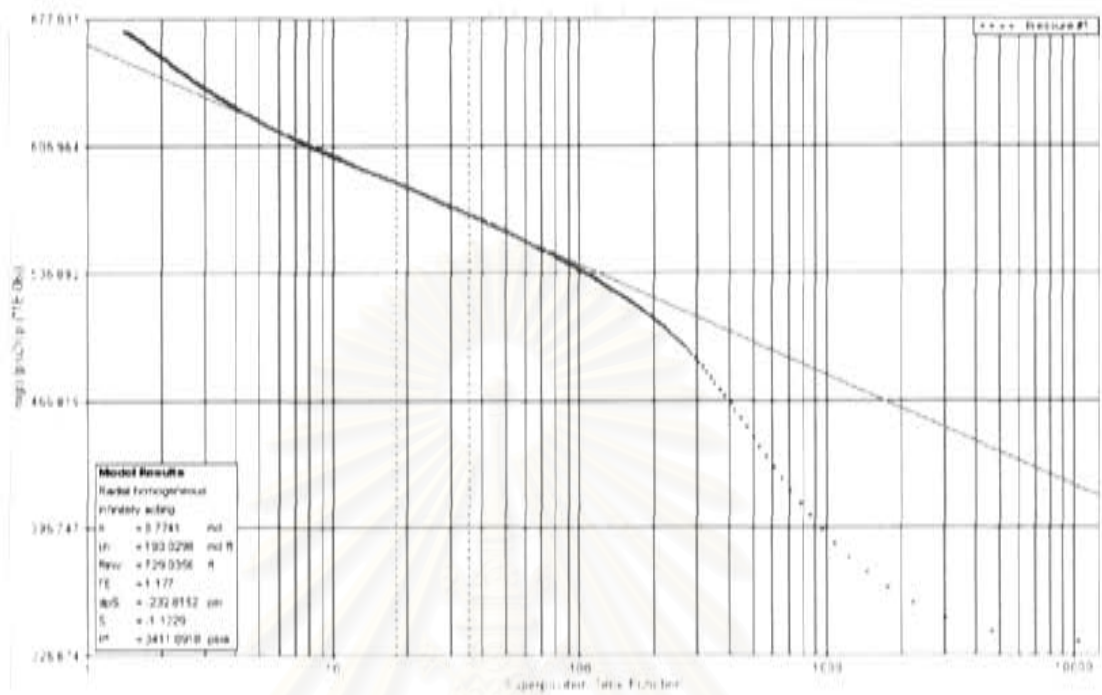


Figure A.67: Well-20 main build-up, semi-log plot.

สถาบันวิทยบริการ
จุฬาลงกรณ์มหาวิทยาลัย

Well-21 Reservoir 73-0

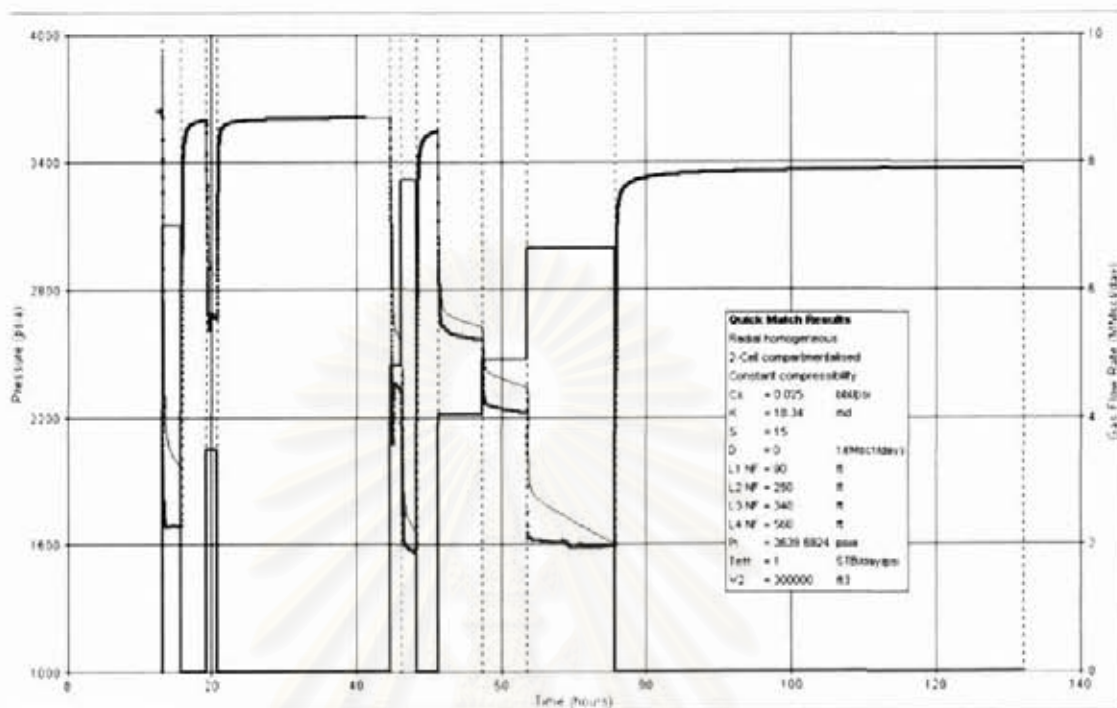


Figure A.68: Well-21 testing overview.

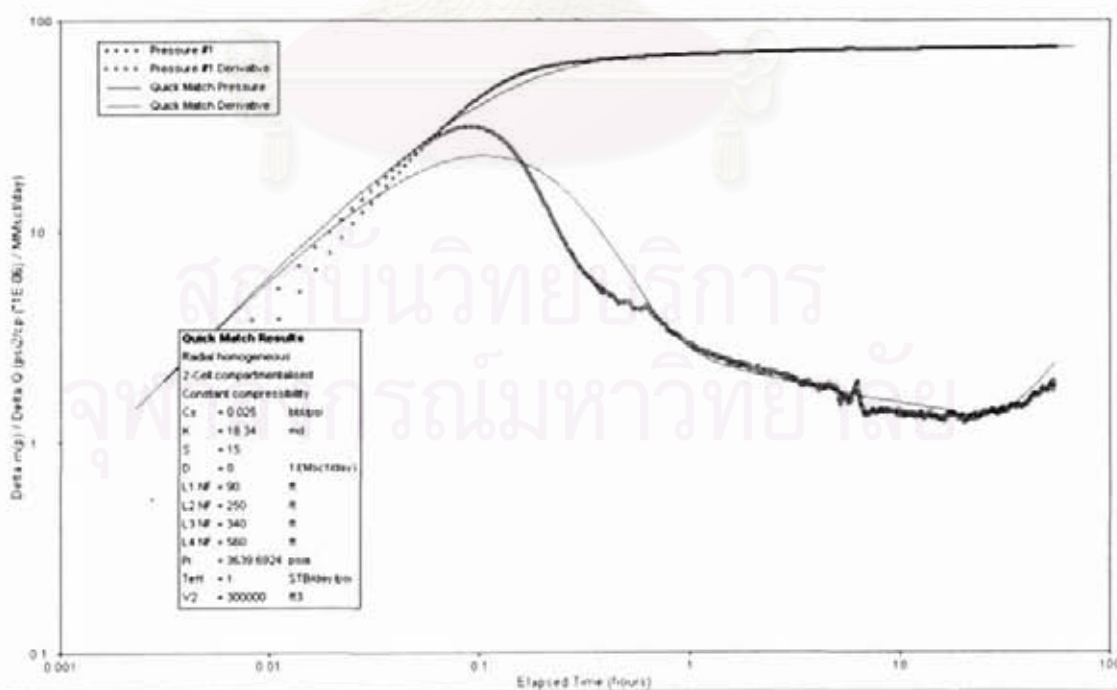


Figure A.69: Well-21 main build-up, log-log plot.

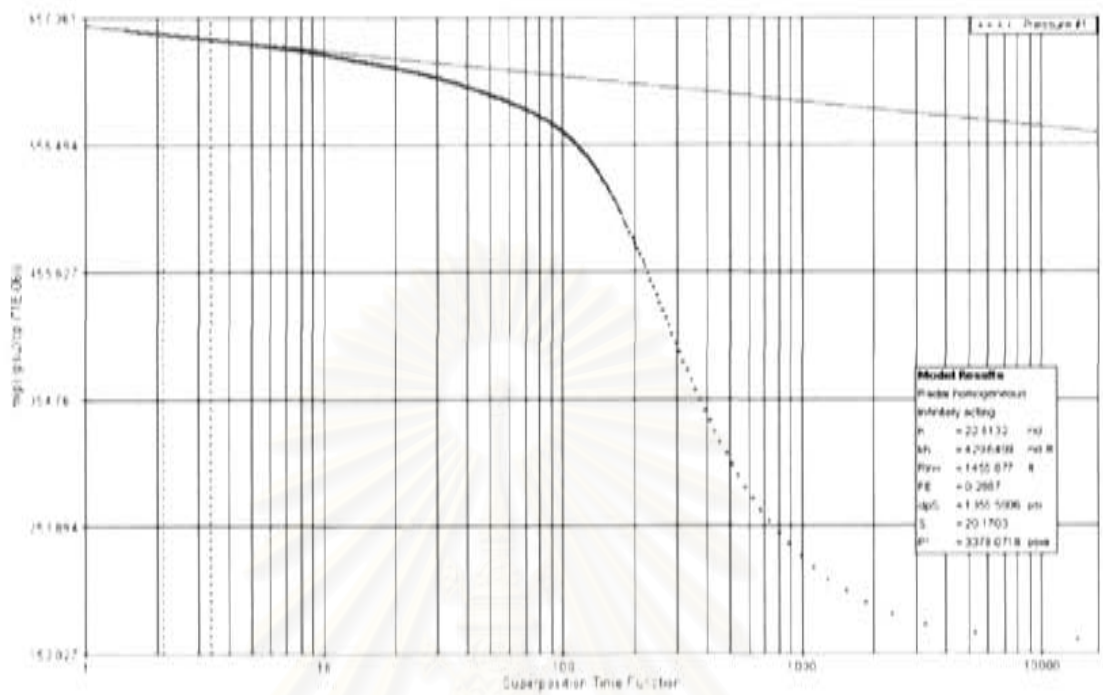


Figure A.70: Well-21 main build-up, semi-log plot.

สถาบันวิทยบริการ
จุฬาลงกรณ์มหาวิทยาลัย

Well-22 Reservoir 78-2

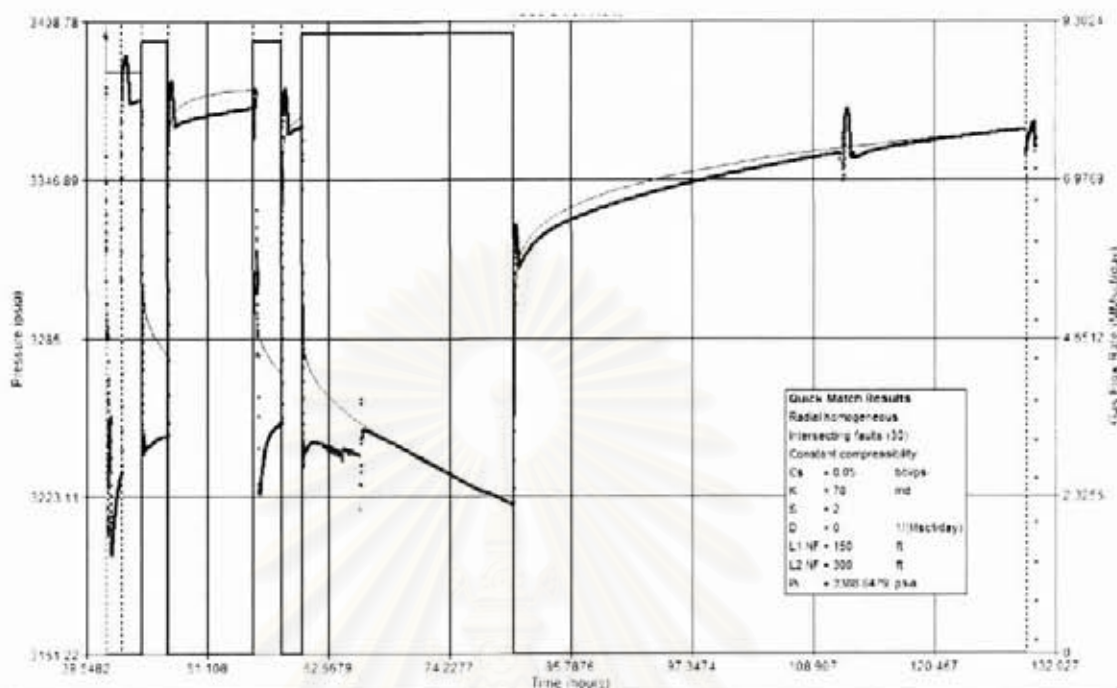


Figure A.71: Well-22 testing overview.

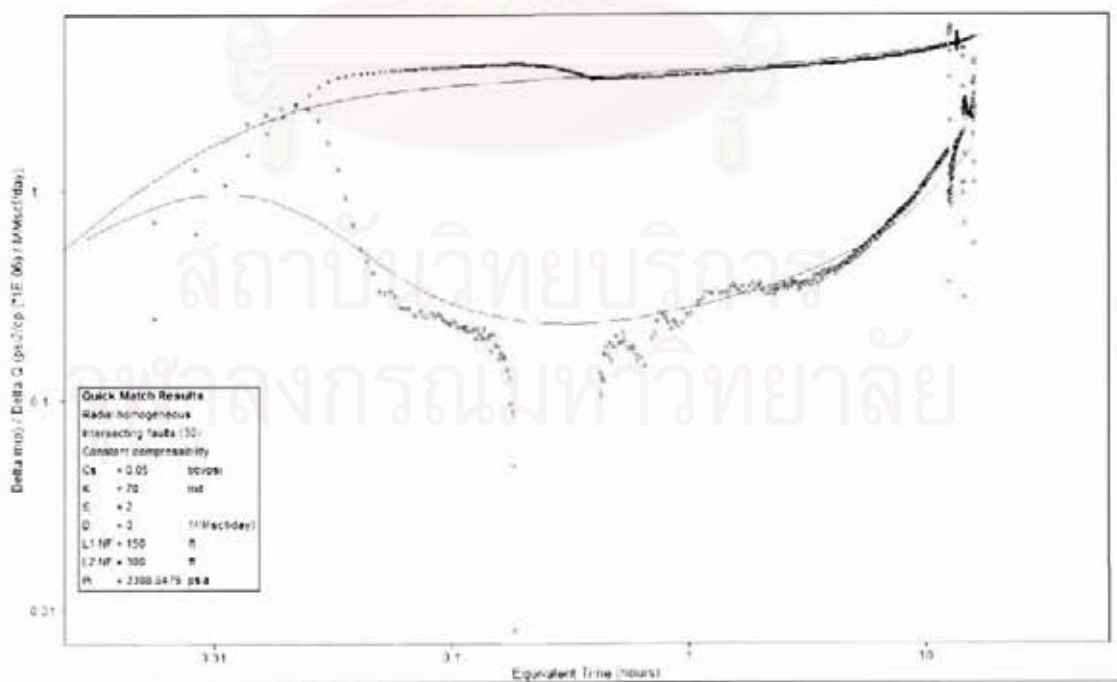


Figure A.72: Well-22 main build-up, log-log plot.

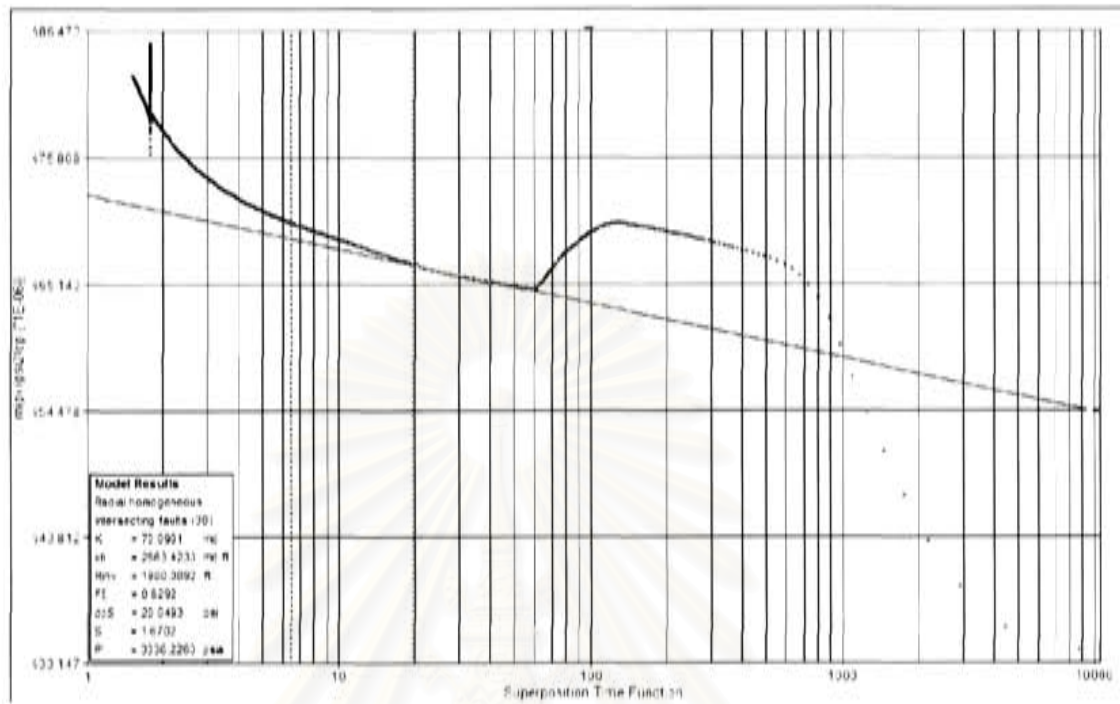


Figure A.73: Well-22 main build-up, semi-log plot.

สถาบันวิทยบริการ
 จุฬาลงกรณ์มหาวิทยาลัย

Well-23 Reservoir 59-4

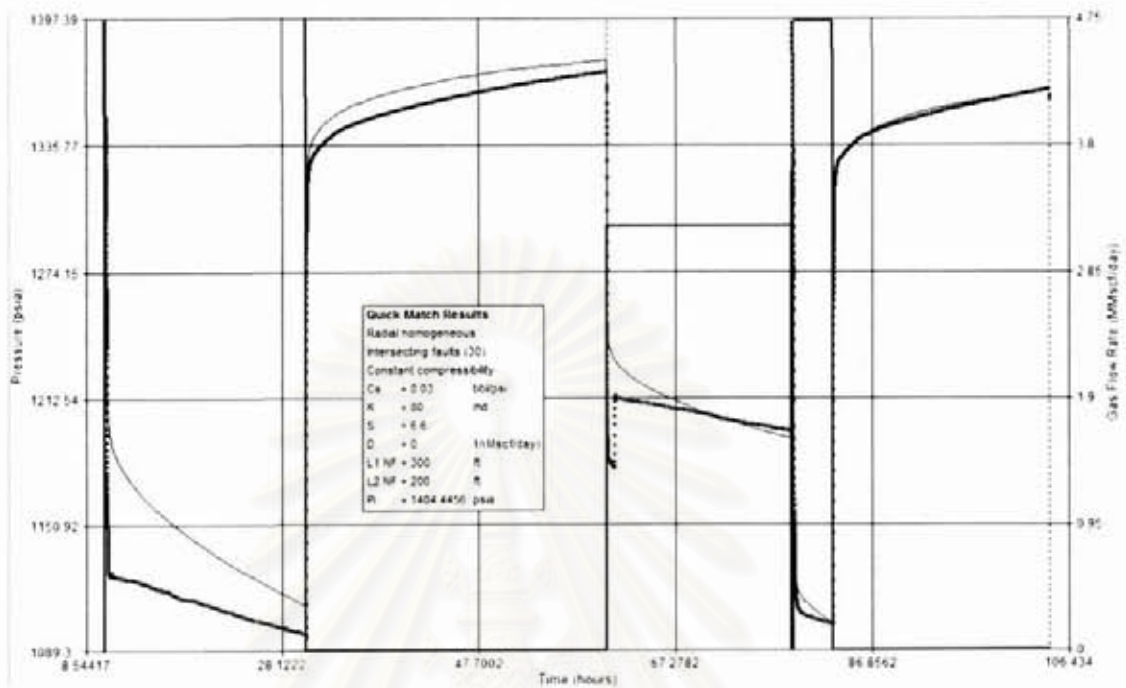


Figure A.74: Well-23 testing overview.

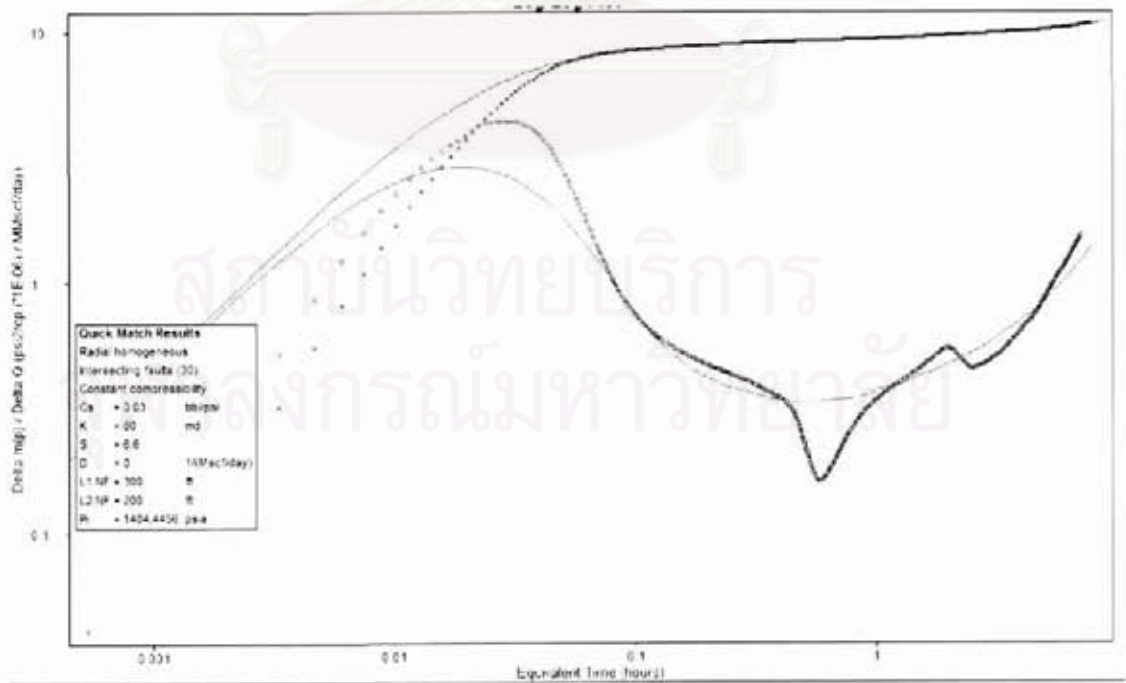


Figure A.75: Well-23 main build-up, log-log plot.

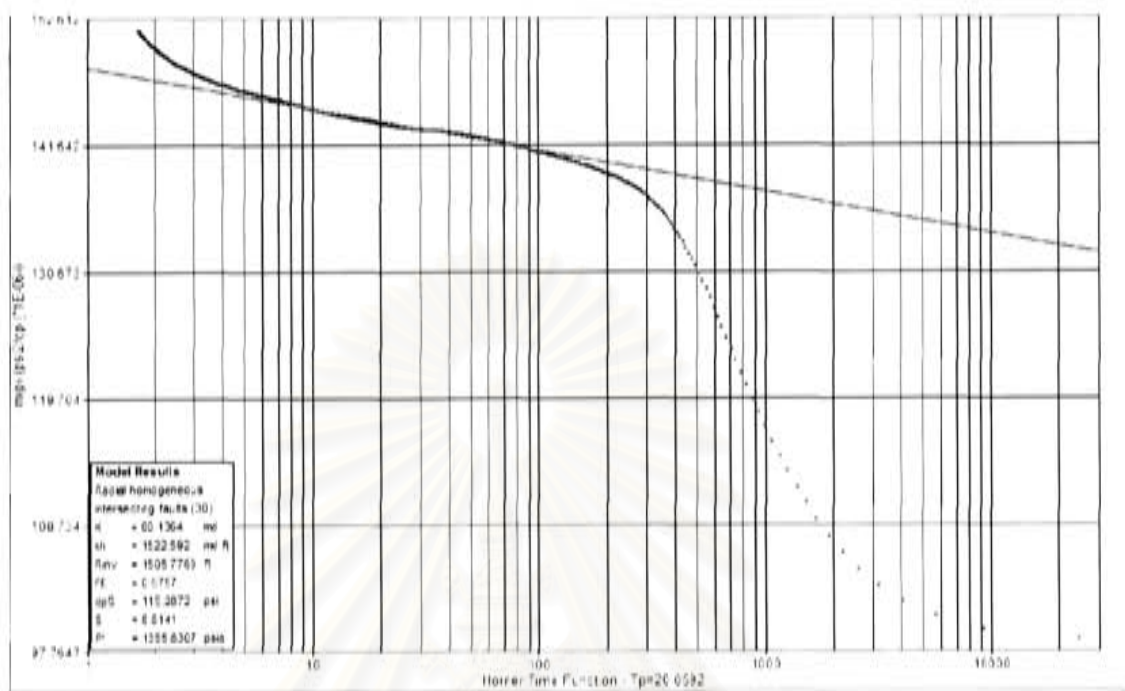


Figure A.76; Well-23 main build-up, semi-log plot.

สถาบันวิทยบริการ
จุฬาลงกรณ์มหาวิทยาลัย

Well-24 Reservoir 88-3

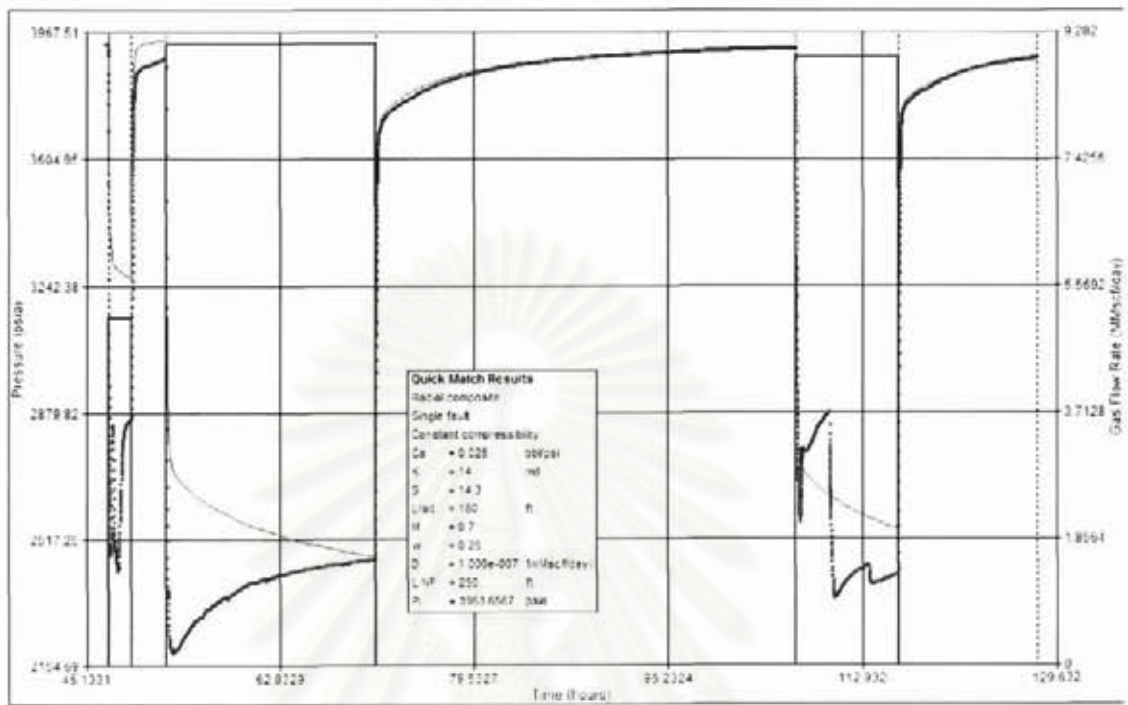


Figure A.77: Well-24 testing overview.

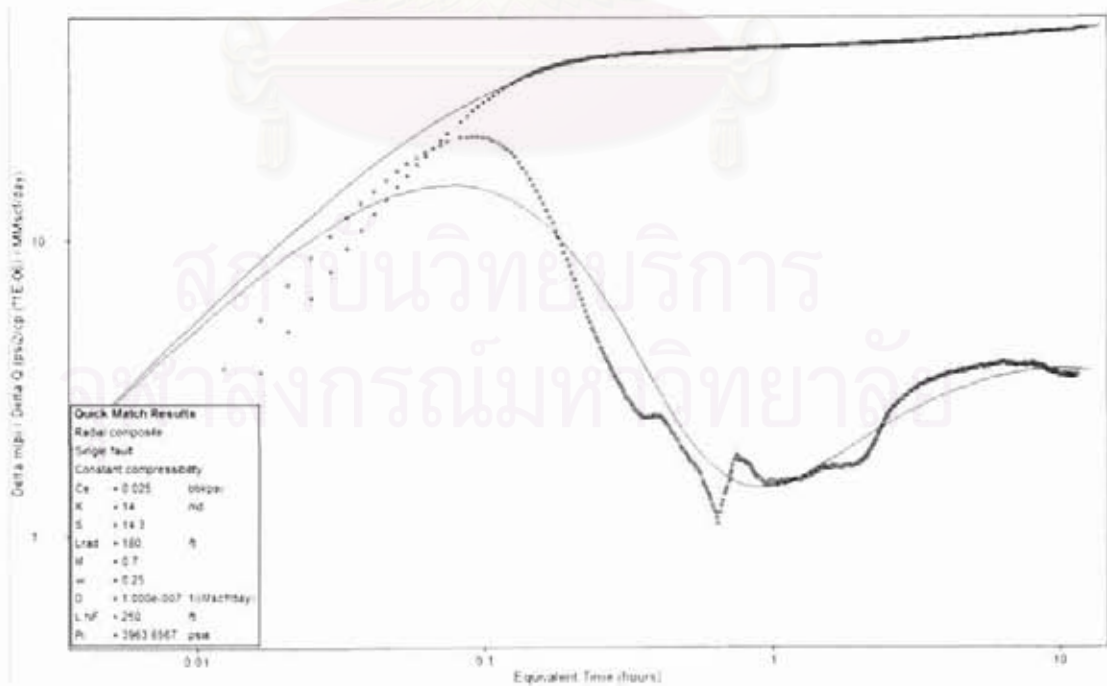


Figure A.78: Well-24 main build-up, log-log plot.

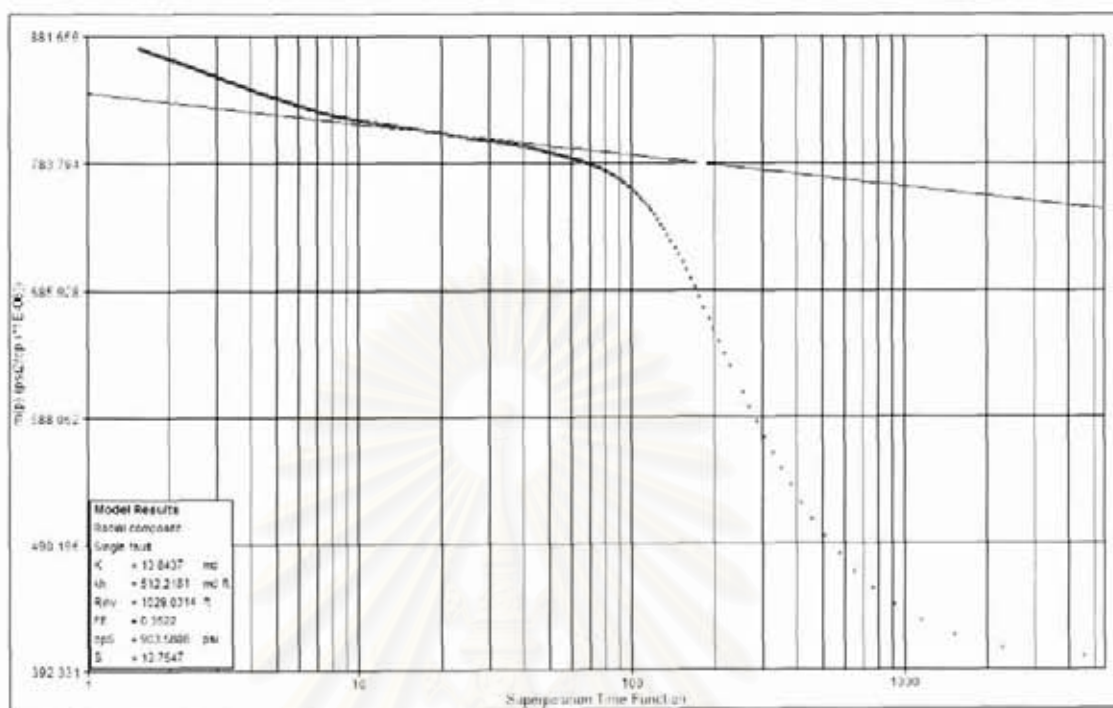


Figure A.79: Well-24 main build-up, semi-log plot.

สถาบันวิทยบริการ
 จุฬาลงกรณ์มหาวิทยาลัย

Well-25 Reservoir 71-0

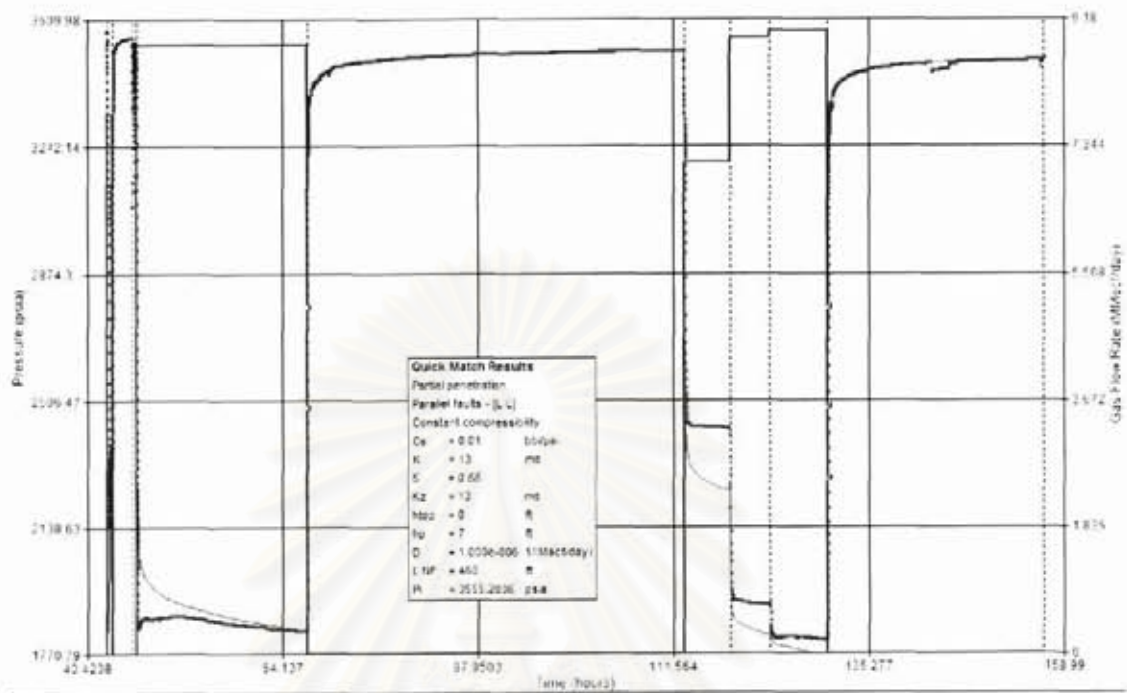


Figure A.80: Well-25 testing overview.

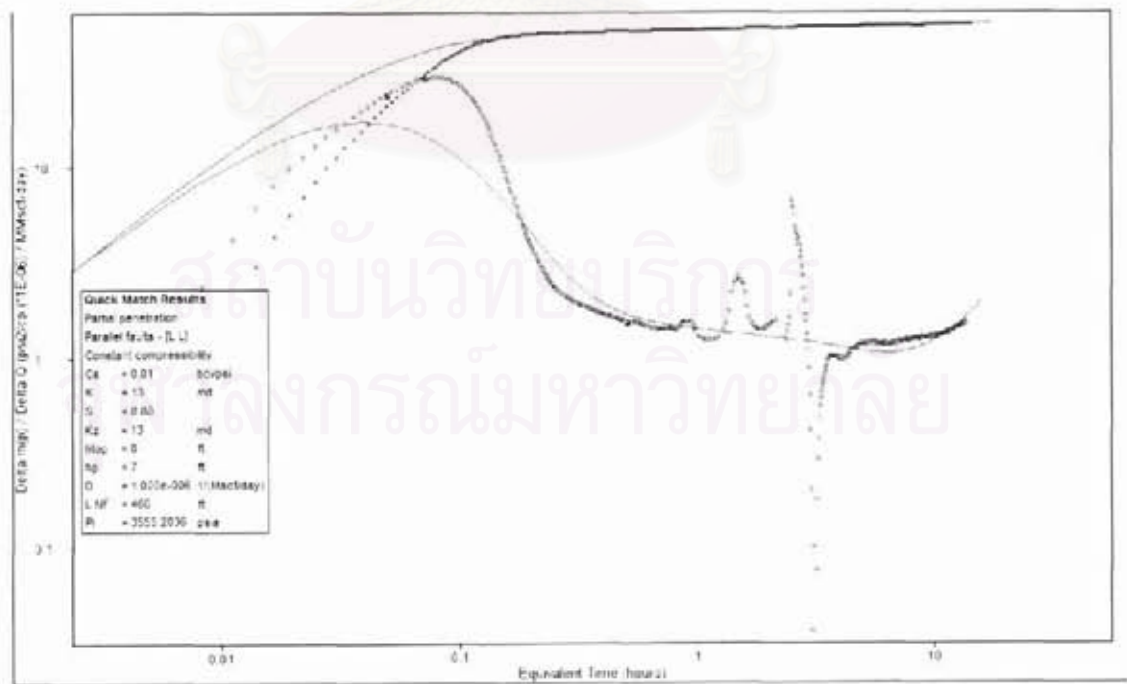


Figure A.81: Well-25 main build-up, log-log plot.

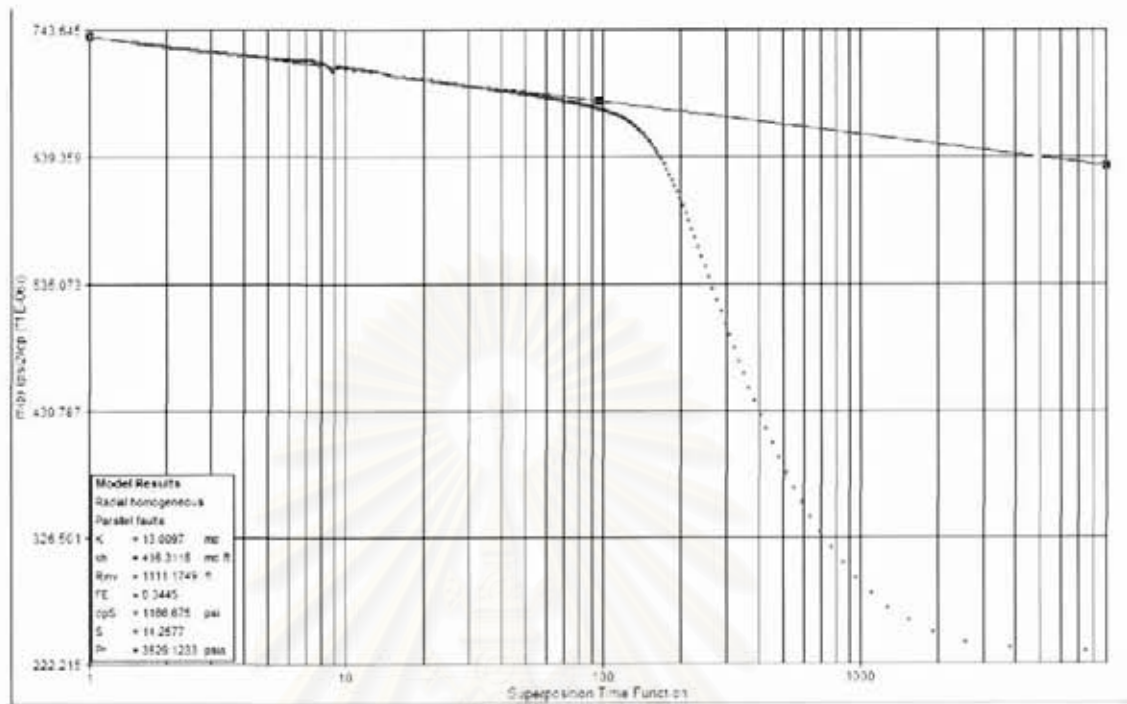


Figure A.82: Well-25 main build-up, semi-log plot.

สถาบันวิทยบริการ
 จุฬาลงกรณ์มหาวิทยาลัย

Well-26 Reservoir 65-3

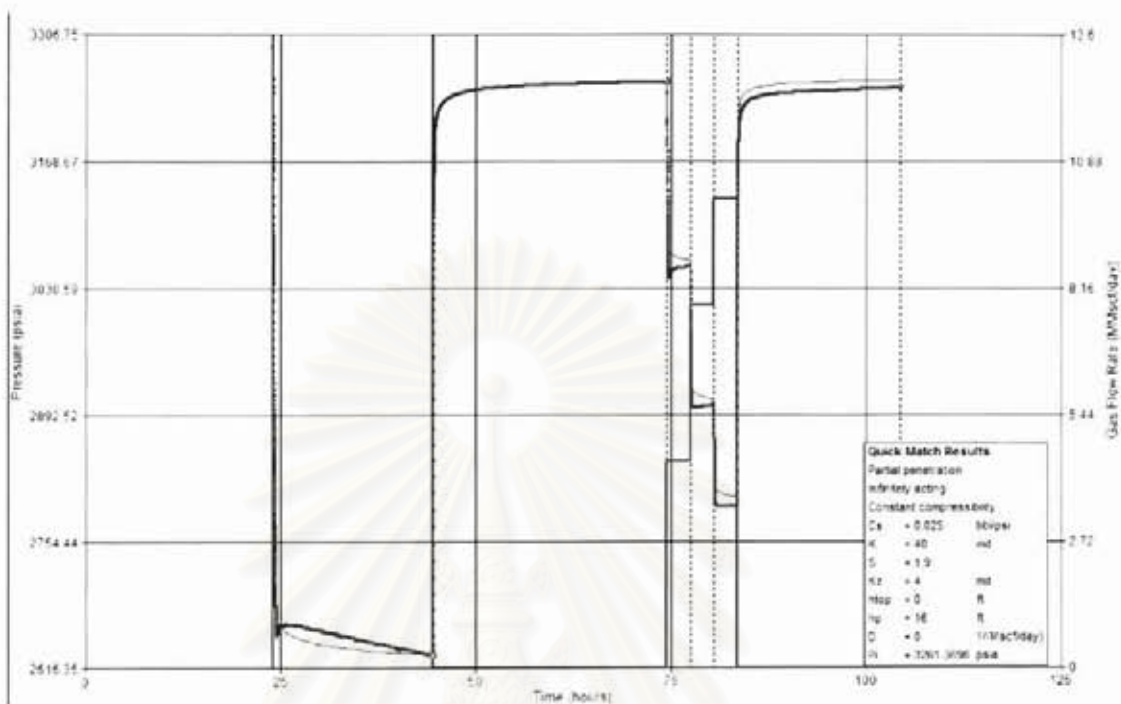


Figure A.83: Well-26 testing overview.

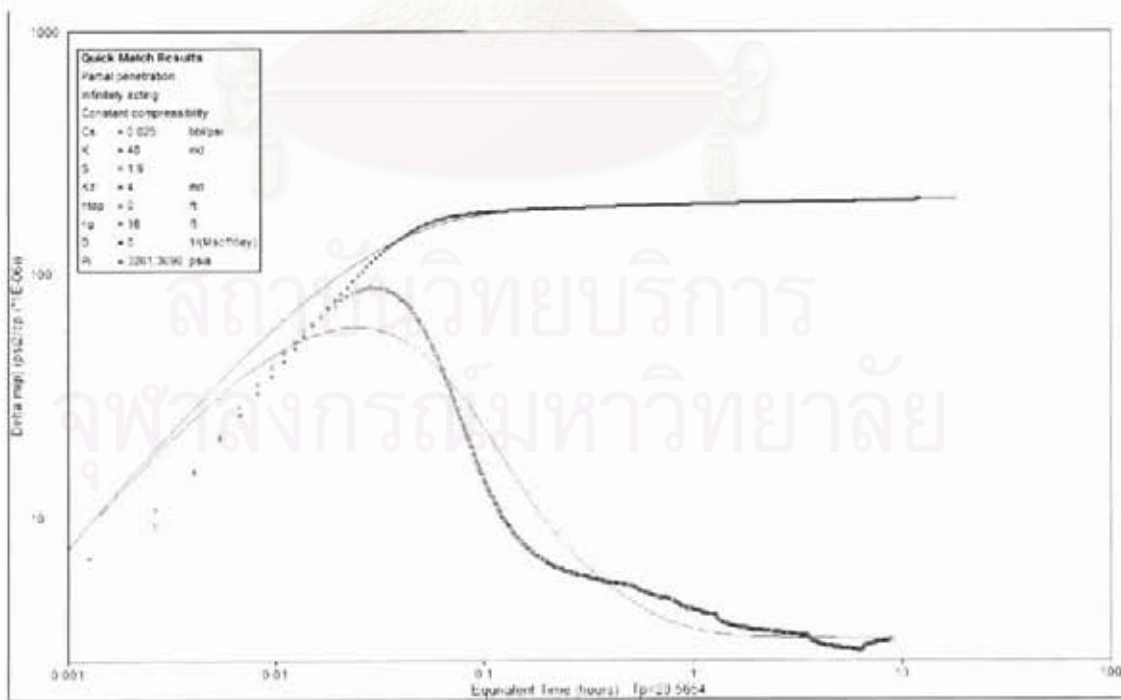


Figure A.84: Well-26 main build-up, log-log plot.

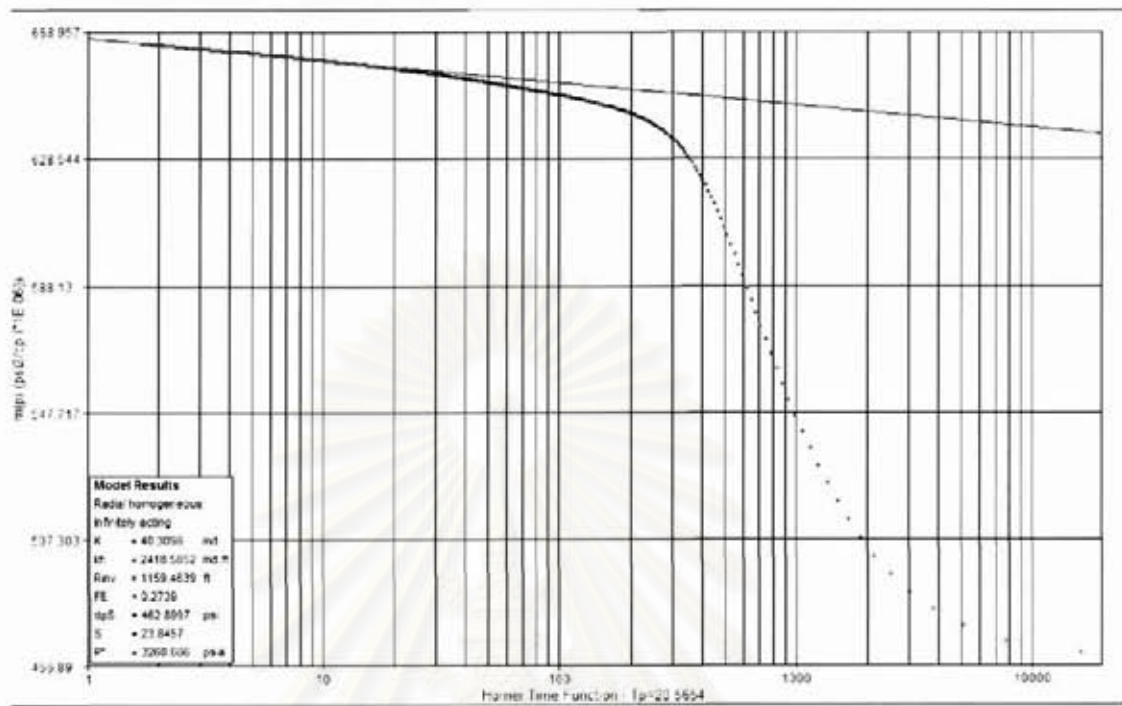


Figure A.85: Well-26 main build-up, semi-log plot.

สถาบันวิทยบริการ
 จุฬาลงกรณ์มหาวิทยาลัย

Well-27 Reservoir 57-0

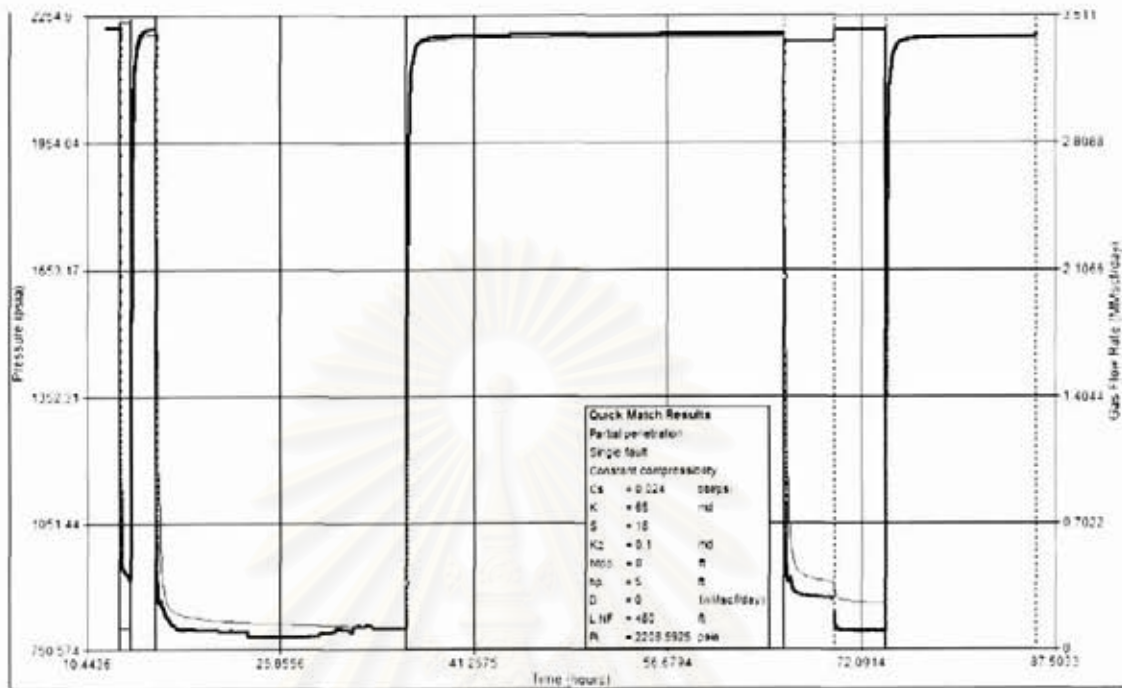


Figure A.86: Well-27 testing overview.

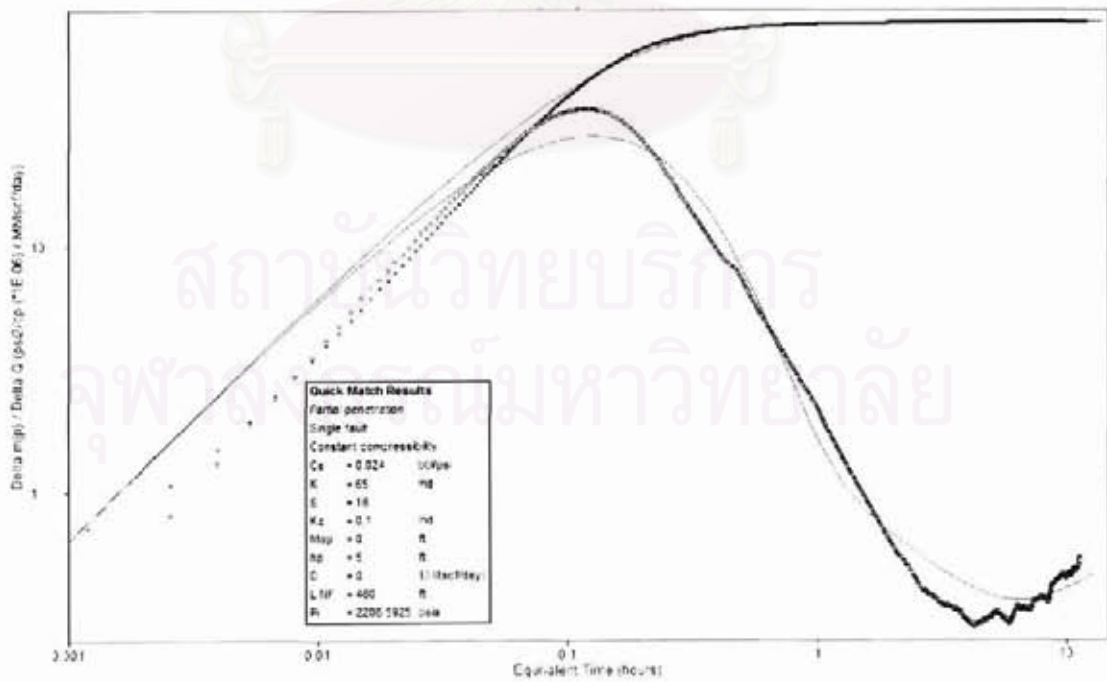


Figure A.87: Well-27 main build-up, log-log plot.

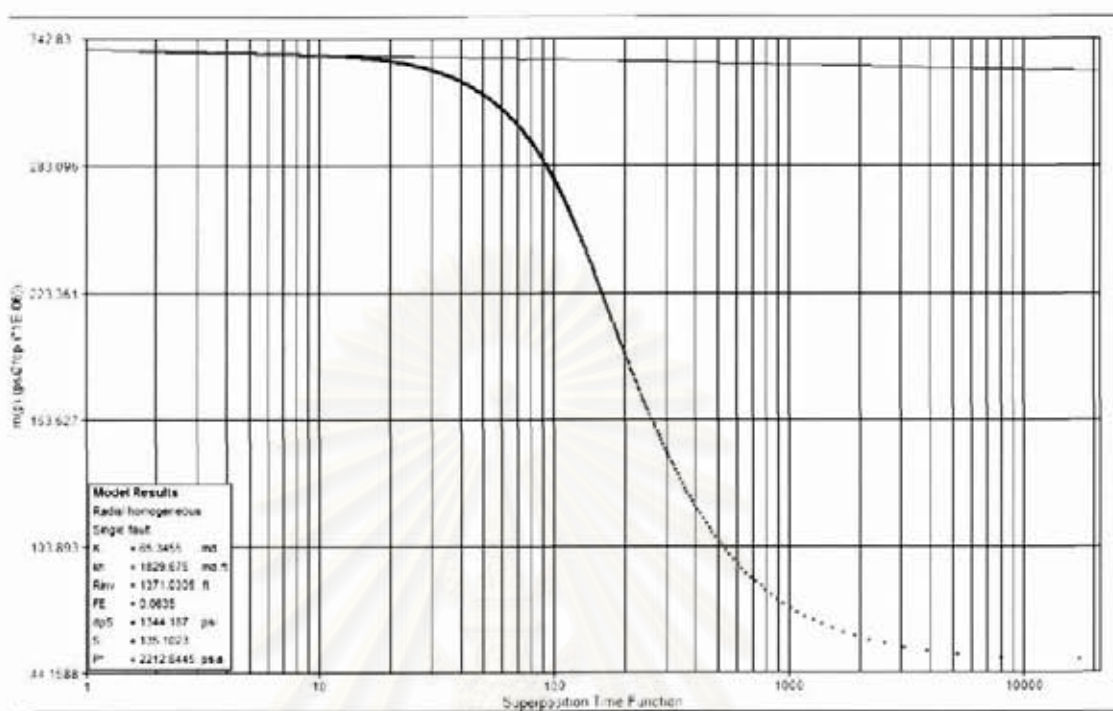


Figure A.88: Well-27 main build-up, semi-log plot.

สถาบันวิทยบริการ
 จุฬาลงกรณ์มหาวิทยาลัย

Well-28 Reservoir 80-6

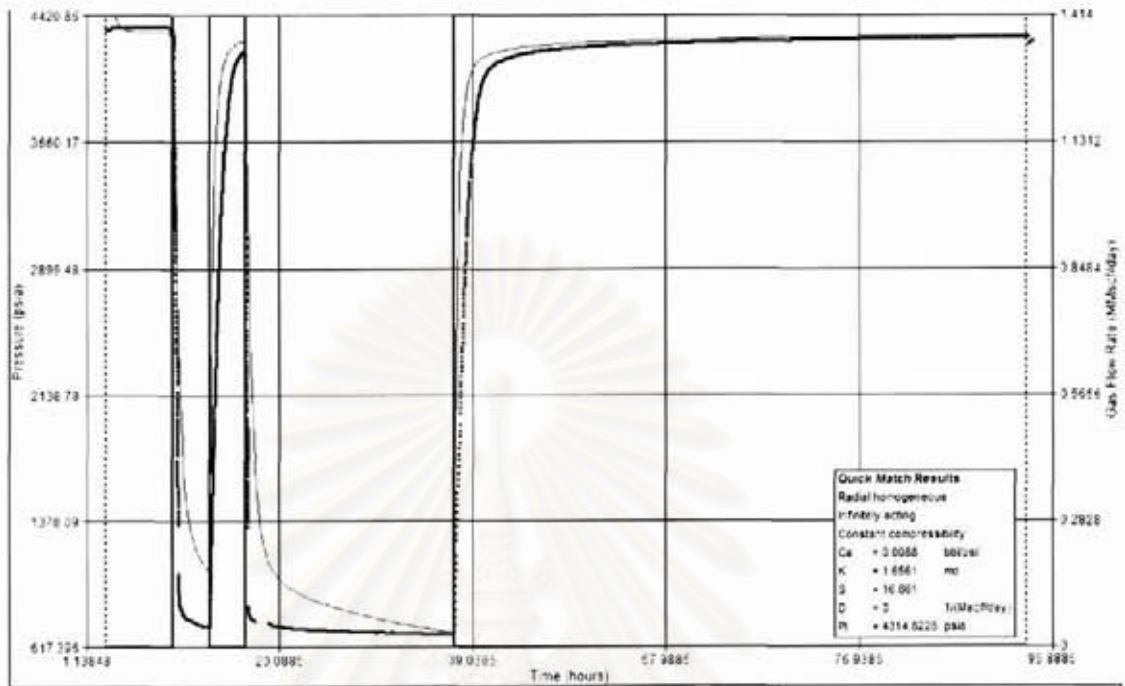


Figure A.89: Well-28 testing overview.

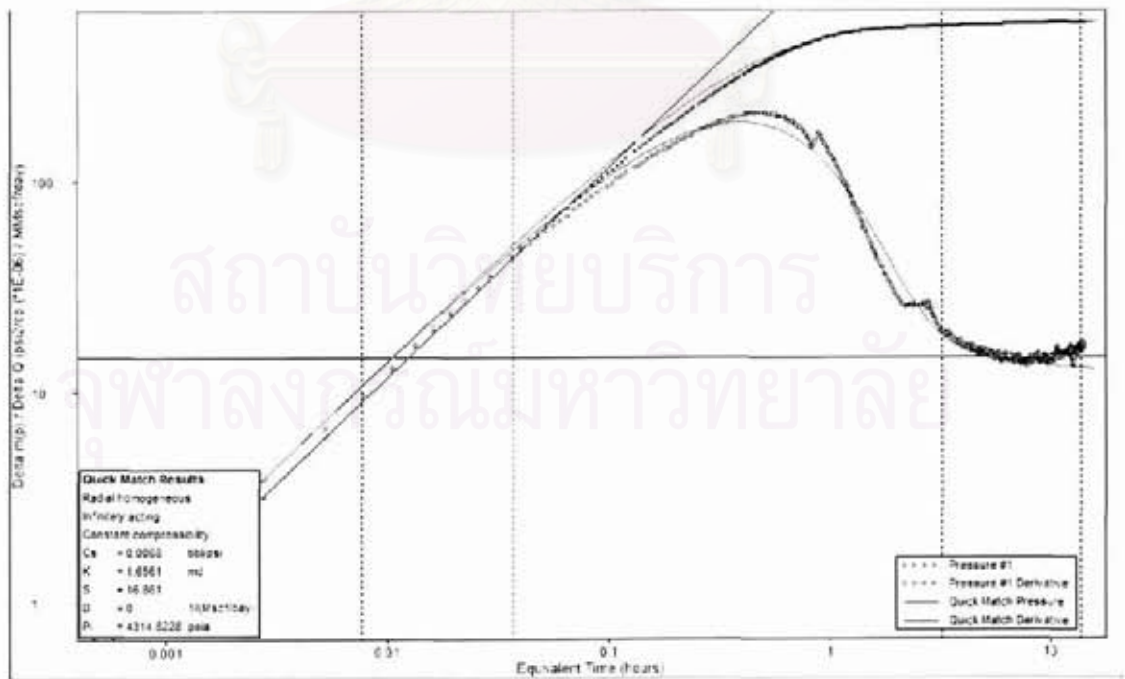


Figure A.90: Well-28 main build-up, log-log plot.

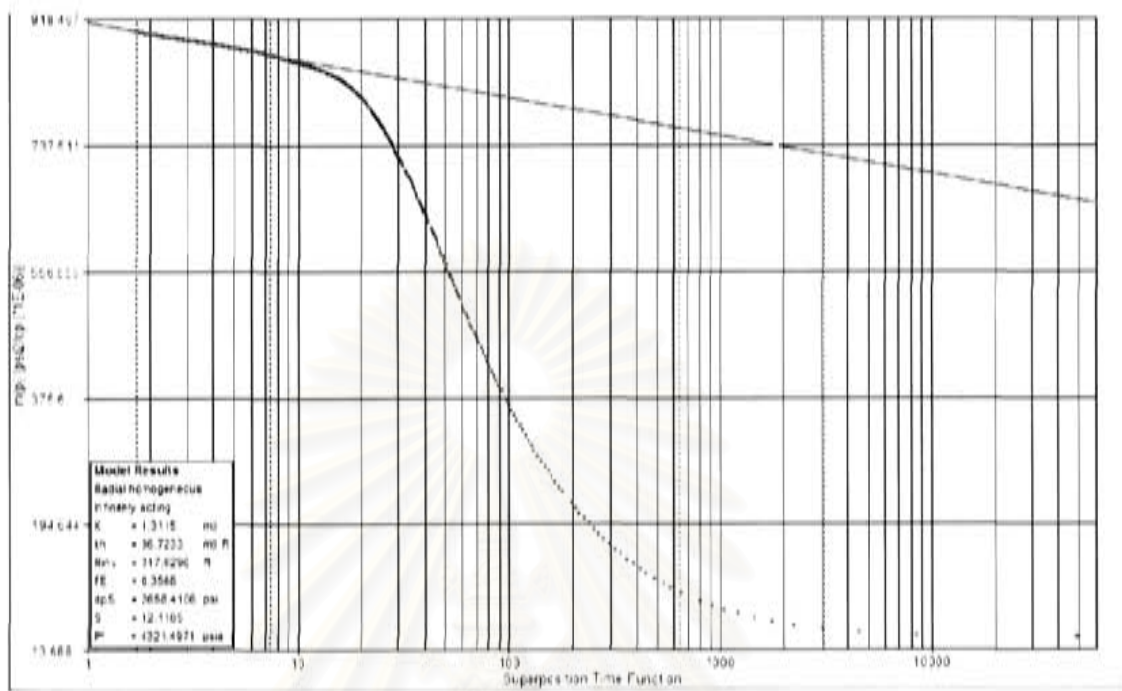


Figure A.91: Well-28 main build-up, semi-log plot.

สถาบันวิทยบริการ
 จุฬาลงกรณ์มหาวิทยาลัย

Well-29 Reservoir 92-5

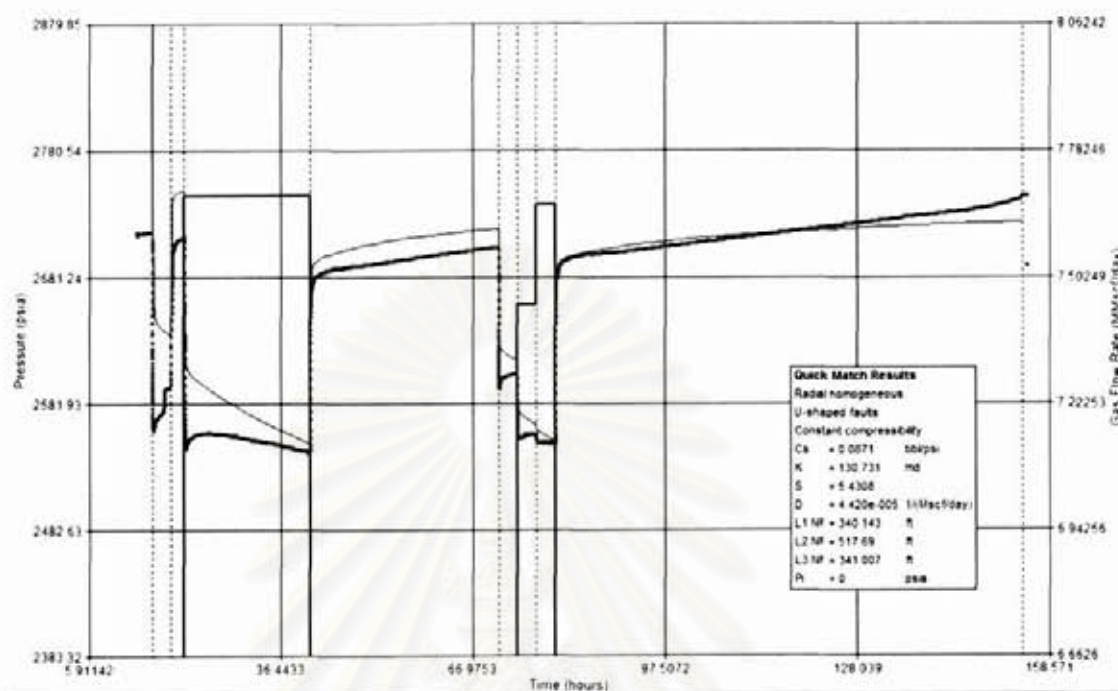


Figure A.92: Well-29 testing overview.

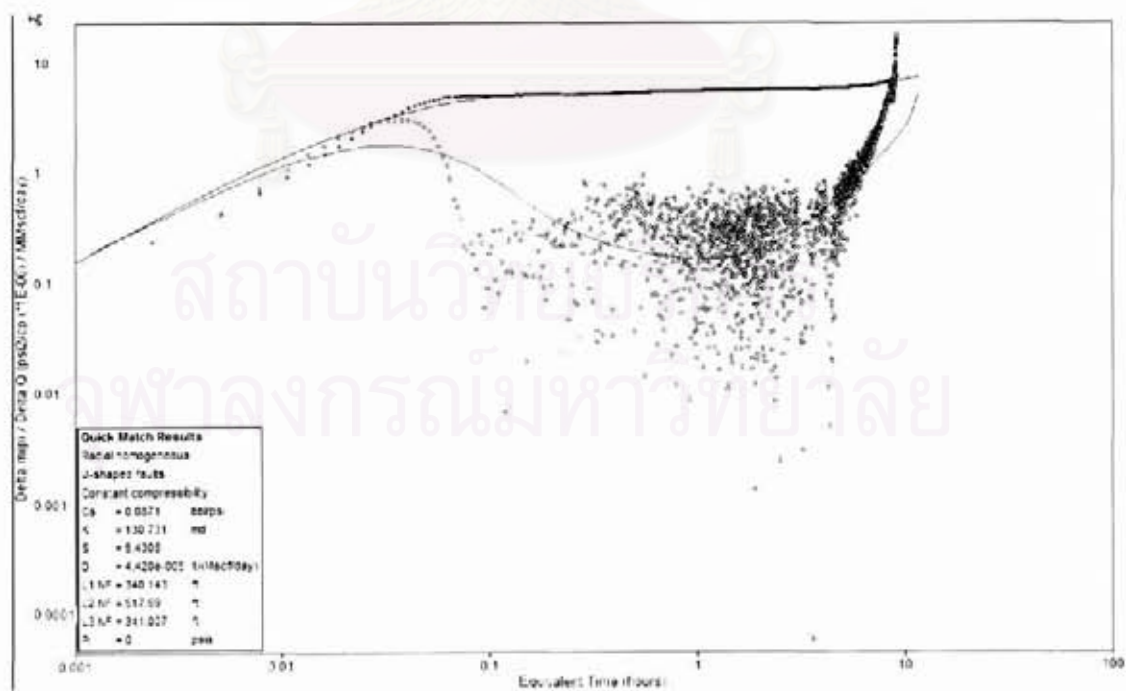


Figure A.93: Well-29 main build-up, log-log plot.

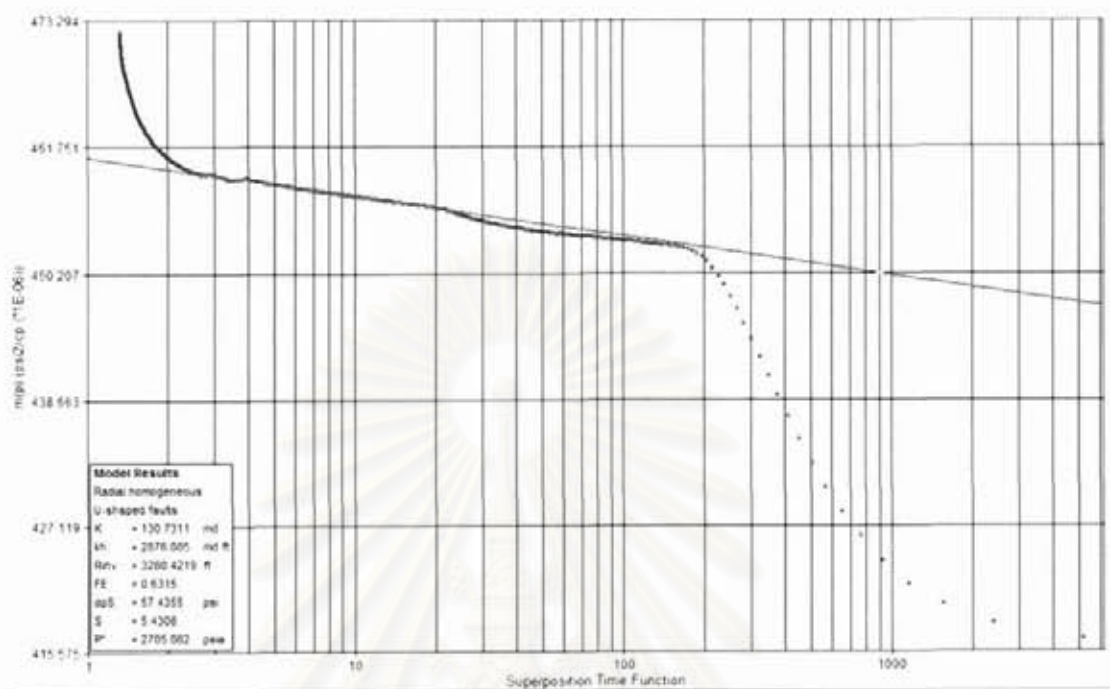


Figure A.94: Well-29 main build-up, semi-log plot.

สถาบันวิทยบริการ
 จุฬาลงกรณ์มหาวิทยาลัย

Well-30 Reservoir 88-4

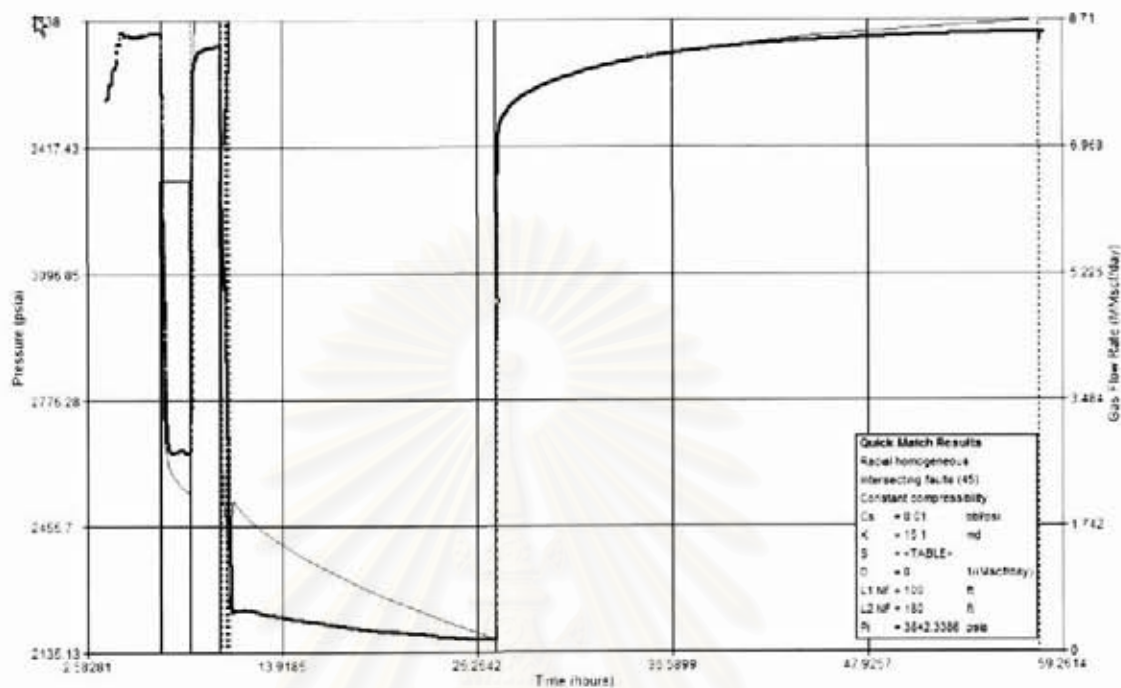


Figure A.95: Well-30 testing overview.

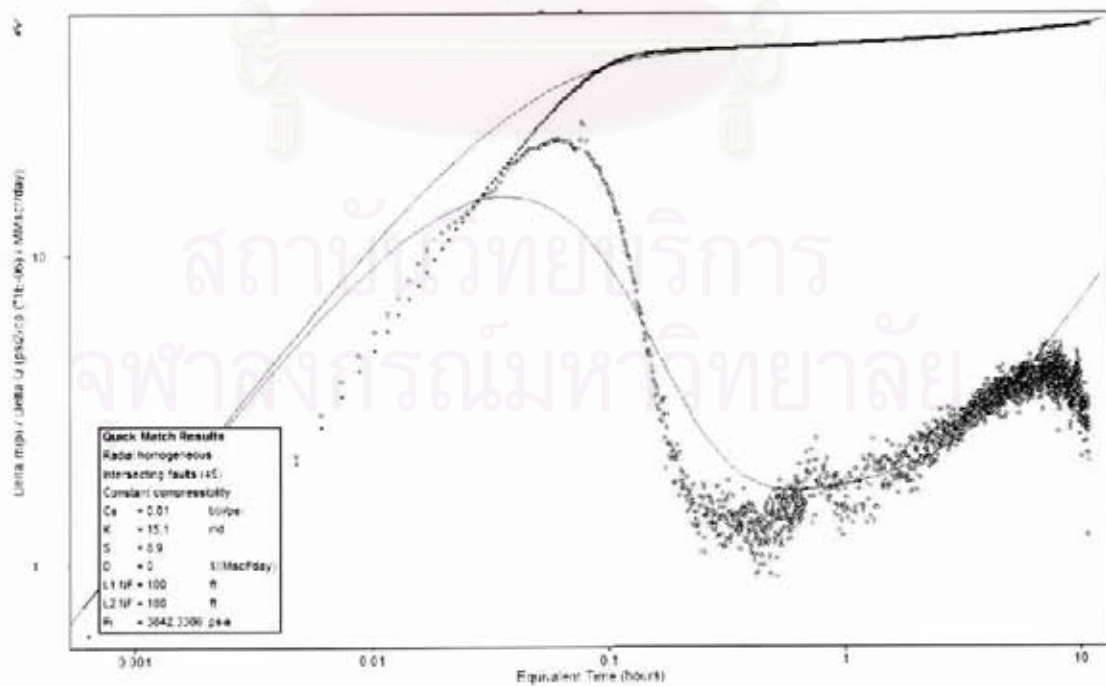


Figure A.96: Well-30 main build-up, log-log plot.

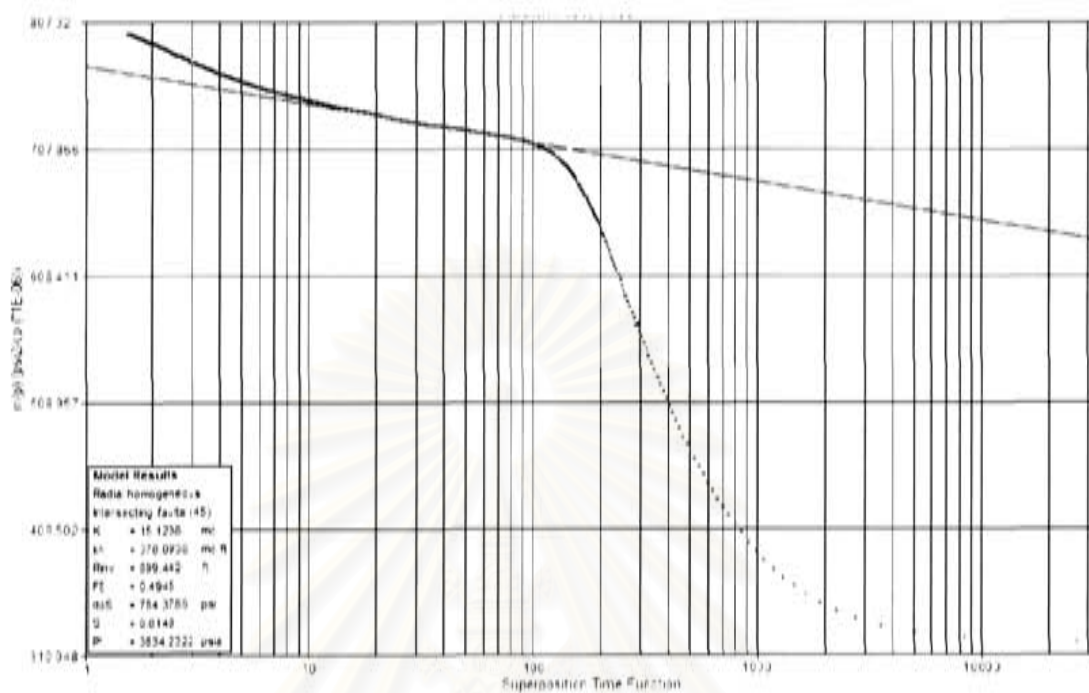


Figure A.97; Well-30 main build-up, semi-log plot.

สถาบันวิทยบริการ
 จุฬาลงกรณ์มหาวิทยาลัย

Well-31 Reservoir 86-1

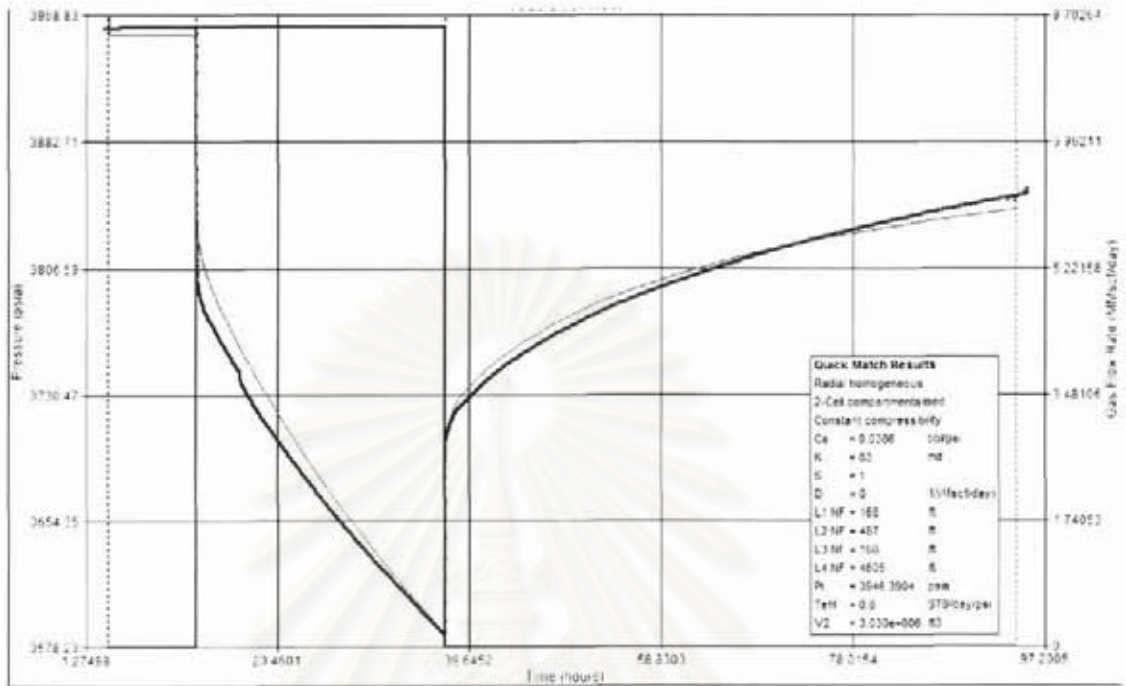


Figure A.98: Well-31 testing overview.

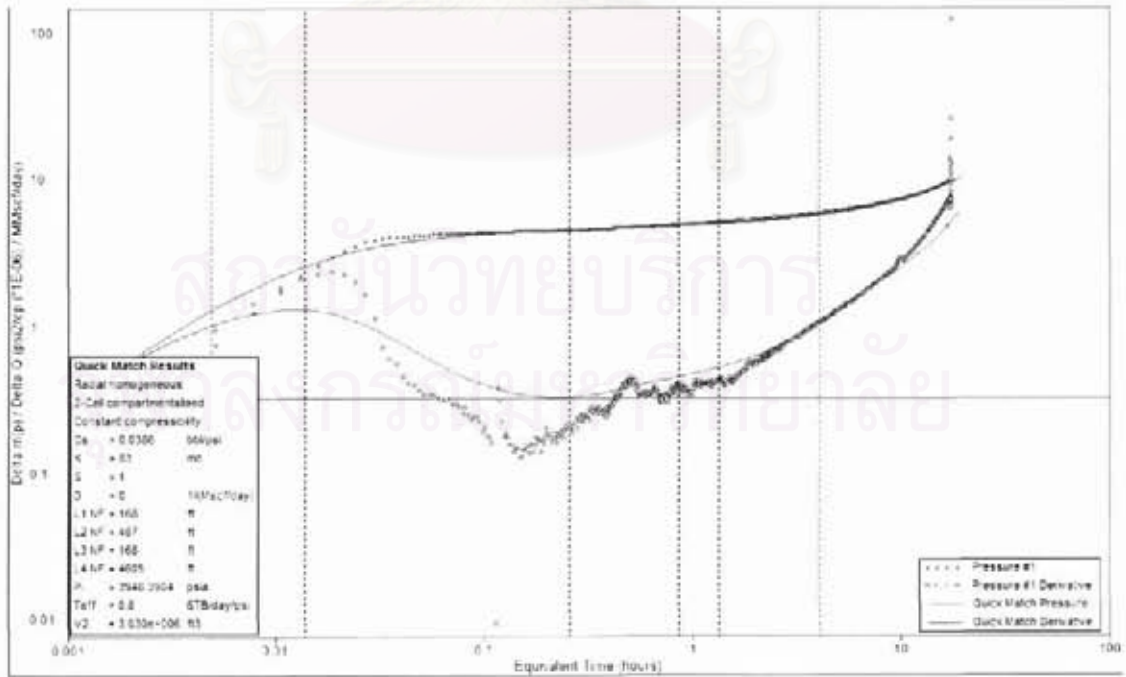


Figure A.99: Well-31 main build-up, log-log plot.

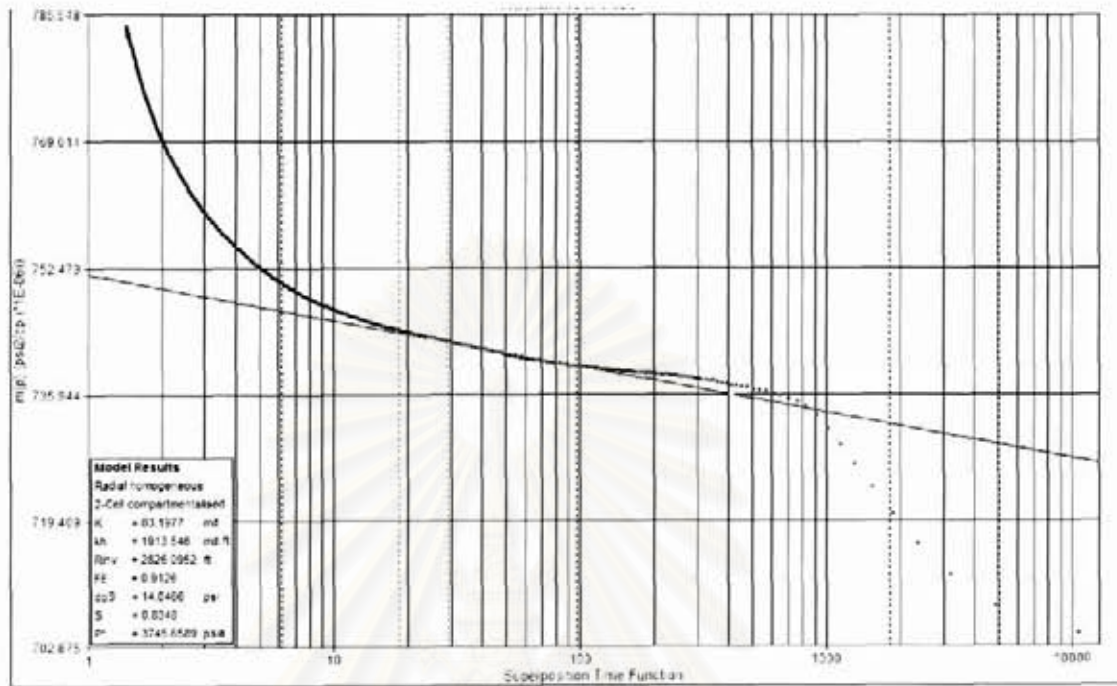


Figure A.100: Well-31 main build-up, semi-log plot.

สถาบันวิทยบริการ
 จุฬาลงกรณ์มหาวิทยาลัย

Well-32 Reservoir 84-0

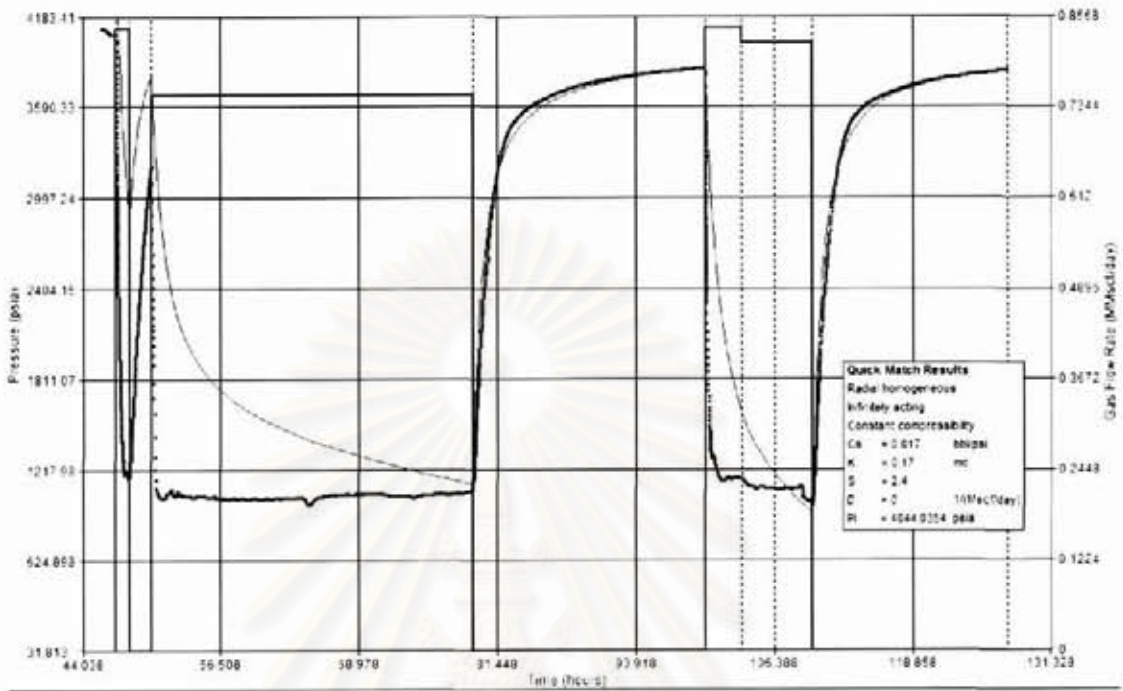


Figure A.101: Well-32 testing overview.

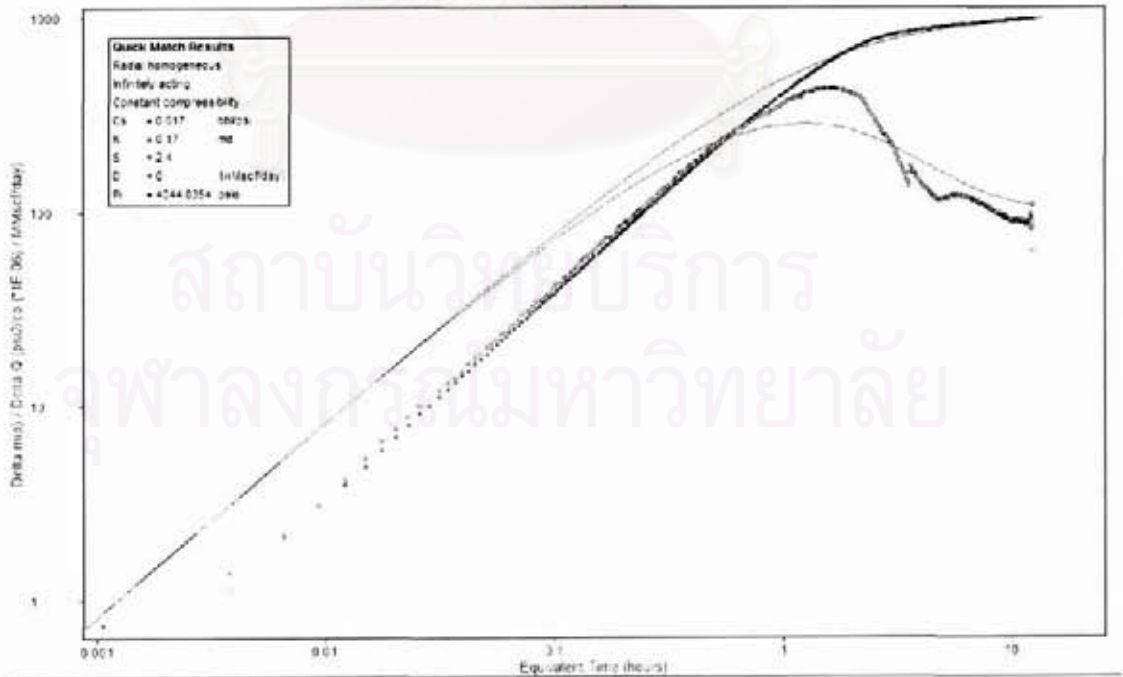


Figure A.102: Well-32 main build-up, log-log plot.

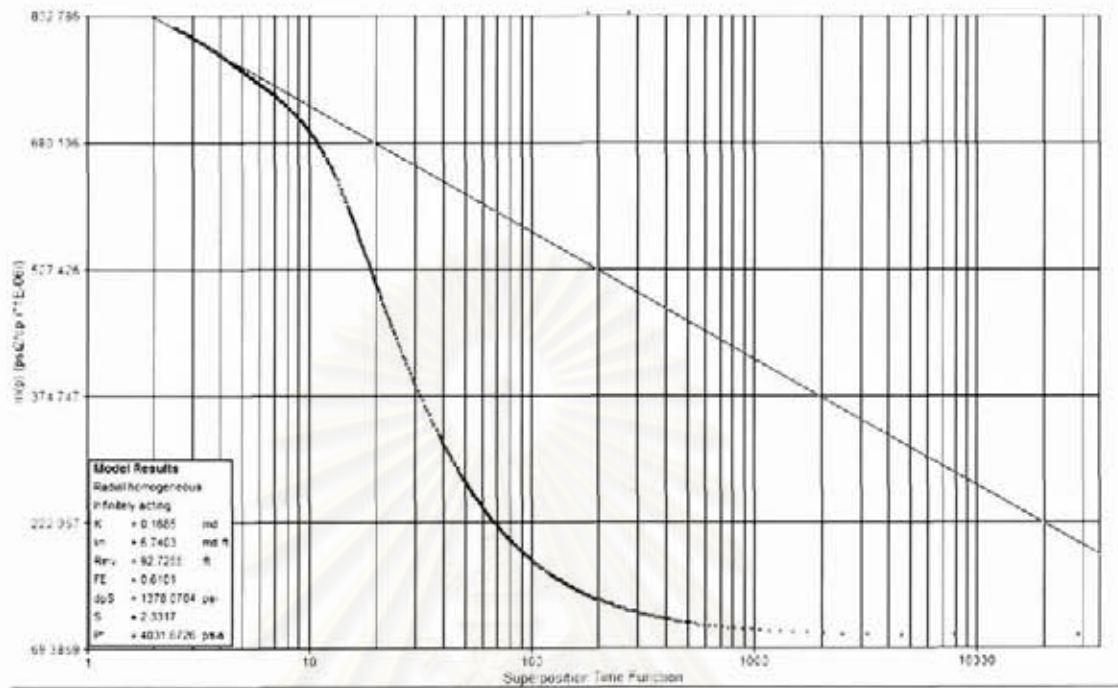


Figure A.103: Well-32 main build-up, semi-log plot.

สถาบันวิทยบริการ
จุฬาลงกรณ์มหาวิทยาลัย

Well-33 Reservoir 78-8

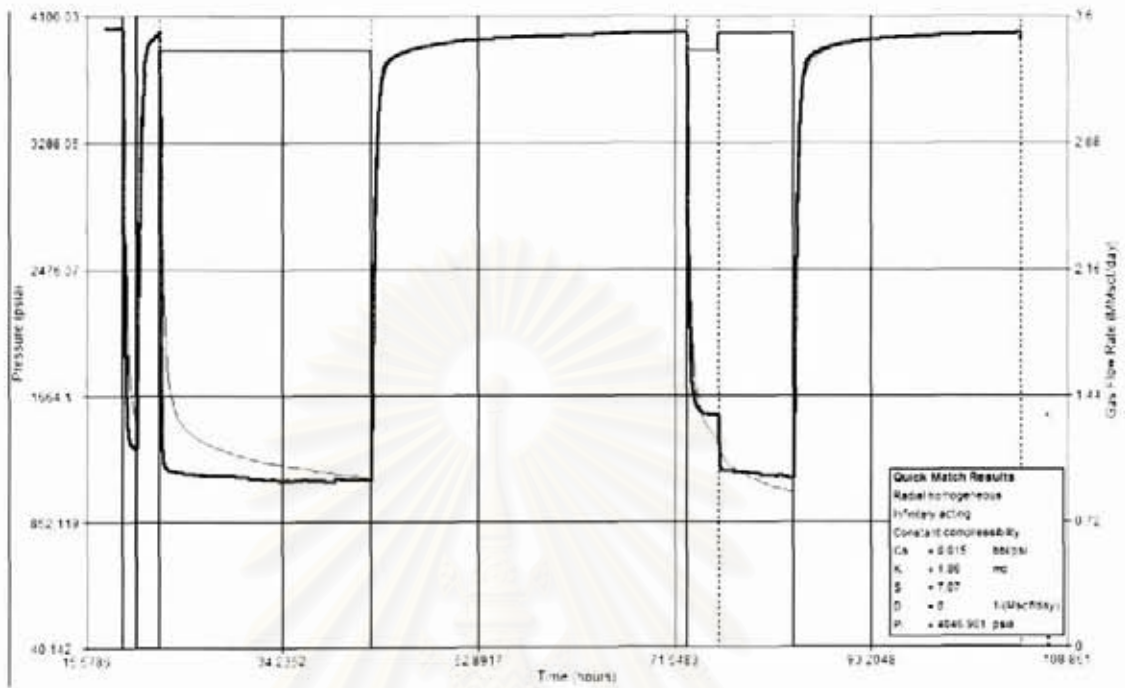


Figure A.104: Well-33 testing overview.

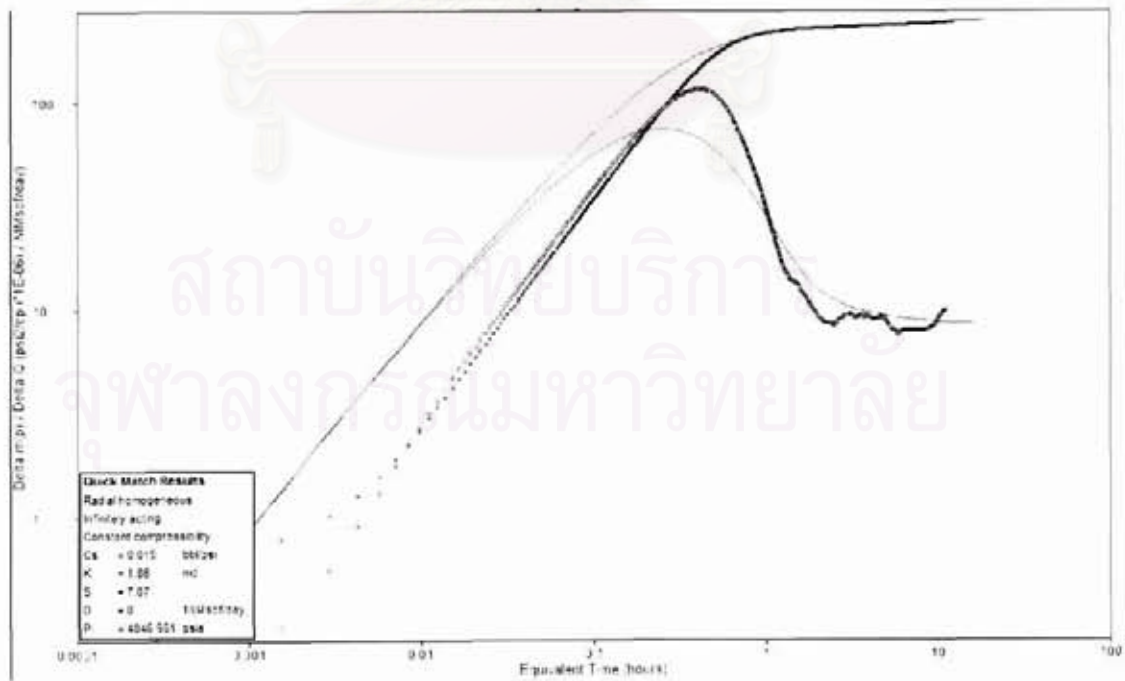


Figure A.105: Well-33 main build-up, log-log plot.

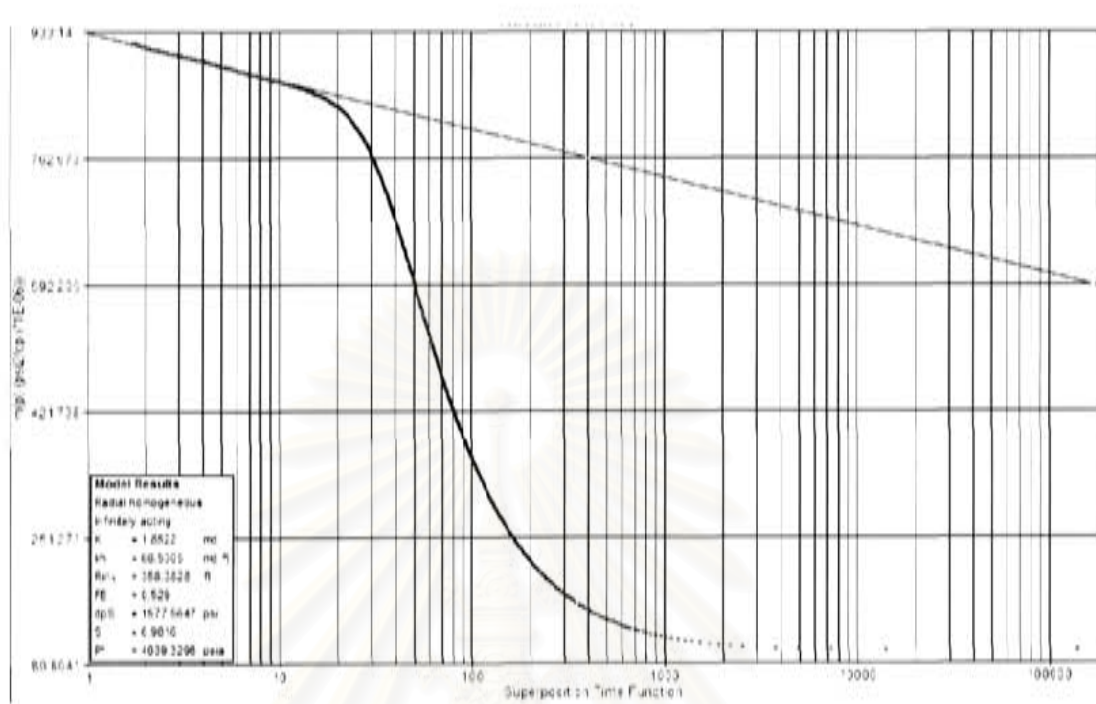


Figure A.106: Well-33 main build-up, semi-log plot.

สถาบันวิทยบริการ
จุฬาลงกรณ์มหาวิทยาลัย

Well-34 Reservoir 92-9

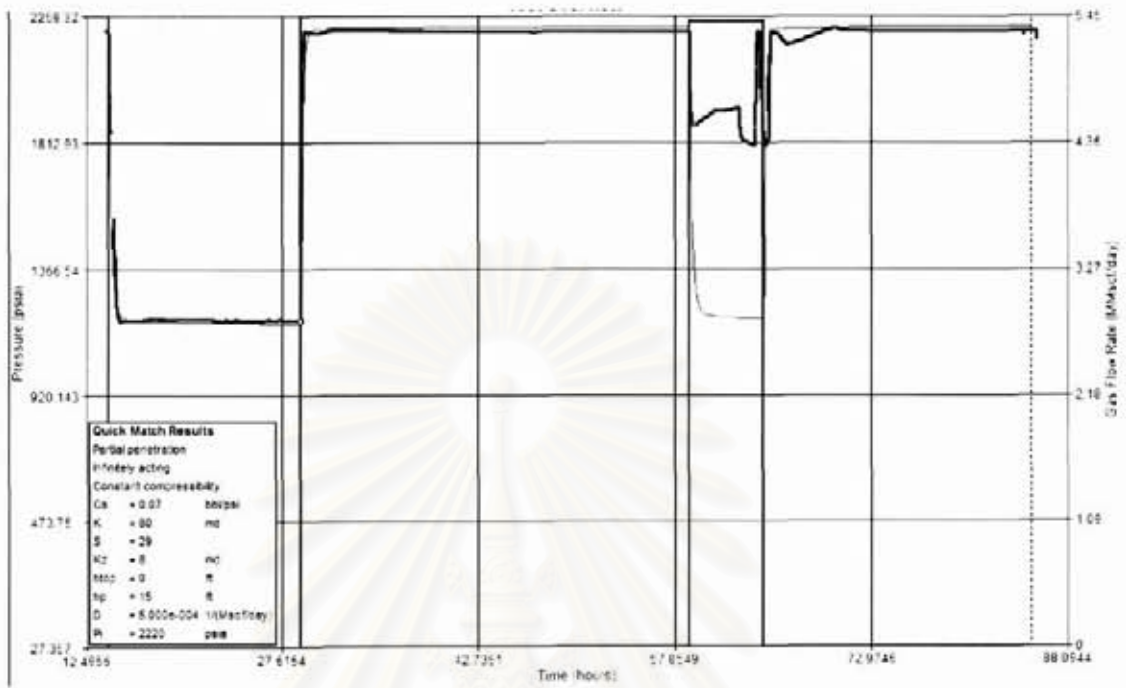


Figure A.107: Well-34 testing overview.

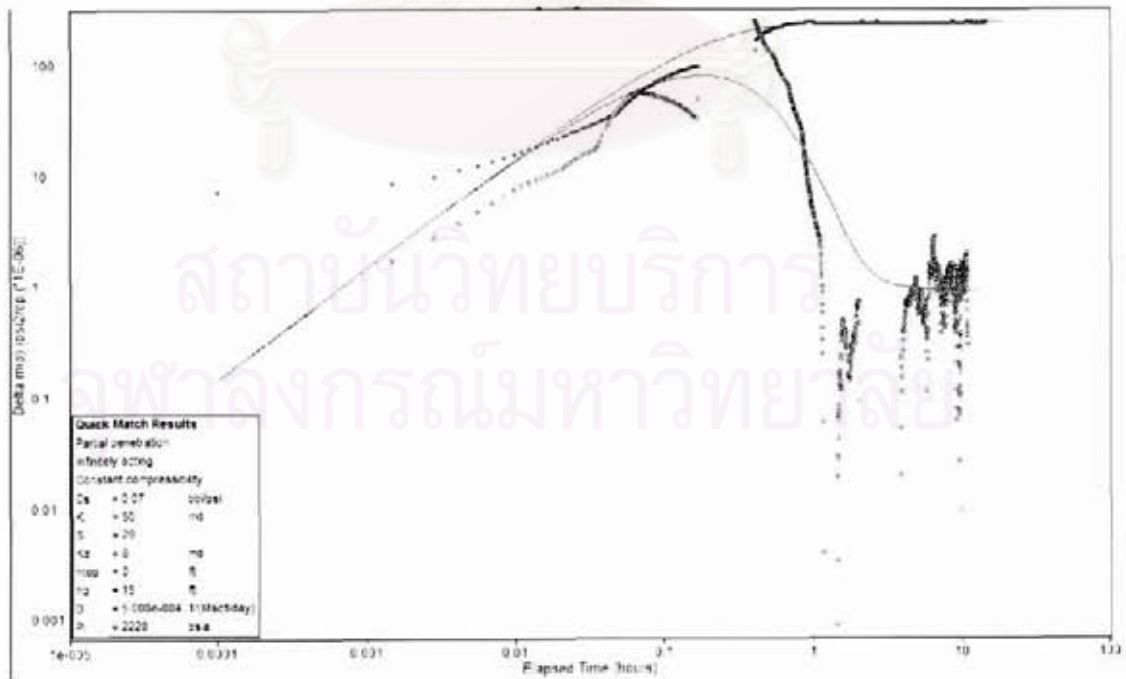


Figure A.108: Well-34 main build-up, log-log plot.

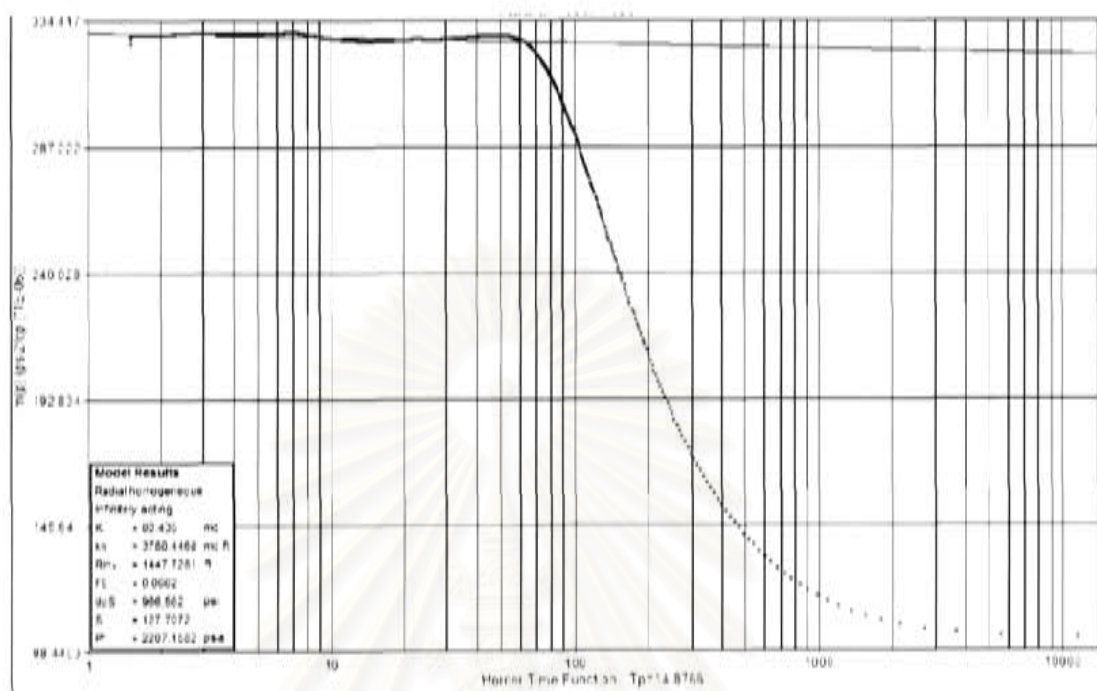


Figure A.109: Well-34 main build-up, semi-log plot.

สถาบันวิทยบริการ
จุฬาลงกรณ์มหาวิทยาลัย

Well-35 Reservoir 87-1

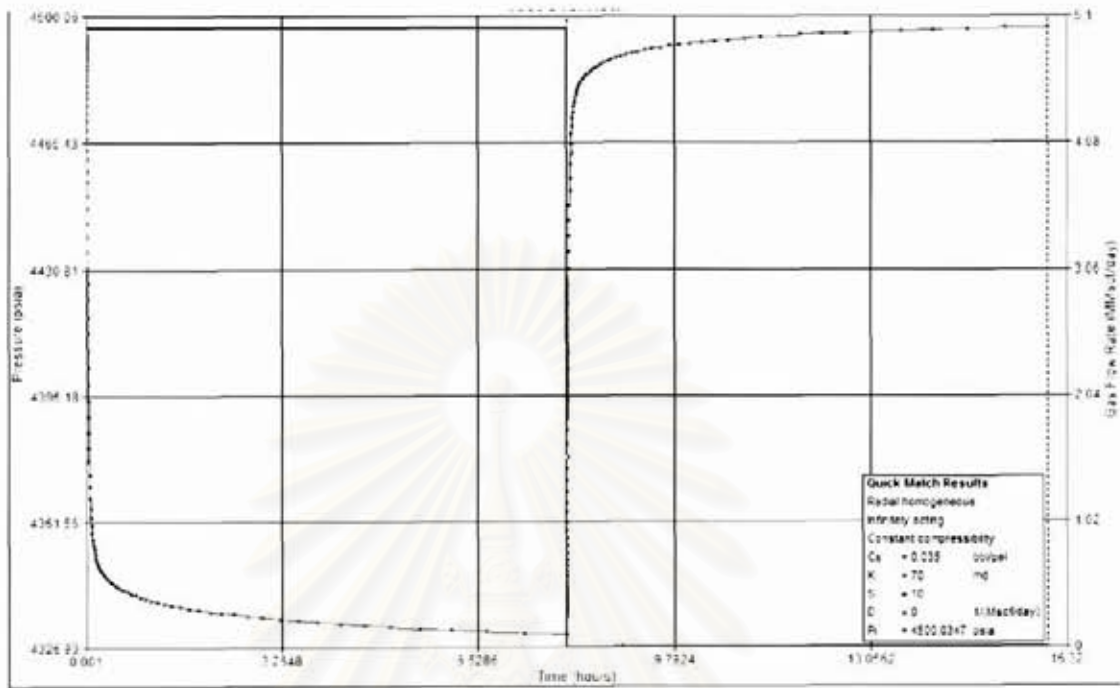


Figure A.110: Well-35 testing overview.

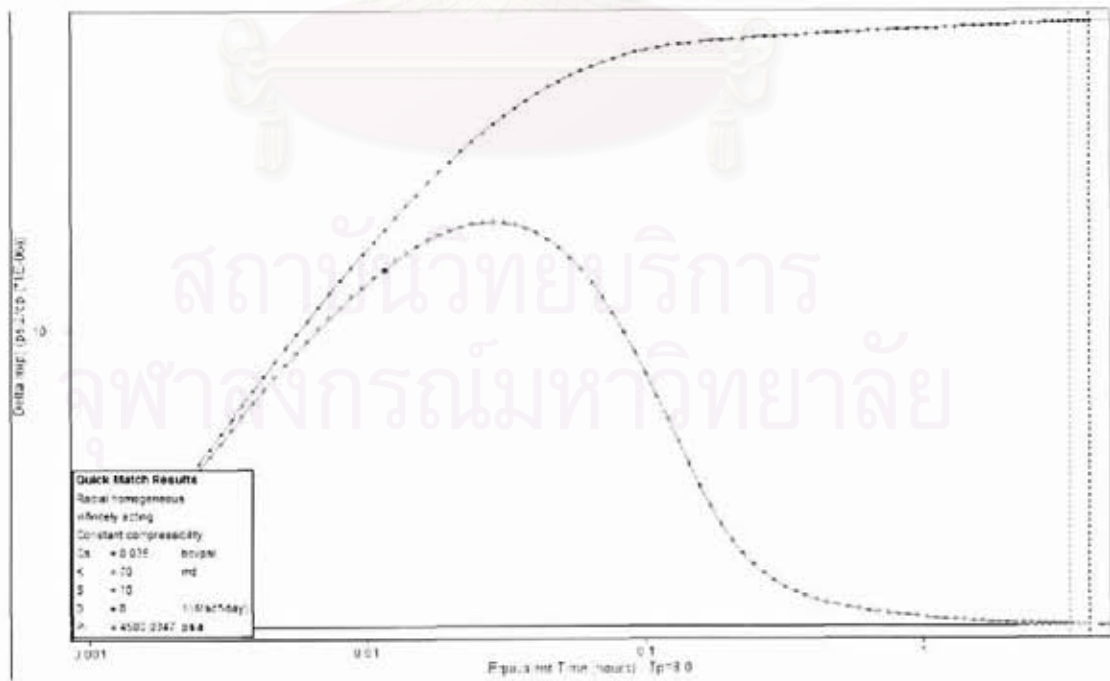


Figure A.111: Well-35 main build-up, log-log plot.

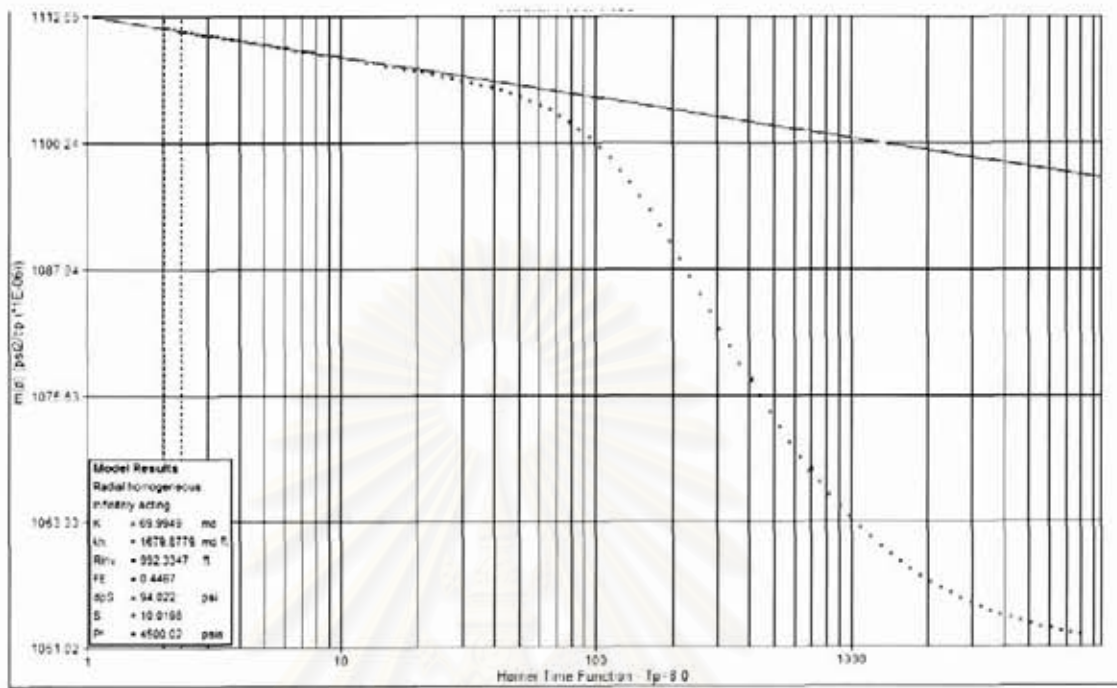


Figure A.112: Well-35 main build-up, semi-log plot.

สถาบันวิทยบริการ
 จุฬาลงกรณ์มหาวิทยาลัย

Well-36 Reservoir 91-7

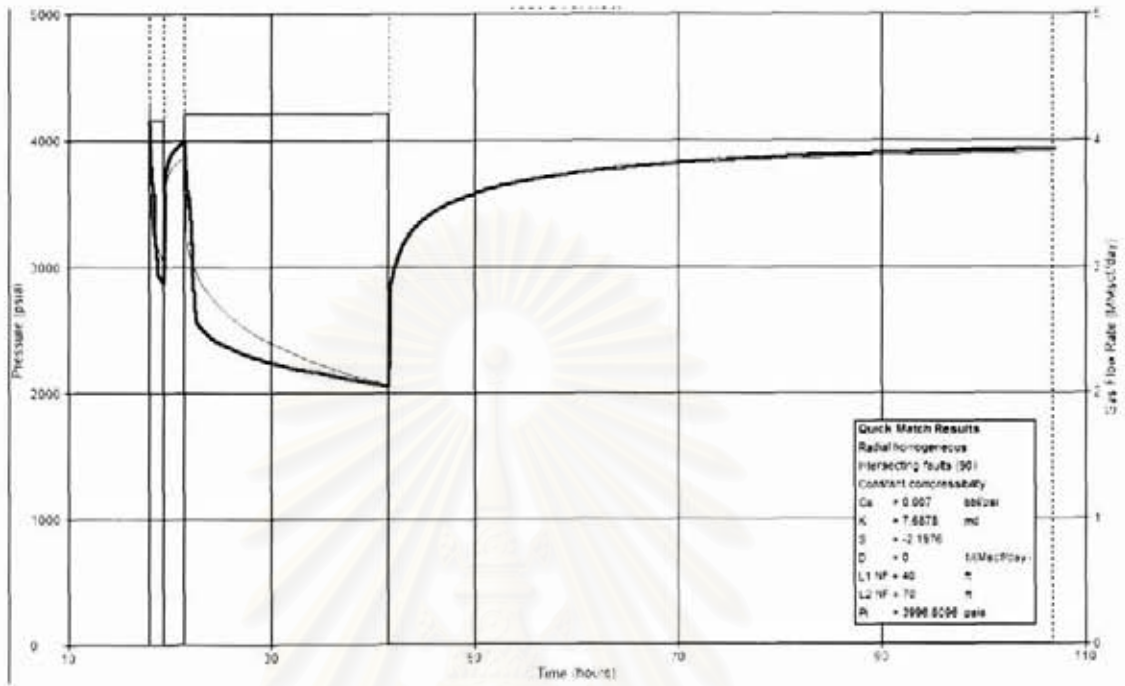


Figure A.113: Well-36 testing overview.

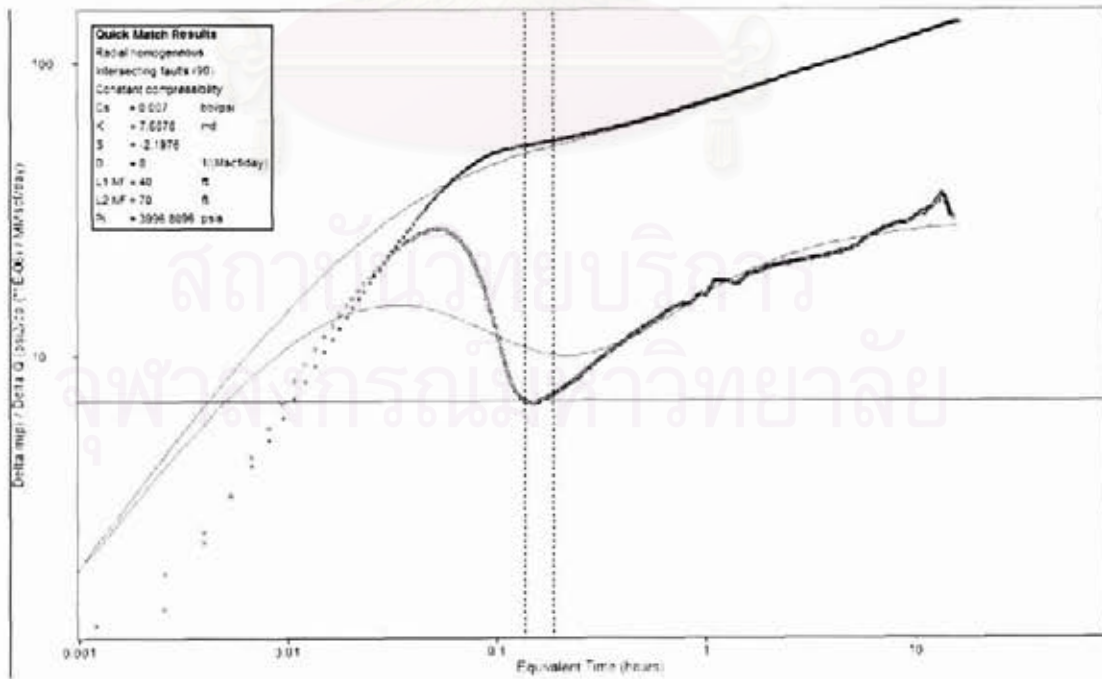


Figure A.114: Well-36 main build-up, log-log plot.

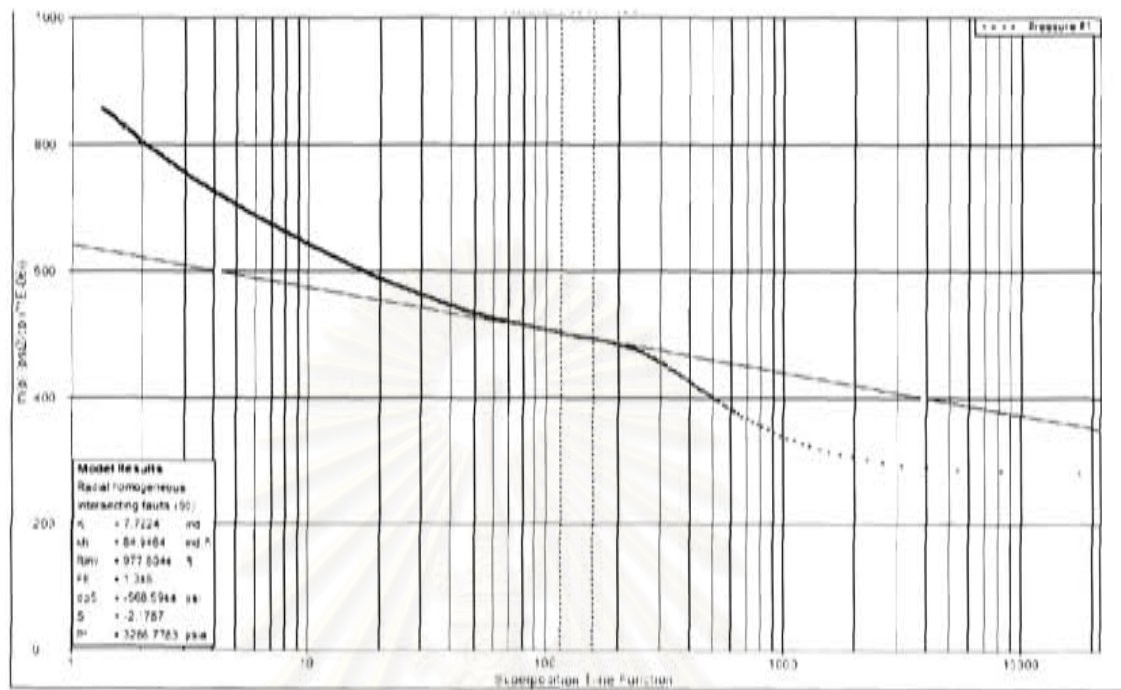


Figure A.115: Well-36 main build-up, semi-log plot.

สถาบันวิทยบริการ
 จุฬาลงกรณ์มหาวิทยาลัย

Well-37 Reservoir 64-0

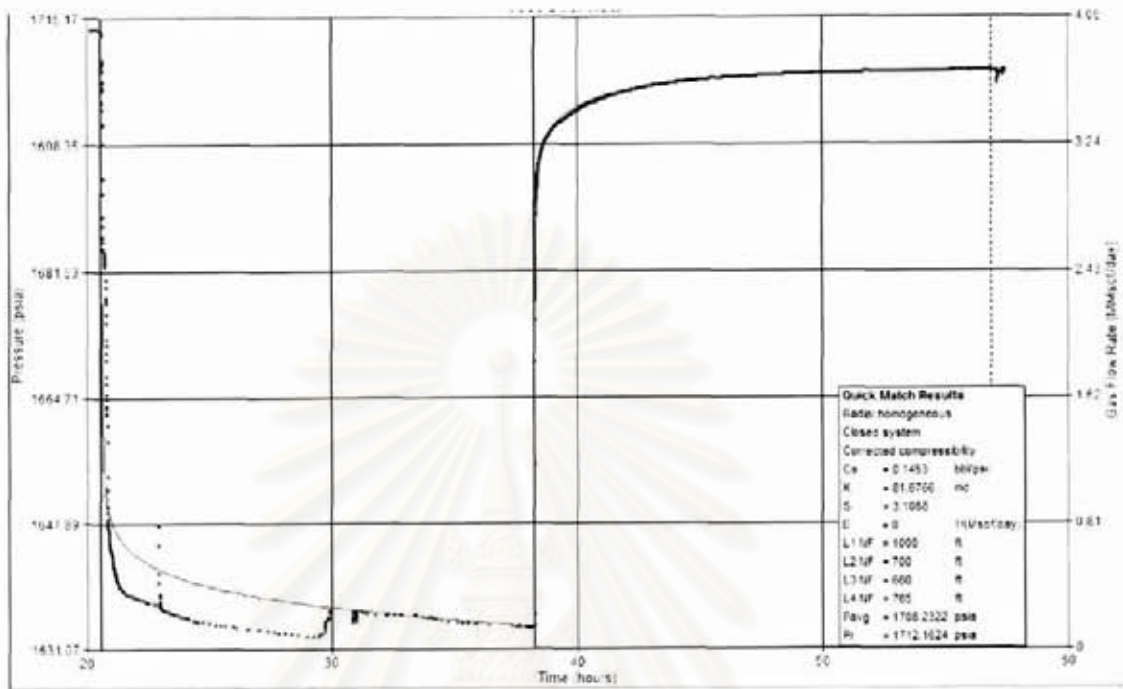


Figure A.116: Well-37 testing overview.

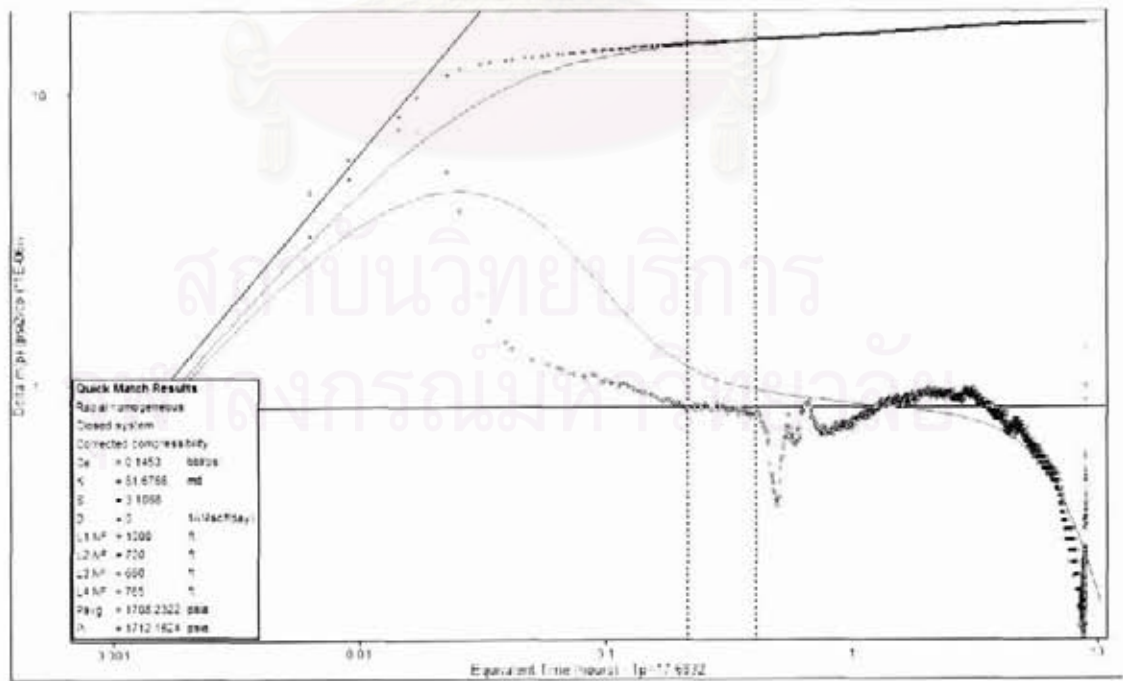


Figure A.117: Well-37 main build-up, log-log plot.

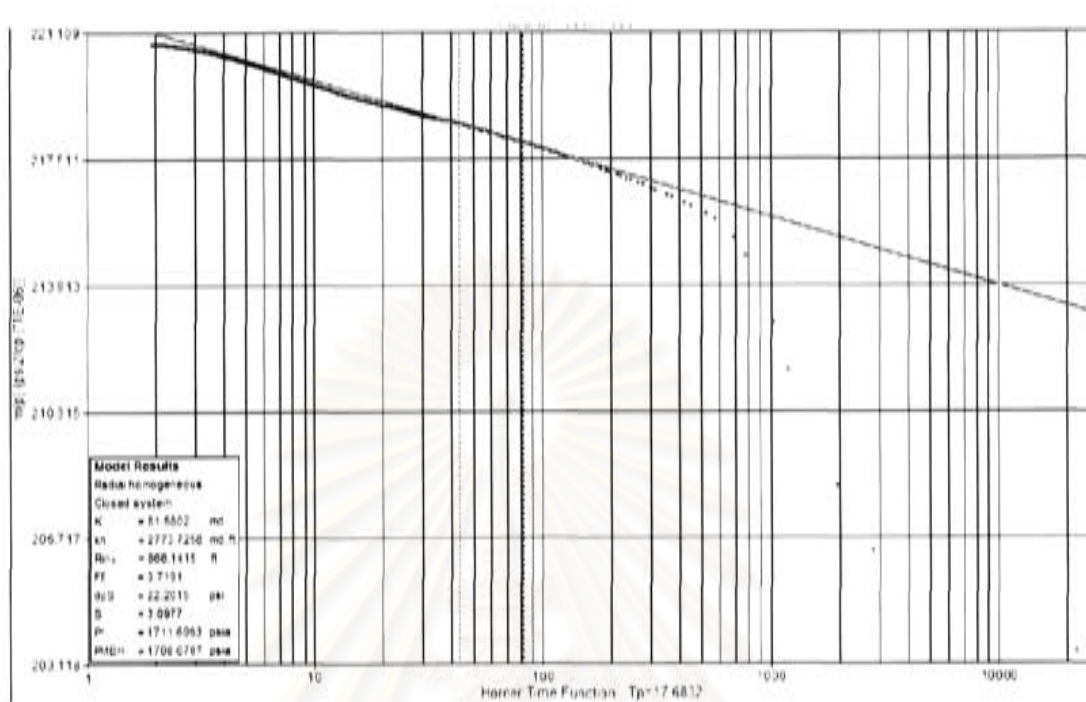


Figure A.118: Well-37 main build-up, semi-log plot.

สถาบันวิทยบริการ
 จุฬาลงกรณ์มหาวิทยาลัย

Well-38 Reservoir 89-9

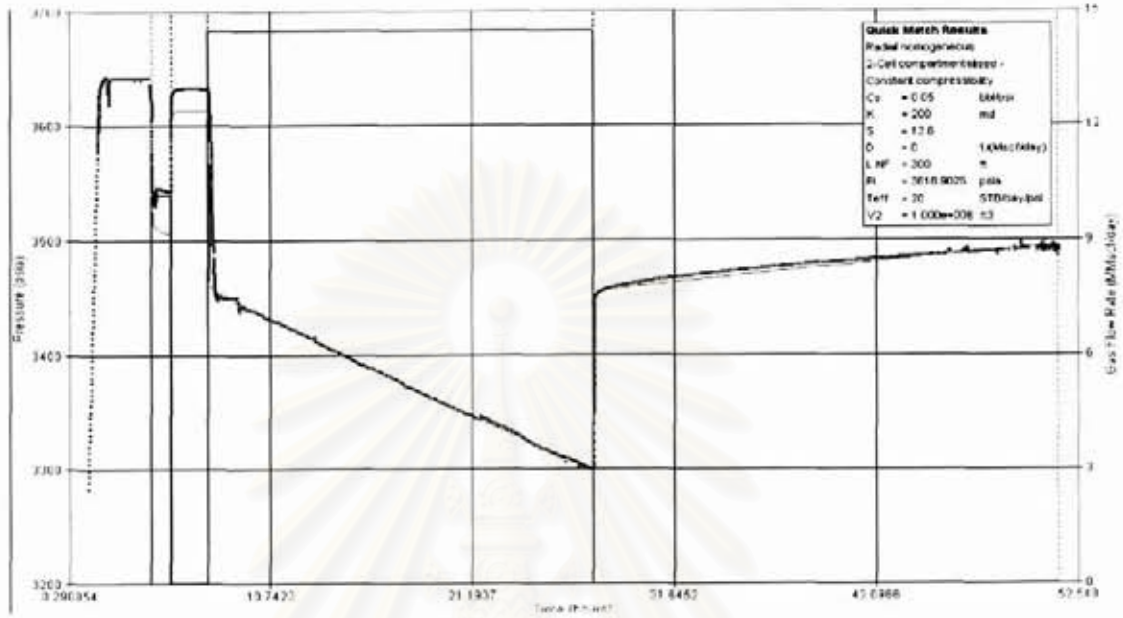


Figure A.119: Well-38 testing overview.

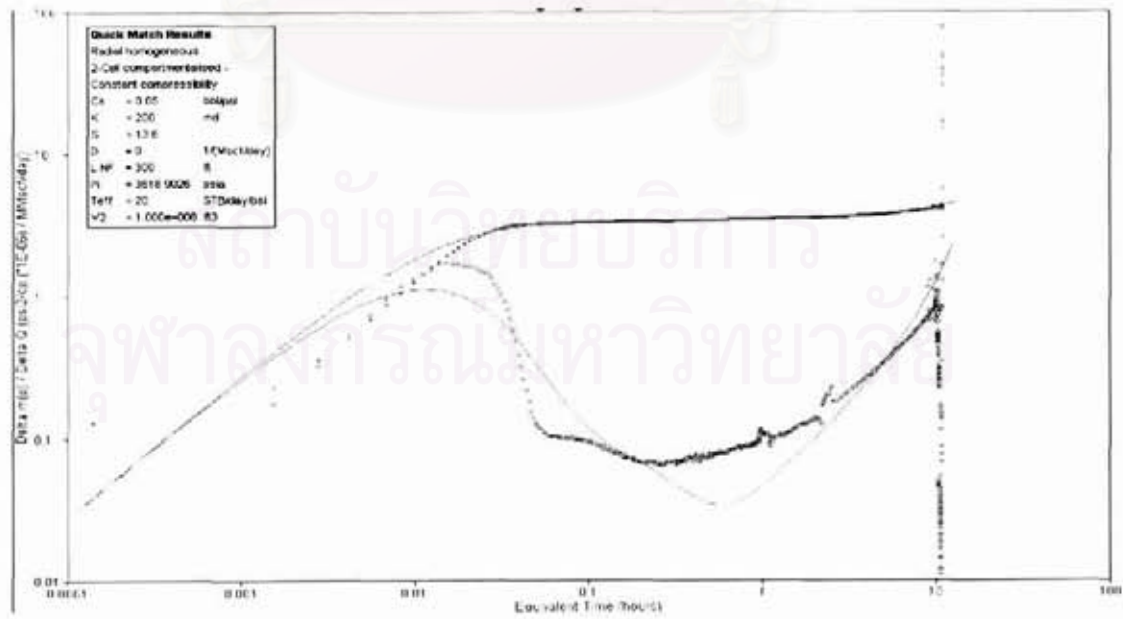


Figure A.120: Well-38 main build-up, log-log plot.

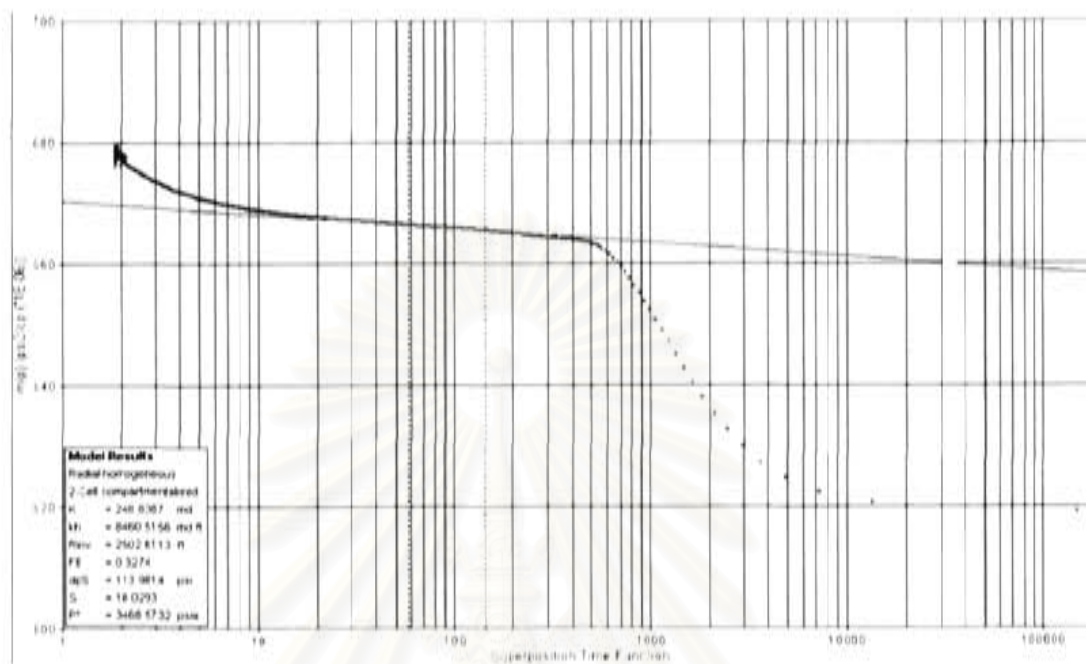


Figure A.121: Well-38 main build-up, semi-log plot.

สถาบันวิทยบริการ
 จุฬาลงกรณ์มหาวิทยาลัย

Well-39 Reservoir 87-1

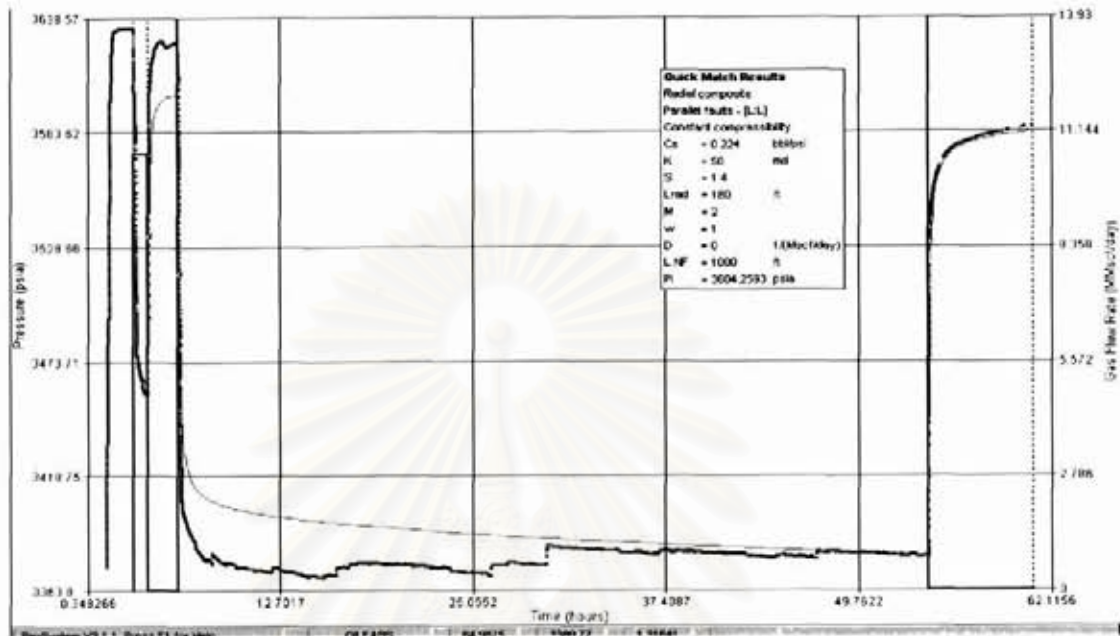


Figure A.122: Well-39 testing overview.

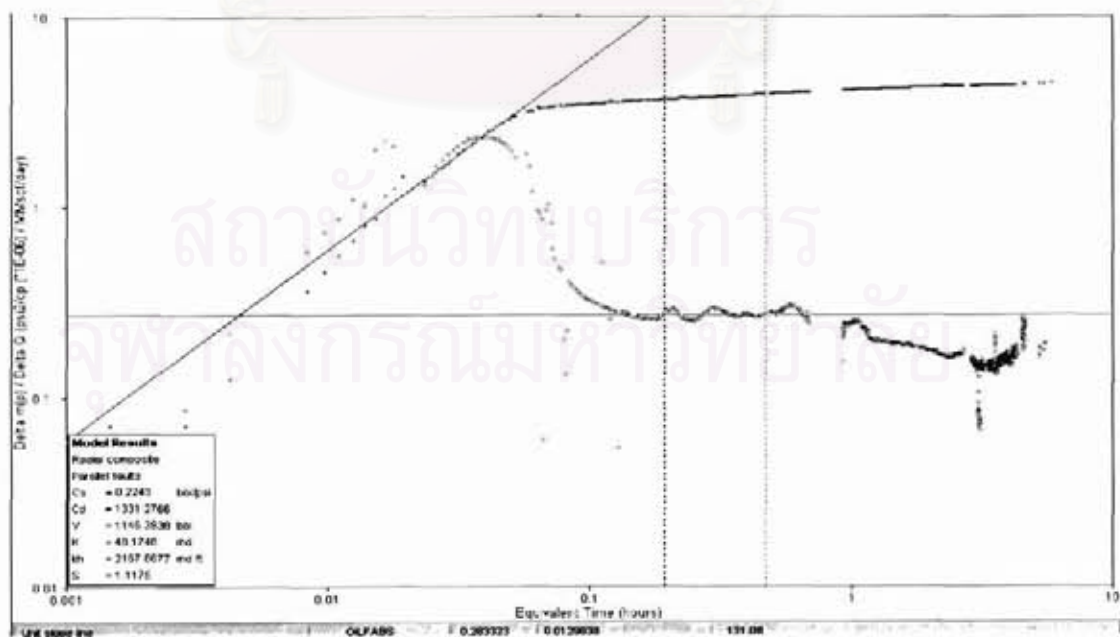


Figure A.123: Well-39 main build-up, log-log plot.

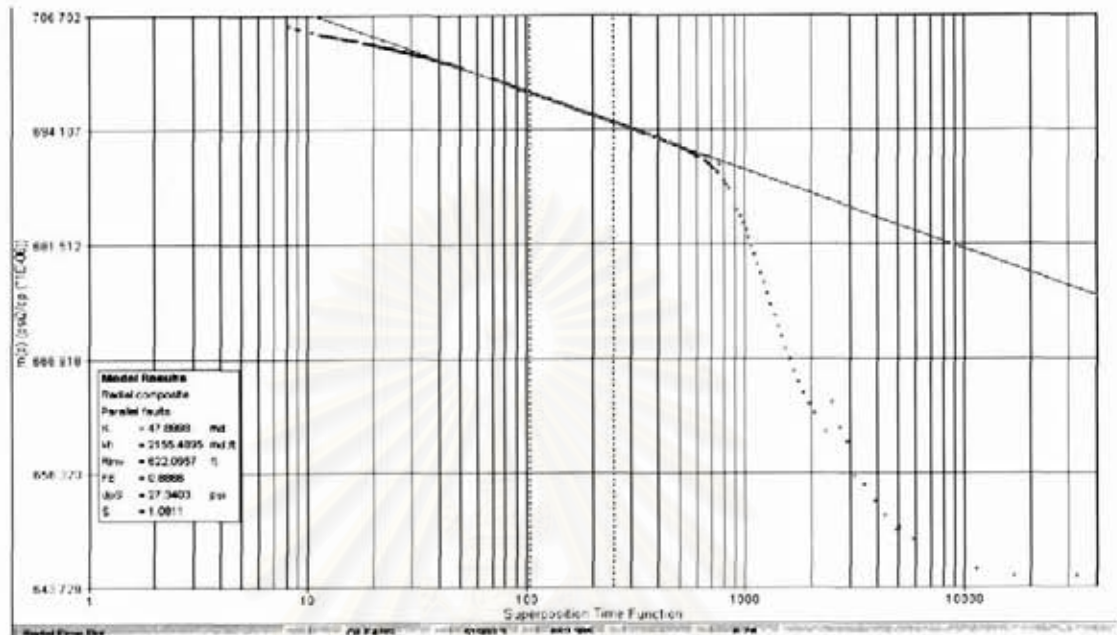


Figure A.124: Well-39 main build-up, semi-log plot.

สถาบันวิทยบริการ
 จุฬาลงกรณ์มหาวิทยาลัย

Well-40 Reservoir 83-4

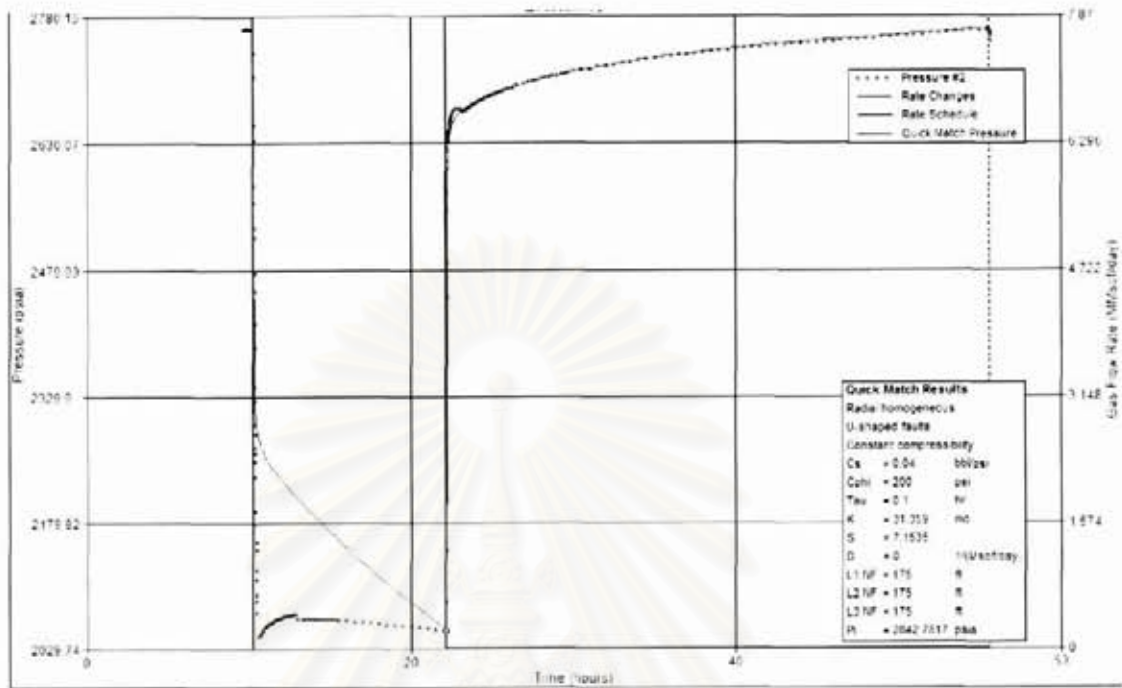


Figure A.125: Well-40 testing overview.

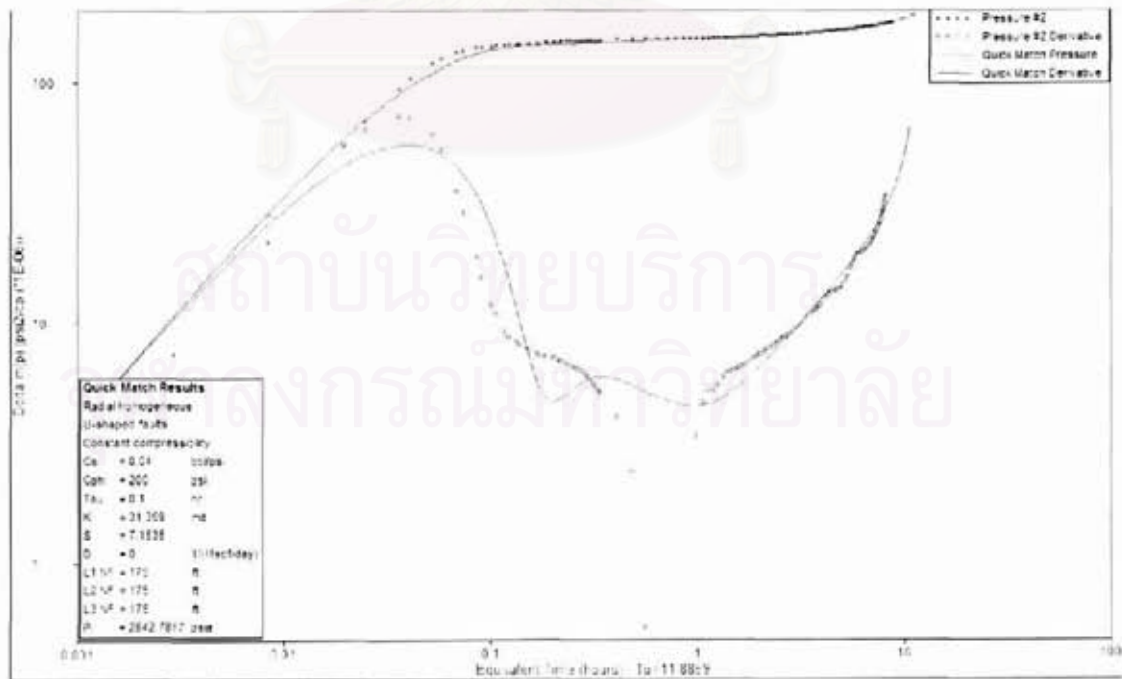


Figure A.126: Well-40 main build-up, log-log plot.

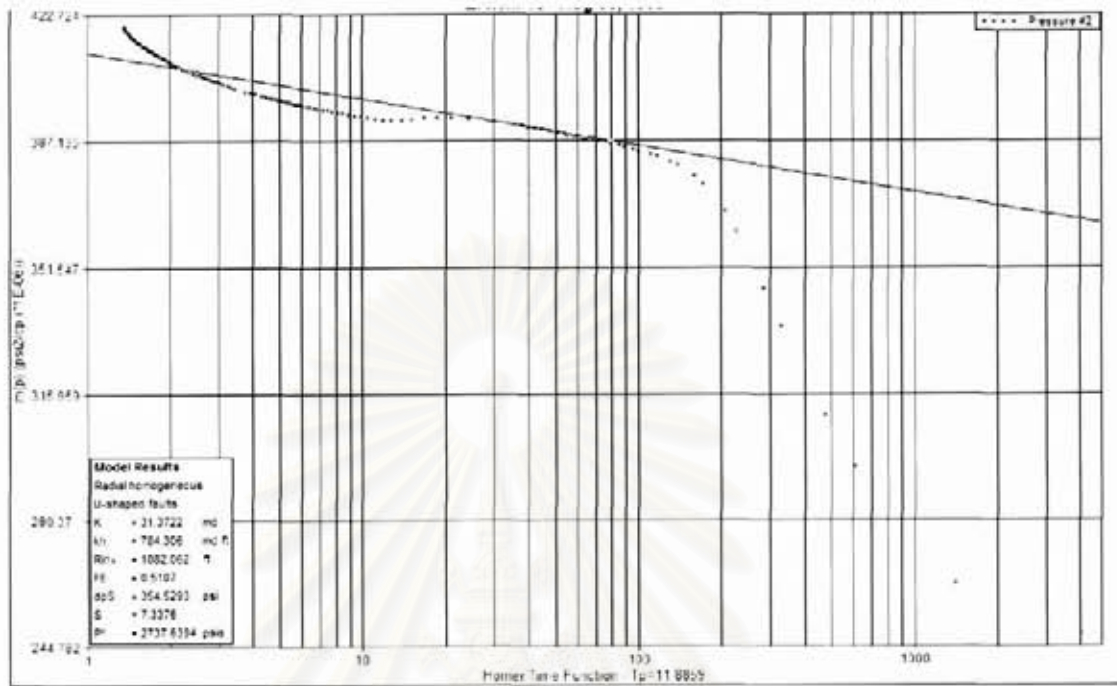


Figure A.127: Well-40 main build-up, semi-log plot.

สถาบันวิทยบริการ
จุฬาลงกรณ์มหาวิทยาลัย

Well-41 Reservoir 69-8

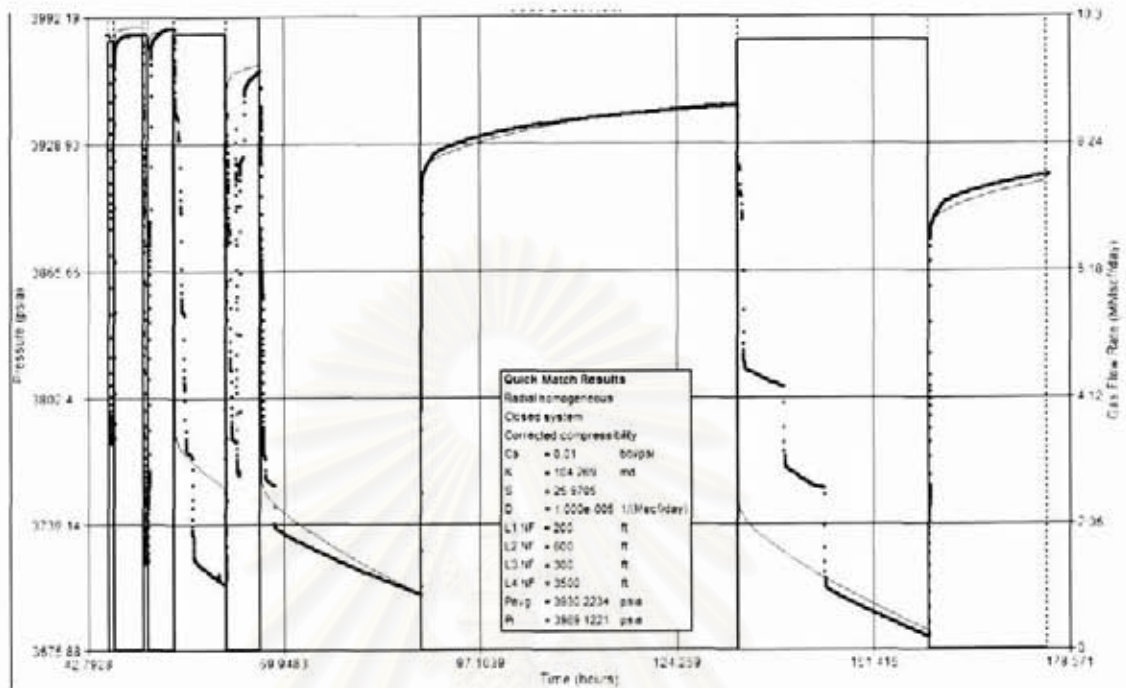


Figure A.128: Well-41 testing overview.

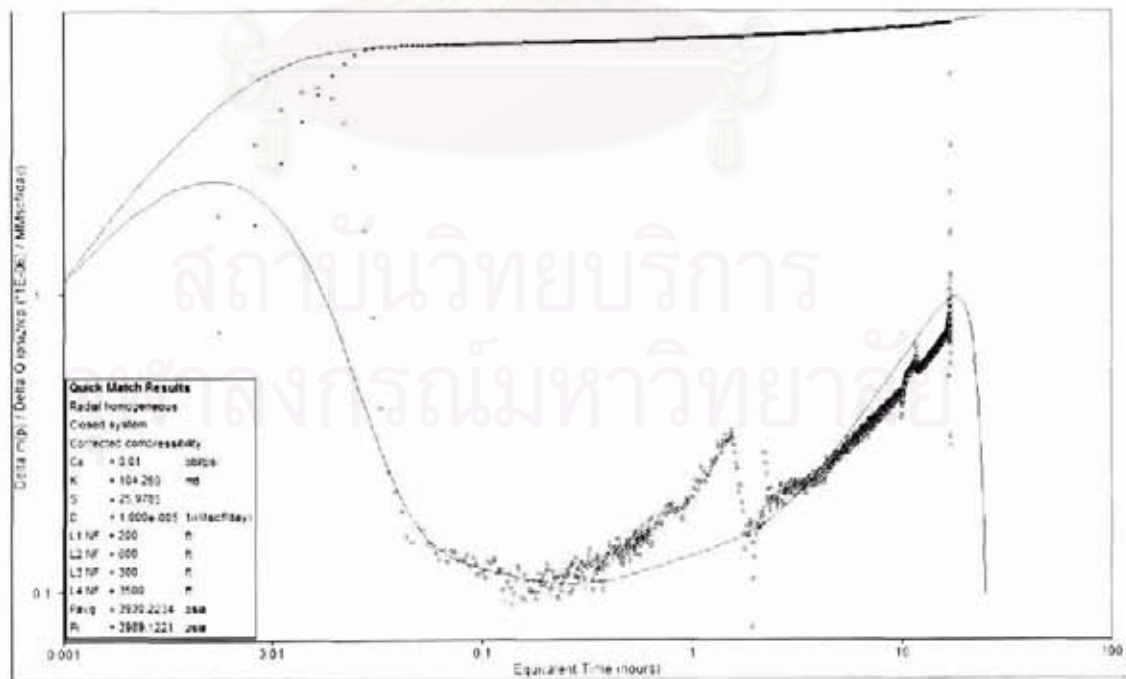


Figure A.129: Well-41 main build-up, log-log plot.

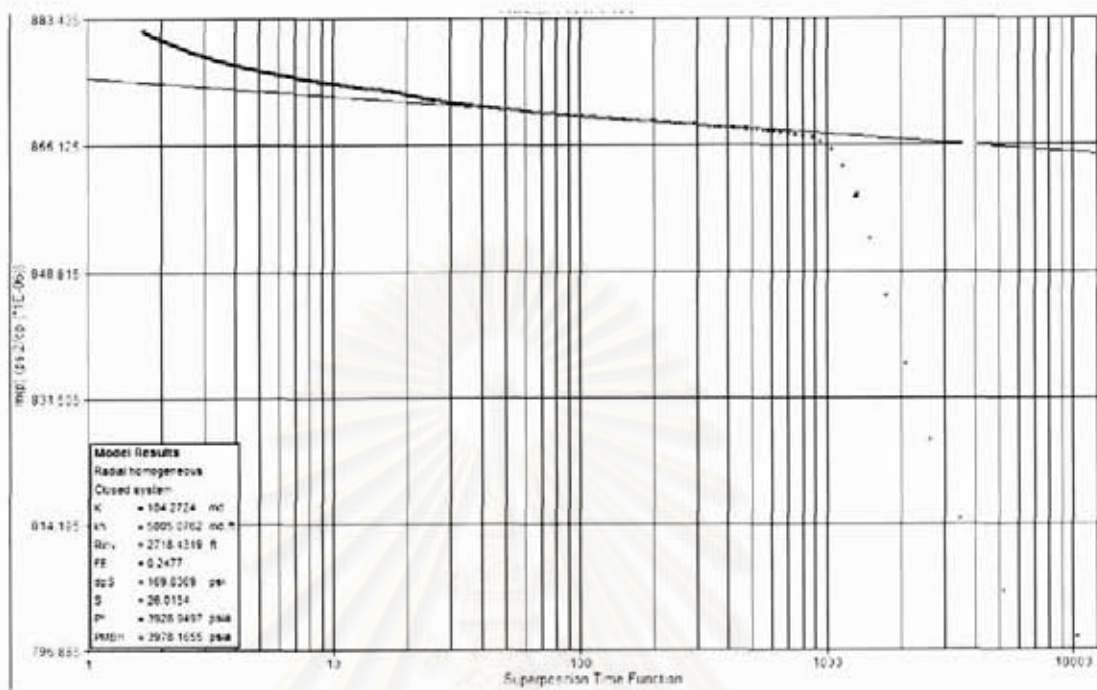


Figure A.130: Well-41 main build-up, semi-log plot.

สถาบันวิทยบริการ
 จุฬาลงกรณ์มหาวิทยาลัย

Well-42 Reservoir 77-5

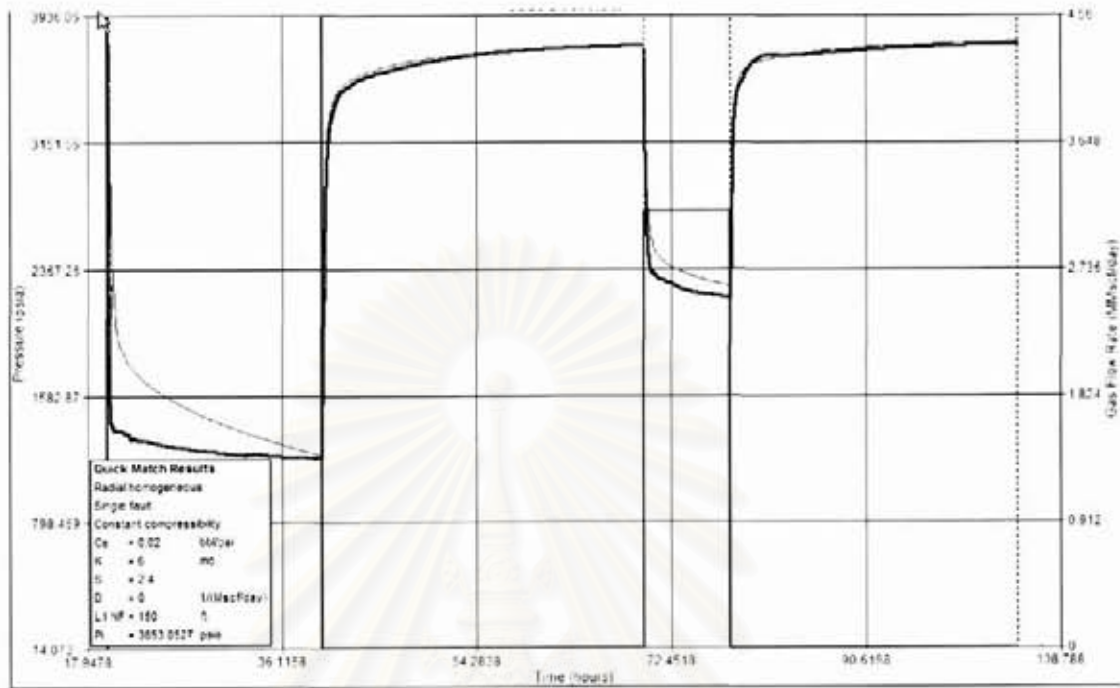


Figure A.131: Well-42 testing overview.

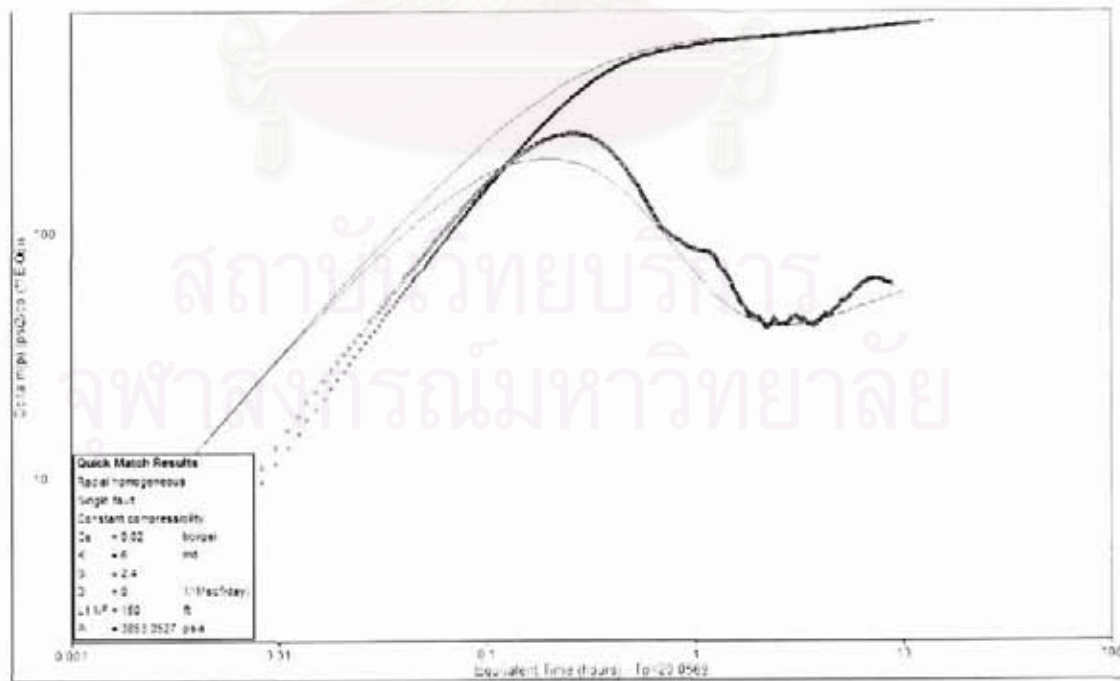


Figure A.132: Well-42 main build-up, log-log plot.

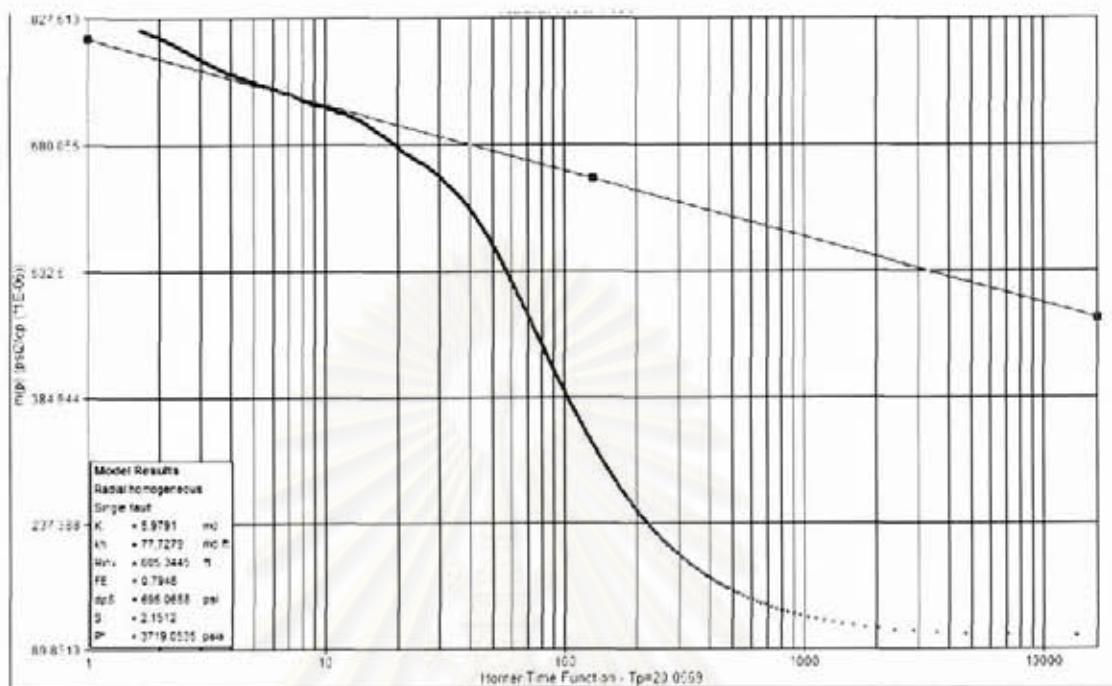


Figure A.133: Well-42 main build-up, semi-log plot.

สถาบันวิทยบริการ
จุฬาลงกรณ์มหาวิทยาลัย

Well-43 Reservoir 75-7

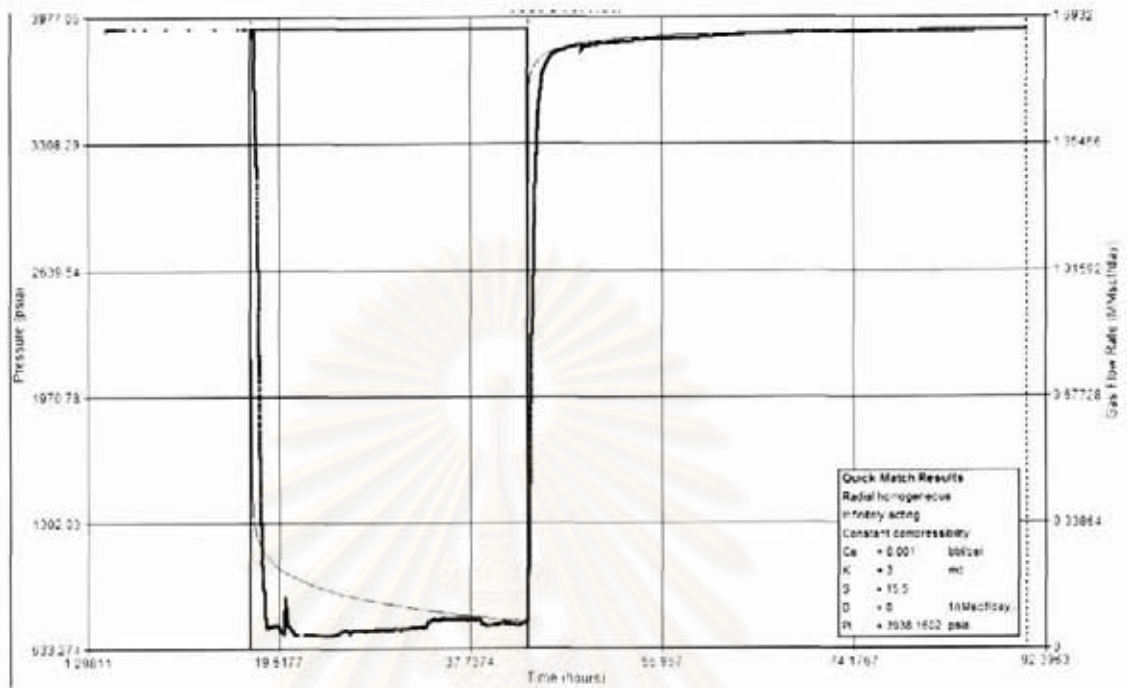


Figure A.134: Well-43 testing overview.

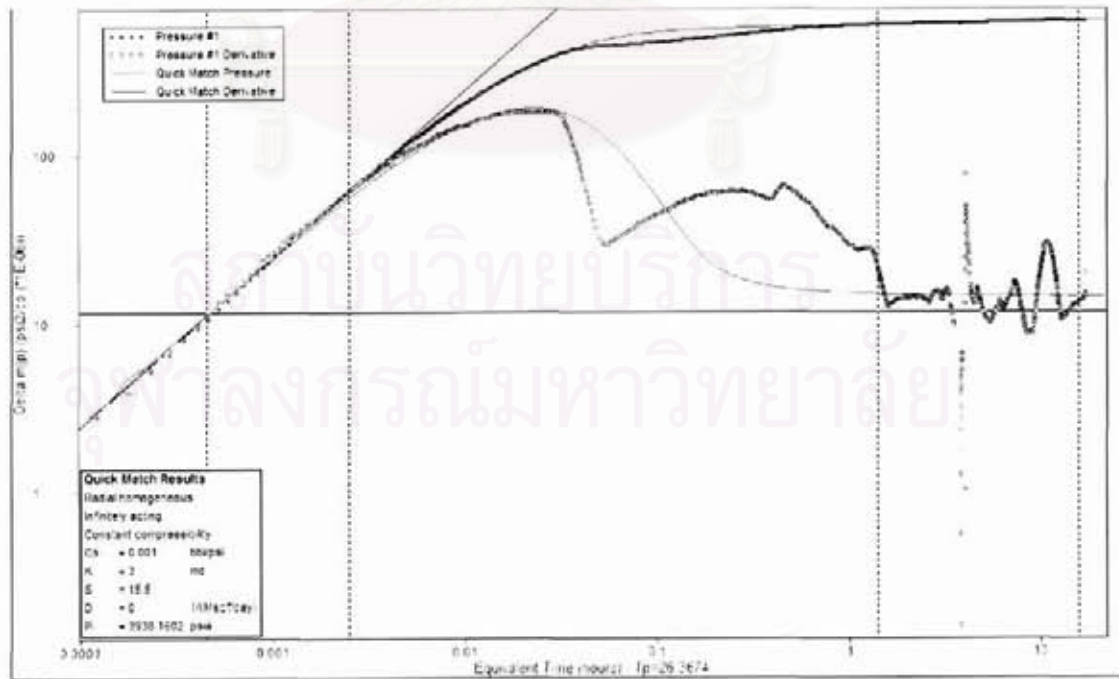


Figure A.135: Well-43 main build-up, log-log plot.

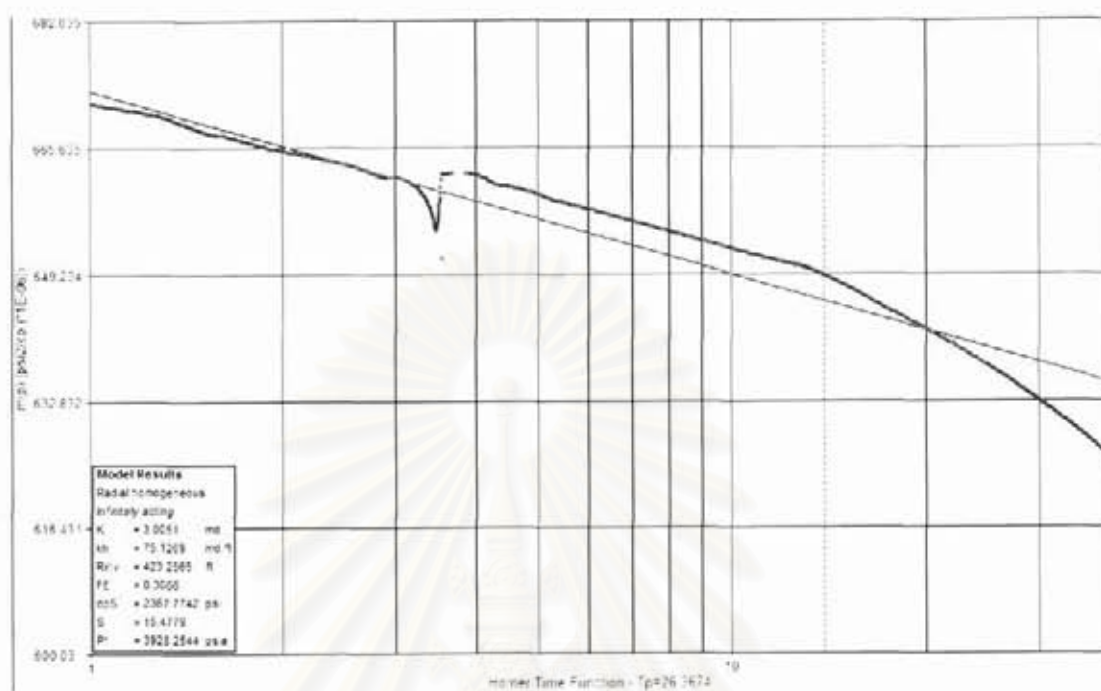


Figure A.136: Well-43 main build-up, semi-log plot.

สถาบันวิทยบริการ
จุฬาลงกรณ์มหาวิทยาลัย

Well-44 Reservoir 79-2

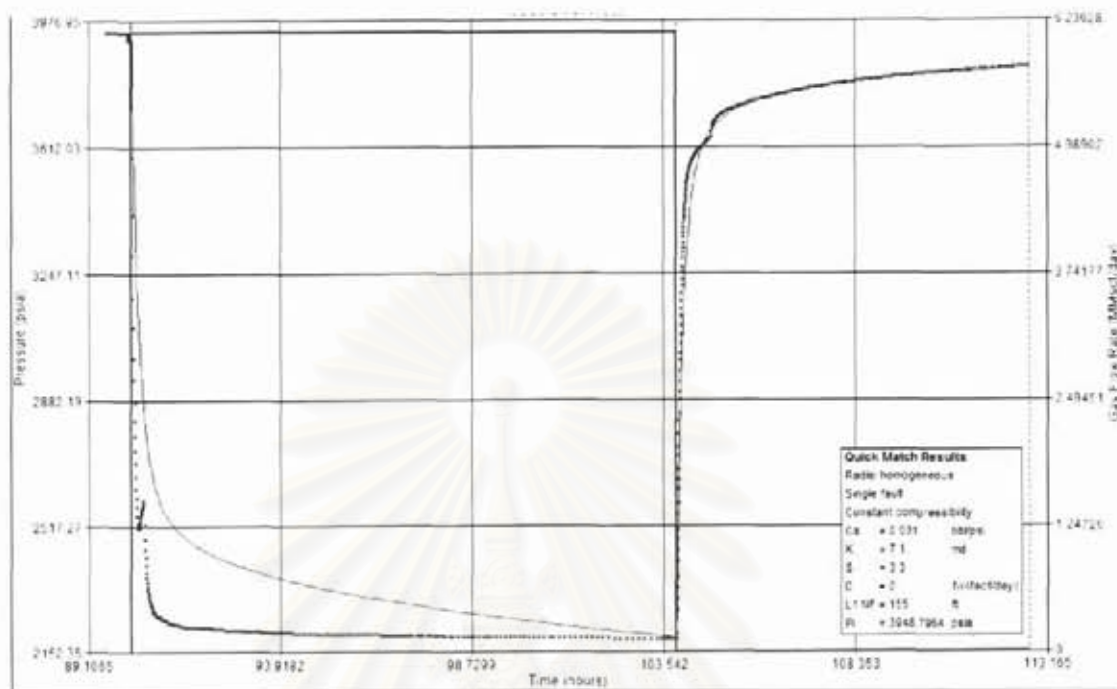


Figure A.137: Well-44 testing overview.

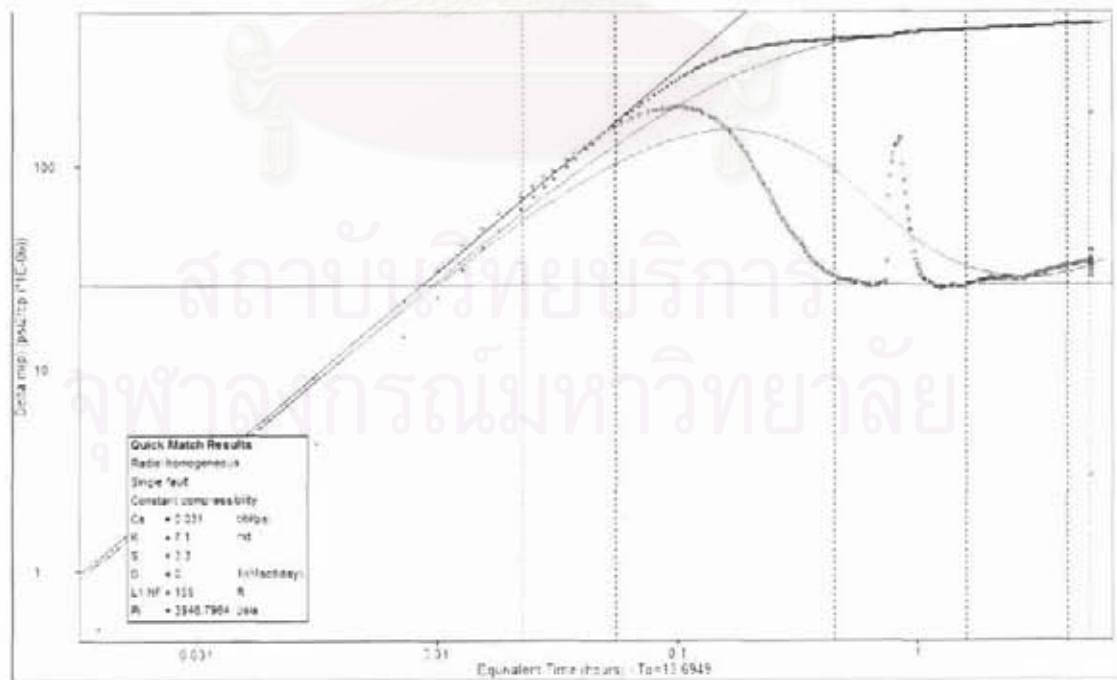


Figure A.138: Well-44 main build-up, log-log plot.

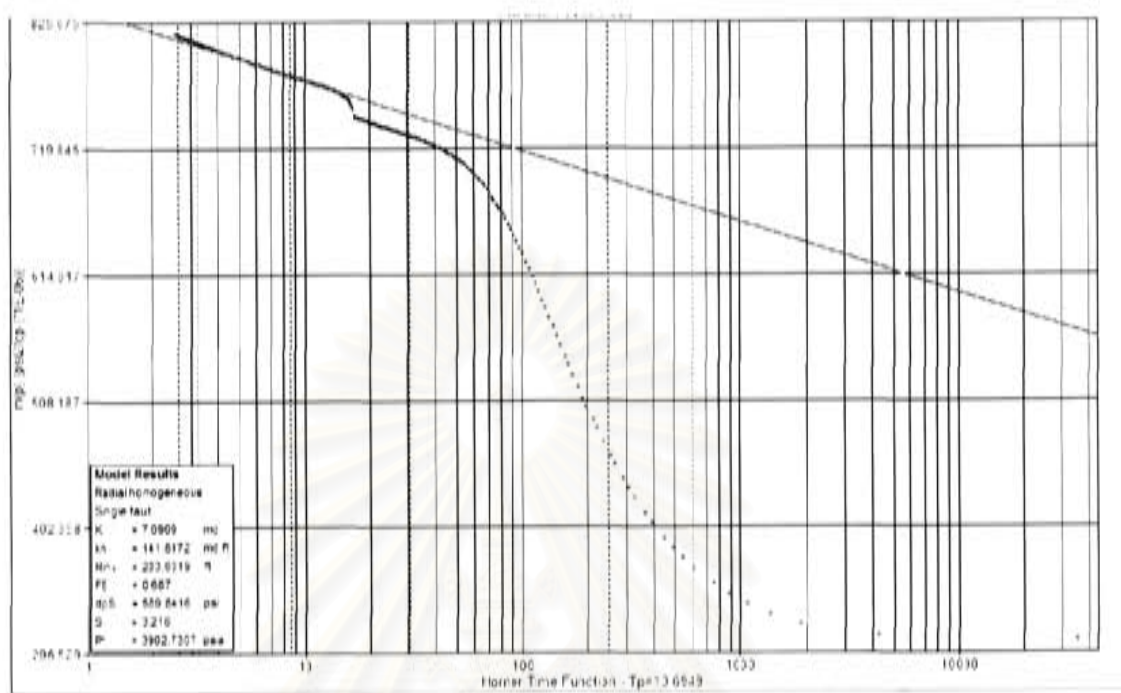


Figure A.139: Well-44 main build-up, semi-log plot.

สถาบันวิทยบริการ
จุฬาลงกรณ์มหาวิทยาลัย

Well-45 Reservoir 80-7

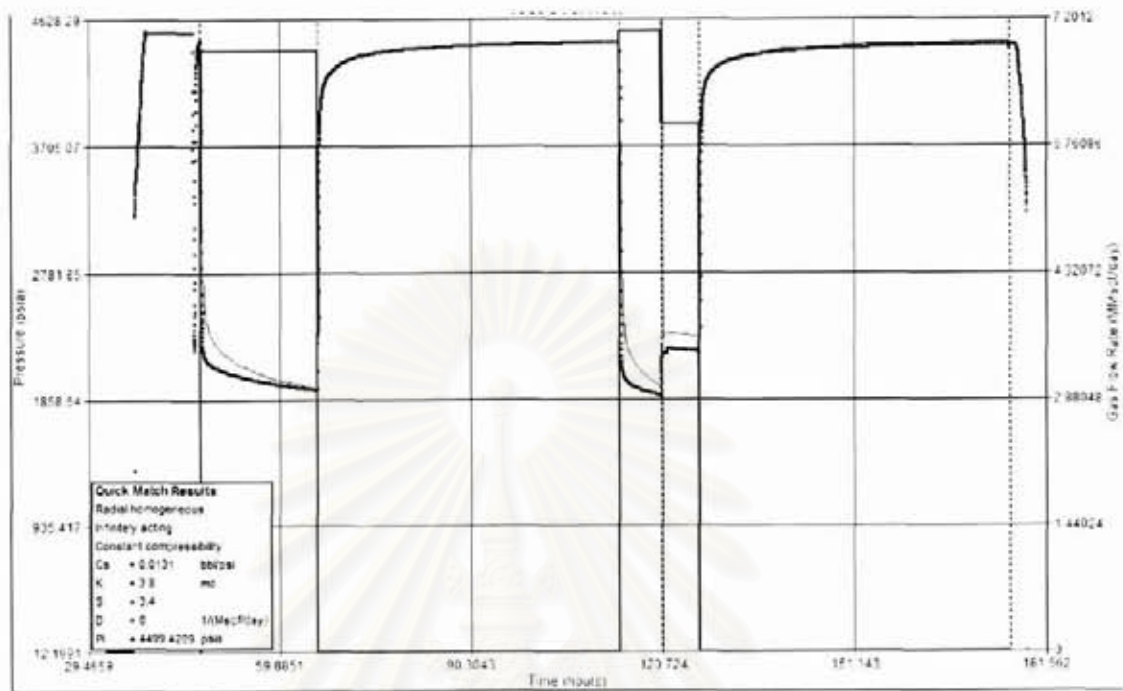


Figure A.140: Well-45 testing overview.

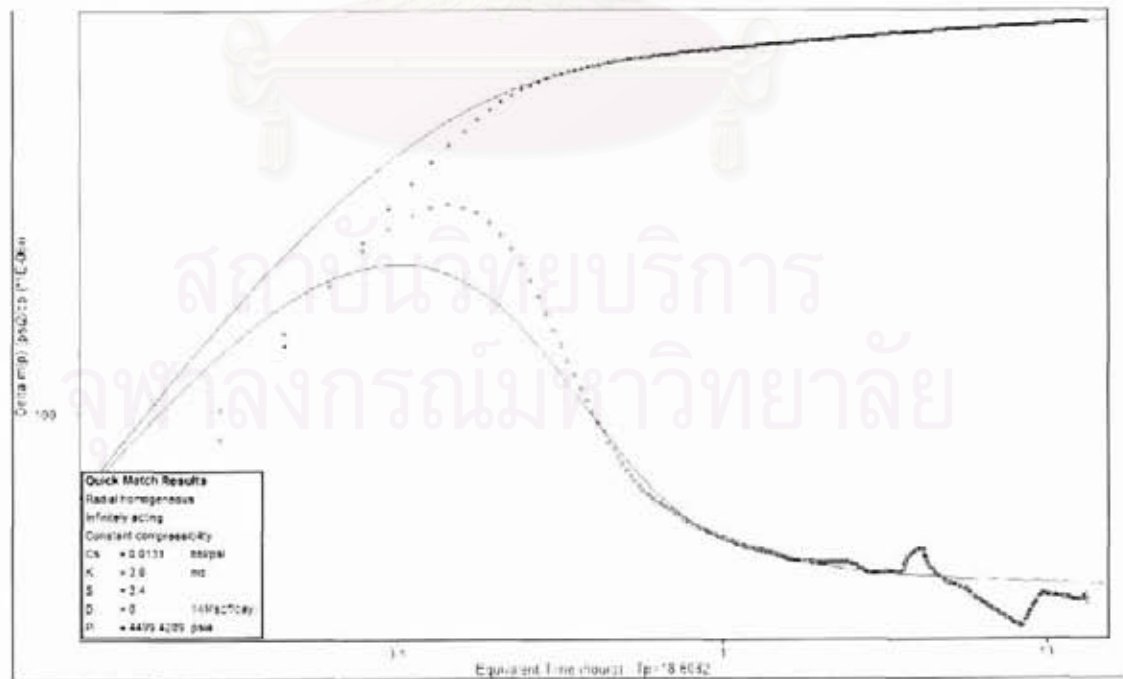


Figure A.141: Well-45 main build-up, log-log plot.

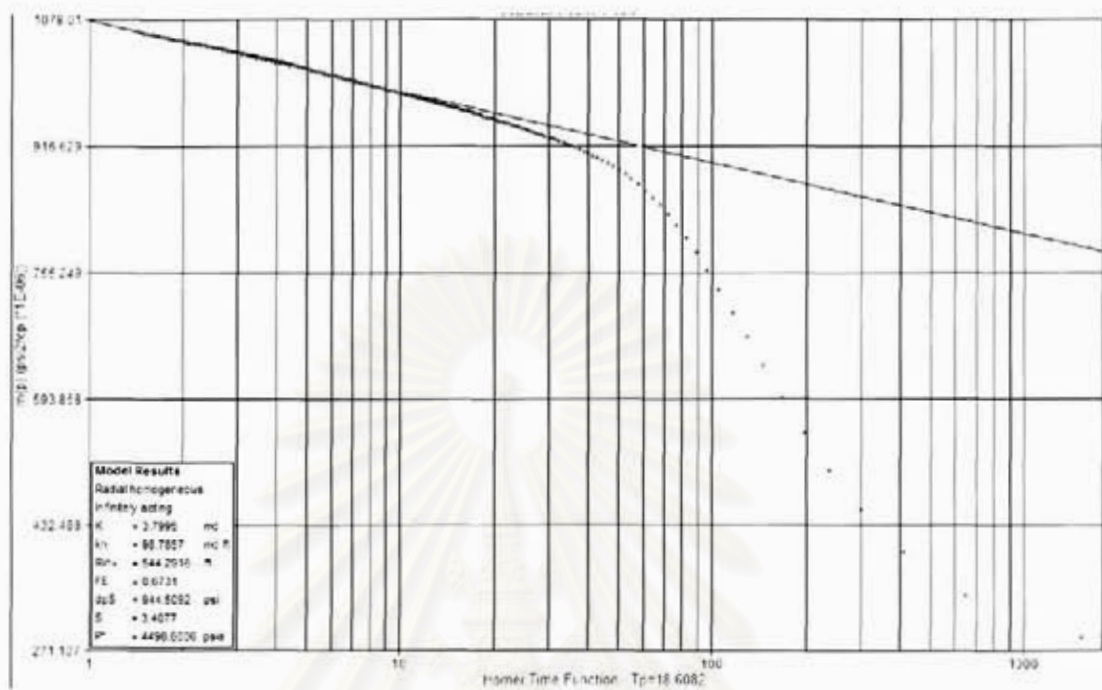


Figure A.142: Well-45 main build-up, semi-log plot.

สถาบันวิทยบริการ
 จุฬาลงกรณ์มหาวิทยาลัย

Well-46 Reservoir 88-6

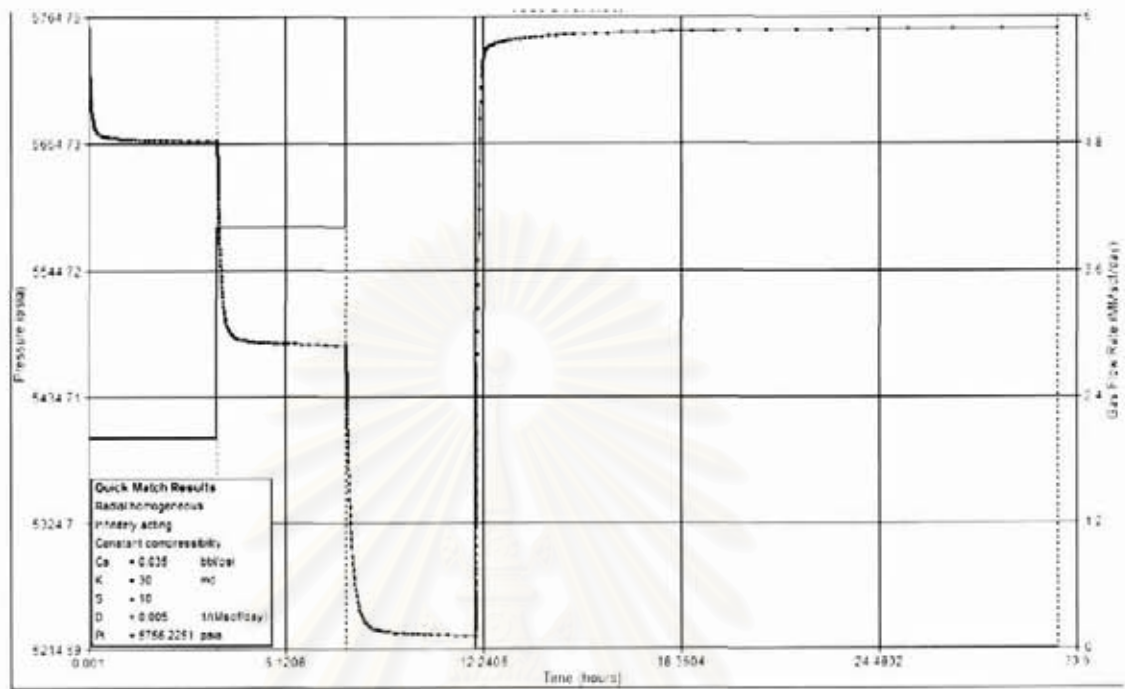


Figure A.143: Well-46 testing overview.

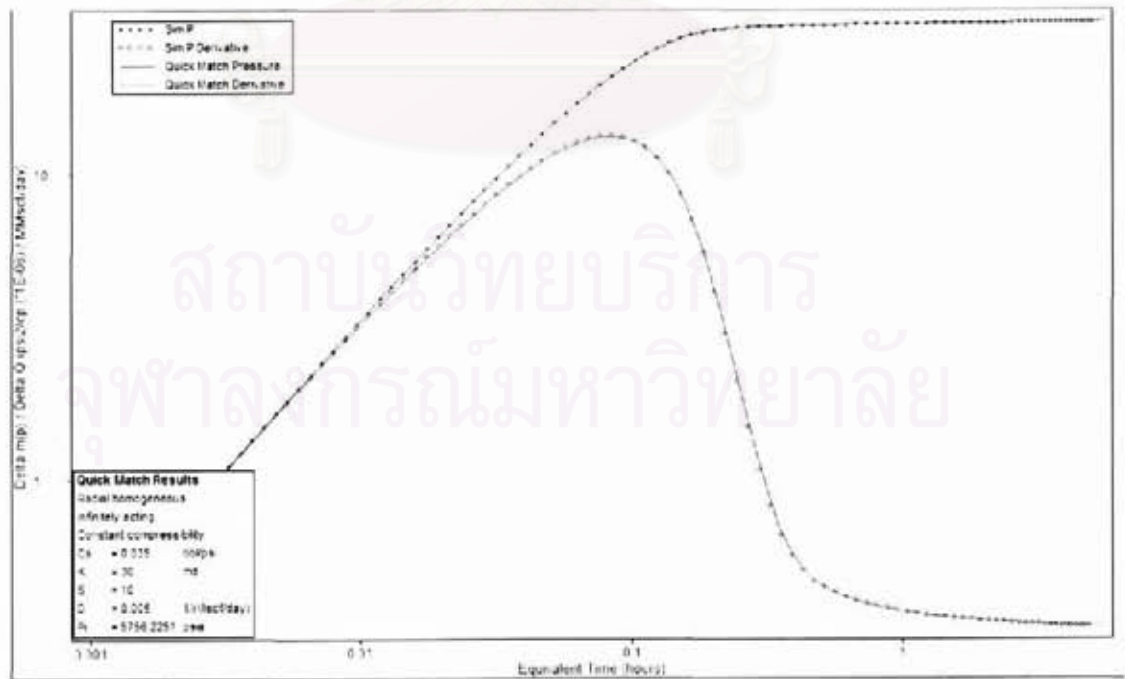


Figure A.144: Well-46 main build-up, log-log plot.

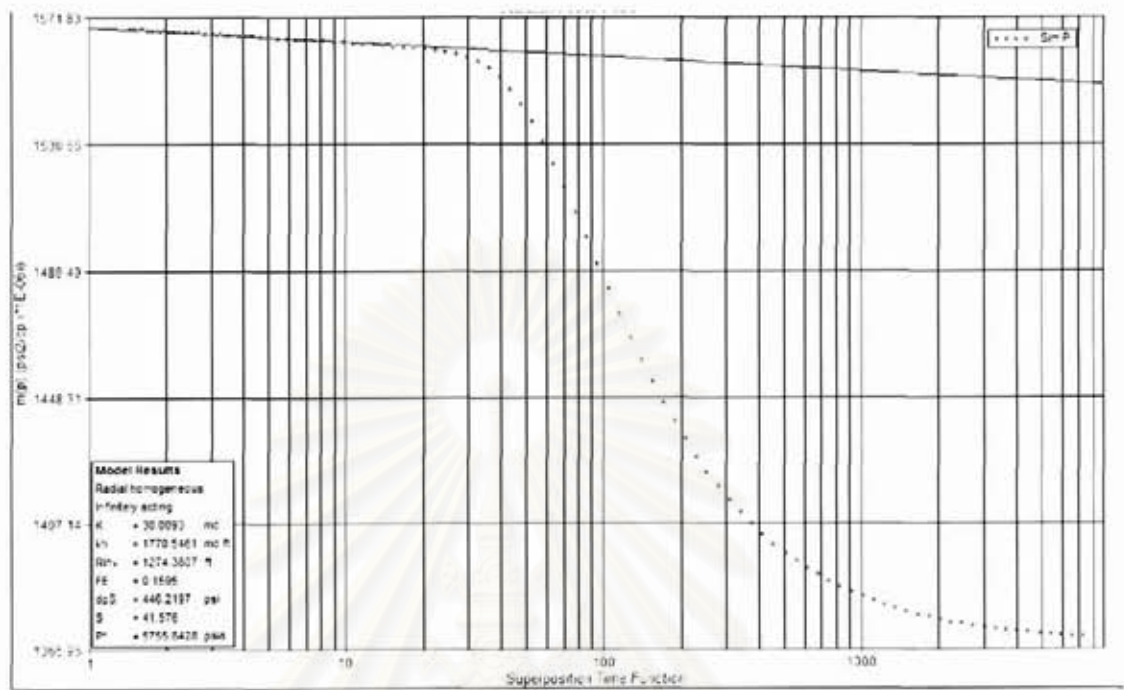


Figure A.145: Well-46 main build-up, semi-log plot.

สถาบันวิทยบริการ
จุฬาลงกรณ์มหาวิทยาลัย

Well-47 Reservoir 77-4

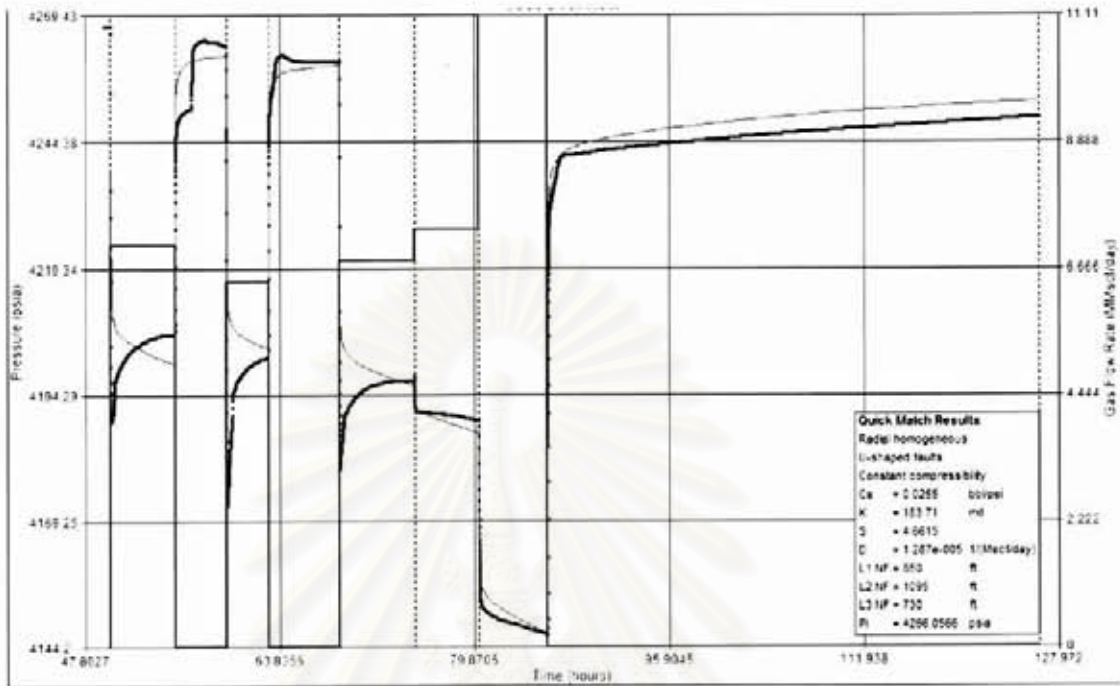


Figure A.146: Well-47 testing overview.

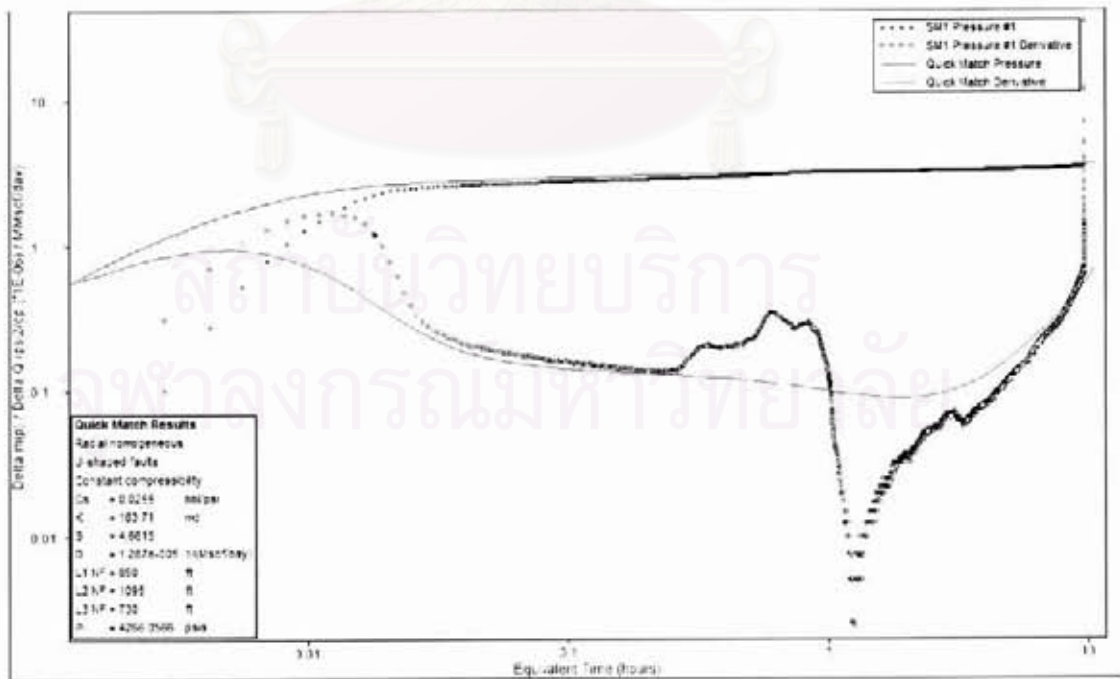


Figure A.147: Well-47 main build-up, log-log plot.

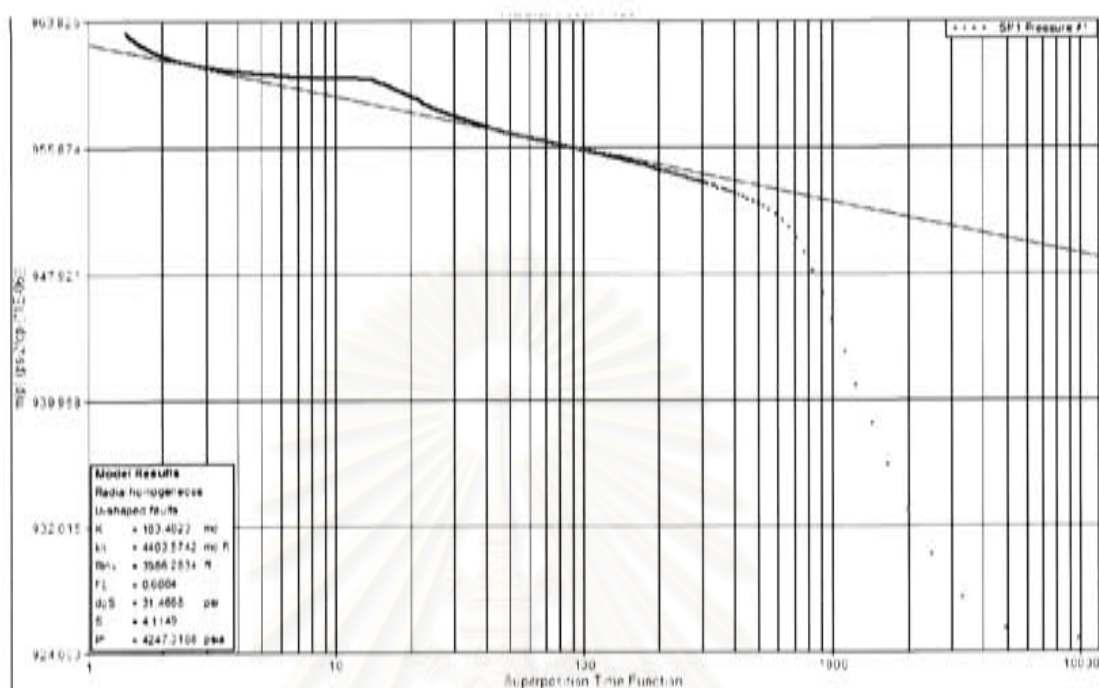


Figure A.148: Well-47 main build-up, semi-log plot.

สถาบันวิทยบริการ
จุฬาลงกรณ์มหาวิทยาลัย

Well-48 Reservoir 76-6

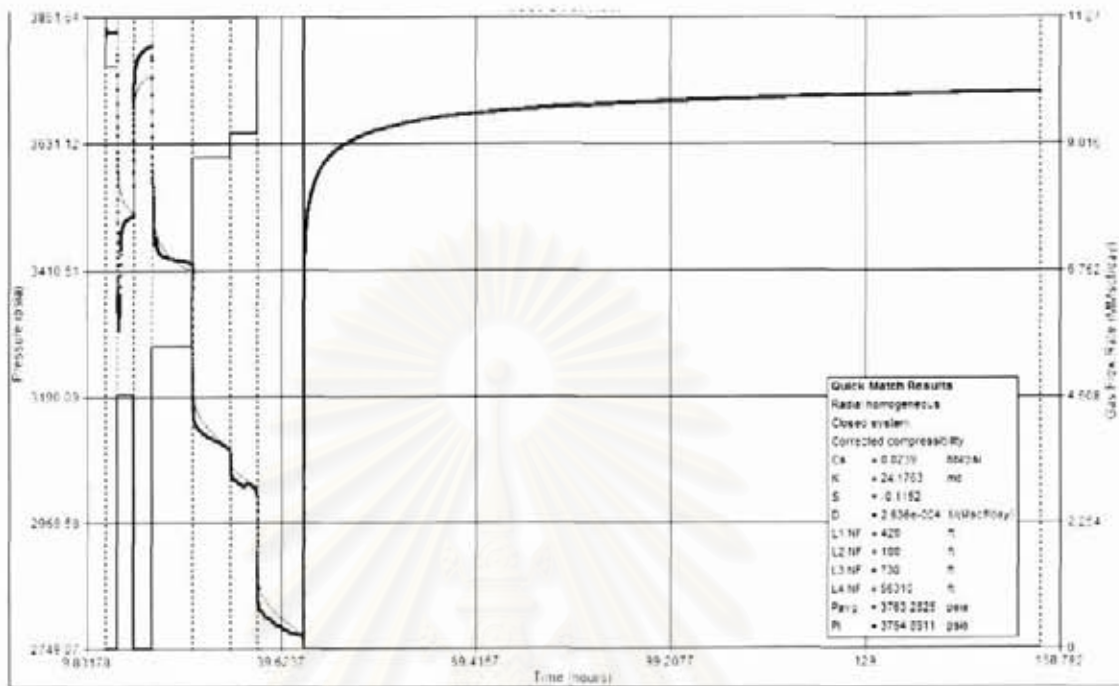


Figure A.149: Well-48 testing overview.

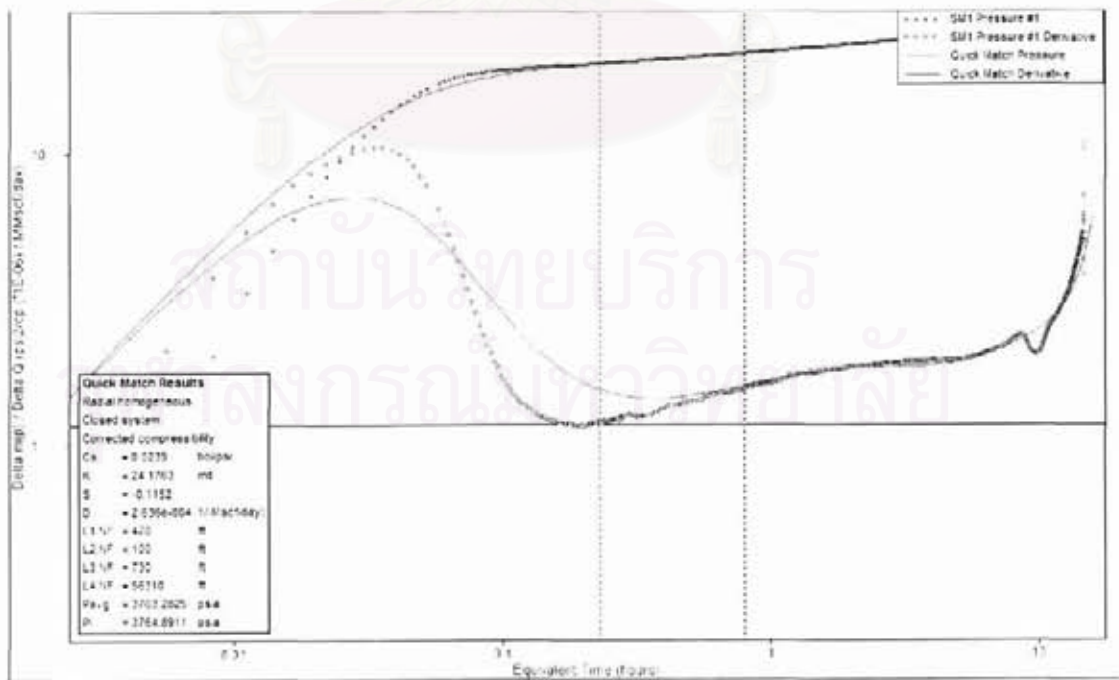


Figure A.150: Well-48 main build-up, log-log plot.

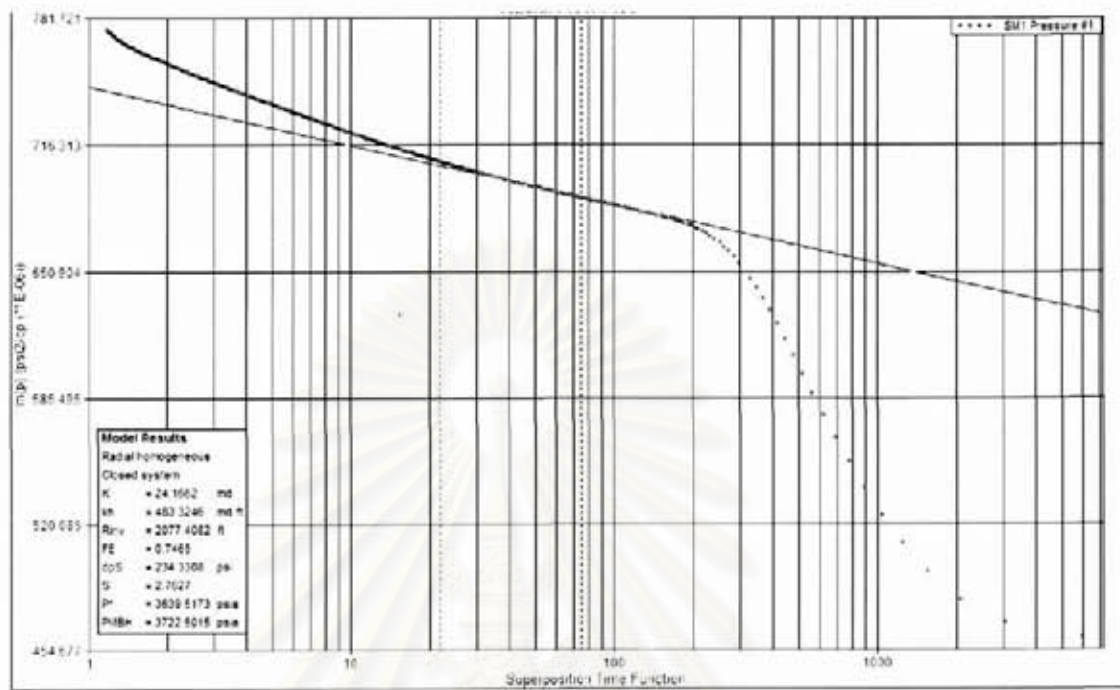


Figure A.151: Well-48 main build-up, semi-log plot.

สถาบันวิทยบริการ
จุฬาลงกรณ์มหาวิทยาลัย

Well-49 Reservoir 79-2

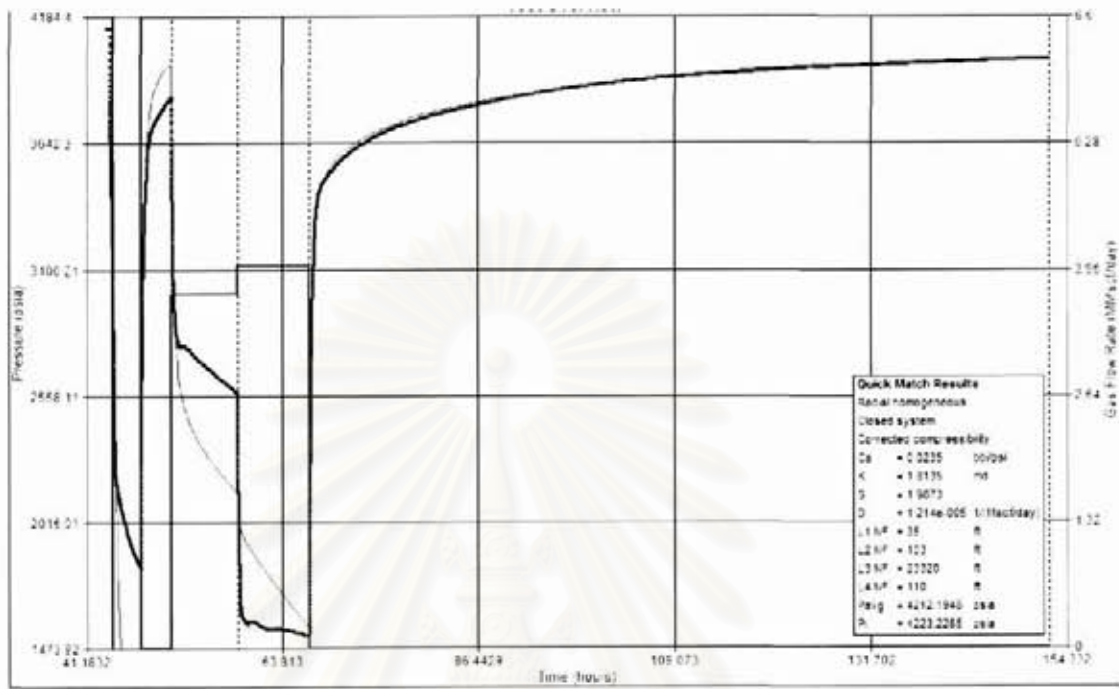


Figure A.152: Well-49 testing overview.

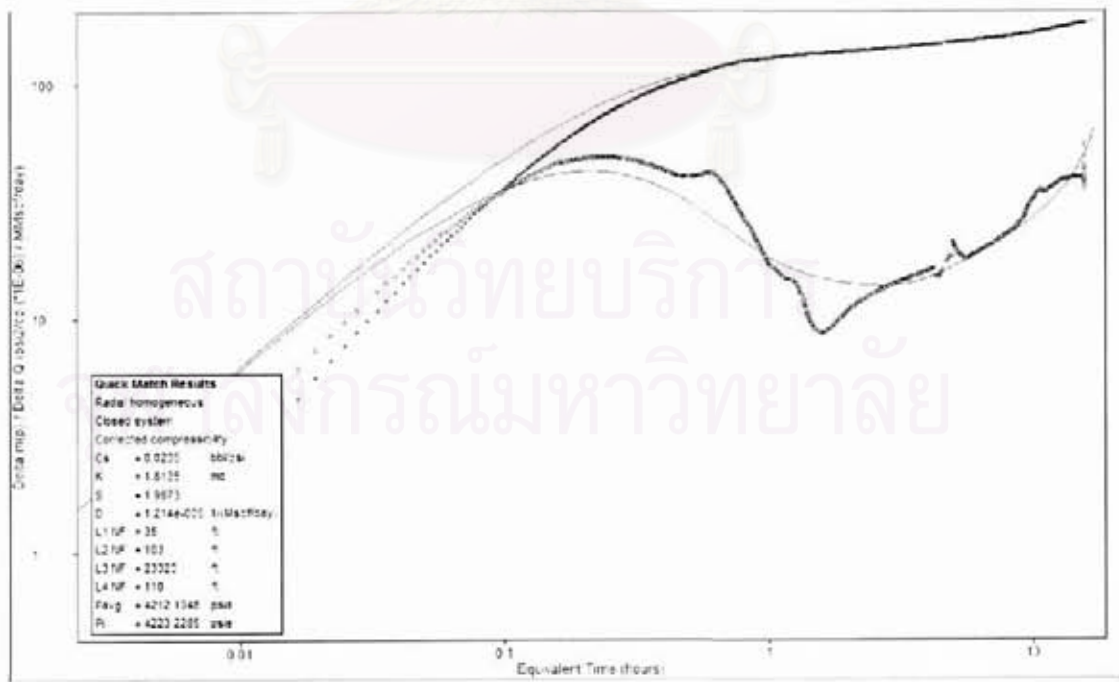


Figure A.153: Well-49 main build-up, log-log plot.

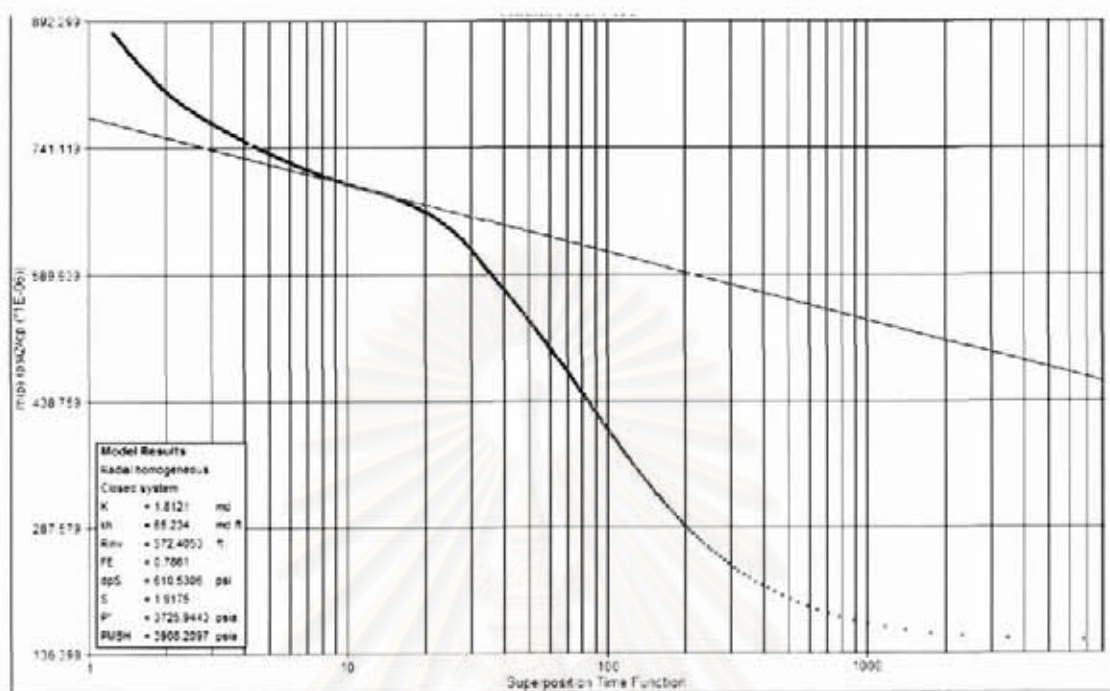


Figure A.154: Well-49 main build-up, semi-log plot.

สถาบันวิทยบริการ
 จุฬาลงกรณ์มหาวิทยาลัย

Well-50 Reservoir 68-7

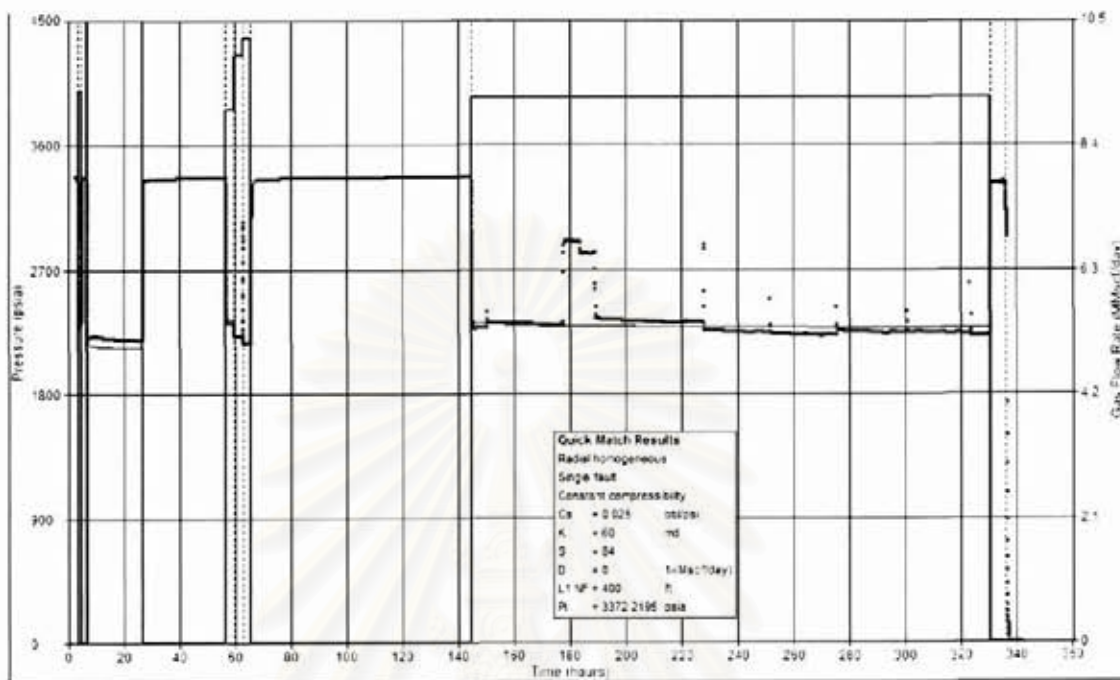


Figure A.155: Well-50 testing overview.

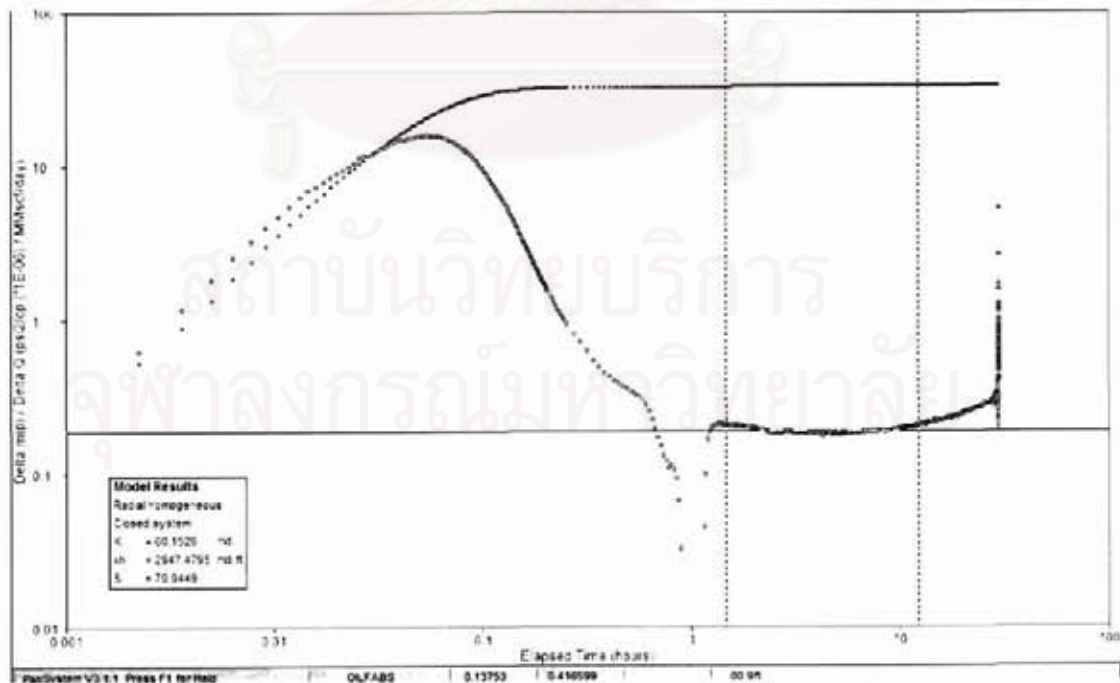


Figure A.156: Well-50 main build-up, log-log plot.

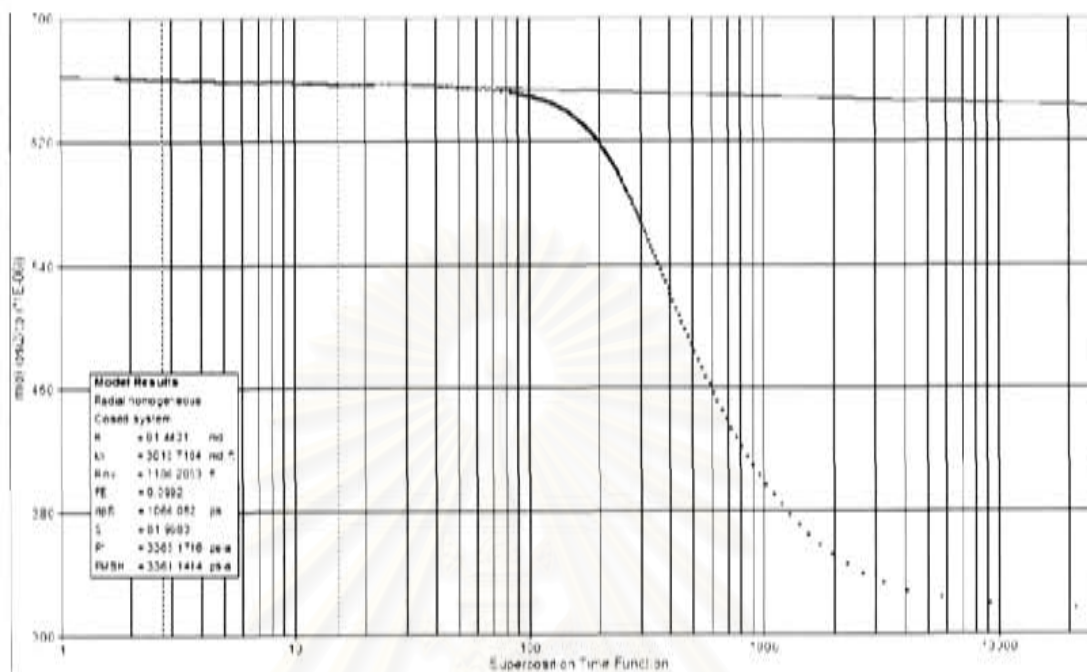


Figure A.157: Well-50 main build-up, semi-log plot.

สถาบันวิทยบริการ
 จุฬาลงกรณ์มหาวิทยาลัย

Well-51 Reservoir 72-8

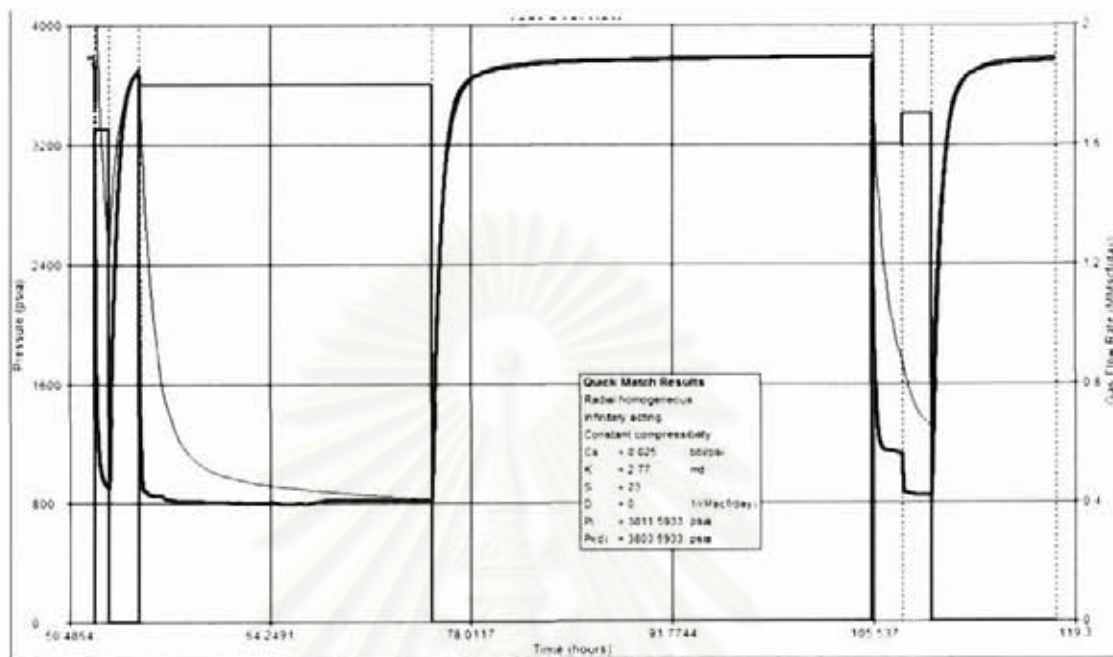


Figure A.158: Well-51 testing overview.

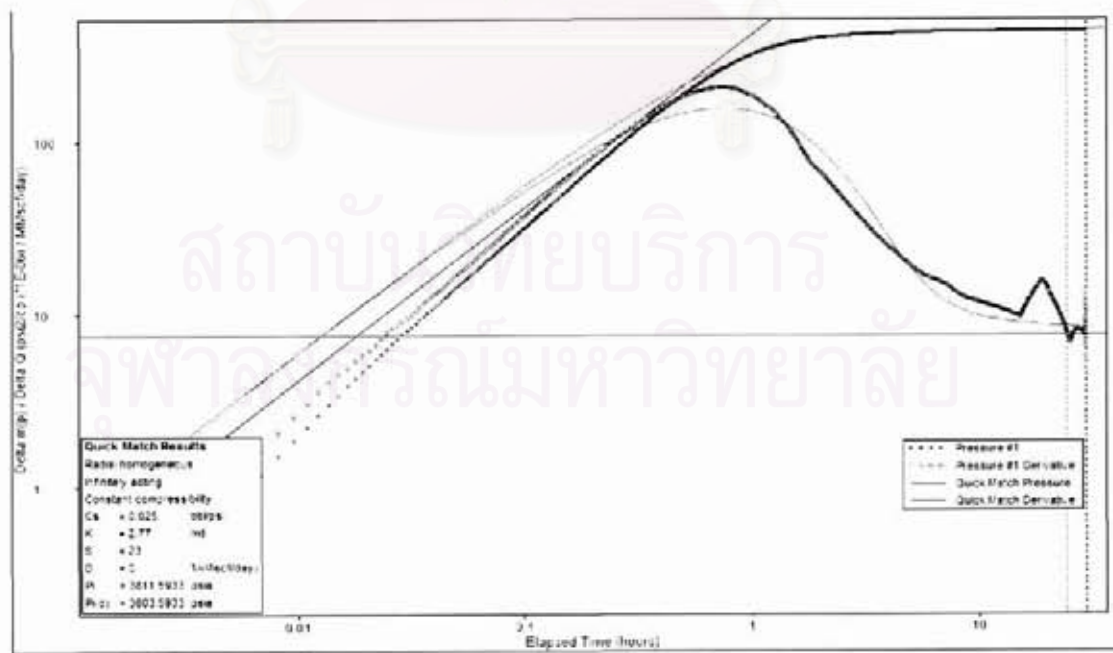


Figure A.159: Well-51 main build-up, log-log plot.

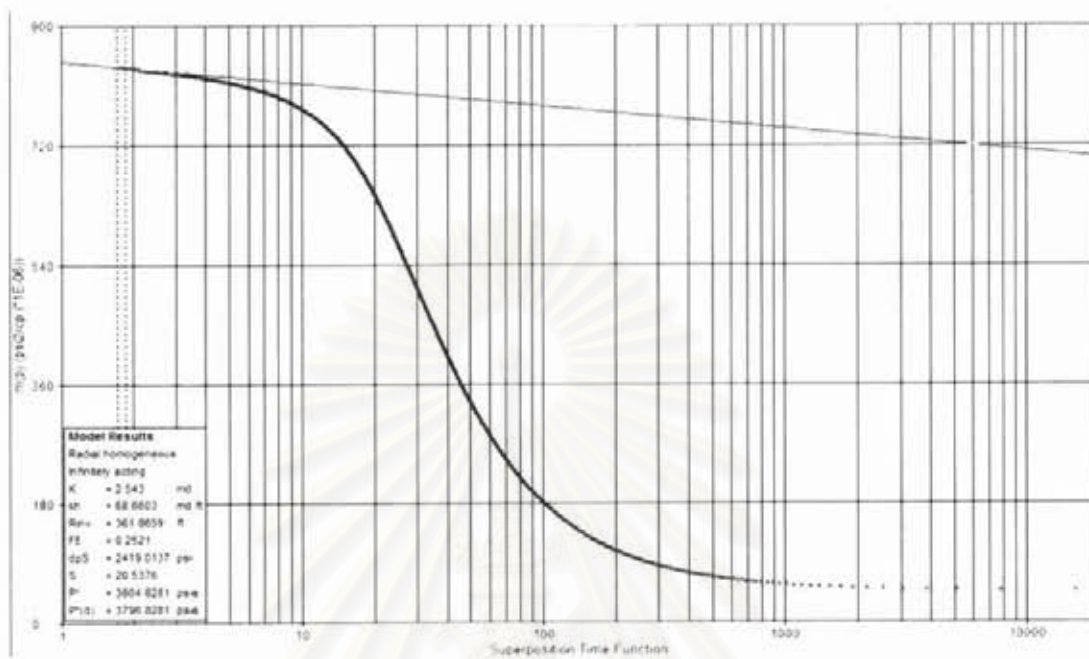


Figure A.160: Well-51 main build-up, semi-log plot.

สถาบันวิทยบริการ
จุฬาลงกรณ์มหาวิทยาลัย

Well-52 Reservoir 68-6

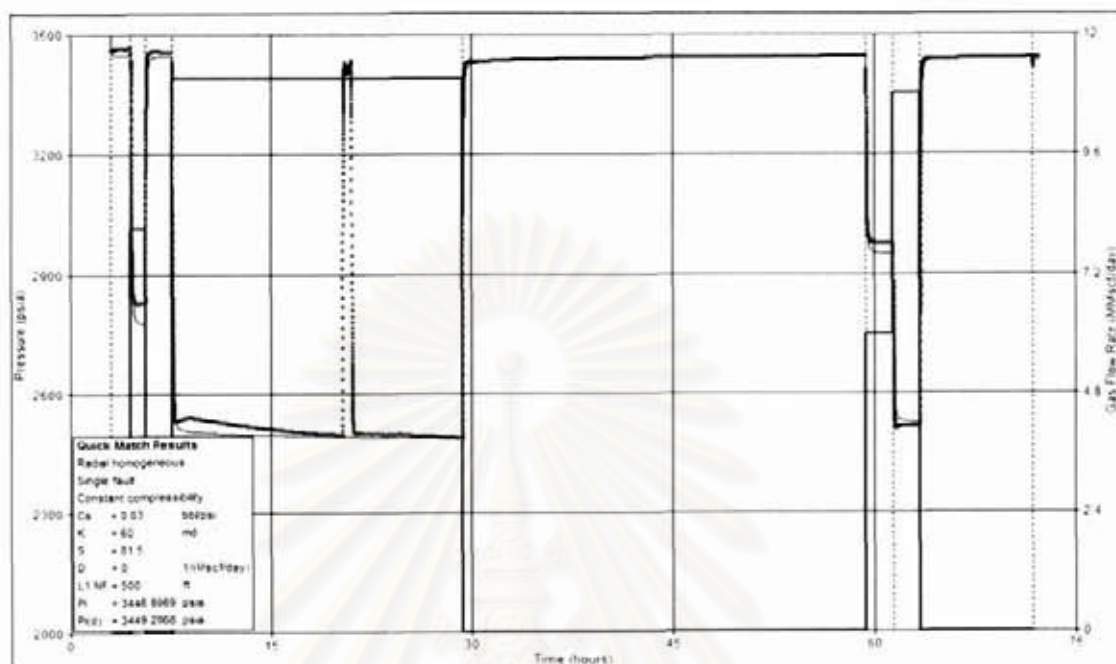


Figure A.161: Well-52 testing overview.

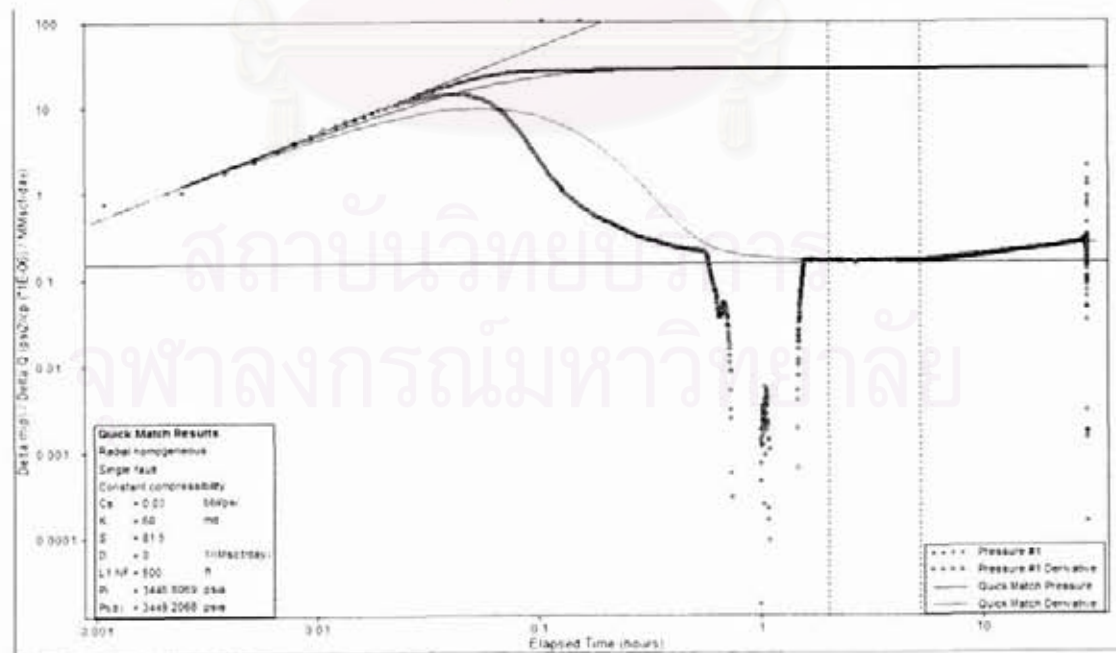


Figure A.162: Well-52 main build-up, log-log plot.

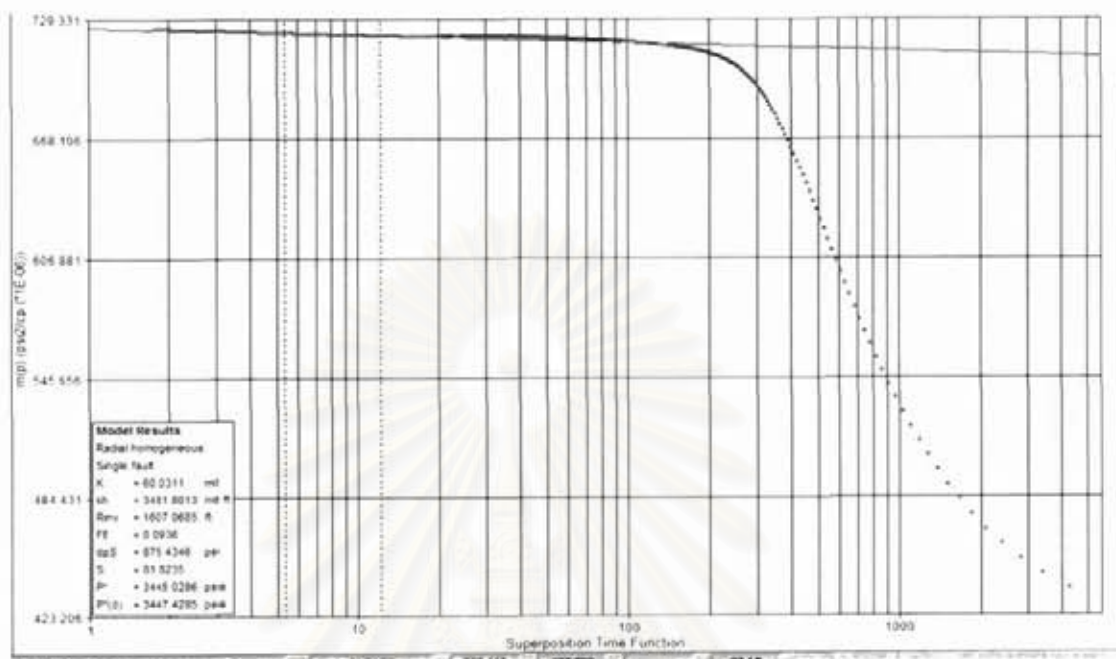


Figure A.163: Well-52 main build-up, semi-log plot.

สถาบันวิทยบริการ
 จุฬาลงกรณ์มหาวิทยาลัย

Well-53 Reservoir 91-1

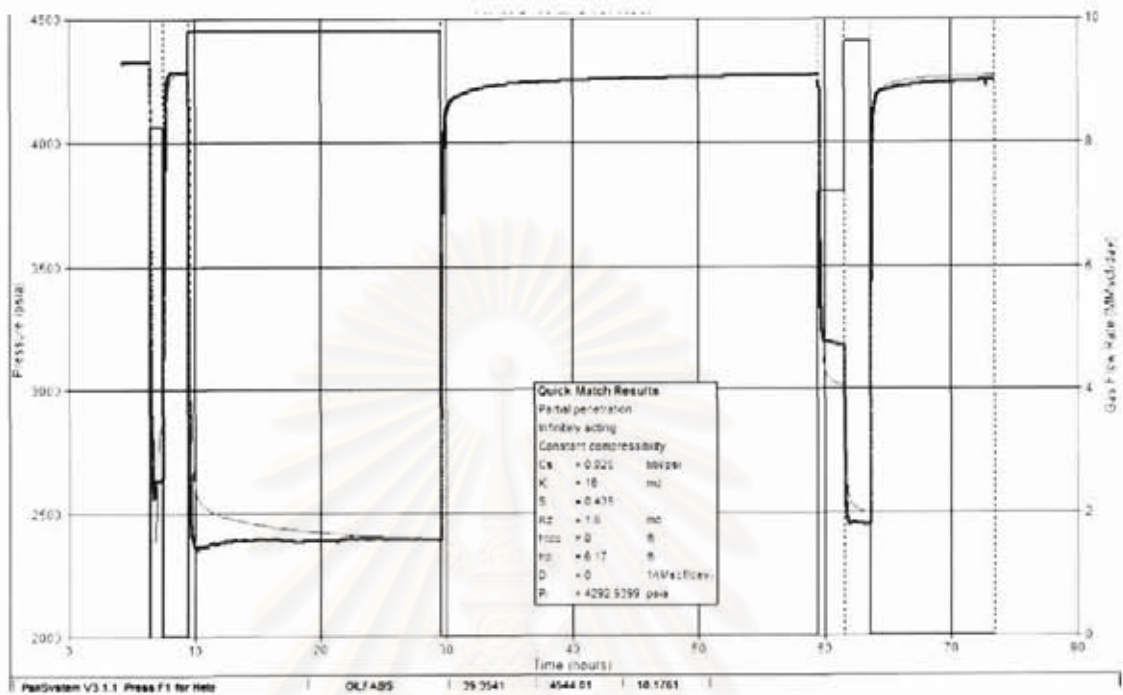


Figure A.164: Well-53 testing overview.

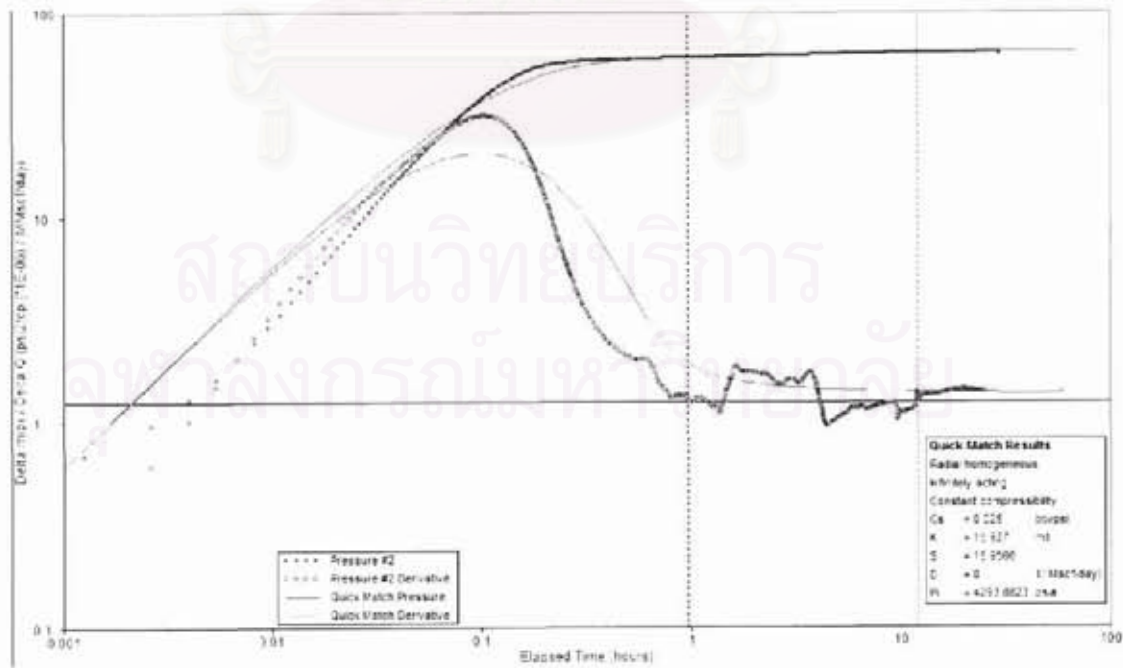


Figure A.165: Well-53 main build-up, log-log plot.

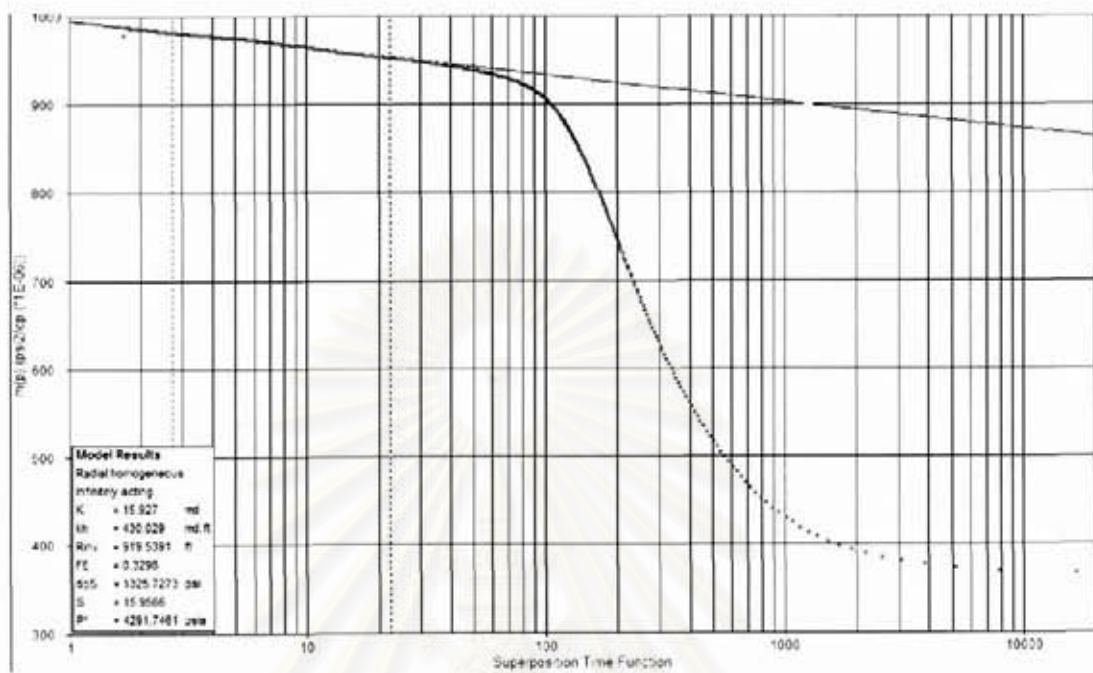


Figure A.166: Well-53 main build-up, semi-log plot.

สถาบันวิทยบริการ
 จุฬาลงกรณ์มหาวิทยาลัย

Well-54 Reservoir 89-4

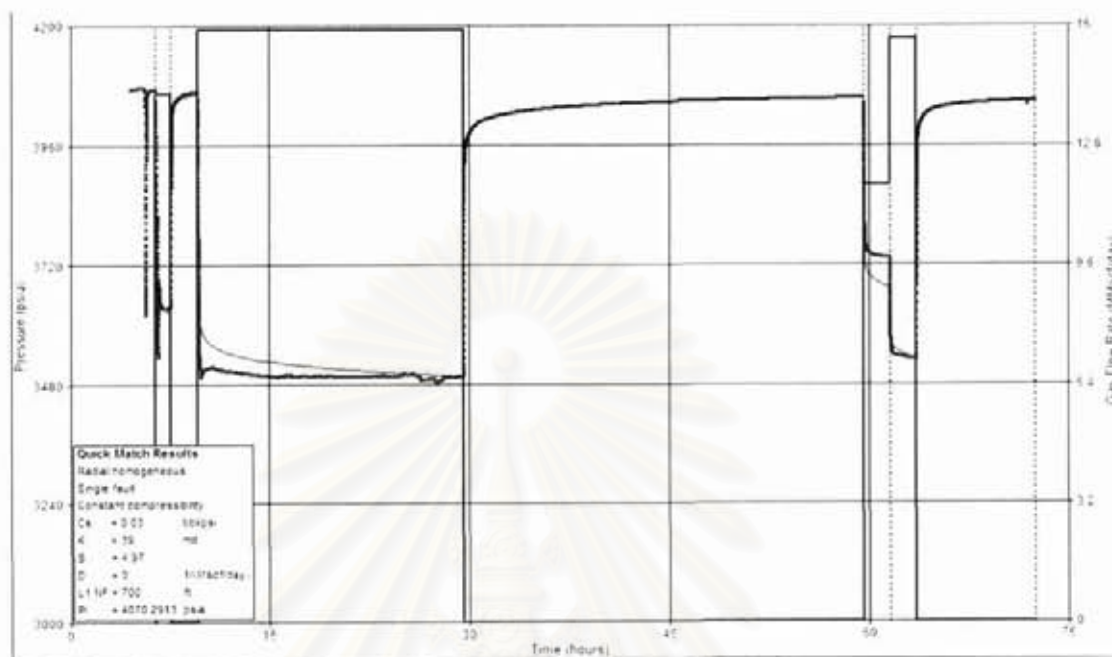


Figure A.167: Well-54 testing overview.

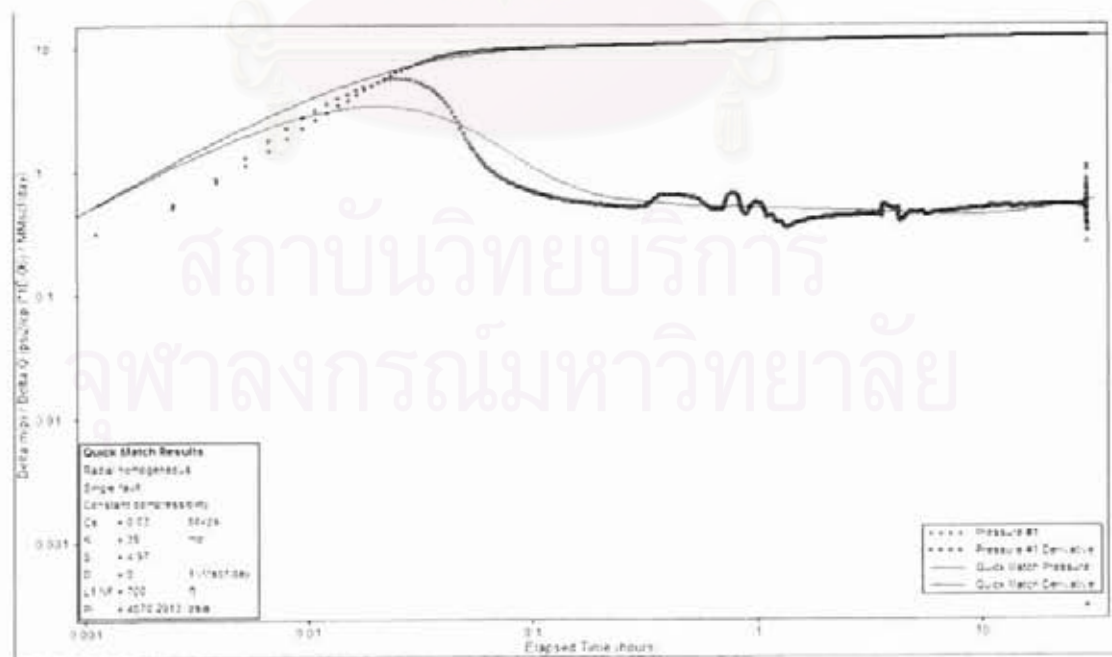


Figure A.168: Well-54 main build-up, log-log plot.

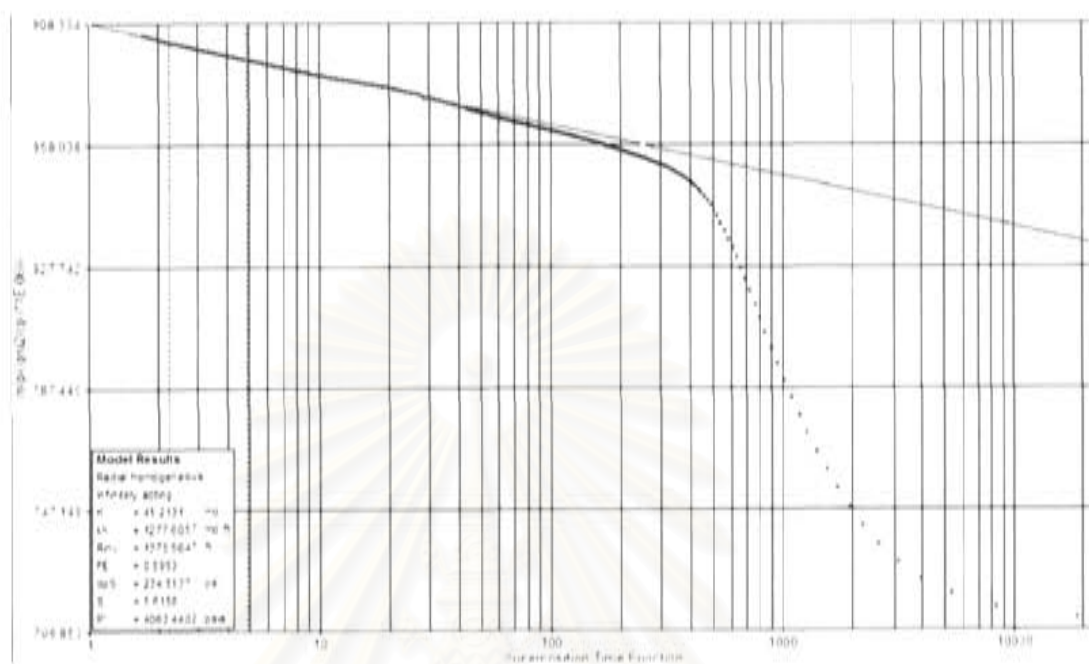


Figure A.169: Well-54 main build-up, semi-log plot.

สถาบันวิทยบริการ
จุฬาลงกรณ์มหาวิทยาลัย

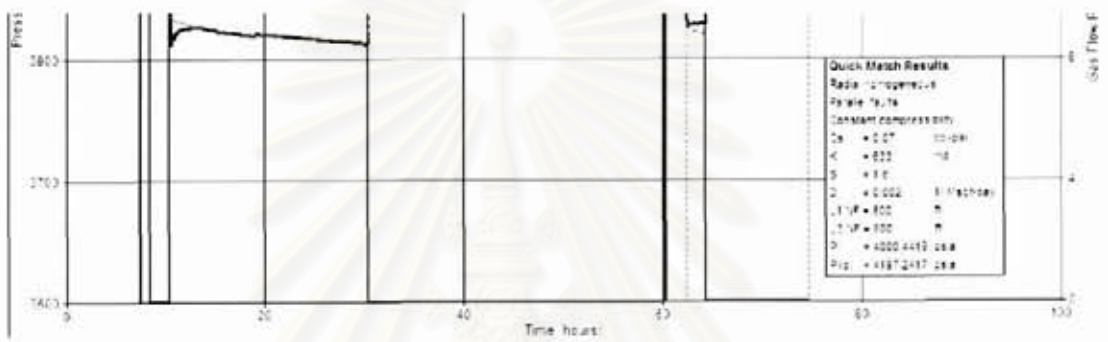


Figure A.170: Well-55 testing overview.

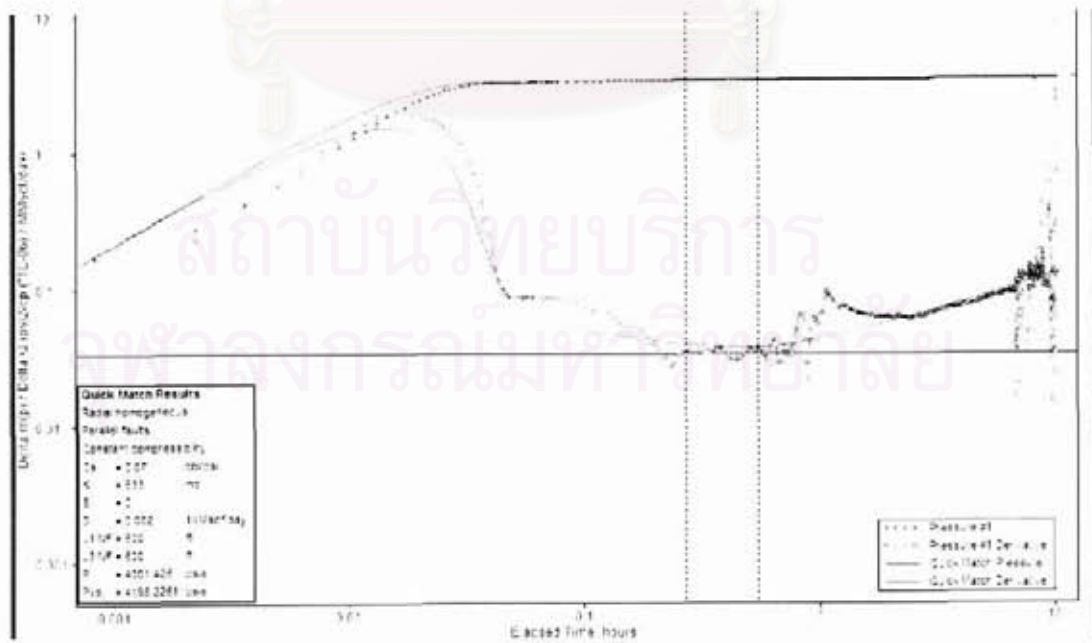


Figure A.171: Well-55 main build-up, log-log plot.

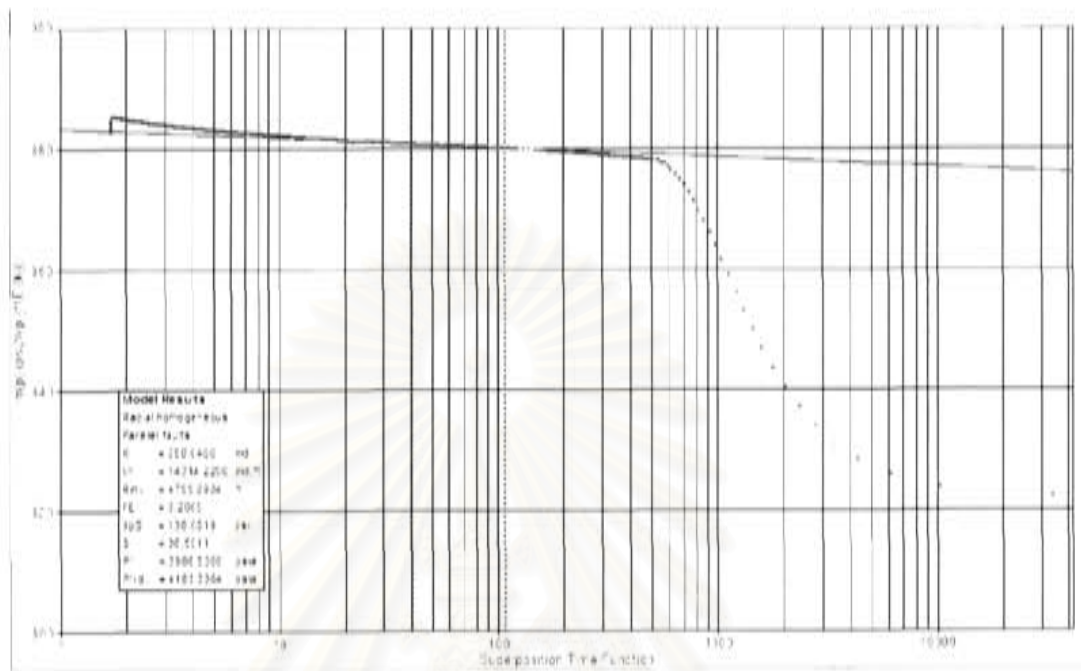


Figure A.172: Well-55 main build-up, semi-log plot.

สถาบันวิทยบริการ
จุฬาลงกรณ์มหาวิทยาลัย

Well-56 Reservoir 75-6

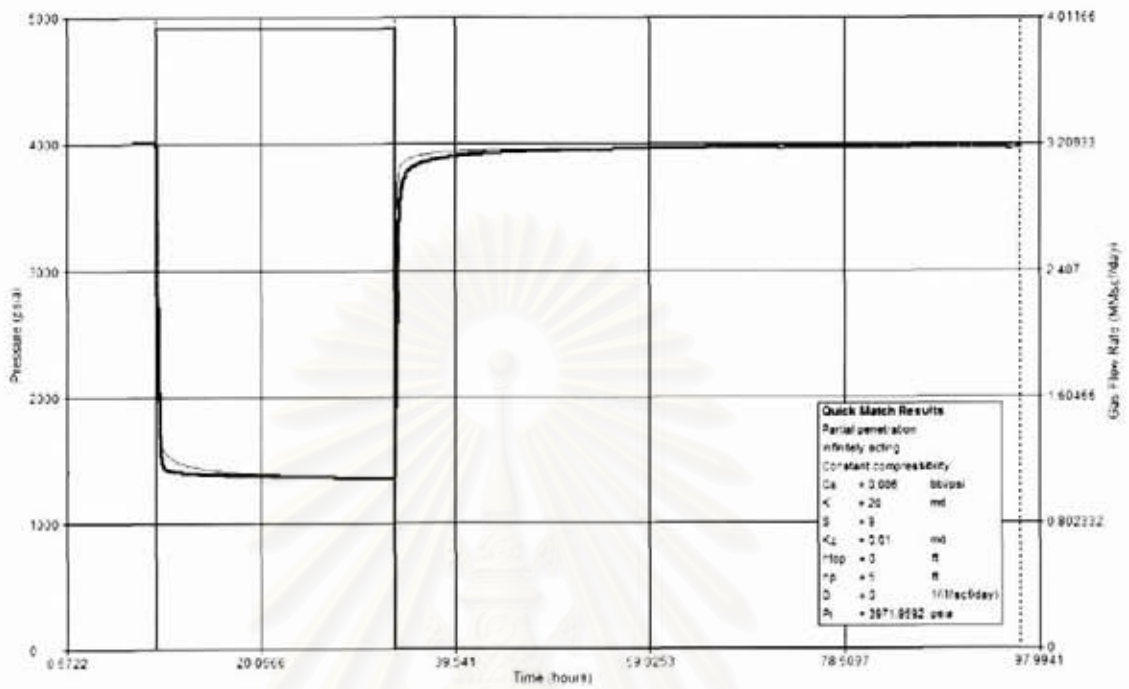


Figure A.173: Well-56 testing overview.

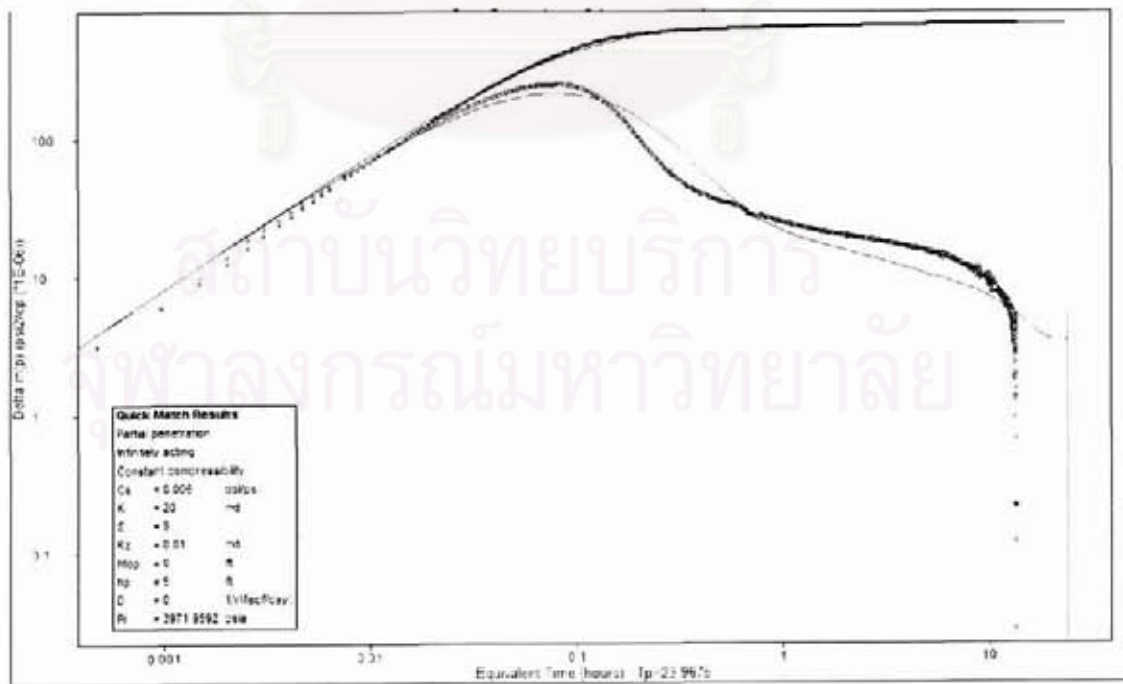


Figure A.174: Well-56 main build-up, log-log plot.

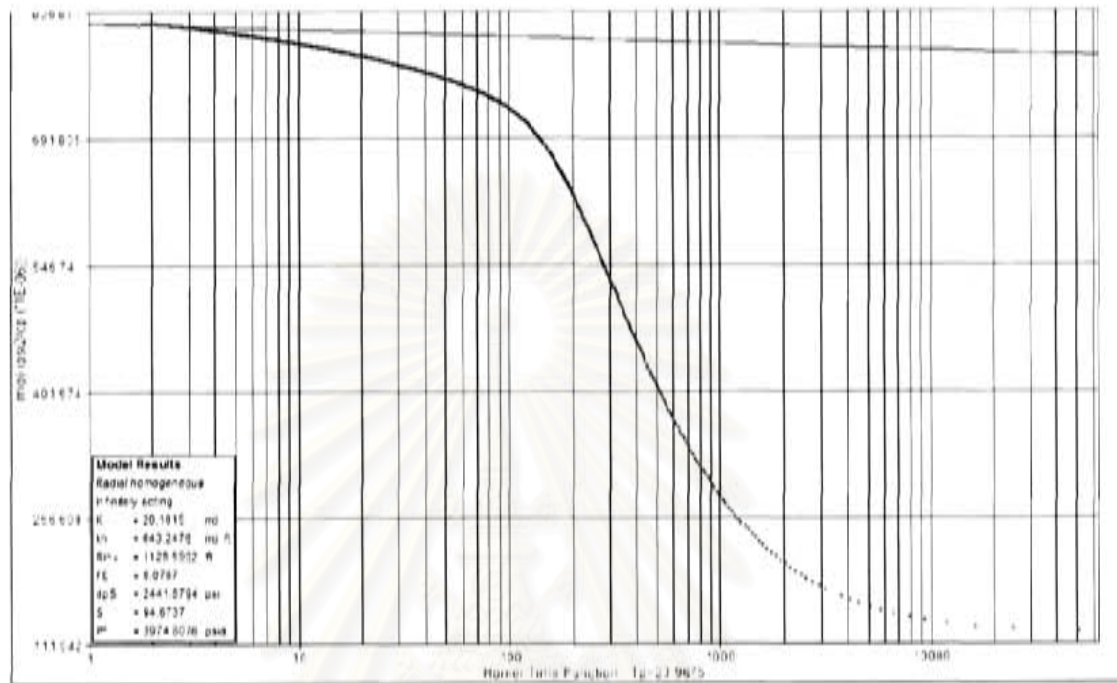


Figure A.175: Well-56 main build-up, semi-log plot.

สถาบันวิทยบริการ
 จุฬาลงกรณ์มหาวิทยาลัย

Well-57 Reservoir 87-6

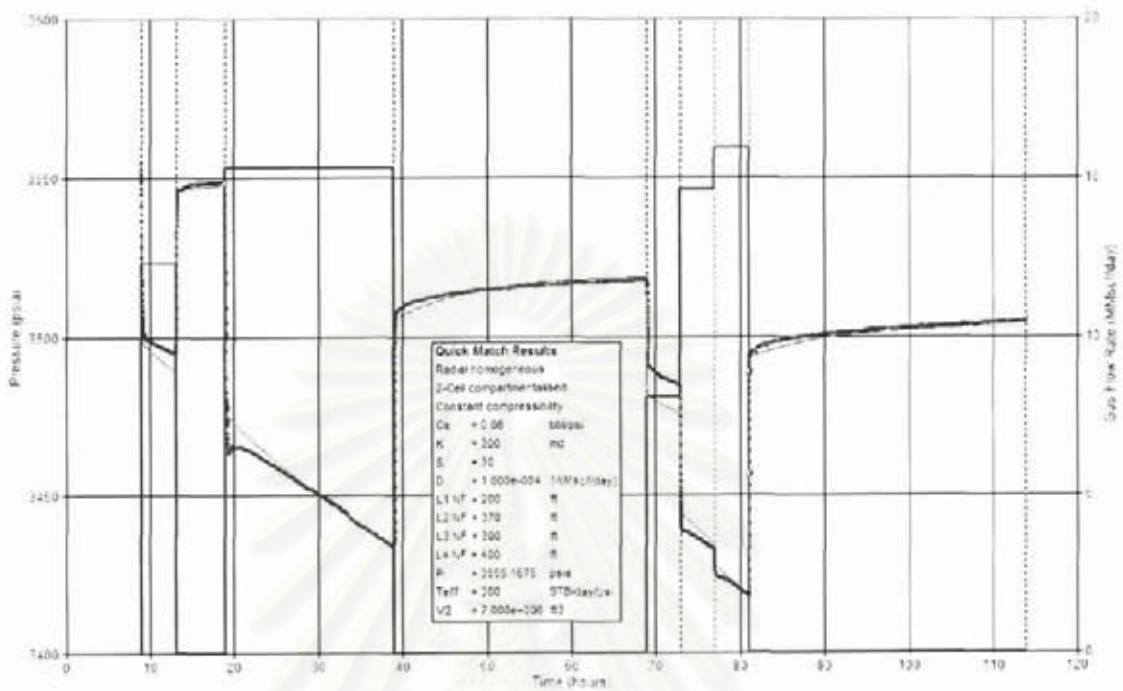


Figure A.176: Well-57 testing overview.

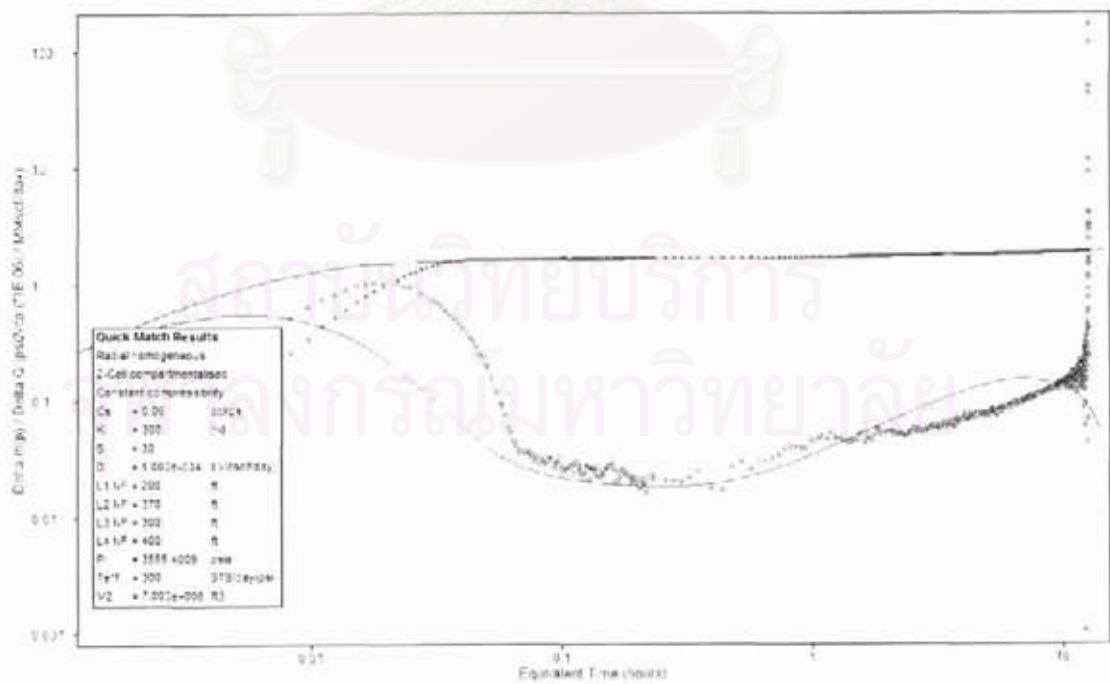


Figure A.177: Well-57 main build-up, log-log plot.

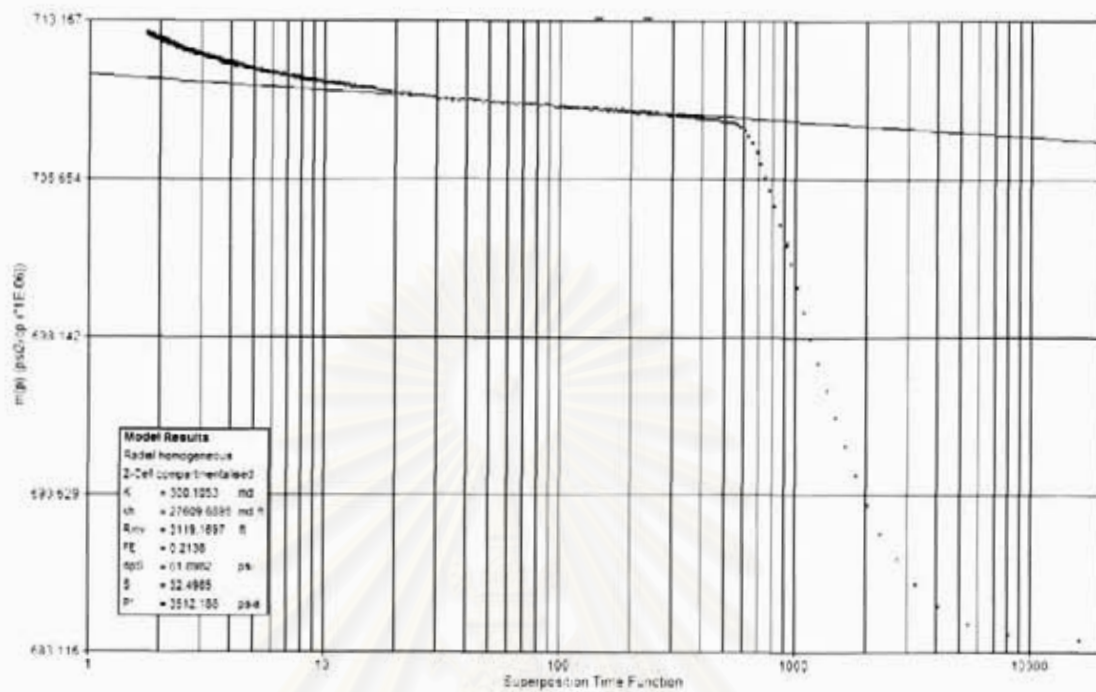


Figure A.178: Well-57 main build-up, semi-log plot.

สถาบันวิทยบริการ
 จุฬาลงกรณ์มหาวิทยาลัย

Well-58 Reservoir 88-9

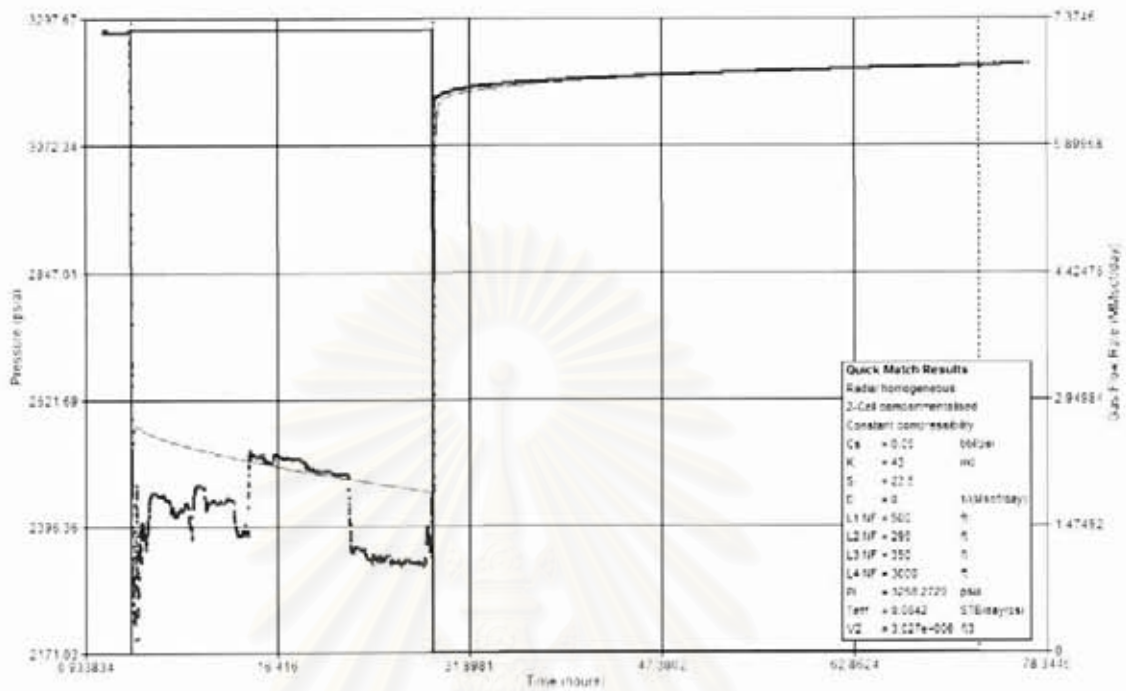


Figure A.179: Well-58 testing overview.

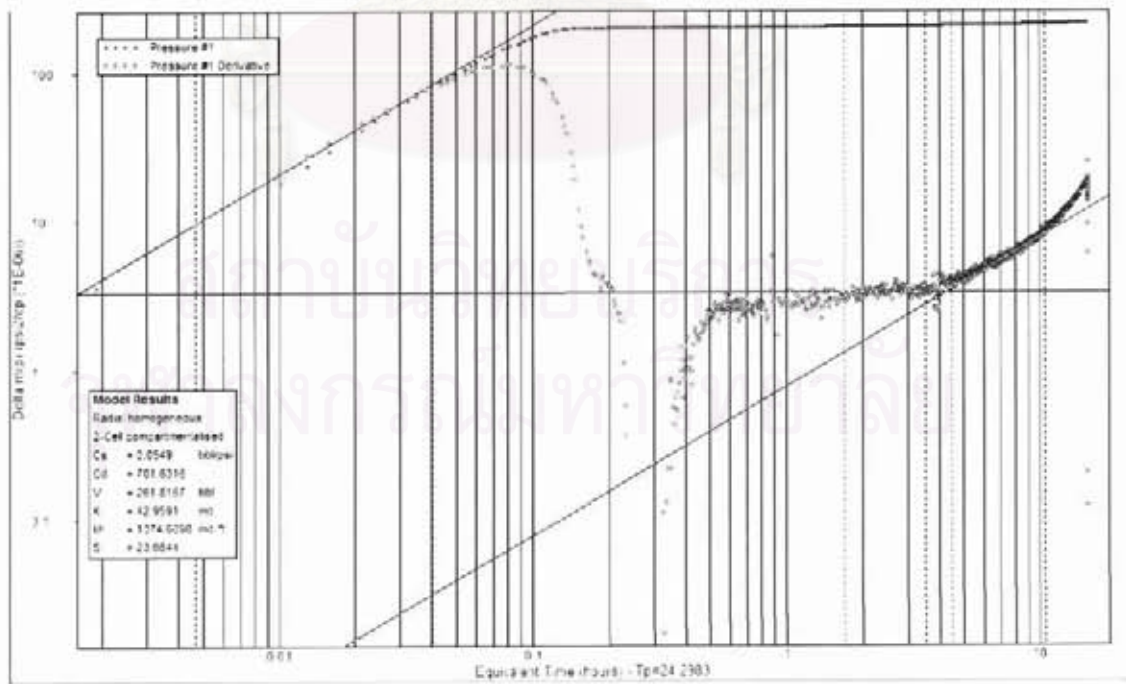


Figure A.180: Well-58 main build-up, log-log plot.

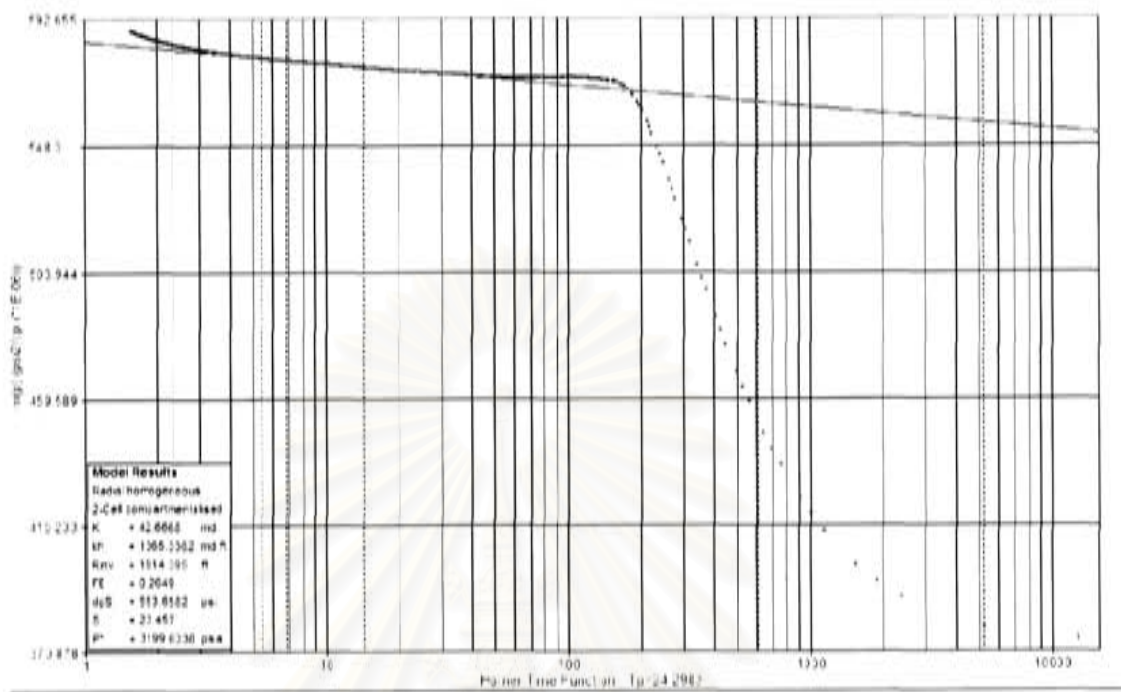


Figure A.181: Well-58 main build-up, semi-log plot.

สถาบันวิทยบริการ
 จุฬาลงกรณ์มหาวิทยาลัย

Well-59 Reservoir 88-8

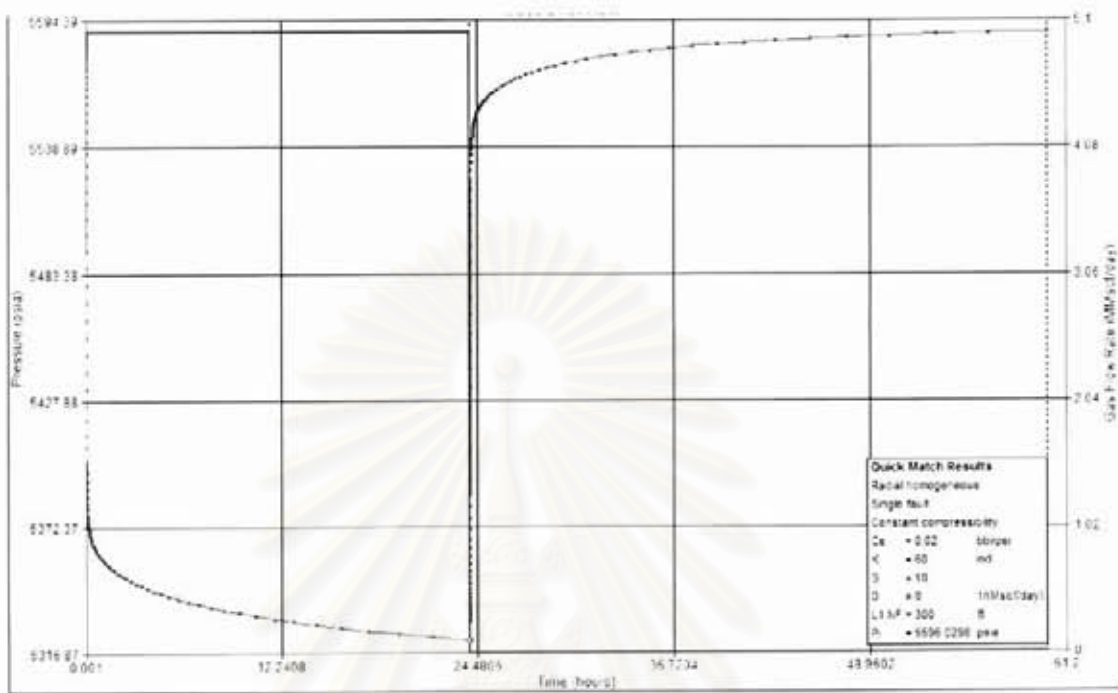


Figure A.182: Well-59 testing overview.

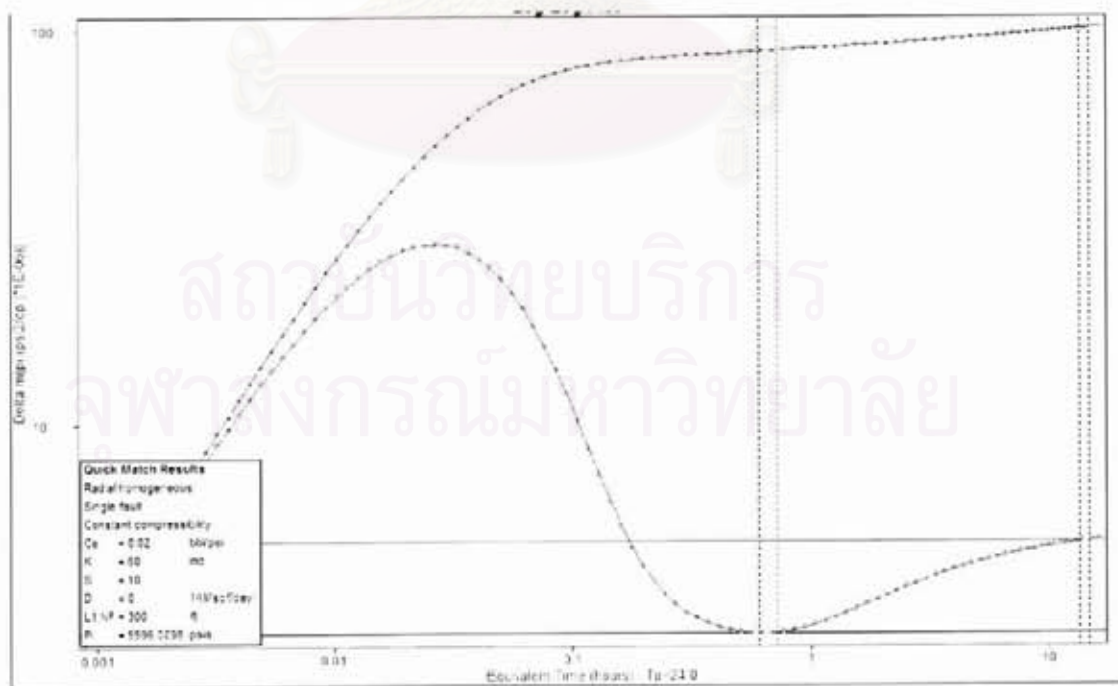


Figure A.183: Well-59 main build-up, log-log plot.

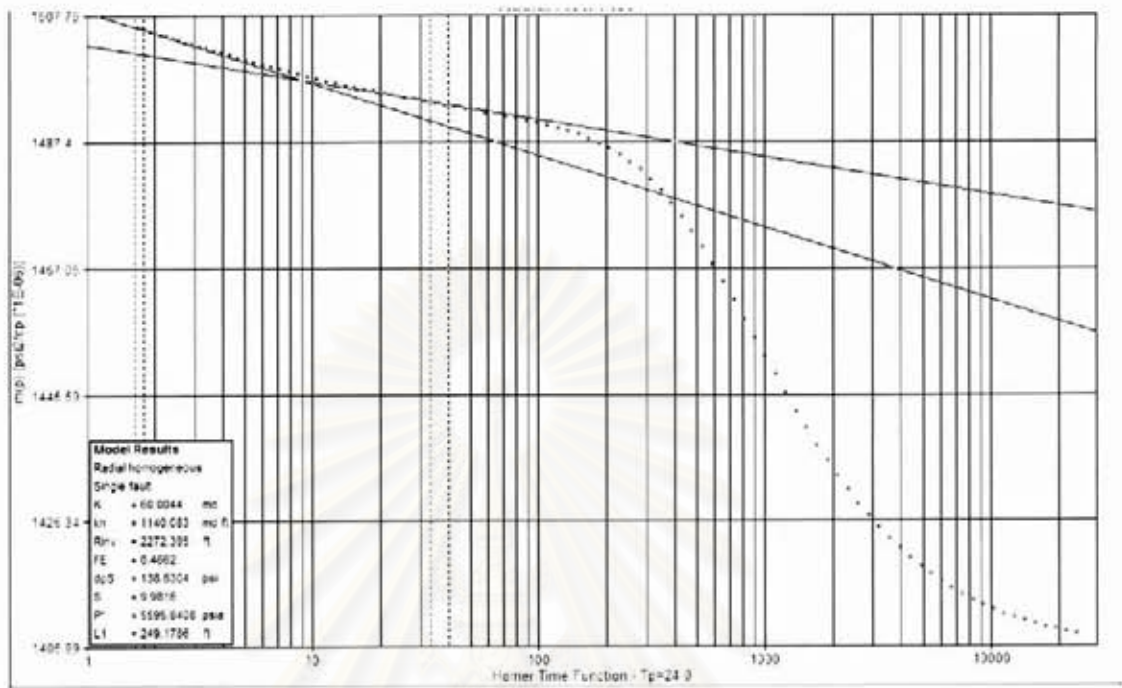


Figure A.184: Well-59 main build-up, semi-log plot.

สถาบันวิทยบริการ
 จุฬาลงกรณ์มหาวิทยาลัย

Well-60 Reservoir 69-2

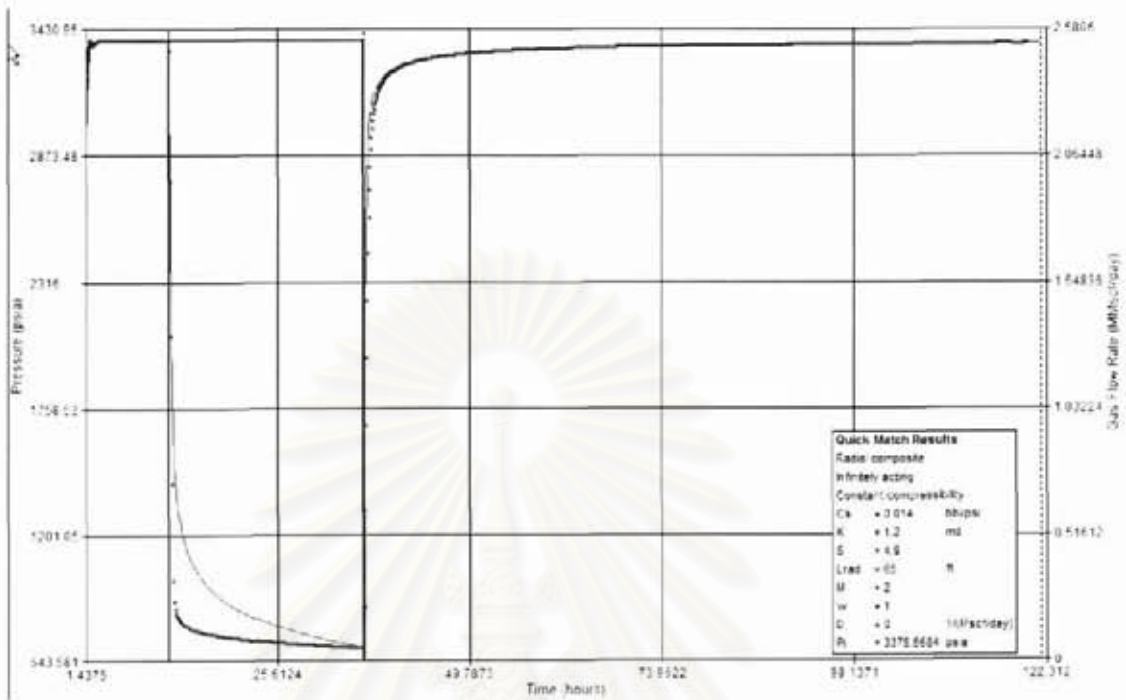


Figure A.185: Well-60 testing overview.

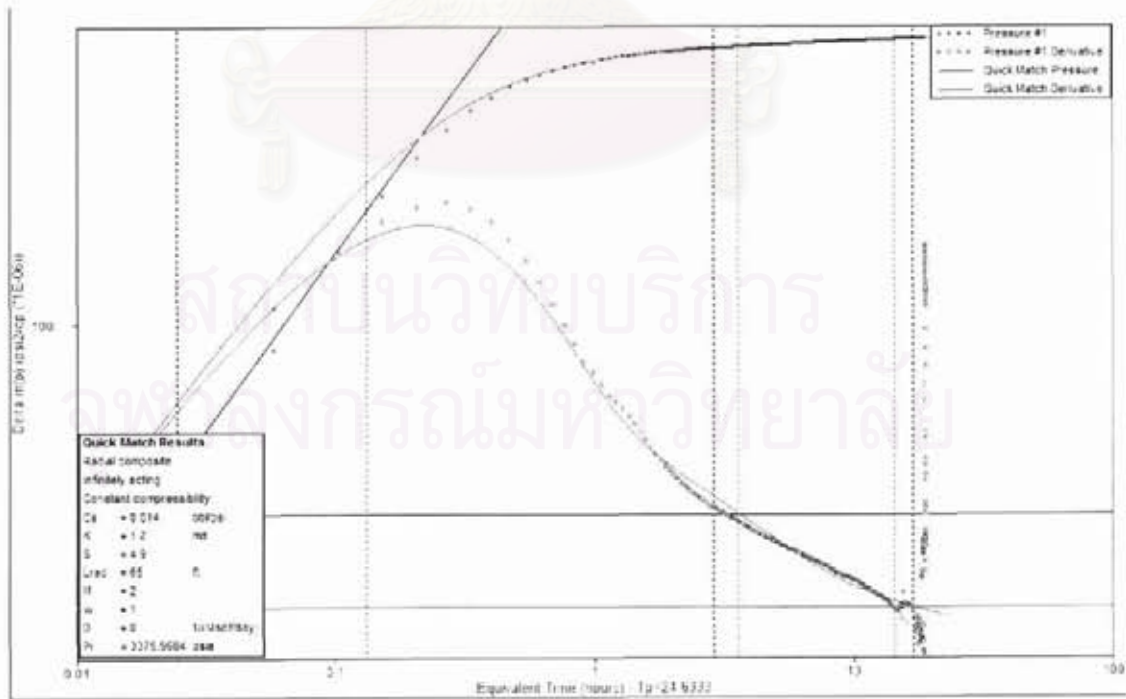


Figure A.186: Well-60 main build-up, log-log plot.

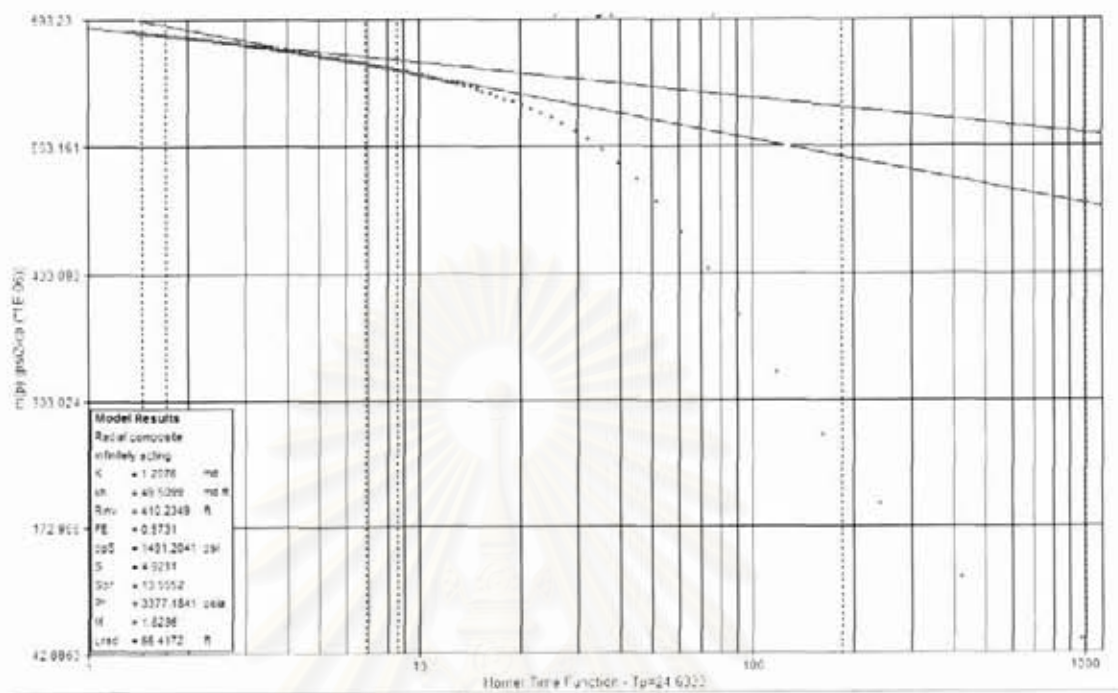


Figure A.187: Well-60 main build-up, semi-log plot.

สถาบันวิทยบริการ
จุฬาลงกรณ์มหาวิทยาลัย

Well-61 Reservoir 78-2

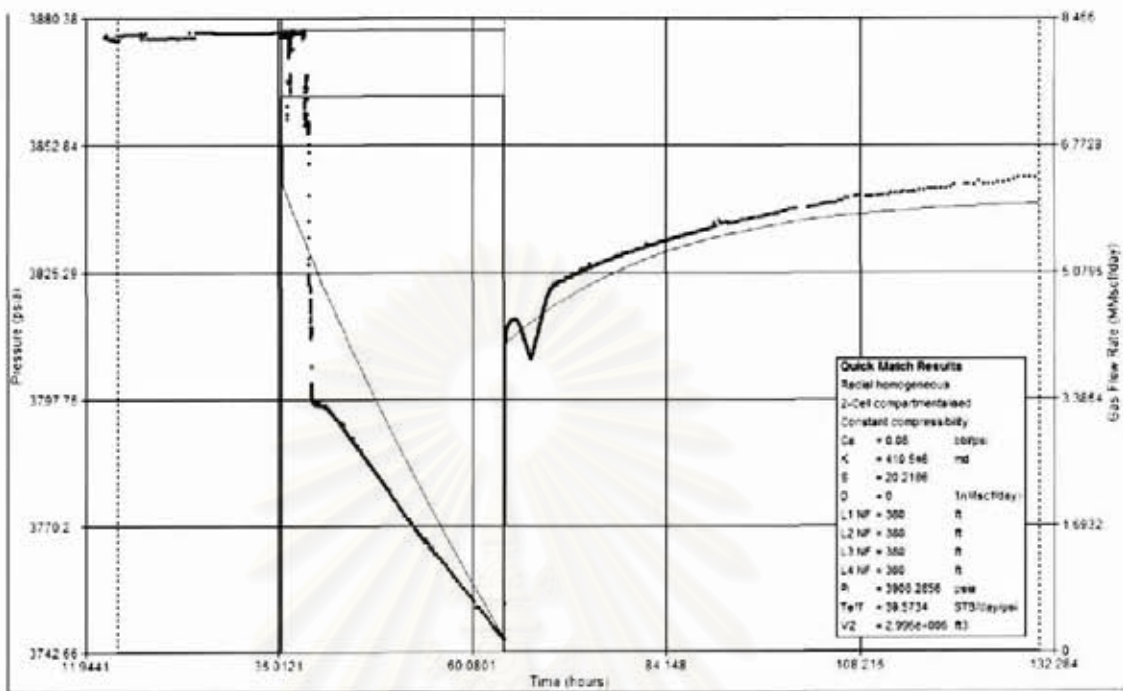


Figure A.188: Well-61 testing overview.

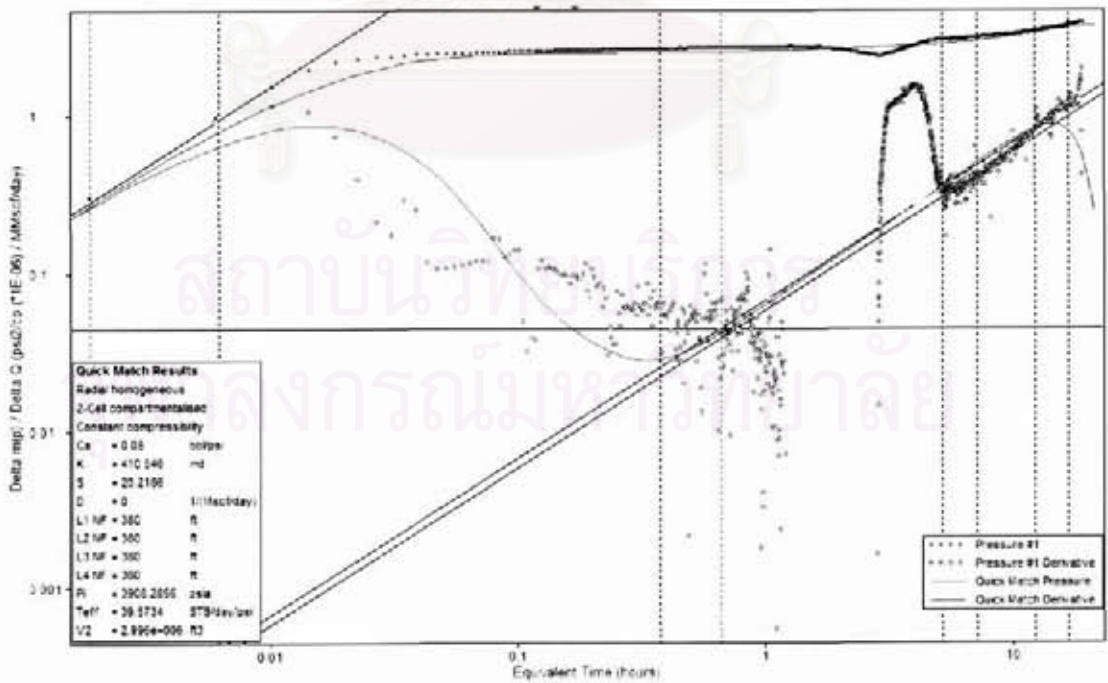


Figure A.189: Well-61 main build-up, log-log plot.

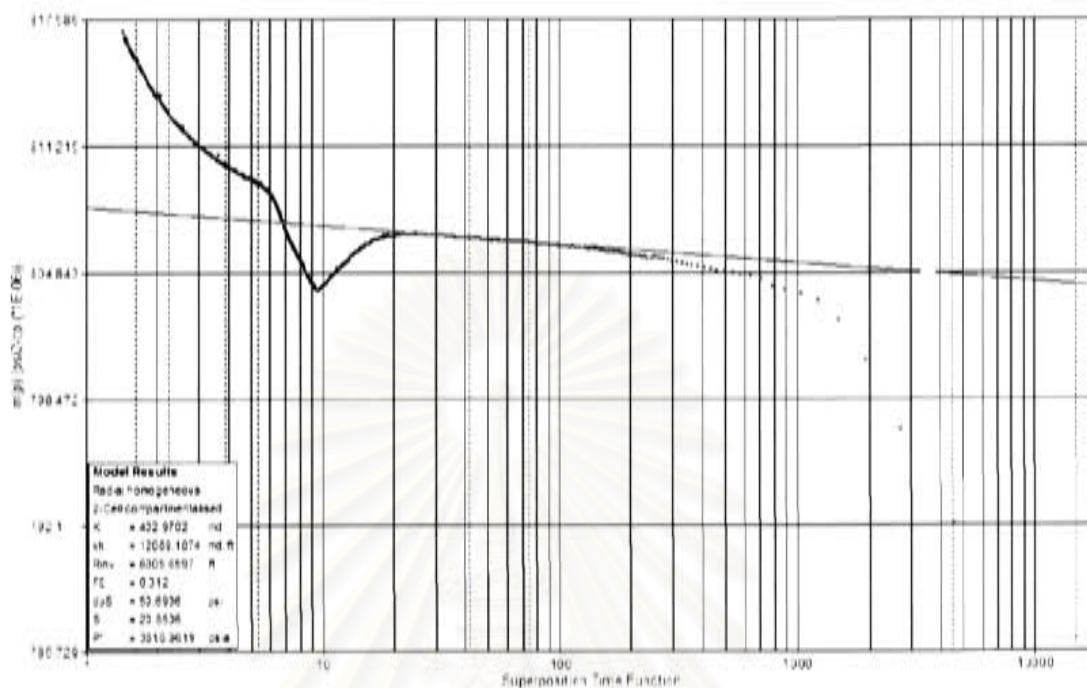


Figure A.190: Well-61 main build-up, semi-log plot.

สถาบันวิทยบริการ
จุฬาลงกรณ์มหาวิทยาลัย

Well-62 Reservoir 70-8

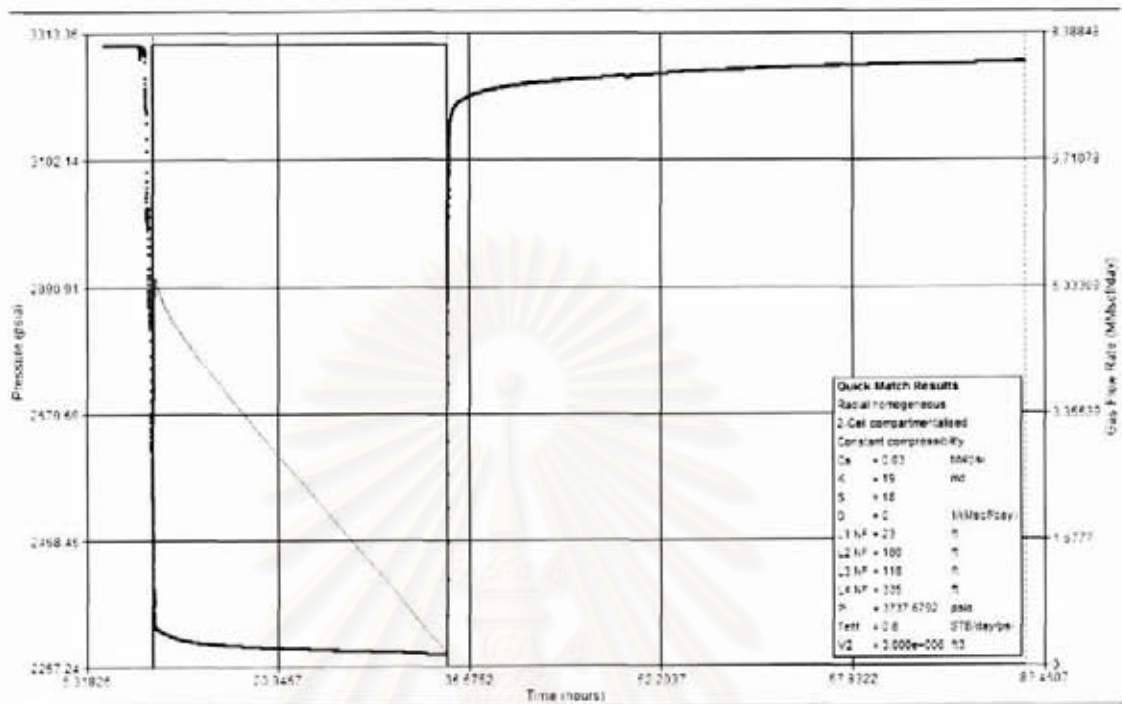


Figure A.191: Well-62 testing overview.

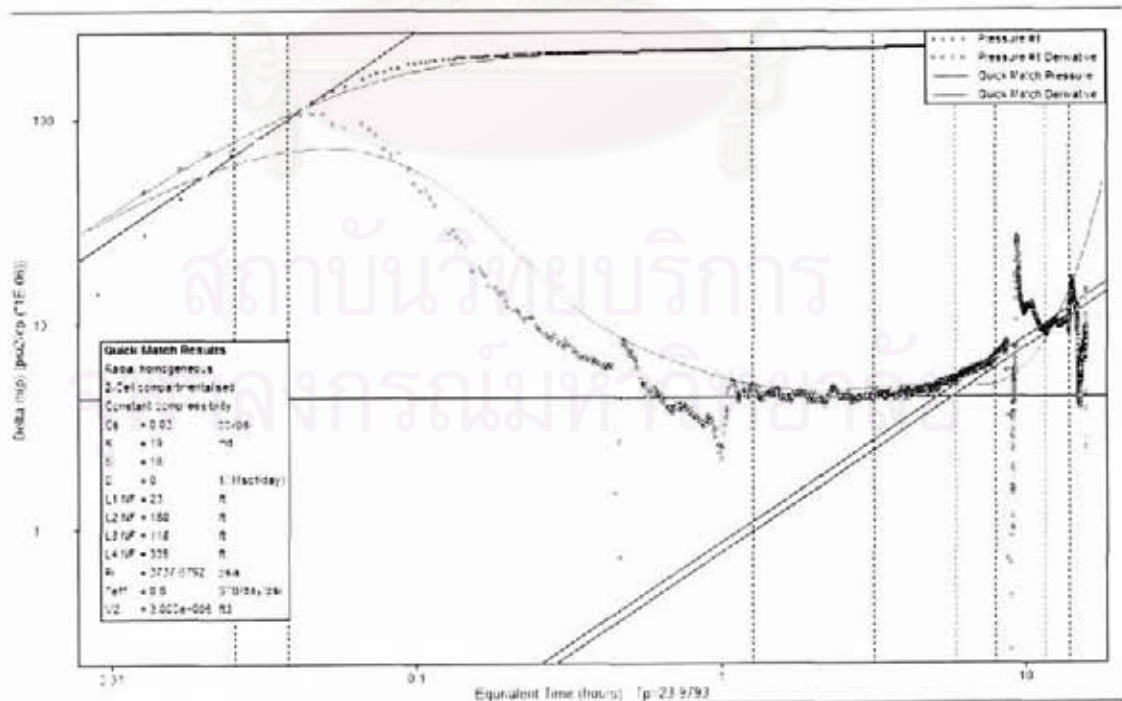


Figure A.192: Well-62 main build-up, log-log plot.

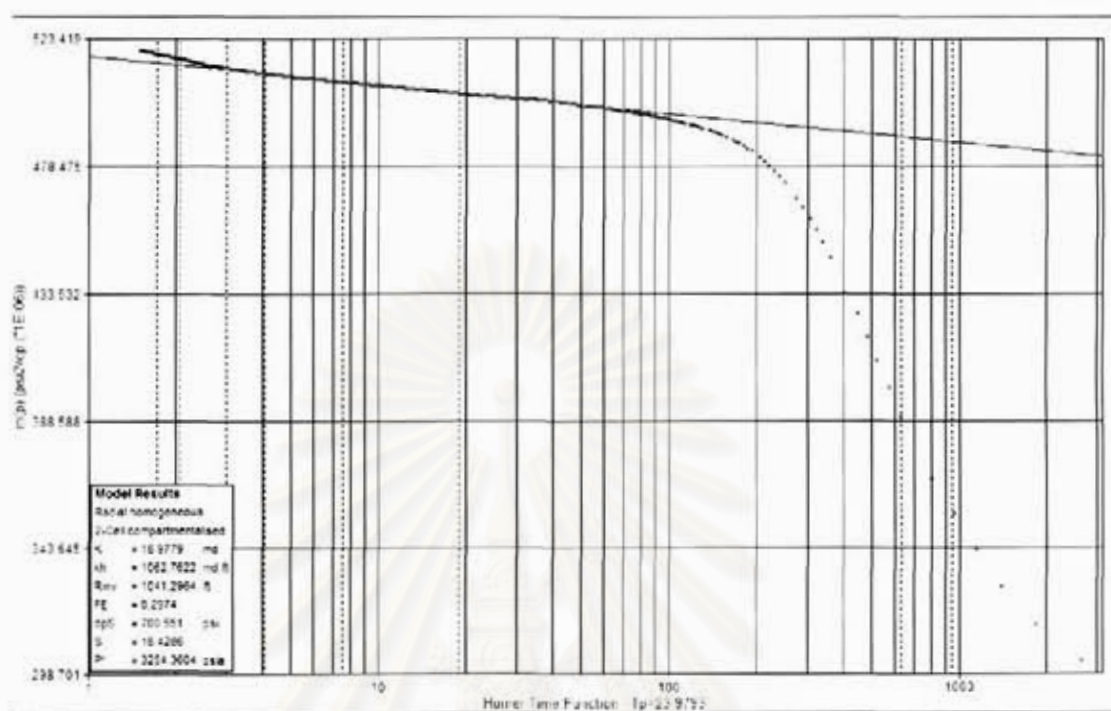


Figure A.193: Well-62 main build-up, semi-log plot.

สถาบันวิทยบริการ
 จุฬาลงกรณ์มหาวิทยาลัย

Well-63 Reservoir 81-2

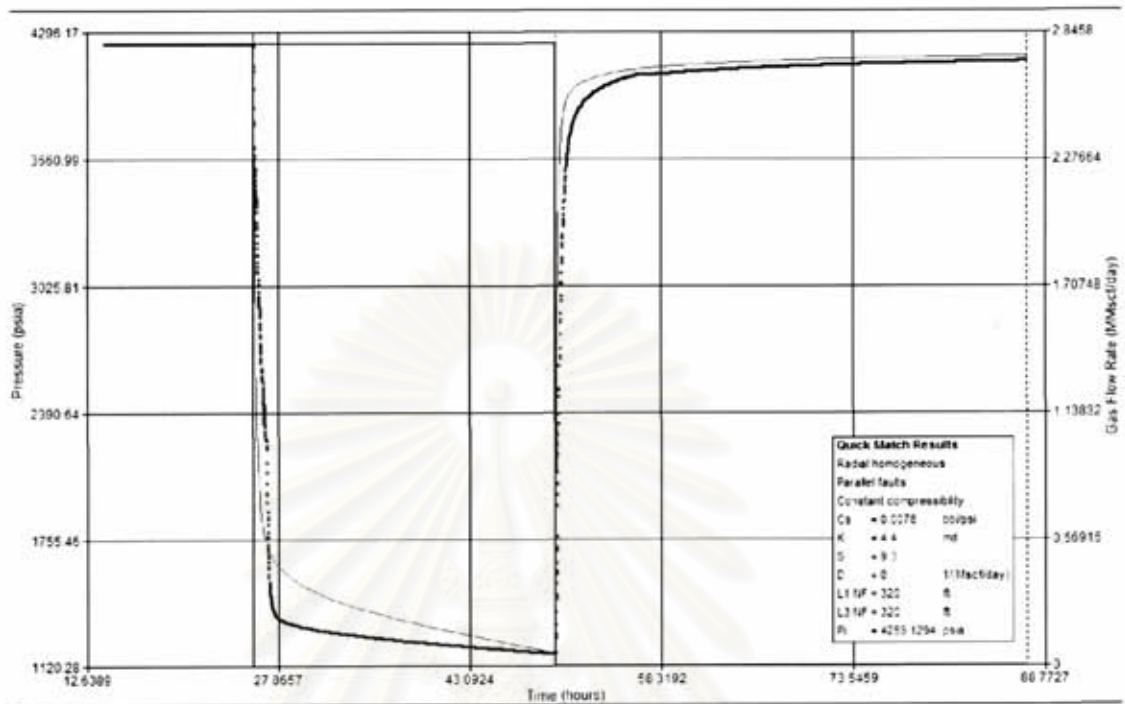


Figure A.194: Well-63 testing overview.

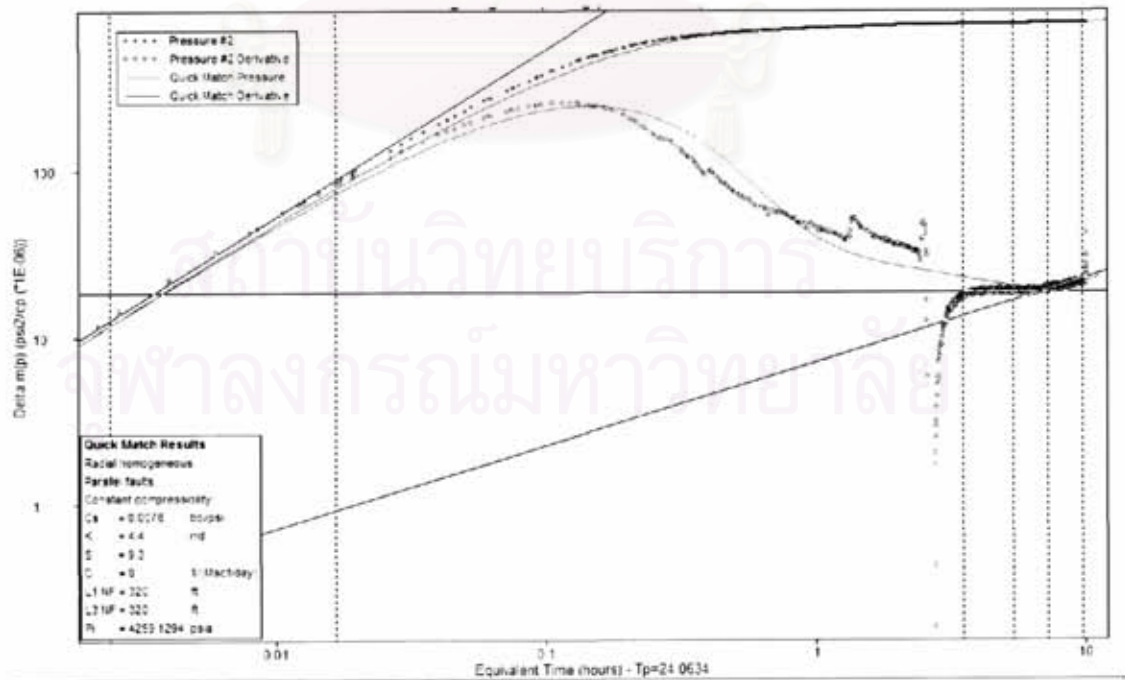


Figure A.195: Well-63 main build-up, log-log plot.

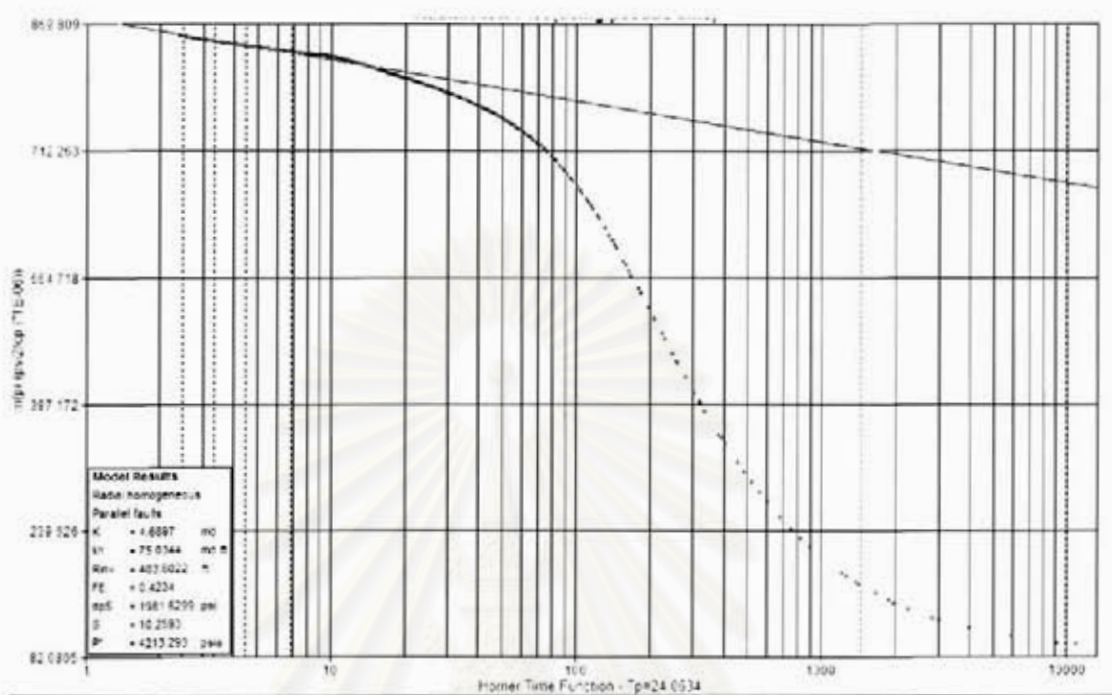


Figure A.196: Well-63 main build-up, semi-log plot.

สถาบันวิทยบริการ
จุฬาลงกรณ์มหาวิทยาลัย

Well-64 Reservoir 92-0

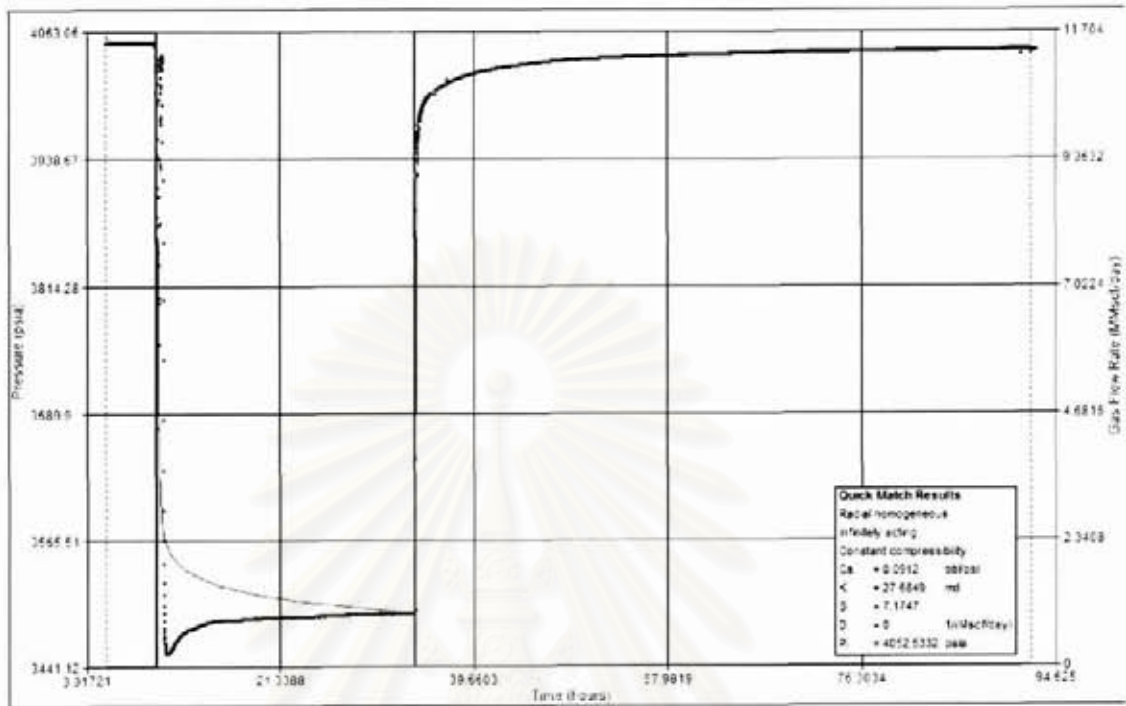


Figure A.197: Well-64 testing overview.

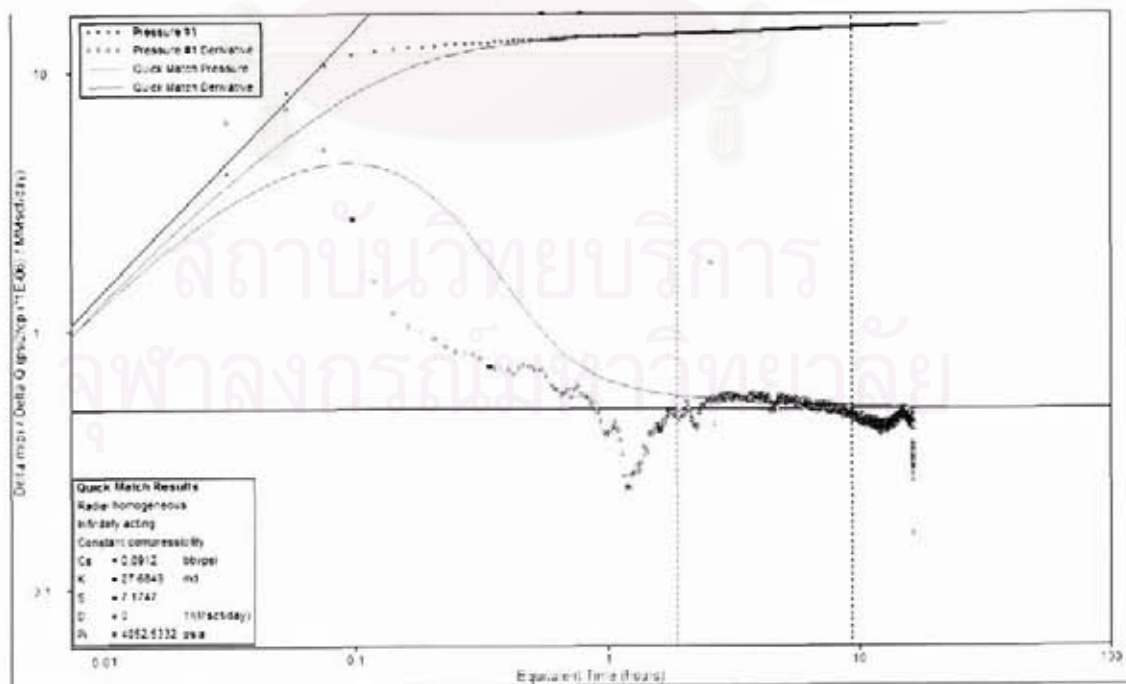


Figure A.198: Well-64 main build-up, log-log plot.

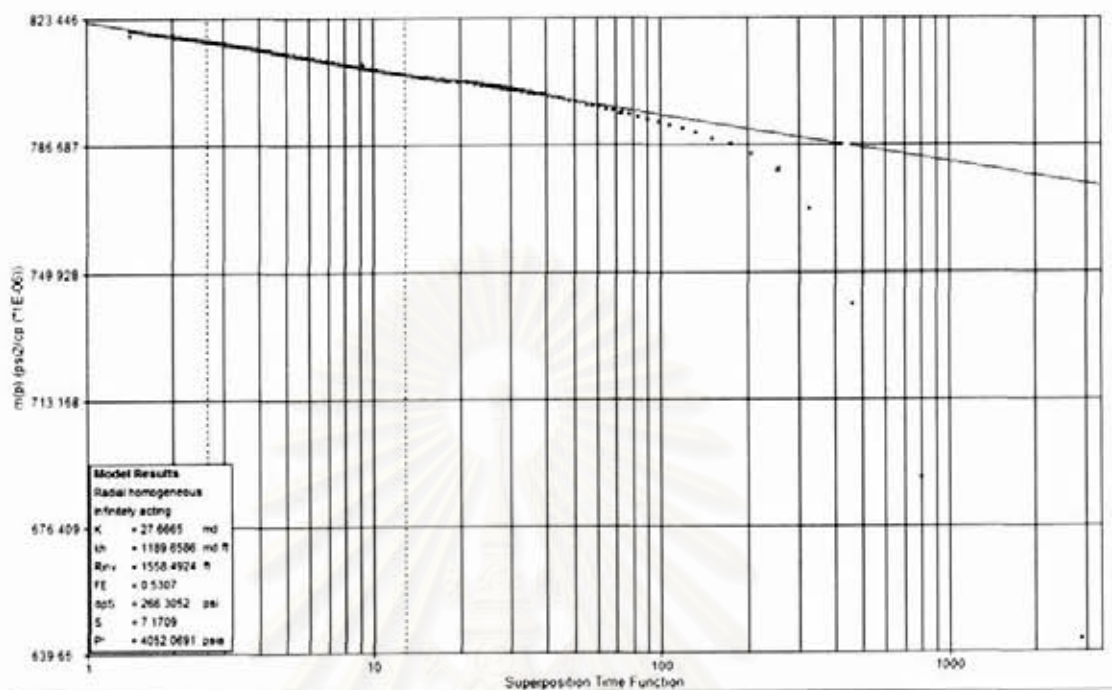


Figure A.199: Well-64 main build-up, semi-log plot.

สถาบันวิทยบริการ
จุฬาลงกรณ์มหาวิทยาลัย

Well-65 Reservoir 89-5

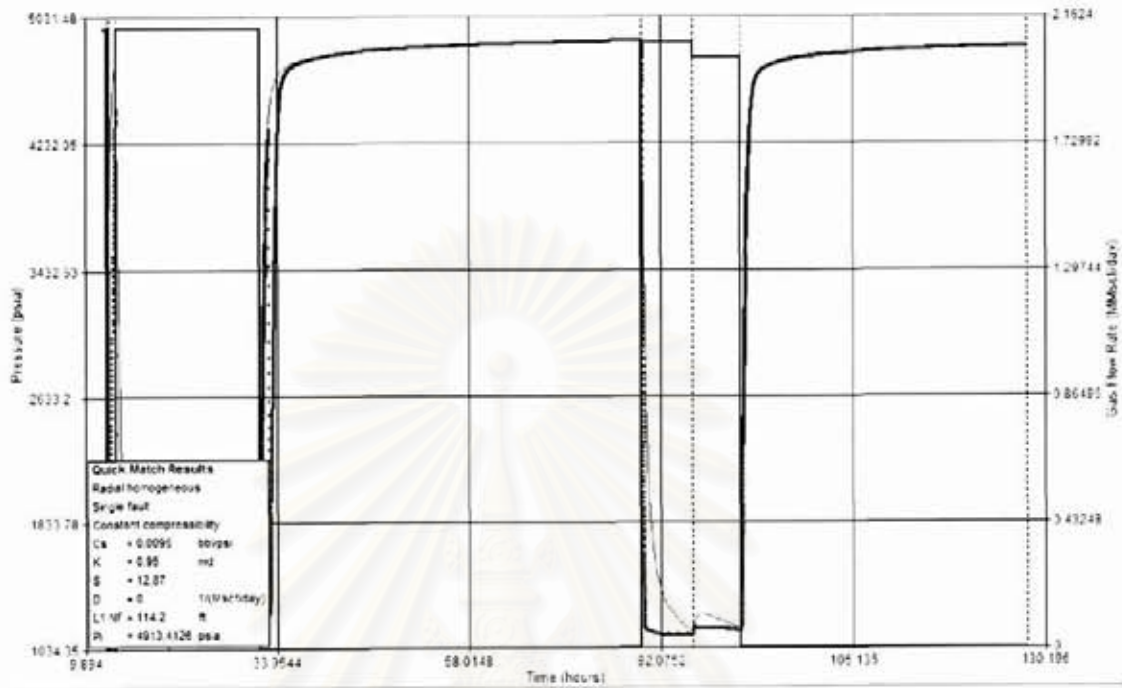


Figure A.200: Well-65 testing overview.

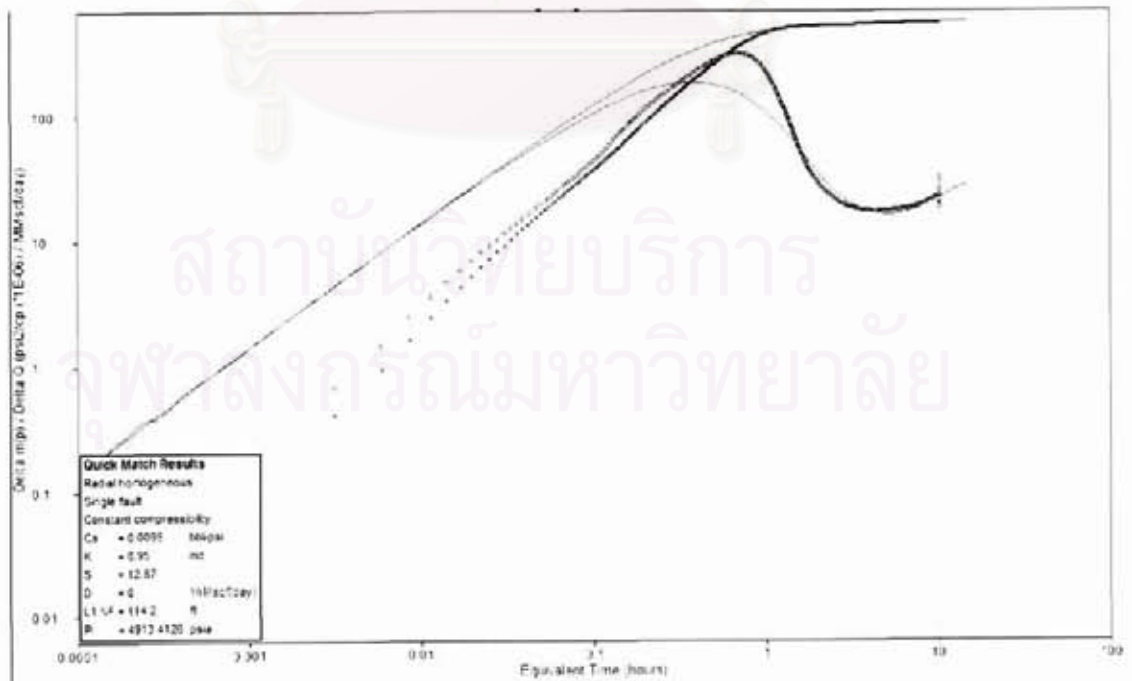


Figure A.201: Well-65 main build-up, log-log plot.

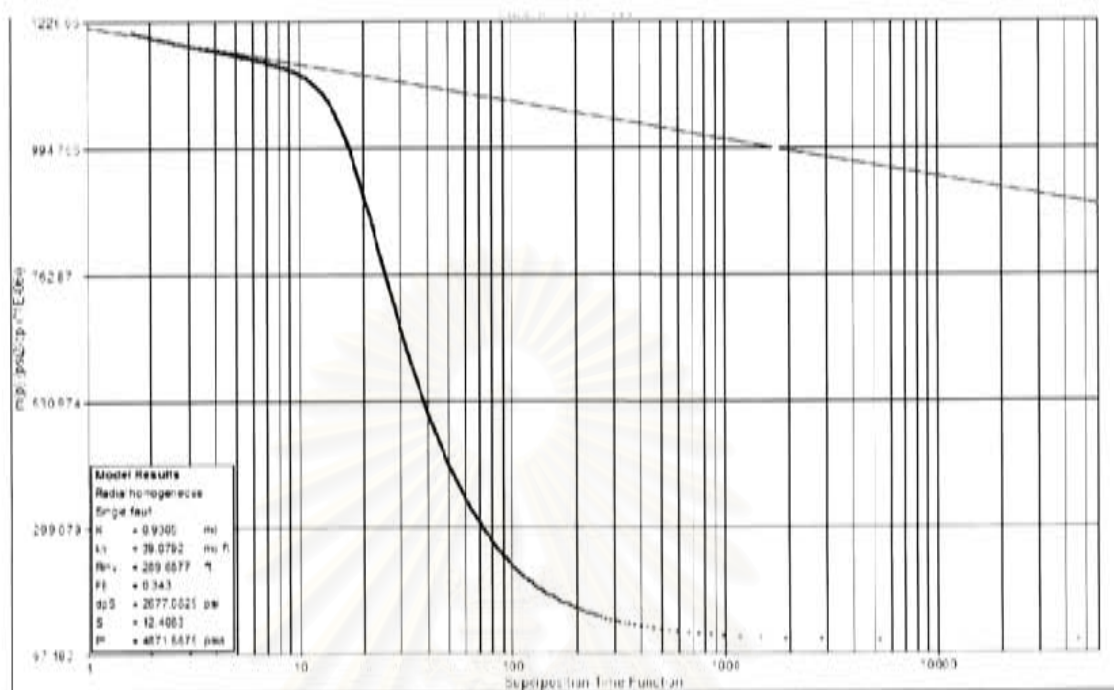


Figure A.202: Well-65 main build-up, semi-log plot.

สถาบันวิทยบริการ
จุฬาลงกรณ์มหาวิทยาลัย

Well-66 Reservoir 64-0

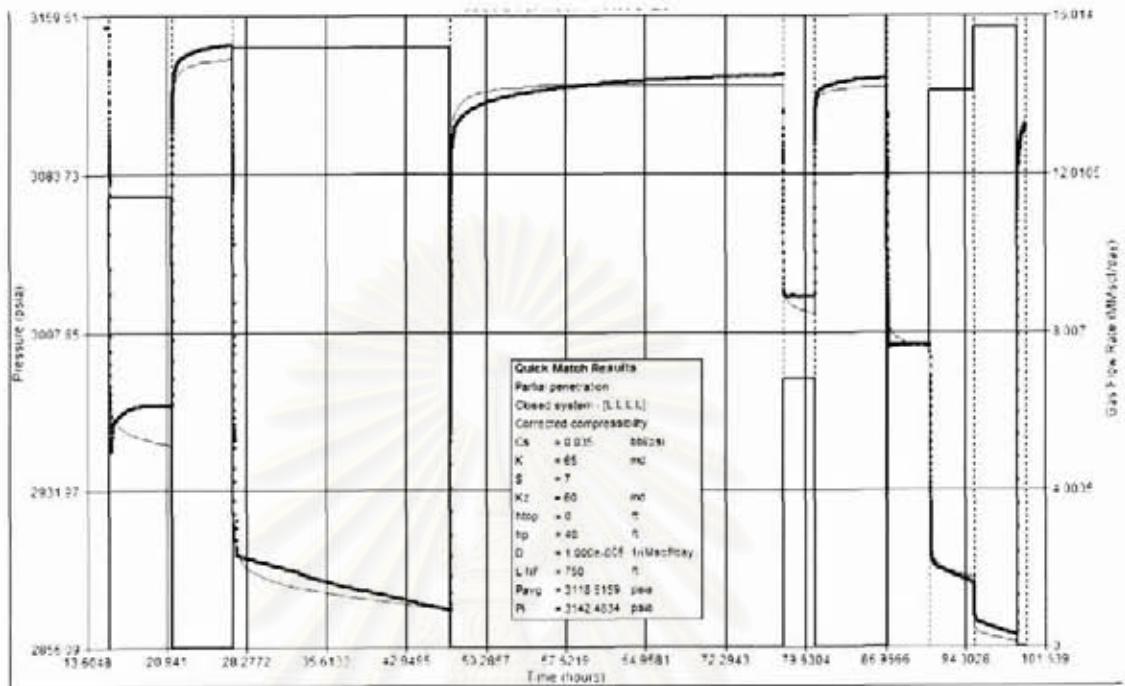


Figure A.203: Well-66 testing overview.

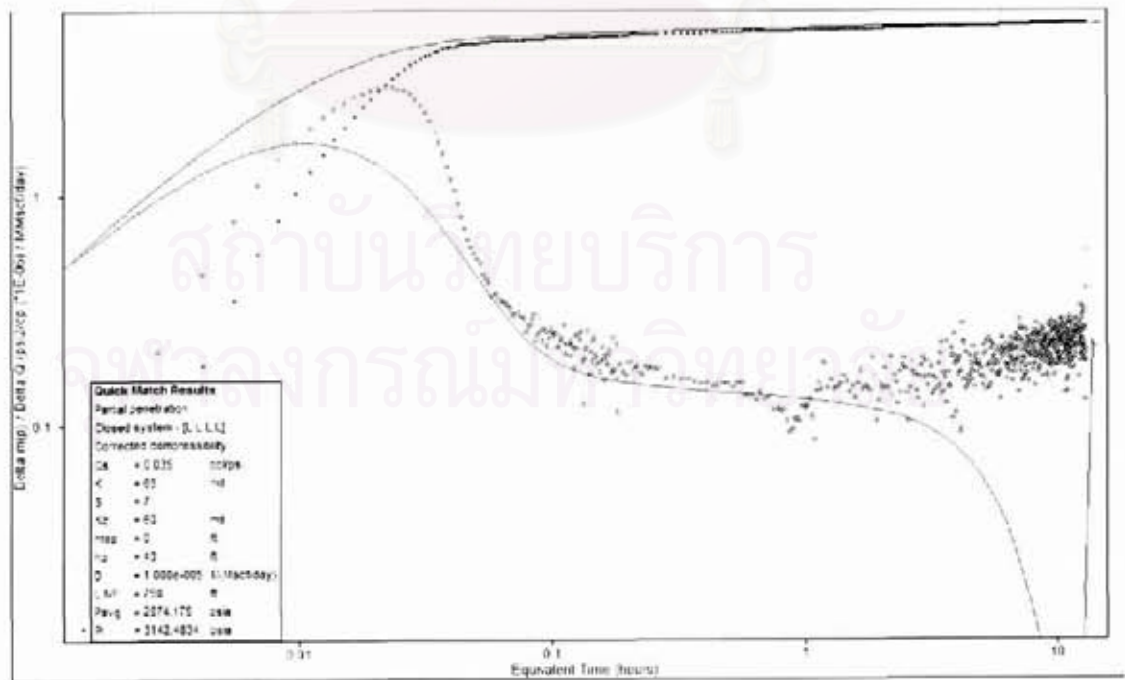


Figure A.204: Well-66 main build-up, log-log plot.

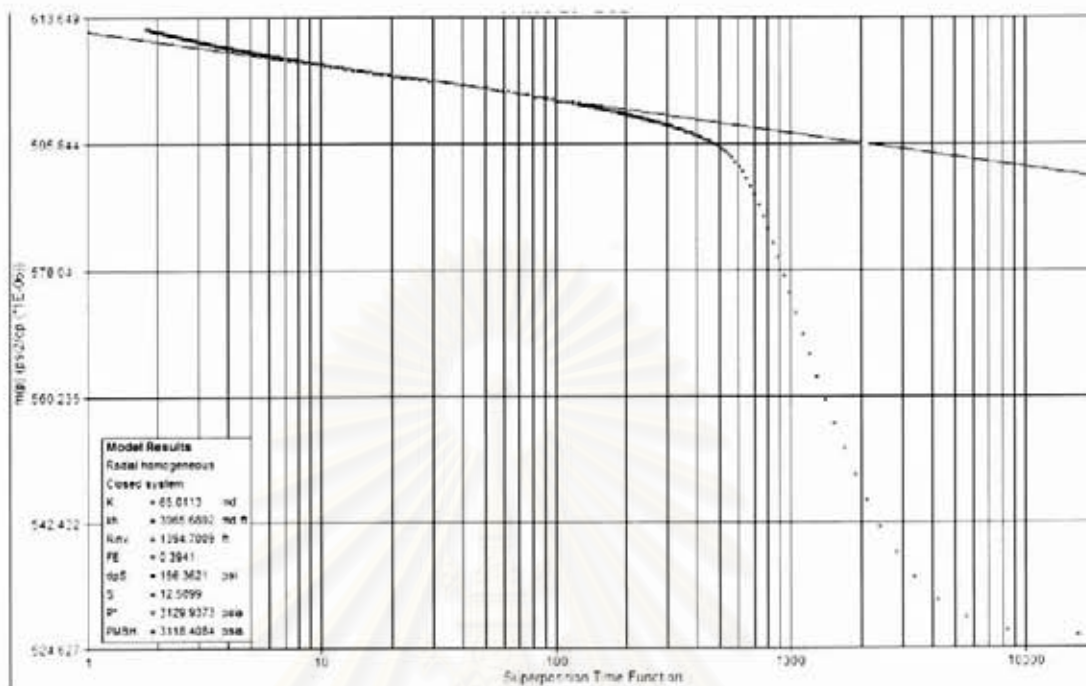


Figure A.205: Well-66 main build-up, semi-log plot.

สถาบันวิทยบริการ
จุฬาลงกรณ์มหาวิทยาลัย

Well-67 Reservoir 81-3

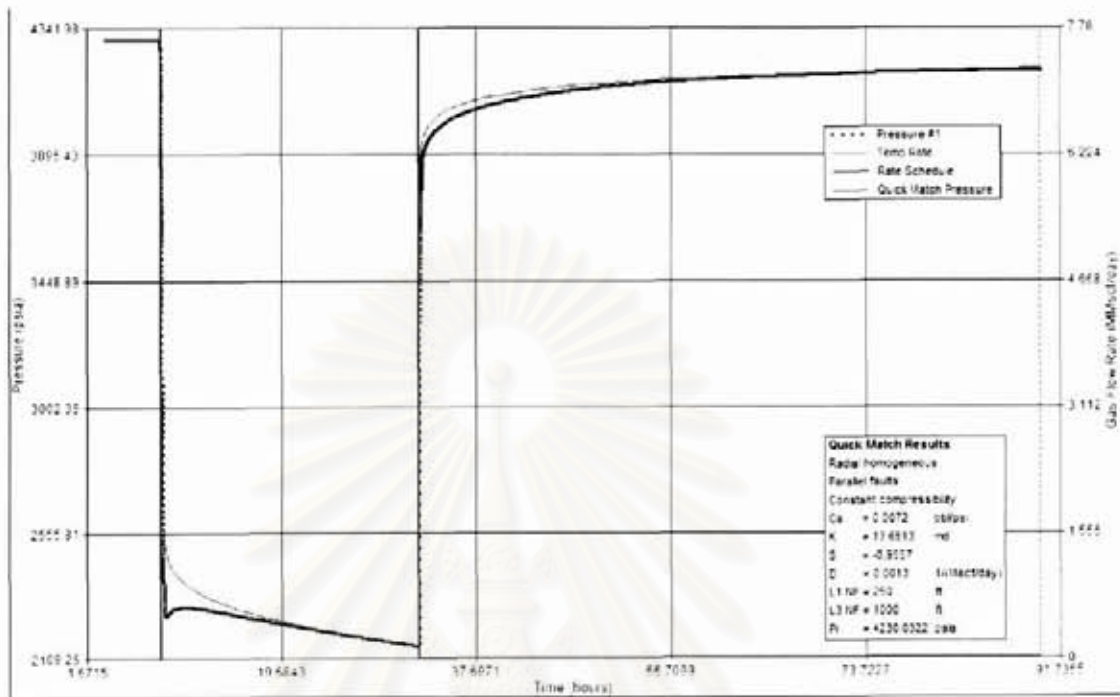


Figure A.206: Well-67 testing overview.

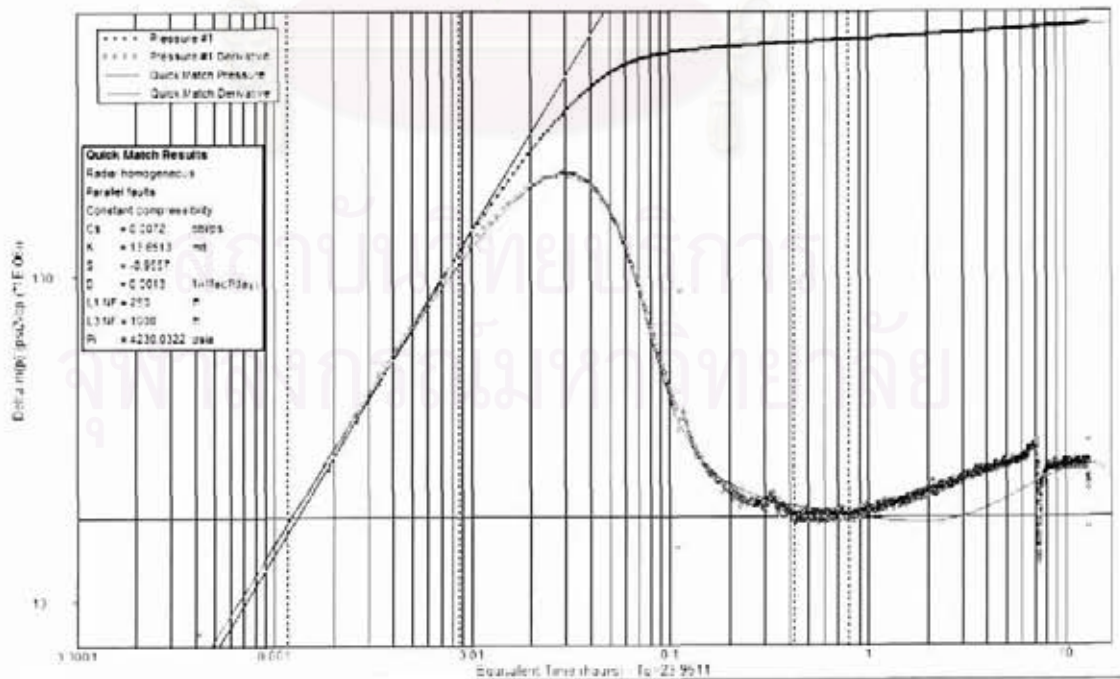


Figure A.207: Well-67 main build-up, log-log plot.

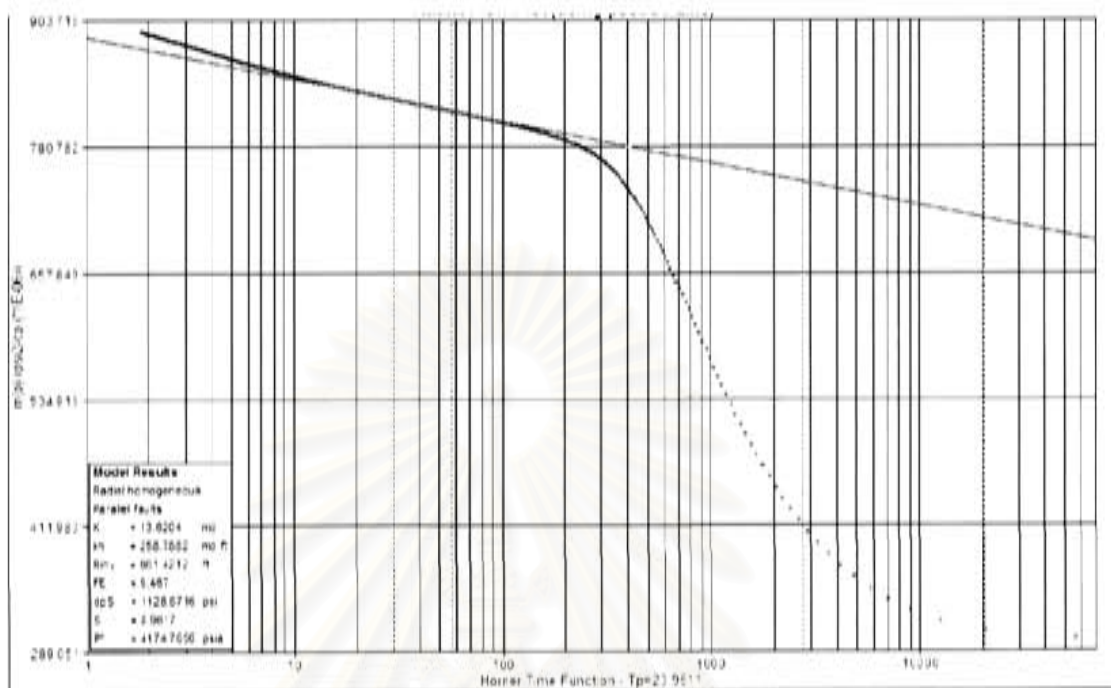


Figure A.208: Well-67 main build-up, semi-log plot.

สถาบันวิทยบริการ
จุฬาลงกรณ์มหาวิทยาลัย

Well 68 Reservoir 71-4

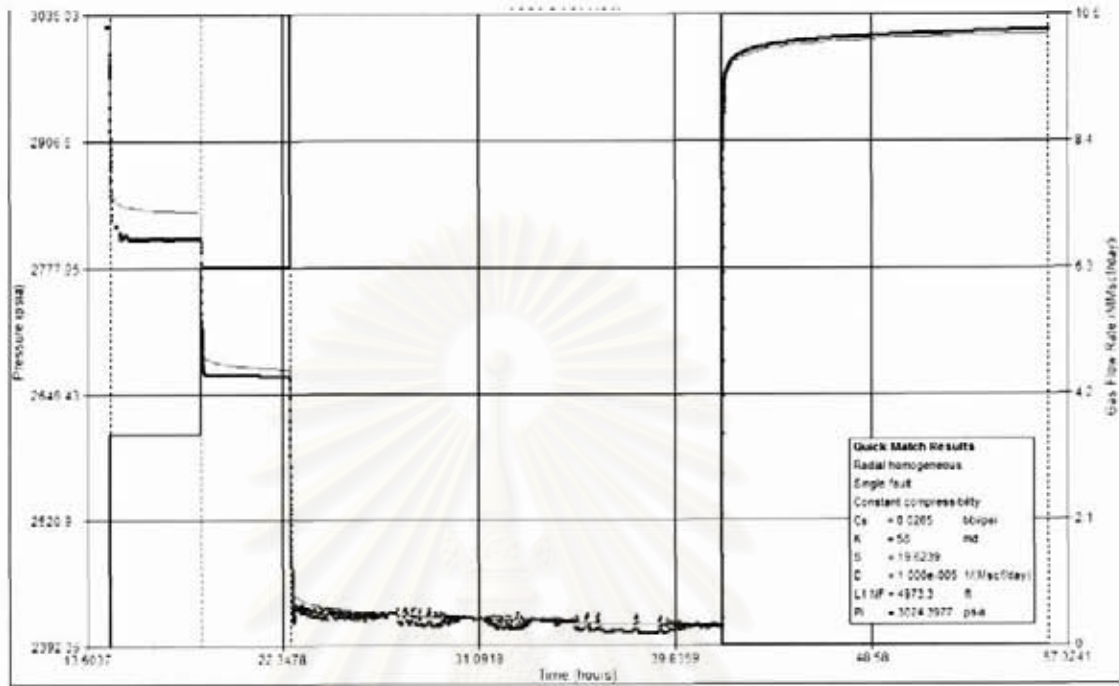


Figure A.209: Well-68 testing overview.

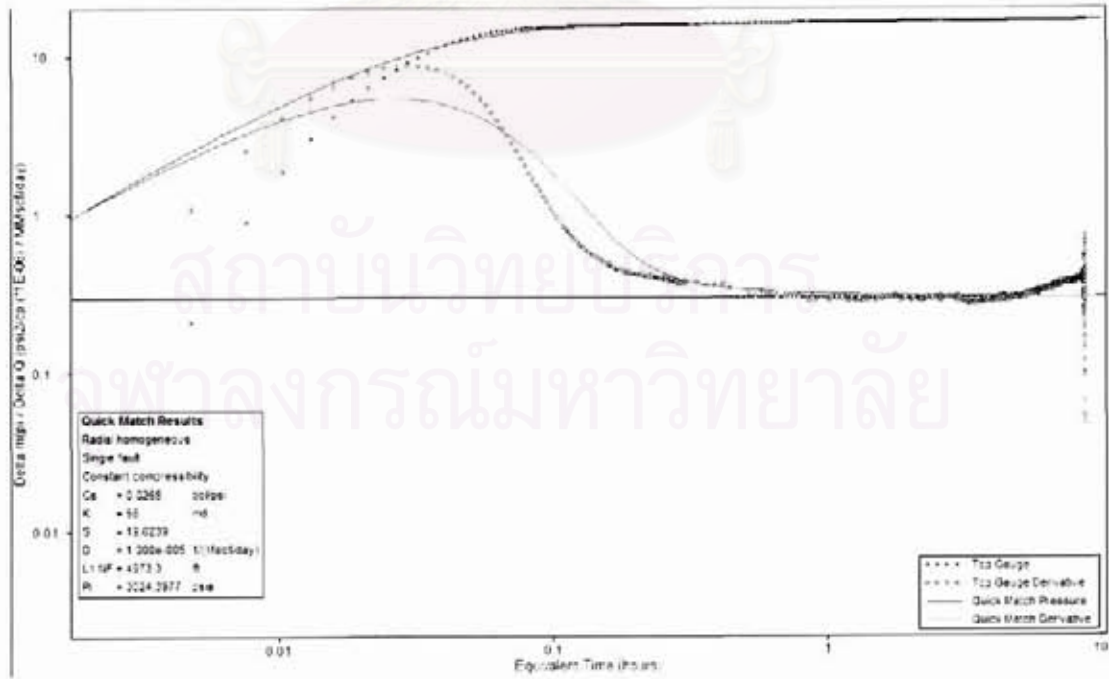


Figure A.210: Well-68 main build-up, log-log plot.

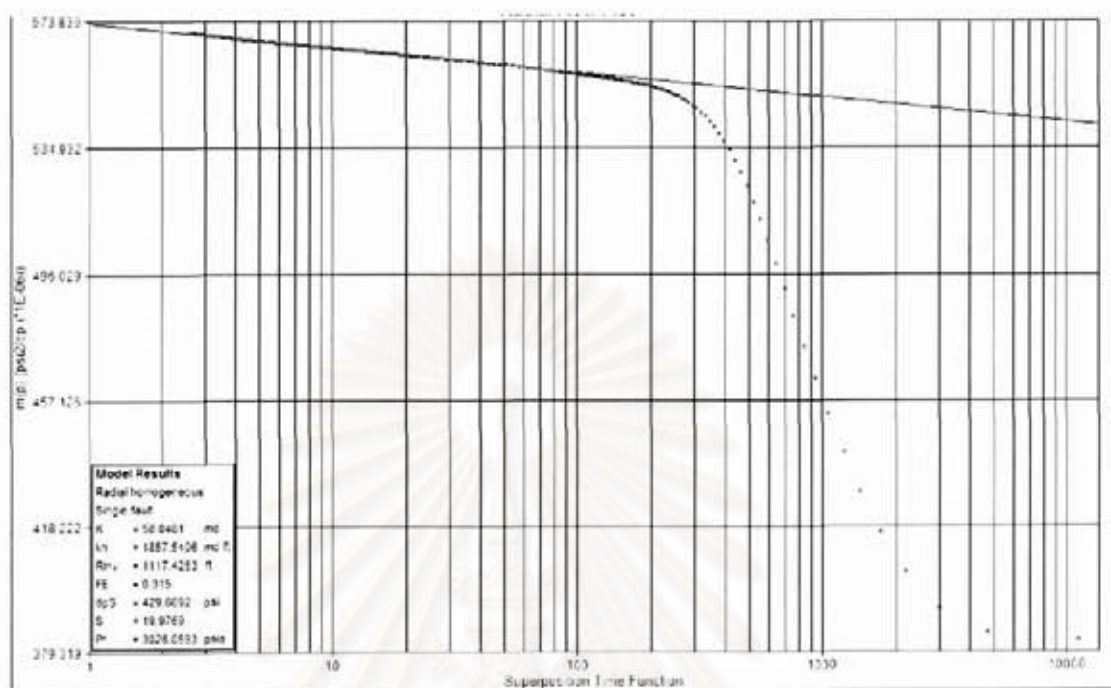


Figure A.211: Well-68 main build-up, semi-log plot.

สถาบันวิทยบริการ
จุฬาลงกรณ์มหาวิทยาลัย

Well 69 Reservoir 72-3

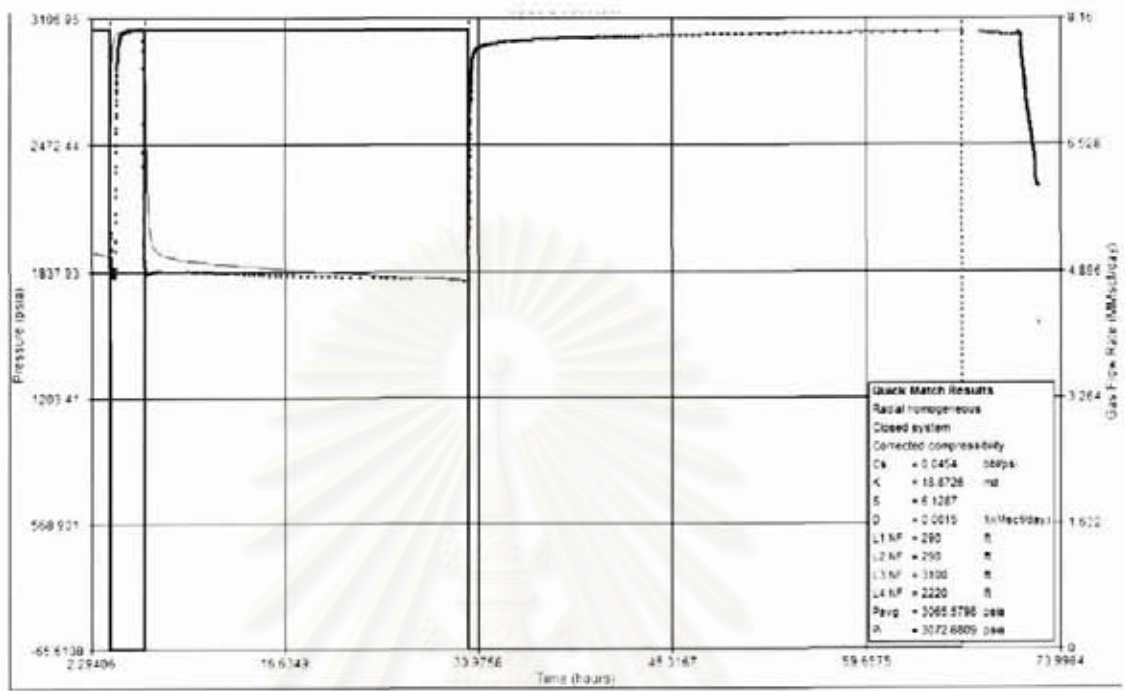


Figure A.212: Well-69 testing overview.

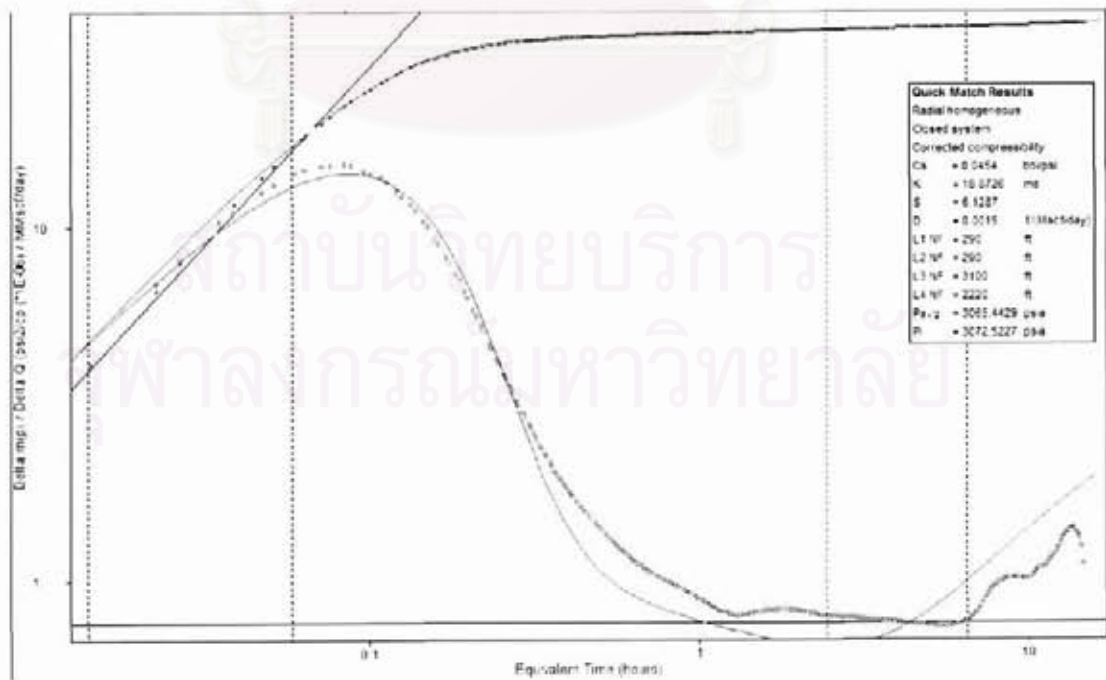


Figure A.213: Well-69 main build-up, log-log plot.

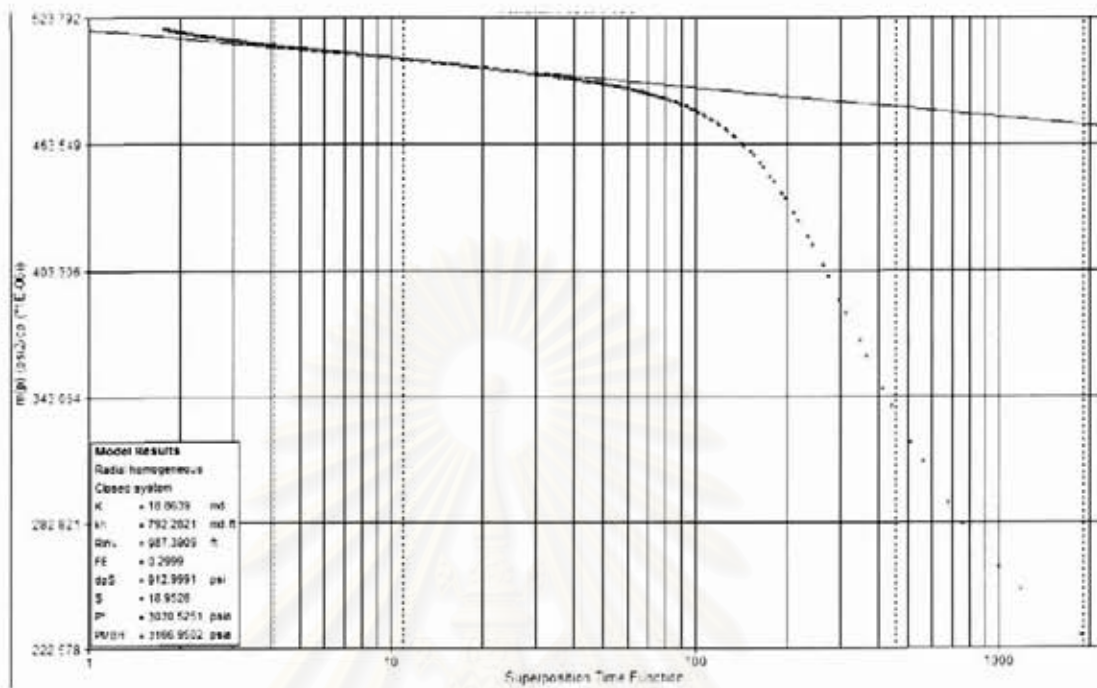


Figure A.214: Well-69 main build-up, semi-log plot.

สถาบันวิทยบริการ
จุฬาลงกรณ์มหาวิทยาลัย

Well 70 Reservoir 65-2

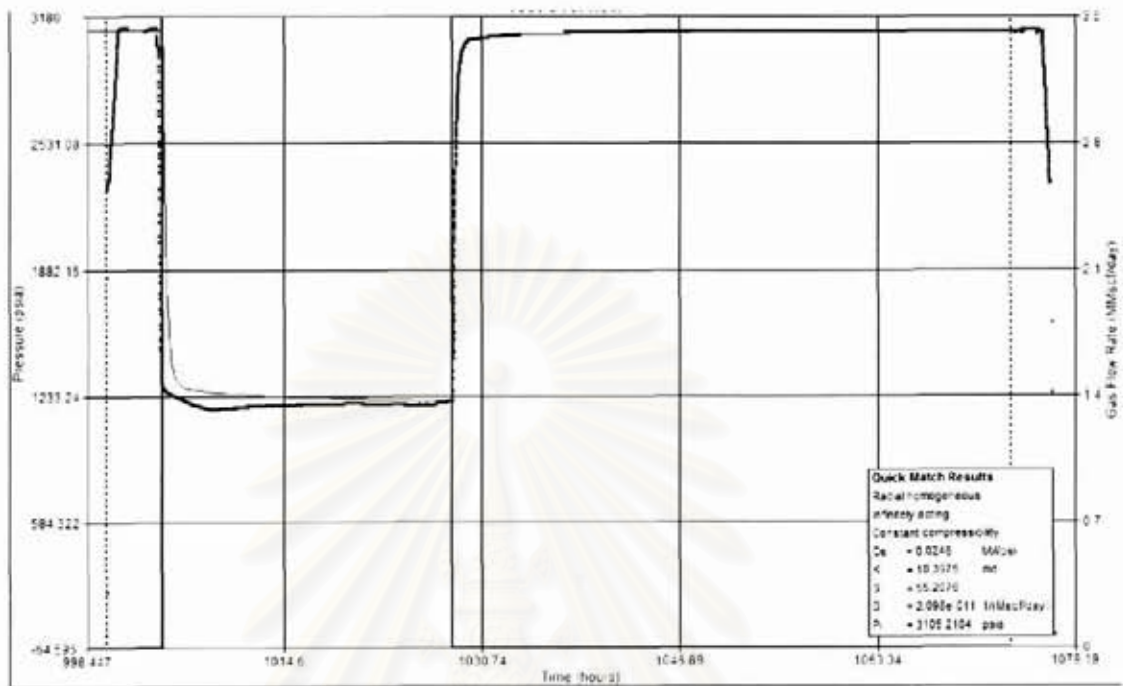


Figure A.215: Well-70 testing overview.

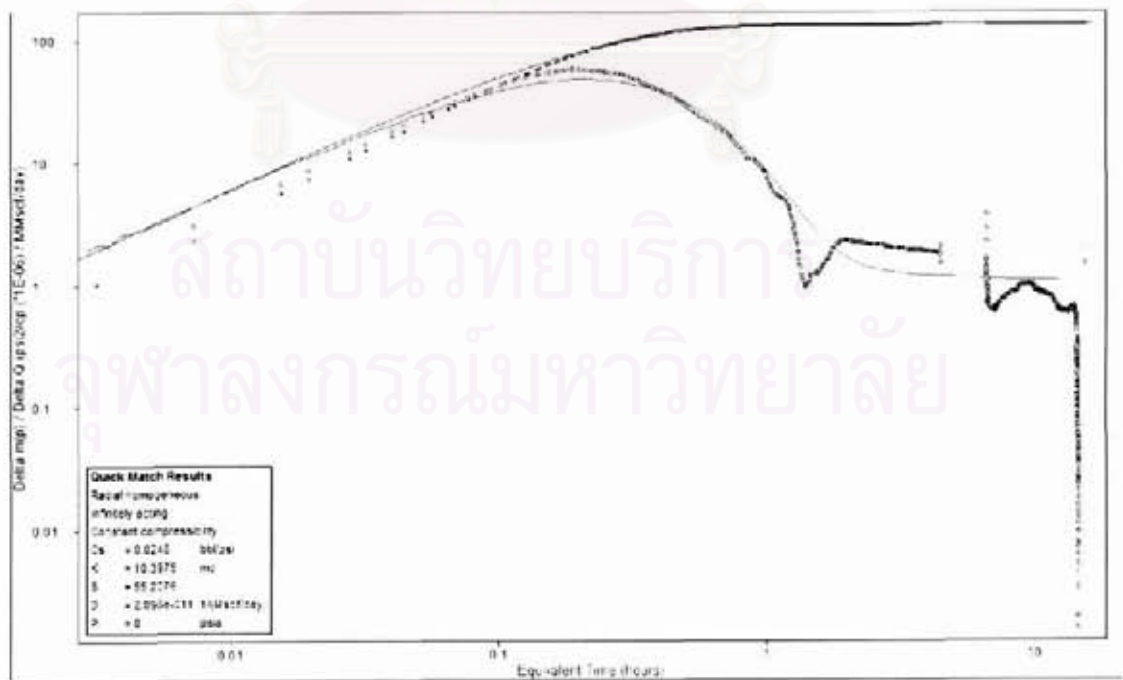


Figure A.216: Well-70 main build-up, log-log plot.

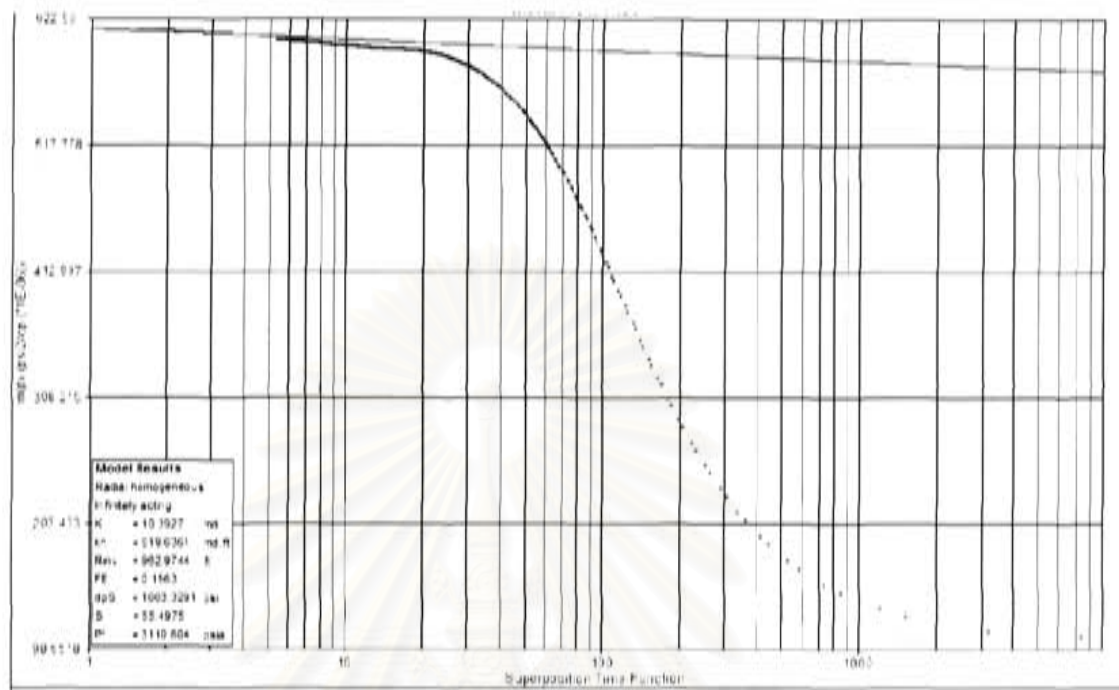


Figure A.217: Well-70 main build-up, semi-log plot.

สถาบันวิทยบริการ
จุฬาลงกรณ์มหาวิทยาลัย

Vitae

Nattapon Nampratchayakul was born on June 25, 1979 in Bangkok, Thailand. He received his B.Eng. in Petroleum Engineering from the Department of Mining and Petroleum Engineering, Faculty of Engineering, Chulalongkorn University in March 2001. He joined Unocal Thailand, Ltd as a training engineer since April 2001. He was promoted to petroleum engineer, for gas asset team, in December 2002. After Unocal Thailand, Ltd was acquired by Chevron in August 2005, he was transferred to be a petroleum engineer of Chevron Thailand Exploration and Production, Ltd. He was assigned to work in oil asset team in February 2006 and promoted to be lead petroleum engineer in April 2006. He has been a graduate student in the Master's Degree Program in Petroleum Engineering in the Department of Mining and Petroleum Engineering, Chulalongkorn University since 2005.



สถาบันวิทยบริการ
จุฬาลงกรณ์มหาวิทยาลัย